9-14-2015

Exploring the Structure of the Proton via Semi-inclusive Pion Electroproduction

Nathan A. Harrison
University of Connecticut - Storrs, nathan.harrison@uconn.edu

Exploring the Structure of the Proton via Semi-inclusive Pion Electroproduction

Nathan Andrew Harrison, Ph.D.

University of Connecticut, 2015

Measurements of the multiplicity, $\cos\phi_h$ moment, and $\cos 2\phi_h$ moment of the semi-inclusive deep inelastic scattering (SIDIS) cross-section have been performed. The data set used was the E1-F run from the CEBAF Large Acceptance Spectrometer (CLAS) at Jefferson National Lab. The run used a 5.498 GeV longitudinally polarized electron beam and an unpolarized liquid hydrogen target. Both charged pion channels were studied over a broad range of kinematics ($0.1 < x < 0.6$, $1.0 < Q^2 < 4.7$ GeV^2, $0.0 < z < 0.9$, $0.0 < P_{h\perp}^2 < 1.0$ GeV^2, and $-180^\circ < \phi_h < 180^\circ$). These measurements give access to transverse momentum dependent parton distribution functions (TMDs) which describe the transverse motion of quarks and gluons inside of the proton. Results show evidence of a TMD known as the Boer-Mulders function being non-zero via a flavor dependence on the $\cos\phi_h$ and $\cos 2\phi_h$ modulations of the data. A non-zero Boer-Mulders function requires a non-zero quark orbital angular momentum (L_q) contribution to the proton spin,

thus giving insights into the 28 year old puzzle of the missing proton spin.

Exploring the Structure of the Proton via Semi-inclusive Pion Electroproduction

Nathan Andrew Harrison

B.S., Rensselaer Polytechnic Institute, Troy, NY, 2009

M.S., University of Connecticut, 2010

A Dissertation

Submitted in Partial Fulfillment of the

Requirements for the Degree of

Doctor of Philosophy

at the

University of Connecticut

2015

APPROVAL PAGE

Doctor of Philosophy Dissertation

Exploring the Structure of the Proton via Semi-inclusive Pion Electroproduction

Presented by

Nathan Andrew Harrison,

Major Advisor

Kyungseon Joo

Associate Advisor

Peter Schweitzer

Associate Advisor

Andrew Puckett

University of Connecticut

2015

To my family and friends, for their unconditional love and support.

ACKNOWLEDGEMENTS

I would first like to thank those who most directly made this Ph.D. thesis possible. My advisor, Dr. Kyungseon Joo, right from the beginning provided me with many great opportunities to get involved in cutting-edge research with some of the top nuclear physicists in the world. My associate advisors, Drs. Peter Schweitzer and Andrew Puckett, have been invaluable as well. They have all always been very patient and willing to share their time and expertise.

I am also grateful to the entire CLAS Collaboration. Although I can't list everyone here, I would especially like to mention Drs. Volker Burkert, Harut Avakian, Maurizio Ungaro, Paul Stoler, Keith Griffioen, F.X. Girod, Youri Sharabian, and Valery Kubarovsky. Whenever I was stuck on something and didn't know where to begin I would start by asking either Harut or Mauri and they always provided valuable feedback.

This accomplishment also would not have been possible without the help, support, and friendship of past and present members of my research group. I am thankful to Dr. Wes Gohn, Dr. Nikolay Markov, Dr. Erin Seder, Dr. Taisiya Mineeva, Dr. Andre Kim, Tom O'Connell, Kevin Wei, David Riser, and Frank Cao.

I would also like to thank the faculty, staff, and students of the UConn

Physics Department, especially Dr. Gerald Dunne, Dr. Michael Rozman, Dr. Richard Jones, Dawn Rawlinson, Kim Giard, Heather Osborne, Micki Bellamy, and Jeanette Jamieson.

I am grateful to all of my former professors and teachers. In particular I would like to thank my high school physics teacher, Mr. Ken Neff, and RPI professors Drs. Jim Napolitano and Paul Stoler. Jim was an excellent teacher of quantum mechanics and also gave me my first ever research experience with the Daya Bay Neutrino Oscillation Experiment. Paul was the one who first got me involved in the CLAS Collaboration which led to many years of intense learning and eventually to this Ph.D. thesis.

On a more personal level, I know I would not be where I am today without the support of family and close friends. I am thankful to my parents for giving me life and always encouraging my curiosity. I am thankful to the extended members of the Harrison, Pasanen, and Smith families for being good role models and for always being supportive. Throughout my life I have been blessed with many good friends, many of whom feel like family, especially the O'Connors, the Faziolis, my many friends from Bethlehem Central High School, RPI, UConn, Jefferson Lab, and surrounding areas, the communities at St. Thomas Aquinas in Storrs and St. Bernard in Rockville, the Wagners, John Sammarco, and Andrew Folsom.

Finally, to the many people I have not mentioned here but have nonetheless positively impacted my life, thank you.

TABLE OF CONTENTS

LIST OF FIGURES

LIST OF TABLES

Chapter 1

Physics Motivation

1.1 Introduction

The quest for a better understanding of the structure of the proton began in the 1950s and 1960s when Hofstadter used a 188 MeV electron beam and hydrogen target to demonstrate the finite size of the proton [1] [2]. Around this same time, physicists were trying to understand the rapidly growing "particle zoo" which consisted of hundreds of known hadrons. Work by Gell-Mann, Ne'eman, and Zweig in the early 1960s led to the idea that hadrons were composed of particles with fractional electric charge that they called quarks [3] [4] [5] [6] [7]. In 1967, electron scattering experiments at the Stanford Linear Accelerator (SLAC) provided the first experimental evidence for this idea [8]. One of the most significant interpretations of these experiments was by Feynman in what he called the "Parton Model," which has evolved over time into the Quark-Parton Model [9] [10].

The SLAC and other deep-inelastic scattering (DIS) experiments at HERA and CERN revealed that the behavior of the partons inside of the proton could be

partially described by parton distribution functions (PDFs) that depend on the fractional parton momentum longitudinal to the nucleon direction of motion, x, and on the square of the momentum transferred between the scattered electron and the struck parton, Q^2. Over the course of the 1970s, 80s, and 90s, these PDFs have been mapped in a wide range of x and Q^2 [11]; examples are shown in figure 1.1. Processes in which transverse spin and momentum are integrated over are described well by these PDFs, however a complete description of the proton depends on transverse quantities.

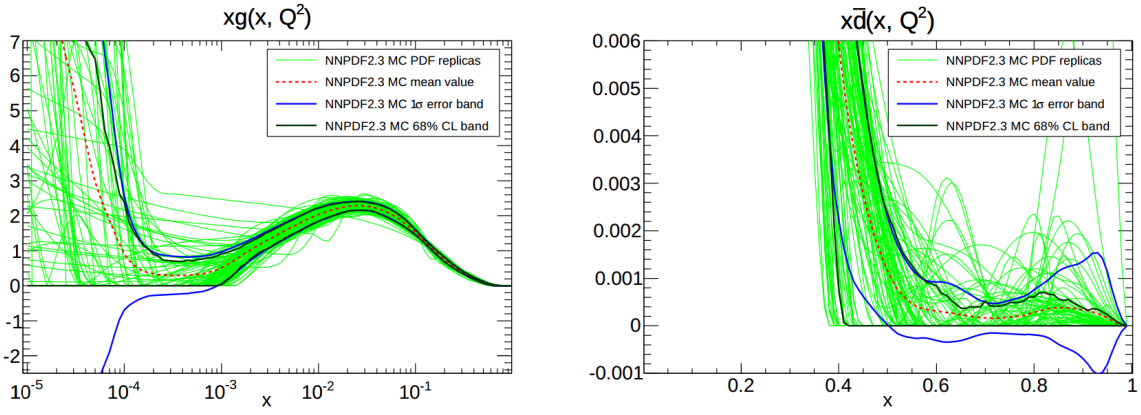

Fig. 1.1: The small x gluon PDF (left) and the large x $\bar{d}$ PDF (right) at $Q^2 = 2\ GeV^2$. Plots taken from reference [11].

A particularly important discovery came in 1987 when the European Muon Collaboration (EMC) showed that only a small portion of the proton's spin comes from the spin of its quarks [12]. This became known as the "Proton Spin Crisis" and remains an unsolved puzzle in physics. It is expected that the "missing"

proton spin is made up of a combination of quark orbital angular (L_q), gluon orbital angular momentum (L_g), and gluon spin (ΔG). Since protons are spin-half particles, we have

$$\frac{\Sigma}{2} + L_q + L_g + \Delta G = \frac{1}{2} \tag{1.1}$$

where $\frac{\Sigma}{2}$ is the contribution from the spin of the quarks. Understanding the transverse motion of quarks and gluons inside the proton is expected to give insights into this puzzle.

In the last 20 years, various experiments have used semi-inclusive deep inelastic scattering (SIDIS) and Drell-Yan ($hh \rightarrow \ell\bar{\ell}X$) to study transverse momentum dependent parton distribution functions (TMDs) which depend on the three-dimensional momentum of the parton. This analysis studies TMDs and related observables via SIDIS electroproduction of charged pions.

1.2 Semi-Inclusive Deep Inelastic Scattering

A SIDIS reaction is one in which a beam lepton, ℓ, scatters off of a target nucleon, N, via the exchange of a photon and the scattered lepton, ℓ', is detected along with a single hadron, h; everything else in the final state, X, is ignored, i.e.,

$$\ell(k) + N(P) \rightarrow \ell'(k') + h(P_h) + X(P_X) \tag{1.2}$$

where k, P, k', P_h, and P_X are the 4-momenta of ℓ, N, ℓ', h, and X, respectively. For this analysis, reactions of the type $ep \rightarrow e\pi^{\pm}X$ are studied. The momentum

transfer (or virtuality), Q^2, is given by

$$Q^2 = -q^2 = -(k - k')^2 \tag{1.3}$$

and the invariant mass of the final state, W, is given by

$$W^2 = (P + q)^2. \tag{1.4}$$

Furthermore, it is convenient to introduce the kinematic variables

$$x = \frac{Q^2}{2P \cdot q}, \qquad y = \frac{P \cdot q}{P \cdot k}, \qquad z = \frac{P \cdot P_h}{P \cdot q}, \qquad \gamma = \frac{2Mx}{Q} \tag{1.5}$$

where x is the longitudinal momentum fraction of the struck quark inside the target nucleon, z is the momentum fraction of the final state hadron, and M is the mass of the target nucleon. An important quantity is the hadron angle, ϕ_h, which is the angle between the lepton plane and the hadron production plane as defined by the Trento convention [17] (see figure 1.2). The hadron angle is given by

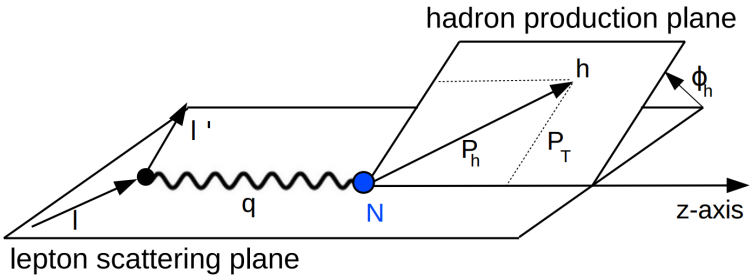

Fig. 1.2: Definition of the hadron angle in semi-inclusive deep inelastic scattering in the target rest frame.

$$\cos\phi_h = -\frac{k_\mu P_{h\nu} g_\perp^{\mu\nu}}{\sqrt{k_\perp^2 P_{h\perp}^2}}, \qquad \sin\phi_h = -\frac{k_\mu P_{h\nu} \epsilon_\perp^{\mu\nu}}{\sqrt{k_\perp^2 P_{h\perp}^2}} \tag{1.6}$$

where $k_\perp^\mu = g_\perp^{\mu\nu} k_\nu$ and $P_{h\perp}^\mu = g_\perp^{\mu\nu} P_{h\nu}$ are the transverse components of k and P_h with respect to the photon momentum. The tensors

$$\begin{aligned} g_\perp^{\mu\nu} &= g^{\mu\nu} - \frac{q^\mu P^\nu + P^\mu q^\nu}{P\cdot q\,(1+\gamma^2)} + \frac{\gamma^2}{1+\gamma^2}\left(\frac{q^\mu q^\nu}{Q^2} - \frac{P^\mu P^\nu}{M^2}\right) \\ \epsilon_\perp^{\mu\nu} &= \epsilon^{\mu\nu\rho\sigma}\frac{P_\rho q_\sigma}{P\cdot q\sqrt{1+\gamma^2}} \end{aligned} \tag{1.7}$$

have non-zero components $g_\perp^{11} = g_\perp^{22} = -1$ and $\epsilon_\perp^{12} = -\epsilon_\perp^{21} = 1$ in the given coordinate system with the convention $\epsilon^{0123} = 1$ for the totally antisymmetric tensor. A simpler form of equation 1.6 is

$$\cos\phi_h = \frac{(\hat{\mathbf{q}}\times\mathbf{k})}{|\hat{\mathbf{q}}\times\mathbf{k}|}\cdot\frac{(\hat{\mathbf{q}}\times\mathbf{P}_h)}{|\hat{\mathbf{q}}\times\mathbf{P}_h|}, \qquad \sin\phi_h = \frac{(\mathbf{k}\times\mathbf{P}_h)\cdot\hat{\mathbf{q}}}{|\hat{\mathbf{q}}\times\mathbf{k}|\,|\hat{\mathbf{q}}\times\mathbf{P}_h|} \tag{1.8}$$

where $\hat{\mathbf{q}} = \mathbf{q}/|\mathbf{q}|$ and all vectors refer to the target rest frame or to any frame reached from the target rest frame by a boost along $\hat{\mathbf{q}}$. Experiments with a polarized target have another important azimuthal angle, ϕ_S, which can be defined by making the replacements $\phi_h \to \phi_S$ and $\mathbf{P}_h \to \mathbf{S}$ in equation 1.8, where $\mathbf{S}$ is the spin of the target nucleon.

Assuming single photon exchange, the leptoproduction cross-section can be written as (see [18])

$$\frac{d^6\sigma}{dx\ dQ^2\ d\psi\ dz\ d\phi_h\ dP_{h\perp}^2} = \frac{1}{2(k\cdot P)x}\frac{\alpha^2 y}{8zQ^4} 2MW^{\mu\nu}L_{\mu\nu} \tag{1.9}$$

where the leptonic tensor is

$$L_{\mu\nu} = 2\left(k_\mu k'_\nu + k'_\mu k_\nu - k\cdot k' g_{\mu\nu}\right) + 2i\lambda_e \epsilon_{\mu\nu\rho\sigma} k^\rho k'^\sigma \tag{1.10}$$

and the hadronic tensor is

$$2MW^{\mu\nu} = \frac{1}{(2\pi)^3}\sum_X \int \frac{d^3\mathbf{P}_X}{2P_X^0}\delta^{(4)}\left(q+P-P_X-P_h\right)\langle P|\, J^\mu(0)\,|h,X\rangle\,\langle h,X|\, J^\nu(0)\,|P\rangle \tag{1.11}$$

where $J^\mu(\xi)$ is the electromagnetic current divided by the elementary charge. A sum is implied over the polarizations of all hadrons in the final state. Now the lepton-hadron cross-section can be written as

$$\begin{aligned}
\frac{d^6\sigma}{dx\; dQ^2\; d\psi\; dz\; d\phi_h\; dP_{h\perp}^2} = \\
\frac{1}{2(k\cdot P)x}\frac{\alpha^2}{xyQ^2}\frac{y^2}{2\,(1-\varepsilon)}\left(1+\frac{\gamma^2}{2x}\right)\{F_{UU,T}+\varepsilon F_{UU,L} \\
+\sqrt{2\varepsilon\,(1+\varepsilon)}\cos\phi_h F_{UU}^{\cos\phi_h}+\varepsilon\cos(2\phi_h)\,F_{UU}^{\cos 2\phi_h}+\lambda_e\sqrt{2\varepsilon\,(1-\varepsilon)}sin\phi_h F_{LU}^{sin\phi_h} \\
+S_\parallel\left[\sqrt{2\varepsilon\,(1+\varepsilon)}sin\phi_h F_{UL}^{sin\phi_h}+\varepsilon sin(2\phi_h)\,F_{UL}^{sin2\phi_h}\right] \\
+S_\parallel\lambda_e\left[\sqrt{1-\varepsilon^2}F_{LL}+\sqrt{2\varepsilon\,(1-\varepsilon)}\cos\phi_h F_{LL}^{\cos\phi_h}\right] \\
+|\mathbf{S}_\perp|\left[sin(\phi_h-\phi_S)\left(F_{UT,T}^{sin(\phi_h-\phi_S)}+\varepsilon F_{UT,L}^{sin(\phi_h-\phi_S)}\right)\right. \\
+\varepsilon sin(\phi_h+\phi_S)\,F_{UT}^{sin(\phi_h+\phi_S)}+\varepsilon sin(3\phi_h-\phi_S)\,F_{UT}^{sin(3\phi_h-\phi_S)} \\
\left.+\sqrt{2\varepsilon\,(1+\varepsilon)}sin\phi_S F_{UT}^{sin\phi_S}+\sqrt{2\varepsilon\,(1+\varepsilon)}sin(2\phi_h-\phi_S)\,F_{UT}^{sin(2\phi_h-\phi_S)}\right] \\
+|\mathbf{S}_\perp|\lambda_e\left[\sqrt{1-\varepsilon^2}\cos(\phi_h-\phi_S)\,F_{LT}^{\cos(\phi_h-\phi_S)}+\sqrt{2\varepsilon\,(1-\varepsilon)}\cos\phi_S F_{LT}^{\cos\phi_S}\right. \\
\left.\left.+\sqrt{2\varepsilon\,(1-\varepsilon)}\cos(2\phi_h-\phi_S)\,F_{LT}^{\cos(2\phi_h-\phi_S)}\right]\right\}
\end{aligned} \tag{1.12}$$

where the Fs are structure functions, λ_e is the helicity of the lepton beam, $S_\parallel$ and

$\mathbf{S}_\perp$ are the components of the polarization of the target, and

$$\varepsilon = \frac{1 - y - \frac{1}{4}\gamma^2 y^2}{1 - y + \frac{1}{2}y^2 + \frac{1}{4}\gamma^2 y^2} \tag{1.13}$$

is the ratio of longitudinal and transverse virtual photon flux. The first subscript on the structure functions represents the beam polarization, the second subscript represents the target polarization, and the third subscript (if there is one) represents the virtual photon polarization, where U, L, and T are short for unpolarized, longitudinally polarized, and transversely polarized, respectively. Since this experiment used an unpolarized target, and since the beam polarization is averaged over, equation 1.12 can be simplified to

$$\begin{aligned}\frac{d^5\sigma}{dx\ dQ^2\ dz\ d\phi_h\ dP_{h\perp}^2} = \frac{2\pi}{2(k\cdot P)x}\frac{\alpha^2}{xyQ^2}\frac{y^2}{2\,(1-\varepsilon)}\left(1+\frac{\gamma^2}{2x}\right)\{F_{UU,T} + \varepsilon F_{UU,L} \\ + \sqrt{2\varepsilon\,(1+\varepsilon)}\cos\phi_h F_{UU}^{\cos\phi_h} + \varepsilon\cos\left(2\phi_h\right) F_{UU}^{\cos 2\phi_h}\Big\}\end{aligned} \tag{1.14}$$

after integrating over ψ to get a factor of 2π (this is the electron θ_{Lab} angle and is perfectly uniform for this experiment). Factoring out the first two structure functions gives

$$\begin{aligned}\frac{d^5\sigma}{dx\ dQ^2\ dz\ d\phi_h\ dP_{h\perp}^2} = \frac{2\pi}{2(k\cdot P)x}\frac{\alpha^2}{xyQ^2}\frac{y^2}{2\,(1-\varepsilon)}\left(1+\frac{\gamma^2}{2x}\right)(F_{UU,T} \\ + \varepsilon F_{UU,L})\left\{1 + A_{UU}^{\cos\phi_h}\cos\phi_h + A_{UU}^{\cos 2\phi_h}\cos 2\phi_h\right\}\end{aligned} \tag{1.15}$$

where

$$\begin{aligned}A_{UU}^{\cos\phi_h} &= \frac{\sqrt{2\varepsilon\,(1+\varepsilon)}F_{UU}^{cos\phi_h}}{F_{UU,T} + \varepsilon F_{UU,L}} \\ A_{UU}^{\cos 2\phi_h} &= \frac{\varepsilon F_{UU}^{cos2\phi_h}}{F_{UU,T} + \varepsilon F_{UU,L}}\end{aligned} \tag{1.16}$$

are the ratio of structure functions and are called the moments of the SIDIS cross-section. Everything in front of the curly brackets is the multiplicity, A_0.

According to the factorization theorem [19] [20], structure functions can, in the Bjorken limit[1], be written as convolutions of TMDs and fragmentation functions (FFs). TMDs give the probability density of a particular quark (or antiquark) existing inside of a nucleon with longitudinal momentum fraction x and intrinsic momentum $\mathbf{k}_T$ and FFs give the probability density of a particular quark (or antiquark) forming into a particular final state hadron with momentum fraction z and transverse momentum (with respect to the quark direction) $\mathbf{p}_T$. In other words, in a SIDIS reaction, a TMD describes the quark just before it absorbs the virtual photon and a FF describes what it does after it is knocked out of the target nucleon.

There are several TMDs; a convenient way of organizing them is by their twist[2] (see table 1.1). The Boer-Mulders function, $h_1^\perp$, is of particular interest for this analysis. A table similar to table 1.1 also exists for FFs and is shown in table 1.2. As scalar particles, pions are always unpolarized, therefore only D_1 and $H_1^\perp$ (the Collins function) are relevant to this analysis. TMDs and FFs are discussed in detail in subsequent sections.

[1] The Bjorken limit is defined as $Q^2 \to \infty$, $2P \cdot q \to \infty$, and $P \cdot P_h \to \infty$ while $x = Q^2/2P \cdot q$ and $z = P \cdot P_h / P \cdot q$ remain fixed.

[2] A thorough discussion of twist is given in [15]. It's formal definition is twist = dimension - spin of the operator, however, twist = 2 + power of M/Q is often used for convenience.

	twist-2			twist-3
N\q	**U**	**L**	**T**	
U	f_1		$h_1^\perp$	$f^\perp, g^\perp, h, e$
L		g_{1L}	$h_{1L}^\perp$	$f_L^\perp, g_L^\perp, h_L, e_L$
T	$f_{1T}^\perp$	g_{1T}	$h_1, h_{1T}^\perp$	$f_T, f_T^\perp, g_T, g_T^\perp, h^\perp, e_T, h_T^\perp, e_T^\perp$

Table 1.1: Twist 2 and 3 TMDs. The **U**, **L**, and **T** in the top row represent the polarization (unpolarized, longitudinally polarized, and transversely polarized) of the quark. Likewise, the left-most column gives the polarization of the nucleon. Twist-3 TMDs describe a quark gluon correlation.

	twist-2		
h\q	**U**	**L**	**T**
U	D_1		$H_1^\perp$
L		G_1	$H_{1L}^\perp$
T	$D_{1T}^\perp$	G_{1T}	$H_1, H_{1T}^\perp$

Table 1.2: Table of leading twist fragmentation functions. The **U**, **L**, and **T** in the top row represent the polarization (unpolarized, longitudinally polarized, and transversely polarized) of the quark. Likewise, the left-most column gives the polarization of the hadron.

Using the notation $\hat{\mathbf{h}} = \mathbf{P}_{h\perp}/\left|\mathbf{P}_{h\perp}\right|$ and

$$\mathcal{C}\left[wfD\right] = x\sum_a e_a^2 \int d^2\mathbf{k}_T\, d^2\mathbf{p}_T\, \delta^{(2)}(\mathbf{k}_T - \mathbf{p}_T - \mathbf{P}_{h\perp}/z) w(\mathbf{k}_T, \mathbf{p}_T) f^a(x, k_T^2) D^a(z, p_T^2) \tag{1.17}$$

where $w(\mathbf{k}_T, \mathbf{p}_T)$ is a weight function and the summation runs over quarks and anti-quarks, the above structure functions are given at tree-level up to twist-3 in [18] as

$$\begin{aligned}
F_{UU,T} &= \mathcal{C}\left[f_1 D_1\right], \\
F_{UU,L} &= 0, \\
F_{UU}^{\cos\phi_h} &= \frac{2M}{Q}\mathcal{C}\left[-\frac{\hat{\mathbf{h}}\cdot\mathbf{p}_T}{M_h}\left(xhH_1^\perp + \frac{M_h}{M} f_1 \frac{\tilde{D}^\perp}{z}\right) - \frac{\hat{\mathbf{h}}\cdot\mathbf{k}_T}{M}\left(xf^\perp D_1 + \frac{M_h}{M} h_1^\perp \frac{\tilde{H}}{z}\right)\right] \\
F_{UU}^{\cos 2\phi_h} &= \mathcal{C}\left[-\frac{2(\hat{\mathbf{h}}\cdot\mathbf{p}_T)(\hat{\mathbf{h}}\cdot\mathbf{k}_T) - \mathbf{p}_T\cdot\mathbf{k}_T}{M M_h} h_1^\perp H_1^\perp\right].
\end{aligned} \tag{1.18}$$

The quantities with a tilde are higher twist FFs; in the Wandzura-Wilczek approximation they are taken to be zero.

Here it can be seen that $A_{UU}^{\cos 2\phi_h}$ is sensitive to the Boer-Mulders effect at the twist-2 level while $A_{UU}^{\cos\phi_h}$ only has higher twist contributions. There is a weakly flavor dependent kinematic effect, known as the Cahn effect [29], which constitutes a known, non-negligible, power correction, to which $A_{UU}^{\cos\phi_h}$ is sensitive at the twist-3 level and to which $A_{UU}^{\cos 2\phi_h}$ is sensitive at the twist-4 level. By measuring both $A_{UU}^{\cos\phi_h}$ and $A_{UU}^{\cos 2\phi_h}$ for both charged pion channels, it may be possible to isolate the flavor dependent Boer-Mulders effect from higher twist contributions such as

the Cahn effect.

Measuring A_0, $A_{UU}^{\cos\phi_h}$, and $A_{UU}^{\cos 2\phi_h}$ as a function of x, Q^2, z, and $P_{h\perp}^2$ is the focus of this thesis. This is done by extracting the ϕ_h distributions in different x, Q^2, z, and $P_{h\perp}^2$ bins from the experimental data, correcting for detector acceptance and radiative effects, and fitting the distributions with the function $A\,(1 + B\cos\phi + C\cos 2\phi)$. The fit parameters A, B, and C then directly give the multiplicity, $\cos\phi_h$ moment, and $\cos 2\phi_h$ moment of the SIDIS cross-section, respectively.

1.3 Transverse Momentum Dependent Parton Distribution Functions

There are 8 leading twist (i.e. twist-2) TMDs, each of which will be discussed here. For unpolarized target experiments, such as the one used for this analysis (see section 2.2.6), only f_1 and $h_1^\perp$ can be studied at leading twist. A separate subsection is dedicated to $h_1^\perp$ due to its importance and relevance to this analysis.

Twist-2 TMDs can be interpreted physically. They depend on x and $\mathbf{k}_T$ and describe a difference of probabilities for a particular quark with a particular polarization to exist inside of a particular nucleon with a particular polarization. The concept is shown in figure 1.3, which is similar to table 1.1 but gives a diagram representing the physical interpretation of each function.

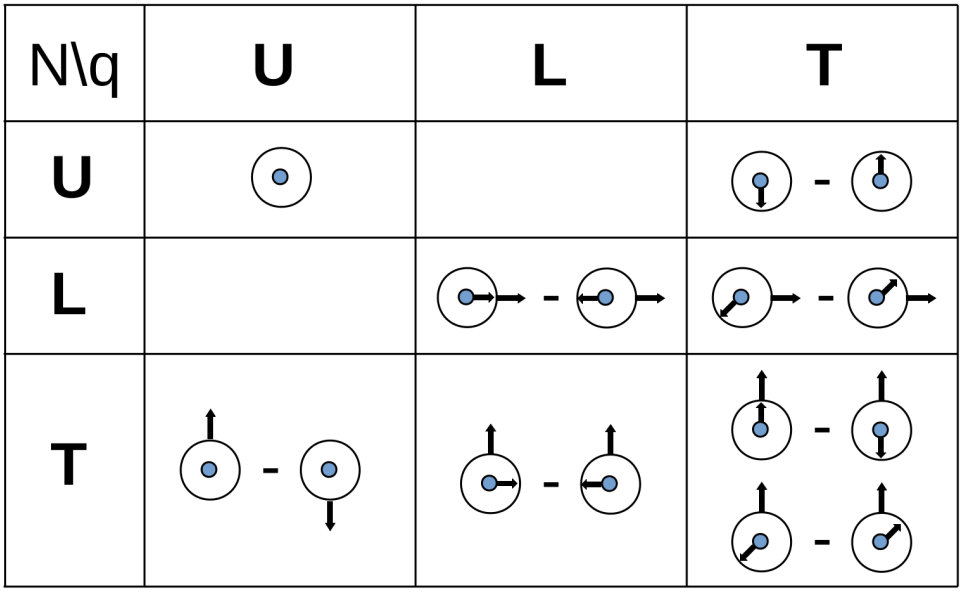

Fig. 1.3: A table of twist-2 TMDs with diagrams representing their physical interpretations. The small circles represent the quark, the big circles represent the nucleon, and the arrows represent their polarizations (the $\hat{z}$ direction (a.k.a. the virtual photon direction) is assumed to go from the left of the page to the right). Arrows pointing down-and-left are coming out of the page and arrows pointing up-and-right are going into the page. In the bottom right cell, the top diagram corresponds to h_1 and the bottom diagram corresponds to $h_{1T}^{\perp}$.

Observables corresponding to the different TMDs can be formed from combinations of the following quantities:

- $\hat{z}$: the direction of the virtual photon
- $\mathbf{k}_T$: the transverse momentum of the quark
- $\mathbf{s}_\perp$: the transverse spin of the quark
- $\mathbf{S}_\perp$: the transverse spin of the nucleon
- h: the quark helicity (the quark spin projection on $\hat{z}$)
- H: the nucleon helicity (the nucleon spin projection on $\hat{z}$)

the simplest one being $\mathbb{1}$, the identity, corresponding to f_1, which describes unpolarized quarks inside of unpolarized nucleons. The product hH corresponds to g_{1L}, sometimes called the "helicity function," which describes longitudinally polarized quarks inside of longitudinally polarized nucleons. The product $\mathbf{s}_\perp \cdot \mathbf{S}_\perp$ corresponds to the "transversity function," h_1, which describes transversely polarized quarks inside of transversely polarized nucleons.

Moving on to combinations containing a power of $\mathbf{k}_T$, we have $h(\mathbf{k}_T \cdot \mathbf{S}_\perp)$ and $H(\mathbf{k}_T \cdot \mathbf{s}_\perp)$ which correspond to g_{1T} and $h_{1L}^\perp$, respectively. These are called the "worm gear" functions. g_{1T} is chiral-even and describes longitudinally polarized quarks inside of transversely polarized nucleons. $h_{1L}^\perp$ is chiral-odd and describes transversely polarized quarks inside of longitudinally polarized nucleons. These

two functions have been shown to be opposite each other ($g_{1T} = -h_{1L}^{\perp}$) in various quark models [23] [24] [25] [26].

Next we have the triple products $\mathbf{S}_\perp \cdot (\mathbf{k}_T \times \hat{z})$ and $\mathbf{s}_\perp \cdot (\mathbf{k}_T \times \hat{z})$. The former expression corresponds to the chiral-even "Sivers function," $f_{1T}^{\perp}$, which describes unpolarized quarks inside of transversely polarized nucleons and the latter corresponds to the Boer-Mulders function discussed in the subsection below. Both of these are T-odd (this is defined in section 1.3.1). The Sivers function generates single-spin asymmetries in transversely polarized SIDIS [21].

Finally, by adding one more power of $\mathbf{k}_T$, we can form the quantity $(\mathbf{S}_\perp \cdot \mathbf{k}_T)(\mathbf{s}_\perp \cdot \mathbf{k}_T) - \frac{1}{2}\mathbf{k}_T^2(\mathbf{S}_\perp \cdot \mathbf{s}_\perp)$ which corresponds to the "pretzelosity function," or the "Mulders-Tangerman distribution", $h_{1T}^{\perp}$, and describes transversely polarized quarks inside of transversely polarized nucleons. A non-zero value for this function could mean that the nucleon has a non-spherical shape [22]. Other combinations either simplify to combinations of these, equal zero (e.g. $\mathbf{k}_T \cdot \hat{z}$), or do not transform like proper scalars under parity inversion.

The diagonal elements of table 1.1 (f_1, g_{1L}, h_1, and $h_{1T}^{\perp}$) are well known and are related to the square of the leading-twist, light-cone wave functions. The off diagonal elements are particularly interesting because they require non-zero orbital angular momentum.

1.3.1 Boer-Mulders Function

The Boer-Mulders function [16], $h_1^\perp$, appears in the top-right corner of table 1.1 and therefore describes transversely polarized quarks in unpolarized nucleons. It is a quark distribution that quantifies a spin-orbit correlation and is of particular interest because it appears in the $A_{UU}^{\cos 2\phi}$ term of the SIDIS cross-section at the leading twist level (see section 1.2). Pictorially, $h_1^\perp$ can be represented by figure 1.4. Here, it can be seen that $h_1^\perp$ is a difference of probabilities that reflects the presence of a handedness inside the proton $(\mathbf{s}_\perp \cdot (\mathbf{k}_T \times \hat{z}))$; if this is non-zero, then there is a net transverse quark polarization inside of unpolarized protons.

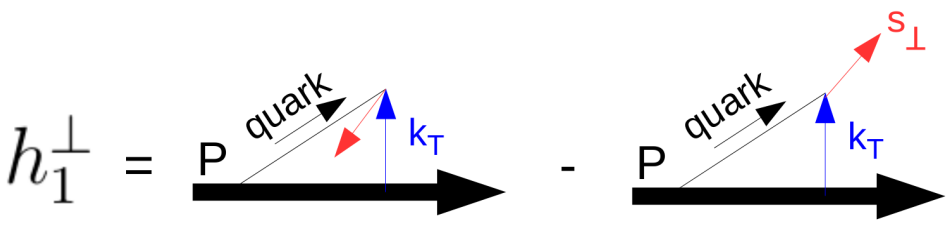

Fig. 1.4: A pictorial representation of the Boer-Mulders function, $h_1^\perp$. P is the momentum of the proton and k_T (blue arrows) and $\mathbf{s}_\perp$ (red arrows) are defined in the text. In the first term on right-hand-side of the equation, $\mathbf{s}_\perp$ is pointing out of the page, and in the second term it is pointing into the page.

$h_1^\perp$ is a naive-T-odd function, i.e. its sign changes under "naive time reversal," which is defined as usual time reversal but without the interchange of initial and final states, and since it is a chiral-odd function it cannot be studied

using inclusive DIS. Due to it's T-odd character, it is predicted that $h_1^\perp$ will have opposite signs when measured using SIDIS and Drell-Yan [13]. This prediction will soon be tested at hadron colliders such as Fermilab, RHIC, and CERN. Another important prediction is that a non-zero measurement of the Boer-Mulders function would suggest that the orbital angular momentum of the quarks inside of the proton is also non-zero; an important insight into the internal dynamics of the proton and the aforementioned "spin crisis."

The Boer-Mulders function has been calculated in a light-cone quark model in [14], these results for up and down quarks are shown in figure 1.5.

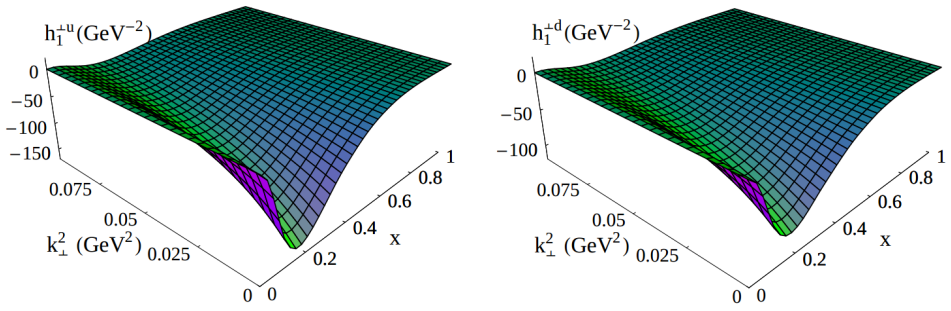

Fig. 1.5: $h_1^\perp$ for up quarks (left) and down quarks (right). Plots taken from [14].

1.4 Fragmentation Functions

FFs describe the process of hadronization, that is, how a quark or gluon forms into a hadron before being detected as a free particle. The phenomenon is a consequence of confinement in Quantum Chromodynamics (QCD), which cannot be studied with inclusive DIS where the final state hadrons are not observed. Al-

though FFs are interesting by themselves, they are made even more relevant by virtue of the fact that they are combined with TMDs in SIDIS processes. A thorough understanding of FFs is therefore needed to make progress on understanding the three dimensional structure of nucleons.

Like TMDs, FFs can be interpreted physically. Figure 1.6 shows the probabilistic interpretations in terms of the quark and hadron polarizations for each leading twist FF in the same way that figure 1.3 does for TMDs. FFs have been determined both experimentally, with results summarized in [27], and in quark models, e.g. in [28].

The convolution of two FFs can be measured with e^+e^- annihilation experiments in a similar way to how the convolution of a TMD and FF can be measured with SIDIS. Results from measurements of these processes along with Drell-Yan, which measures the convolution of two TMDs, give a complete picture of TMDs and FFs.

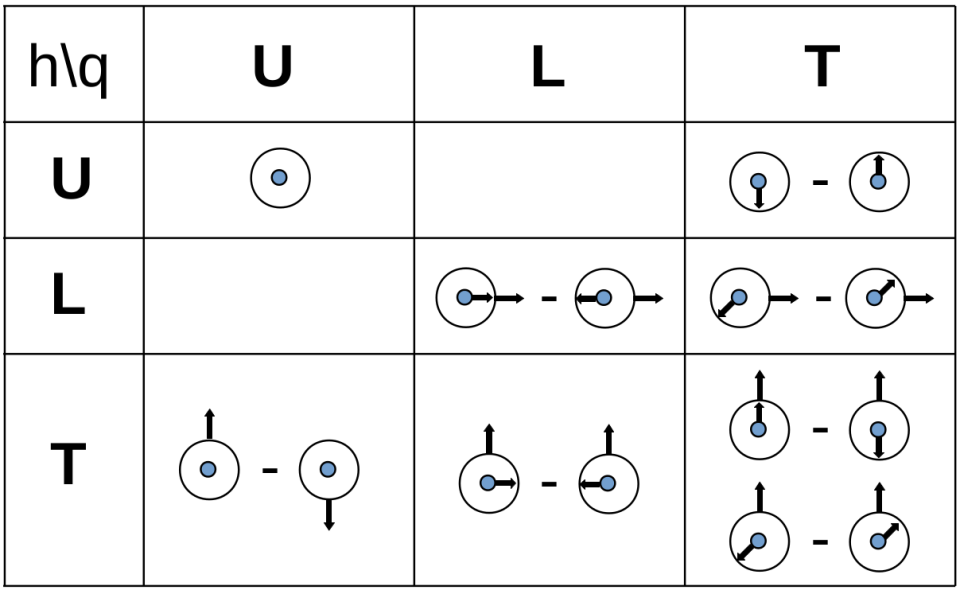

Fig. 1.6: A table of twist-2 FFs with diagrams representing their physical interpretations. The small circles represent the quark, the big circles represent the hadron, and the arrows represent their polarizations. Arrows pointing down-and-left are coming out of the page and arrows pointing up-and-right are going into the page. In the bottom right cell, the top diagram corresponds to H_1 and the bottom diagram corresponds to $H_{1T}^{\perp}$. The polarization arrows are with respect to the quark direction (before hadronization), which is assumed to go from the left of the page to the right.

Chapter 2

The Experiment

2.1 The CEBAF Accelerator

The Continuous Electron Beam Accelerator Facility (CEBAF) is located at the Thomas Jefferson National Laboratory (Jefferson Lab) in Newport News, VA. Construction of the facility began in 1987 and the first electron scattering experiments started in 1995. Electrons are produced at the CEBAF injector site by shining a laser onto a Gallium Arsenide (GaAS) photocathode and are then directed into one of two linear accelerators (LINACs). Nine recirculation arcs use magnetic fields to bend the electron beam such that it passes through each LINAC up to five times before entering one of the three experimental halls as shown in figure 2.1. The CLAS detector used in this experiment and discussed in detail below is located in Hall-B. The LINACs use superconducting radio-frequency (SRF) cavities made of niobium which operate at 2K (-456°F) to boost the electrons by up to 1.140 GeV with each pass. After five passes around the 7/8 mile track, the polarized electrons delivered by CEBAF arrive at the experimental halls in

bunches of one million every 2 ns with energies up to 6 GeV. The maximum beam polarization is approximately 88%.

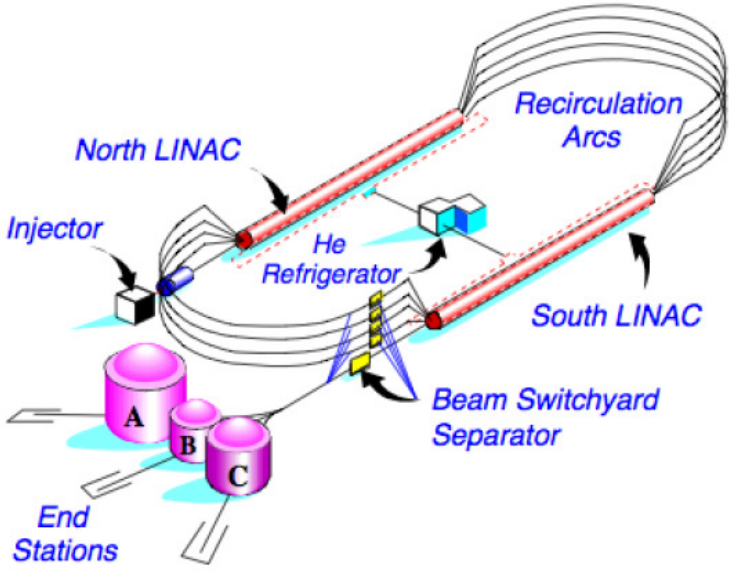

Fig. 2.1: The Continuous Electron Beam Accelerator Facility (CEBAF) at Jefferson National Lab. The beam is created at the injector site and passes a pair of linear accelerators and recirculating arcs with each loop before being delivered to one of the three experimental halls (Hall A, B, or C).

2.2 The CLAS Detector

The CEBAF Large Acceptance Spectrometer (CLAS) is a particle detector with a nearly 4π solid angle coverage that measures approximately 30 feet across located in Hall-B of Jefferson Lab. CLAS is composed of six identical sectors and

four detector subsystems along with a torus magnet [30], see figure 2.2. Each of the four subsystems, which are drift chambers, Čerenkov counters, time-of-flight scintillators, and electromagnetic calorimeters, will be discussed in detail below.

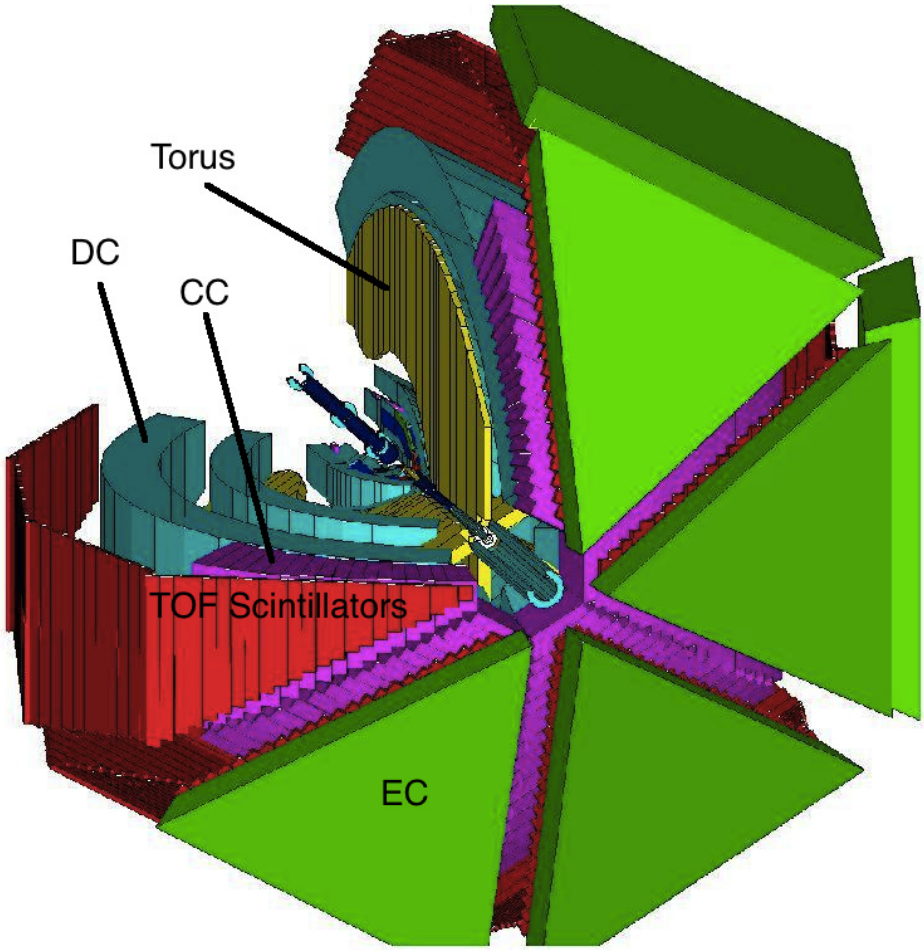

Fig. 2.2: The CEBAF Large Acceptance Spectrometer (CLAS) particle detector with the different components labeled.

2.2.1 The Torus Magnet

The CLAS torus magnet is shown if figure 2.3, the six sectors of CLAS fit between the six arms of the magnet. Unlike other common magnets, such as dipolar and solenoidal, toroidal magnets preserve polar angle, afford a uniform momentum resolution over a broad momentum range, and produce a vanishing magnetic field at its center where the target is located, thus allowing us to have targets of various polarizations. The magnet uses superconducting coils to produce currents up to 3680 Amps corresponding to a magnetic field of 2 Tesla.

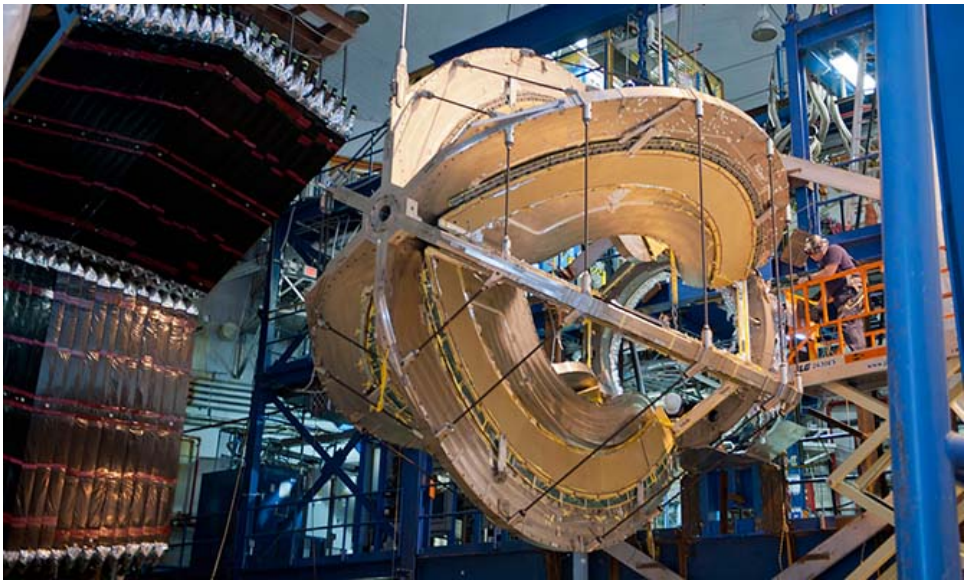

Fig. 2.3: A photograph of the CLAS torus magnet being installed in Hall-B of Jefferson National Lab.

2.2.2 Drift Chambers

The inner-most detector subsystem is the drift chambers (DCs) [31] which surround the torus magnet. Located within the toroidal magnetic field, the DCs are used to determine the momenta of charged particles by measuring the curvatures of their paths and the relationship given in Eq. 2.1, where q is the charge of the particle, B is the magnetic field strength, and ρ is the curvature of the path.

$$p = qB\rho \tag{2.1}$$

There are three layers, or regions, of drift chambers, each filled with an ionizing gas with a high ion drift velocity (90% argon and 10% CO_2). As charged particles pass through the gas, a trail of ions is left behind which drift (via an electric field) to wires that detect the ions. Using the known magnetic field shown in figure 2.4, the trajectories, and therefore the curvatures and momenta, of the particles can be determined.

The aforementioned sensing wires are 20 μm diameter gold-plated tungsten with a surface electric field of 280 kV/cm. Each sensing wire is surrounded by a hexagonal field wire as shown in figure 2.5. There are a total of 35,148 hexagonal "drift cells."

2.2.3 Čerenkov Counter

When a charged particle travels through a medium with velocity $v > \frac{c}{n}$, where n is the refractive index of the medium, radiation known as Čerenkov radiation is

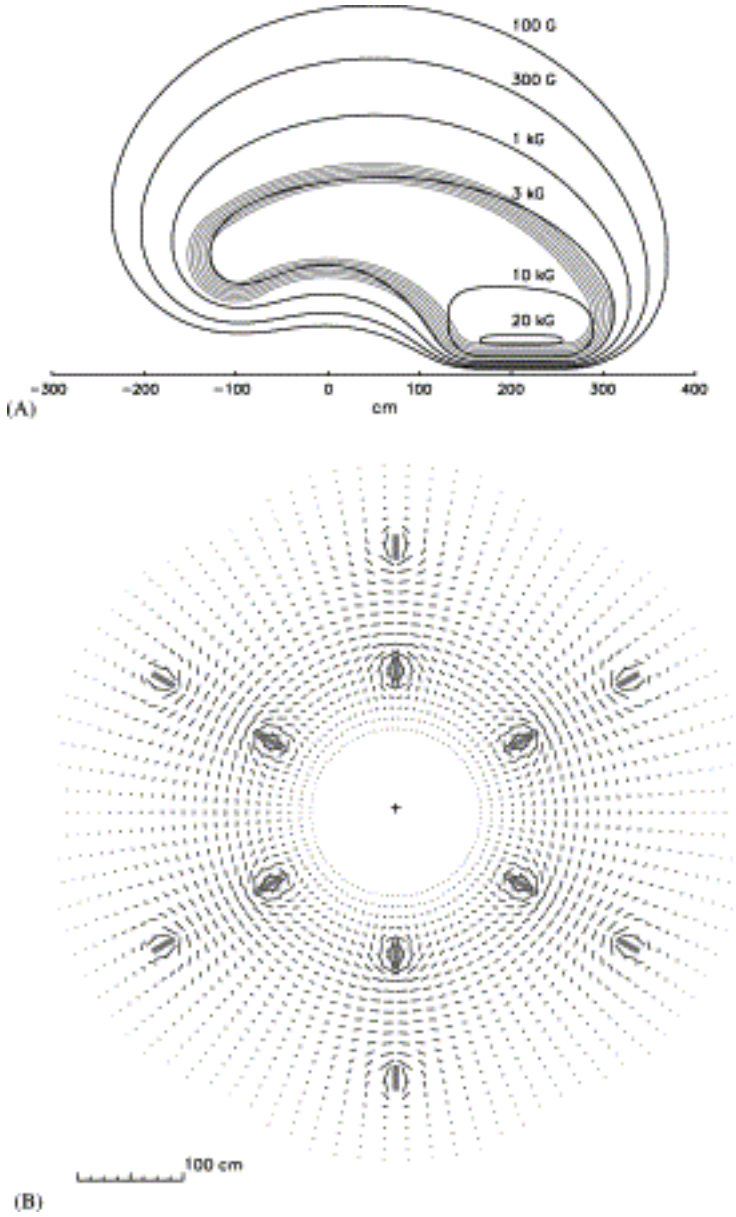

Fig. 2.4: "(A) Contours of constant absolute magnetic field for the CLAS toroid in the midplane between two coils. The projection of the coils onto the midplane is shown for reference; (B) Magnetic field vectors for the CLAS toroid transverse to the beam in a plane centered on the target. The length of each line segment is proportional to the field strength at that point. The six coils are seen in cross-section. [30]"

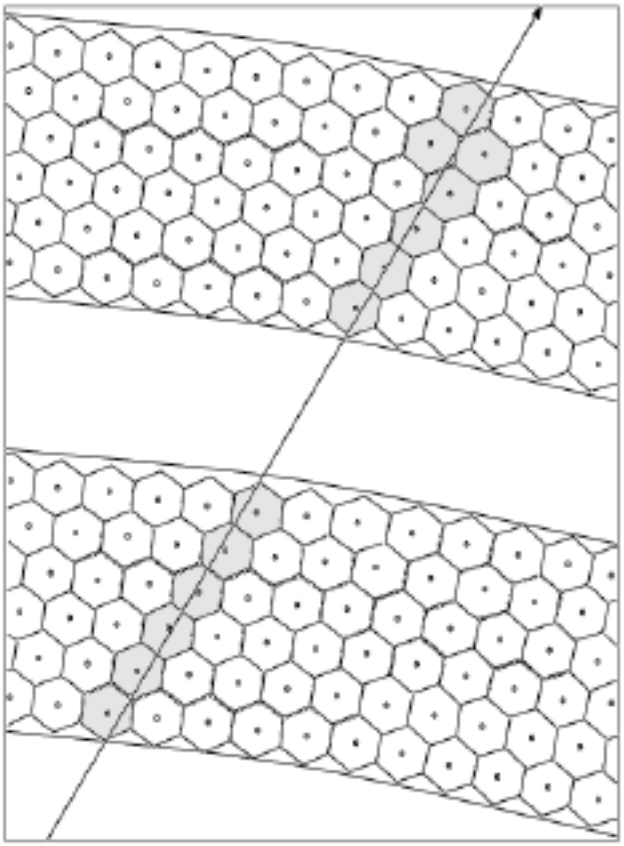

Fig. 2.5: A cross-section of one of the drift chambers showing the hexagonal wire cells. A typical track is indicated by the black line and shaded regions.

emitted. The CLAS Čerenkov Counter (CC) [32] uses this principle to distinguish between electrons and negatively charged pions, which are often misidentified as electrons. The medium used in the CC is gaseous perfluorbutane, C_4F_{10}, which has a refractive index of 1.00153. With this gas, the threshold for radiating for electrons is 9 MeV and for negative pions it is 2.5 GeV, which gives good electron-pion separation at the energy scales of this experiment.

Each of the six identical sectors of the CC consists of 18 segments. Each segment consists of a pair of elliptical mirrors, a pair of hyperbolic mirrors, and a pair of PMTs arranged in a way to optimize detection of Čerenkov radiation, see figures 2.6 and 2.7; each PMT is also surrounded by a magnetic shield and an Winston cone to improve detection efficiency.

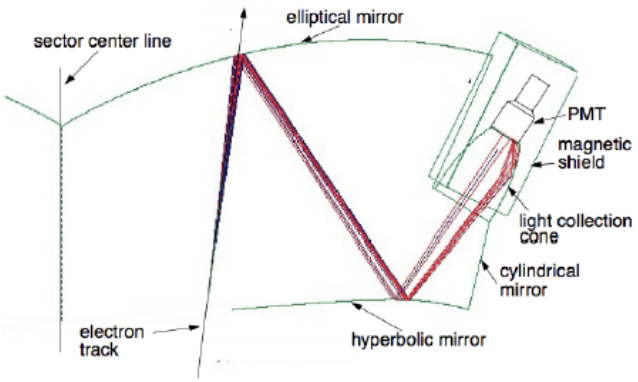

Fig. 2.6: A diagram of half of one CLAS CC segment with a typical electron track shown. The electron produces Čerenkov light which is reflected off of an elliptical mirror, then off of a hyperbolic mirror, before being detected by a PMT.

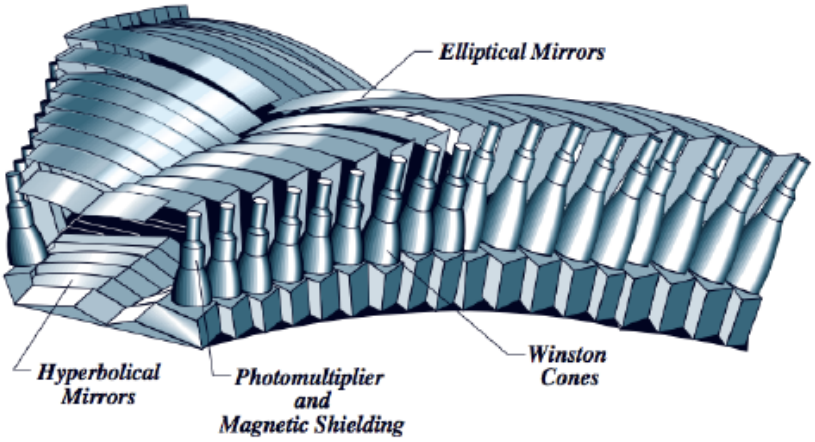

Fig. 2.7: An entire sector of the CLAS CC. Each sector has 18 segments consisting of a pair of elliptical mirrors, a pair of hyperbolic mirrors, and a pair of PMTs with shieldings and Winston Cones.

2.2.4 Time-of-Flight Scintillators

The CLAS time-of-flight scintillators (TOF or SC) [33] consists of six identical sectors; each sector has four panels with a total of 57 Bicron-408 scintillators, see figure 2.8. Each scintillator paddle is 5 cm thick, either 15 or 22 cm wide, and has a length between 32 and 450 cm; the shorter paddles at forward angles and the longer paddles at larger angles, for a total coverage area of 206 m^2. When a charged particle passes through one of the scintillators, ionization radiation is detected by the PMTs at the end of the paddles and the timing information is recorded. This information, along with the event start time and the path length measured by the DC, is used to calculate the velocity of charged particles. The

time resolution varies from 60 to 120 ps depending on the length of the paddle; the system is capable of pion-kaon separation up to 2 GeV.

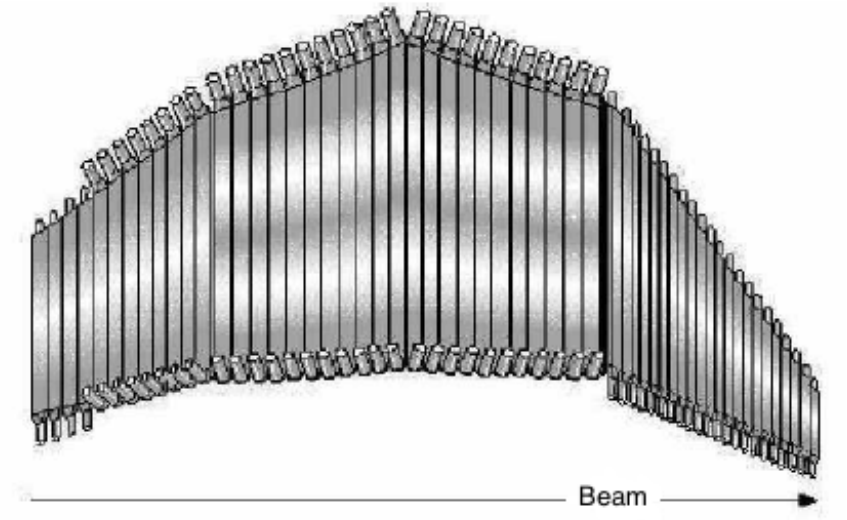

Fig. 2.8: A drawing of one sector of the CLAS TOF. There are 48 scintillator strips, each with a PMT on each end.

2.2.5 Electromagnetic Calorimeter

The CLAS electromagnetic calorimeter (EC) [34] records energy, position, and timing information for each track in the forward region ($8^\circ < \theta < 45^\circ$). Each of the six identical sectors of the EC is composed of three planes of lead-scintillator strips arranged in a triangular pattern, each offset by 120° (see figure 2.9) to allow for the triangulation of hits. When a charged particle enters the EC, its interaction with the media generates photons that are collected by PMTs. When entering the EC, relativistic electrons lose most of their energy via bremsstrahlung radiation,

while negatively charged pions tend to create radiation via ionization processes. These two different processes generate different signals in the EC making it easy to use the EC to separate electrons and negatively charged pions.

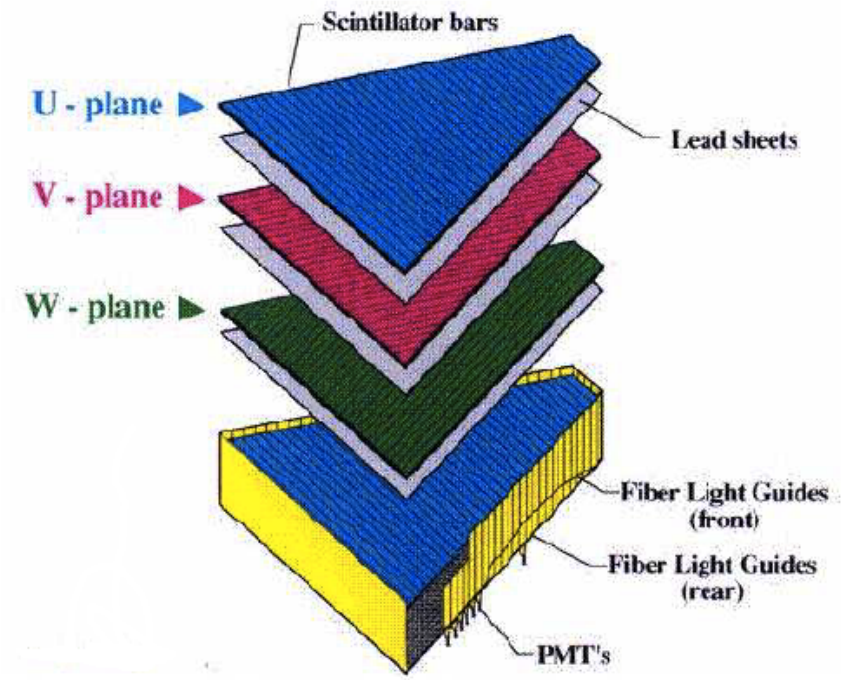

Fig. 2.9: A schematic of one of the CLAS electromagnetic calorimeters with the different components labeled.

2.2.6 E1-f Run

The E1-f run at at Jefferson Lab operated from April through June of 2003. The run used a 5.498 GeV electron beam with a 75.1±0.2% polarization. The target was an unpolarized liquid hydrogen. It was determined that running the torus magnet at 60% of its maximum value would improve acceptance. In this

analysis, two pion channels - π^+ and π^- - were studied over a broad kinematic range ($Q^2 \approx 1 - 5GeV^2, P_T \approx 0 - 1.5GeV, z \approx 0.4 - 0.7$, and $x \approx 0.1 - 0.9$).

Chapter 3

Data Analysis

3.1 Data Processing

During the running of the experiment, raw data (TDC and ADC values) from each of the detector subsystems is captured by the Data Acquisition System (DAQ) and stored in files in a format known as BOS format. After the completion of the experiment, these files are processed, or "cooked," using the CLAS Reconstruction and Analysis software package (RECSIS). RECSIS essentially translates the raw data into understandable information for each event, such as each track's momentum, θ, ϕ, and charge, along with some other specifics such as the number of photoelectrons produced in the CC, and the energy deposited in the EC, for example. At this stage, the data files can be converted into a preferred format, such as a ROOT tree, which was used for this analysis. A good run list for the E1-f experiment was determined in [35] and is printed in appendix A.

3.2 Recalibration of the SC

It was discovered that the original calibration was off for some of the SC paddles during certain portions of the run period. To fix this, a run number dependent t_0 offset is added or subtracted to the time value for certain paddles. Some paddles were too bad to be fixed; these paddles are cut from the analysis. Most of these paddles are in the very backward direction (paddle number greater than ~ 40) and have low statistics.

It is not sufficient to do paddle calibration with just electrons because they do not go to backward angles, therefore positive and negative hadrons were used (primarily pions). For each paddle, the quantity $\Delta t = t_{measured} - t_{calculated}$ is calculated for each track hitting that paddle. $t_{calculated}$ is the calculated time based on the track's momentum measured in the drift chamber, path length, and the assumed pion mass. $t_{measured}$ is the time measured by the specific paddle with the event start time subtracted off. The event start time depends on the time value given by the paddle hit by the electron, which is the trigger. In principle, it may not be safe to rely on the timing information from the electron side either, but since the majority of the paddles are good, this can be ignored. For a given paddle, then, Δt is plotted vs momentum. For a good paddle, pions will form a horizontal band centered at $\Delta t = 0$. For bad paddles, this band will be shifted up or down by several nanoseconds. This is done in bins of run number to look for any run number dependence. Any deviation from $\Delta t = 0$ is then corrected

by simply subtracting off the time shift. Figure 3.1 shows an example of this procedure, and tables 3.1 and 3.2 summarize the corrected and cut paddles.

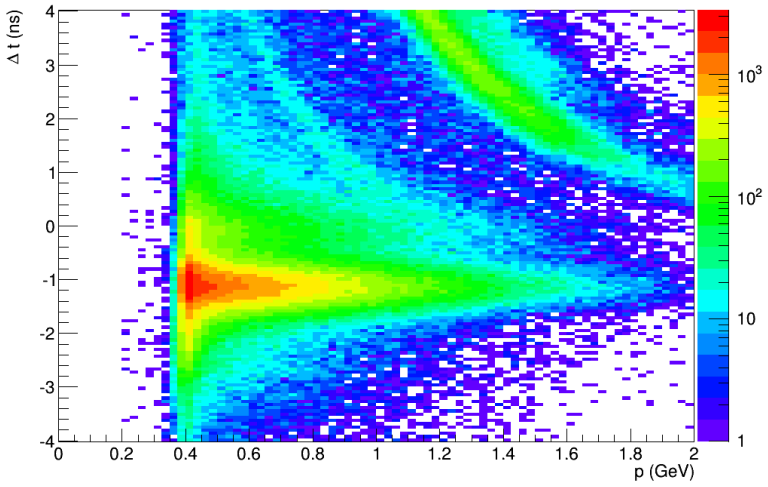

Fig. 3.1: Δt versus momentum for positive tracks hitting paddle number 24 of sector 1. This paddle was incorrectly calibrated; the events in the horizontal band centered near $\Delta t = -1.13ns$ are positive pions that should be centered at $\Delta t = 0$. The timing information from this paddle is corrected by adding $1.13334ns$ to it for runs numbered greater than or equal to 37749. Runs numbered less than 37749 were correctly calibrated and need no correction, these events are faintly visable. Protons and a small number of kaons are also visable in this plot.

Table 3.1: A summary of the t_0 offsets applied to the incorrectly calibrated SC paddles.

sector	paddle	run range	time shift (ns)
1	24	run no. >= 37749	1.13334
2	38	run no. >= 38535	-1.89592
3	2	run no. >= 0	-15.45
3	11	run no. >= 37777	-2.26126
3	24	run no. >= 37855 and run no. <= 38546	-1.78266
3	25	run no. >= 37743 and run no. <= 38266	2.44804
3	27	run no. >= 37854 and run no. <= 38546	-1.85815
3	28	run no. >= 37854	1.21704
4	2	run no. <= 37853	-1.9
4	5	run no. >= 38549	1.91688
4	19	run no. >= 37854	-0.365798
4	34	run no. >= 37854	-2.33721
4	42	run no. >= 37750	-1.4118
4	45	run no. >= 38551	-3.36406
5	2	run no. >= 38241	-19.15
5	2	run no. <= 38240	-17.9

Continued on next page

Table 3.1 – *Continued from previous page*

sector	paddle	run range	time shift (ns)
5	18	run no. >= 37854 and run no. <= 38545	1.24884
5	20	run no. >= 37809	-0.468722
5	34	run no. <= 37853	-1
5	34	run no. >= 37854	6
5	36	run no. >= 37748	1.07962
6	1	run no. >= 0	18.25
6	18	run no. >= 37854 and run no. <= 38545	-1.69106

sector	paddles
1	41, 42, 44, 45, 46, 47
2	16, 40, 41, 42, 43, 45, 46
3	2, 40, 41, 42, 43, 44, 45, 46
4	43, 46
5	3, 40, 41, 42, 43, 44, 46, 47
6	40, 42, 44, 45

Table 3.2: A summary of the SC paddles that are cut from the analysis because their calibration is unreliable and uncorrectable.

3.3 Electron Identification

Electrons are identified by putting each negative track for a given event through a series of nine cuts. A candidate electron is considered a "good" electron only if it passes all nine cuts. If an event has more than one good electron, the highest momentum one is chosen. The nine cuts, described in detail in the subsequent sections, are: matching cuts on the θ and ϕ angles in the CC, a θ vs ϕ fiducial cut, a momentum dependent cut on the EC energy, a cut on the energy in the inner EC, a geometric cut on the EC, fiducial cuts on regions 1 and 3 of the DC, and a cut on the z vertex.

3.3.1 CC θ Matching

Due to the geometry of the CC, the correspondence between polar angle in the CC, θ_{CC}, and the CC segment number for scattered electrons is manifestly surjective. A cut is therefore applied on θ_{CC} for each segment of the CC by fitting the θ_{CC} distribution with a gaussian plus a polynomial background; events within 3σ of the mean pass the cut, see figure 3.2.

3.3.2 CC ϕ Matching

Each sector of the CC is divided in half such that each side is a mirror image of the other (see section 2.2.3). If a track is on one side of the sector but the PMT that fired was on the other side, then the event was likely background and not a

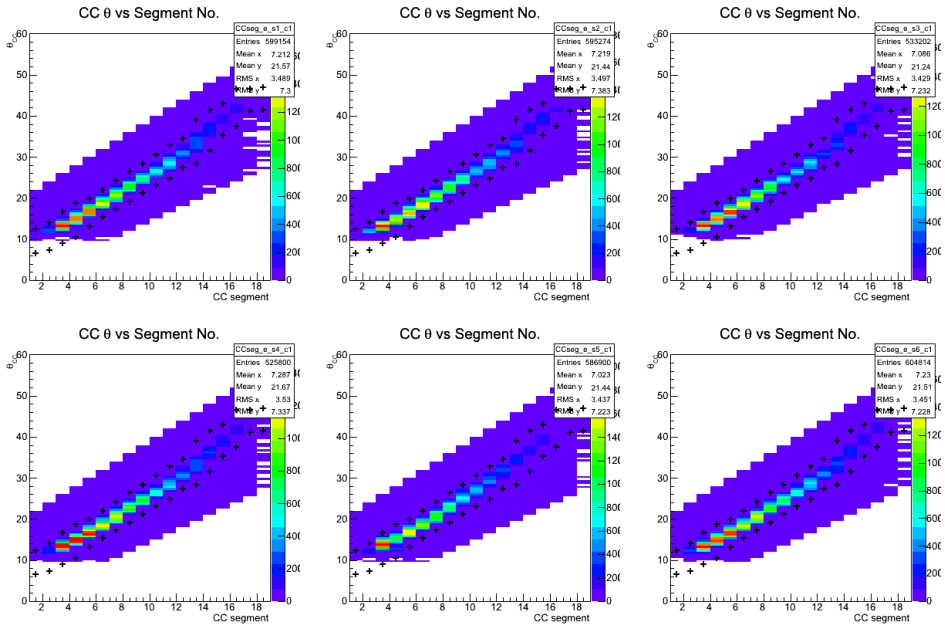

Fig. 3.2: θ_{CC} vs CC segment number for each of the six sectors of CLAS. These plots already have the other eight cuts applied and the current cut is given by the black crosses.

good event. A CC ϕ matching algorithm is used that returns 0 if both PMTs fire, ± 1 if the track and PMT are on the same side, and ± 2 if the track and PMT are on opposite sides. Events that return ± 2 are rejected, all other events are kept. See figures 3.3 and 3.4.

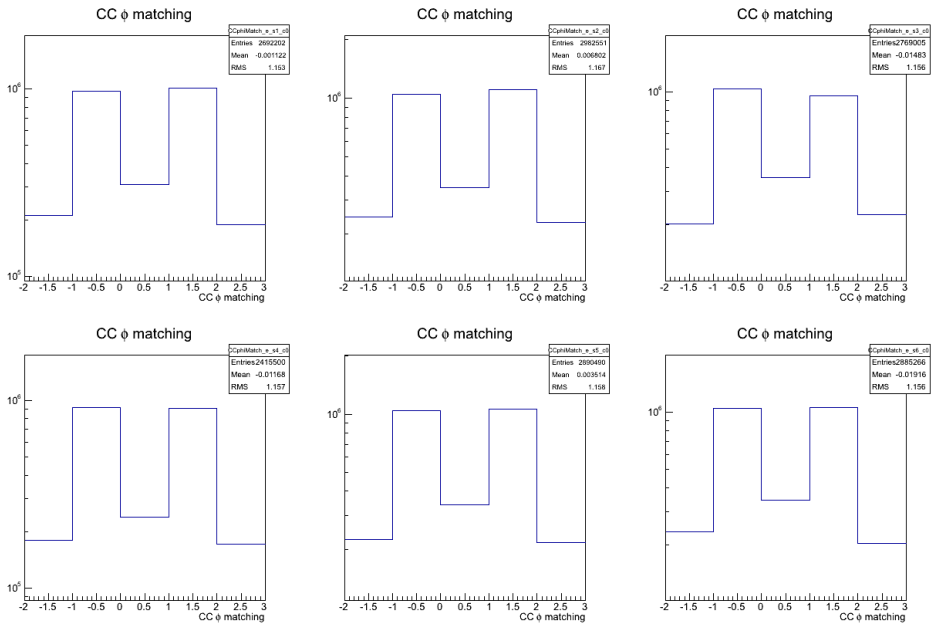

Fig. 3.3: CC ϕ matching distribution for negative tracks for each sector. The matching algorithm returns 0 if both PMTs fire, ± 1 if the track and PMT are on the same side, and ± 2 if the track and PMT are on opposite sides.

3.3.3 CC Fiducial Cut

A geometric cut of the form $\theta_{CC} > 46.0 - 35\sqrt{1 - \frac{\phi^2}{350}}$ (units of degrees) is applied to the CC. The equation was obtained empirically based on the θ_{CC} vs ϕ (lab

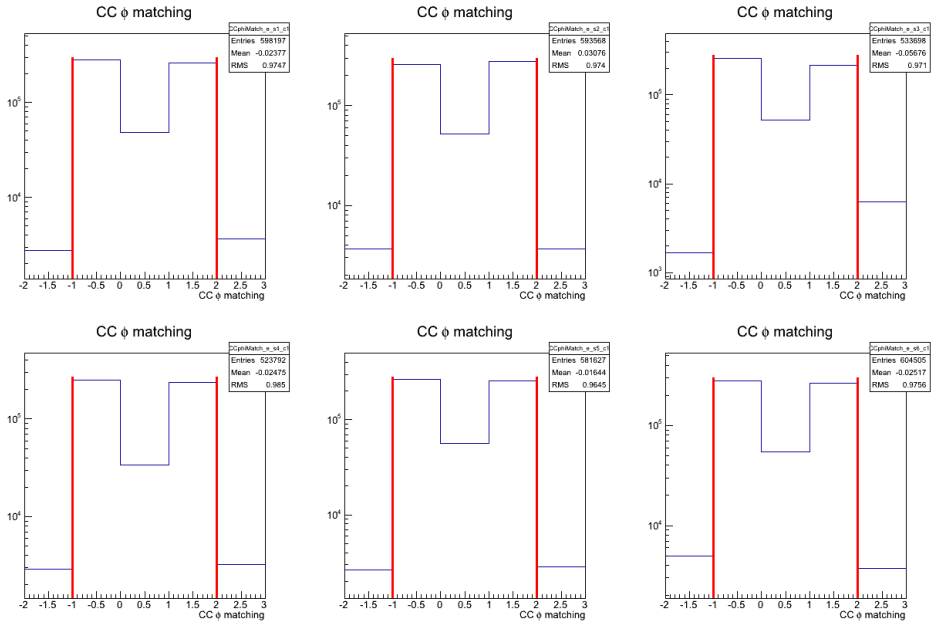

Fig. 3.4: CC ϕ matching distribution for electron candidates with all other electron ID cuts applied for each sector. This cut is shown in red and removes candidate electrons for which the PMT and track are on opposite sides of the sector.

angle) distribution with and without other electron ID cuts applied. See figure 3.5.

3.3.4 EC E_{in} vs E_{out} Cut

The EC can be used to separate negatively charged pions from electrons in several ways. Firstly, the scattered electron always travels in a forward direction while pions can have any direction; since the EC only covers forward angles, any track not producing a signal in the EC is immediately rejected. Secondly, any pion over 0.5 GeV is minimum ionizing in the EC and produces less light in the PMTs than electrons do. Therefore, only candidate electrons with an energy in the inner part of the EC greater than 0.06 GeV are kept (see figure 3.6).

3.3.5 EC Sampling Fraction Cut

The ratio of total energy to momentum stays nearly constant as a function of momentum for electrons. To eliminate background as well as contamination from other negative tracks, each momentum bin is fit with a gaussian and the points at $\mu + 5\sigma$ and $\mu - 3\sigma$ are fit with a second order polynomial to define the cut. Figure 3.7 shows the E/p vs p distribution candidate electrons along with the cut described here.

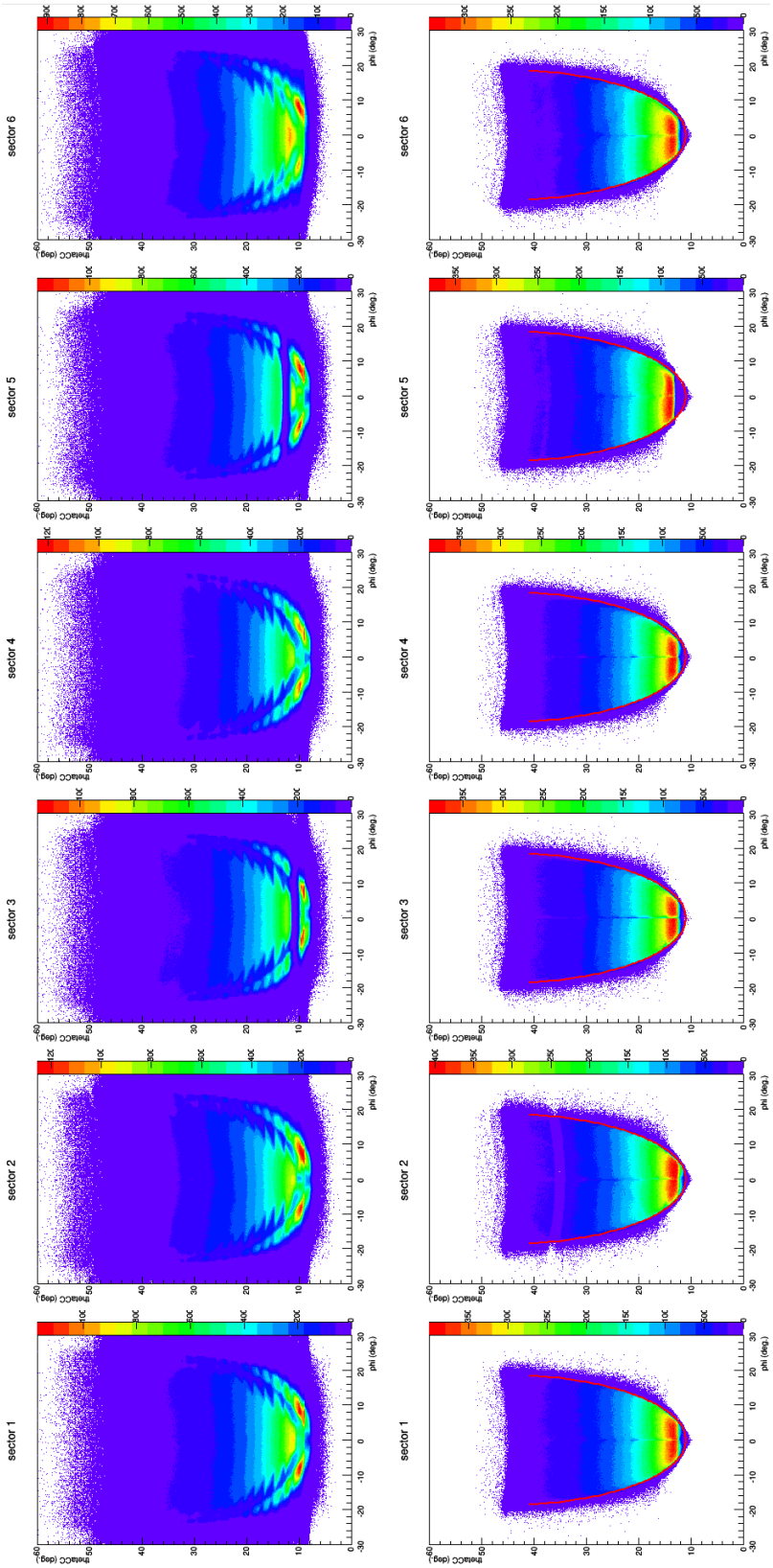

Fig. 3.5: θ_{CC} vs ϕ (lab angle) for each of the six CLAS sectors. The top row shows all negative tracks and the bottom row shows negative tracks which pass all the other electron ID cuts with this cut shown in red.

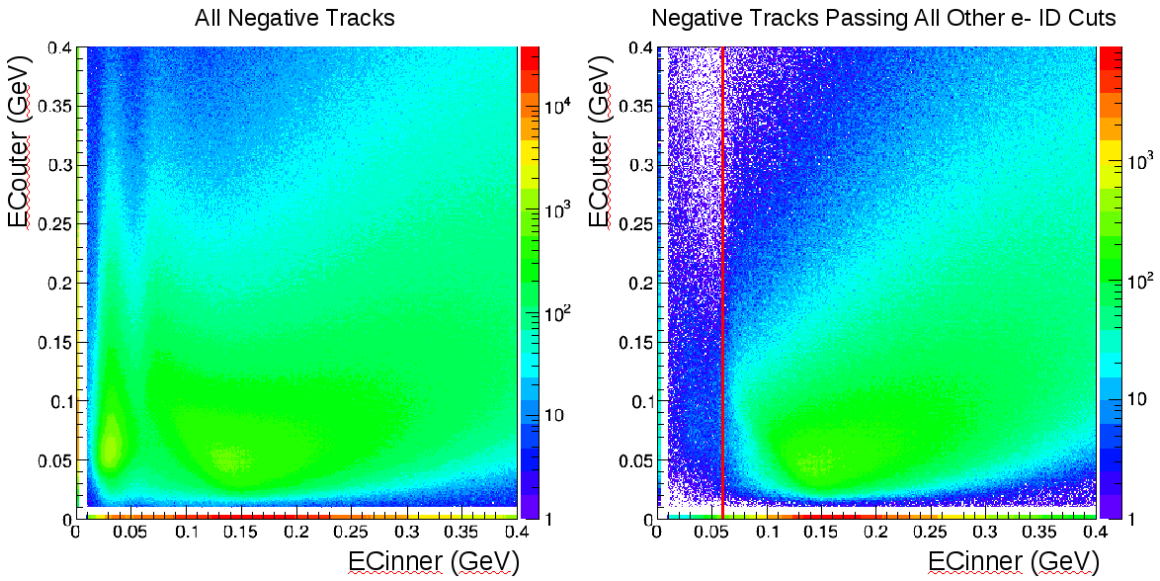

Fig. 3.6: outer EC energy vs inner EC energy plots for (left) all negative tracks and (right) negative tracks passing all other electron ID cuts. Tracks with and inner EC energy greater than 0.06 GeV pass this cut (shown by the red line in the plot on the right).

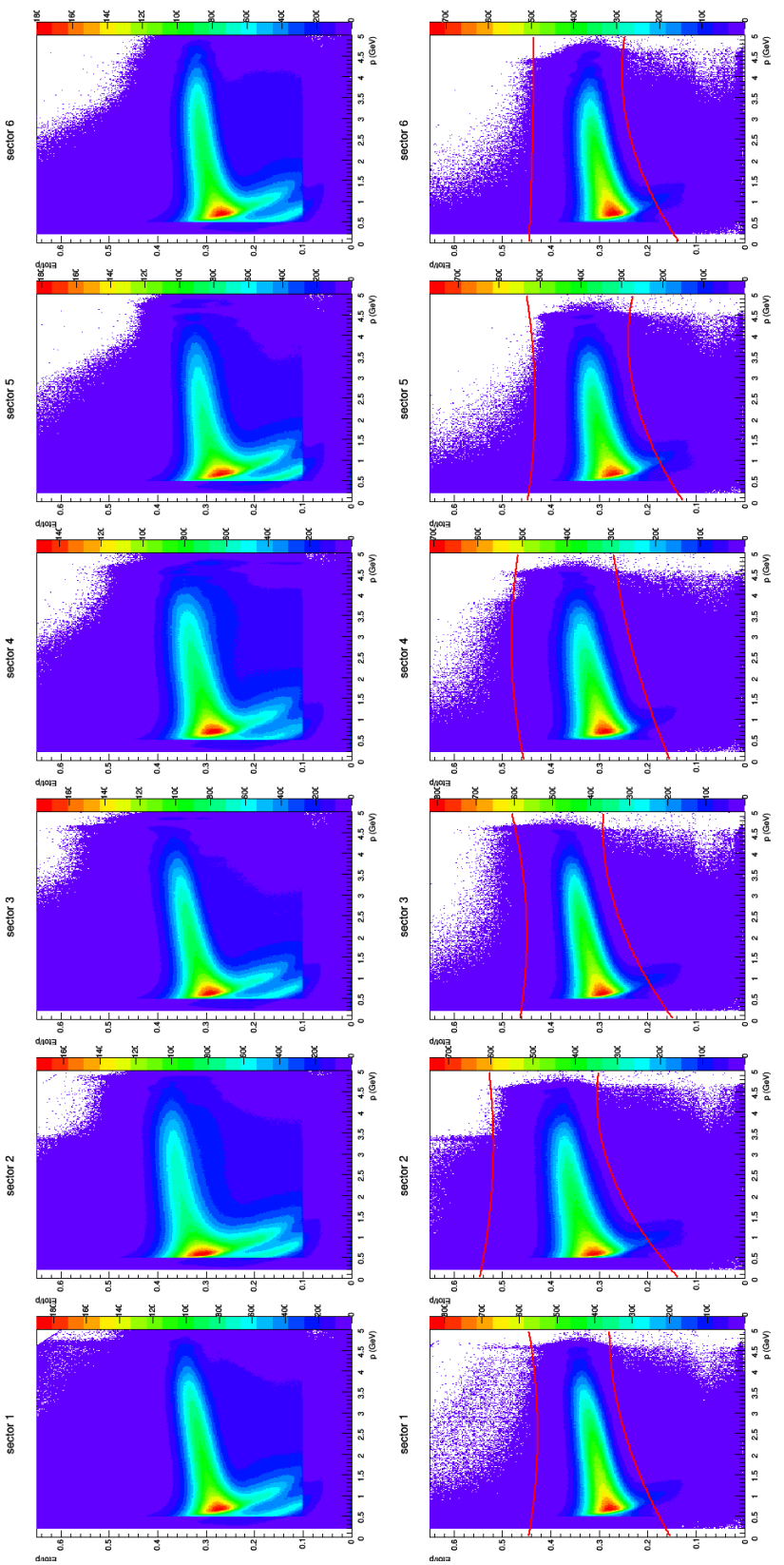

Fig. 3.7: The energy deposited in the EC divided by momentum as a function of momentum for electron candidates for each of the six CLAS sectors. The top row shows all negative tracks and the bottom row shows the tracks passing all other electron ID cuts with this cut shown in red.

3.3.6 EC Geometric Cut

When a particle deposits its energy in the EC a "shower" is created. If this shower occurs close to the edge of one of the EC triangles only a fraction of the particle's energy is reconstructed. Since energy information about these particles is unreliable they are cut via a geometric cut on the EC (see figure 3.8).

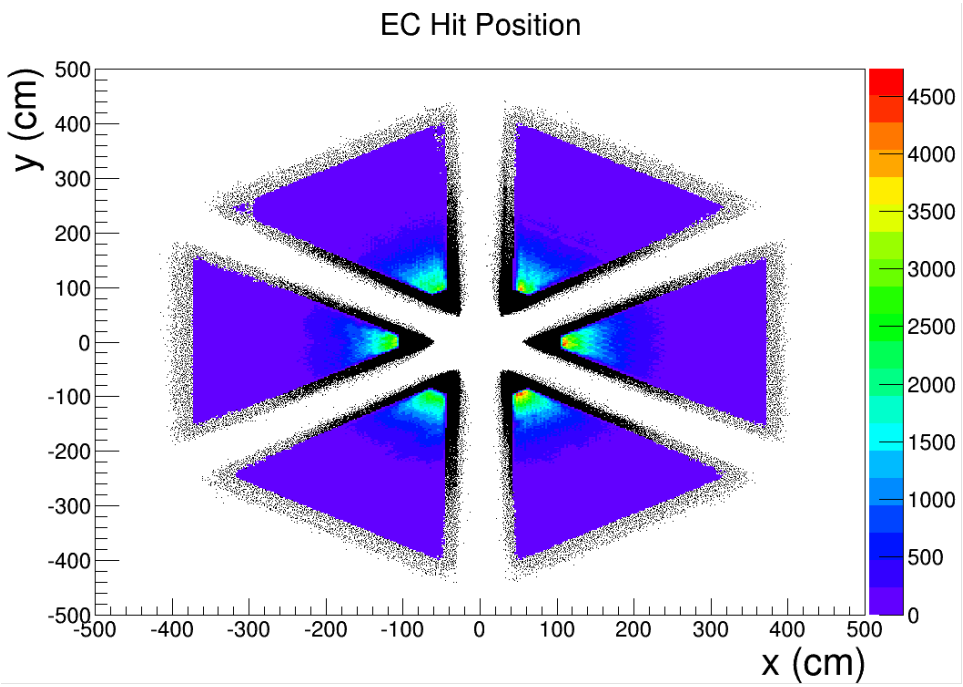

Fig. 3.8: The distribution of hits in the EC. The black points show the hit positions for all negative tracks and the colored points show the hit positions for the final electron sample. It can clearly be seen that tracks hitting near any of the edges have been removed.

3.3.7 Region 1 Fiducial Cut

A geometric fiducial cut is applied to X-Y position of tracks in region 1 of the DC. The cut is shown with red lines in figure 3.9. The lines are symmetric about Y=0, form a 60° angle, and intersect at X=22 cm.

3.3.8 Region 3 Fiducial Cut

A geometric fiducial cut is applied to X-Y position of tracks in region 3 of the DC. The cut is shown with red lines in figure 3.10. The lines are symmetric about Y=0, form a 49° angle, and intersect at X=83 cm.

3.3.9 z Vertex Correction and Cut

A cut is made on the z vertex to remove candidates that do not originate from the target. The efficacy of the cut can be improved by first applying a vertex correction. During reconstruction, a vertex (x, y, z) is calculated for each charged track based on the intersection of the track with the midplane of the corresponding sector. The midplane of a sector is the plane that divides the sector in half and contains the supposed beamline $(0, 0, z)$. However, during the E1-f experiment the beam was not centered at $(x, y) = (0, 0)$, therefore a correction to the z vertex is applied. Figure 3.11 shows the (x, y) offset of the beam; events in this plot were selected from the aluminium foil located downstream from the target to fix the z position. The calculated value for the beam position is $(x, y) =$

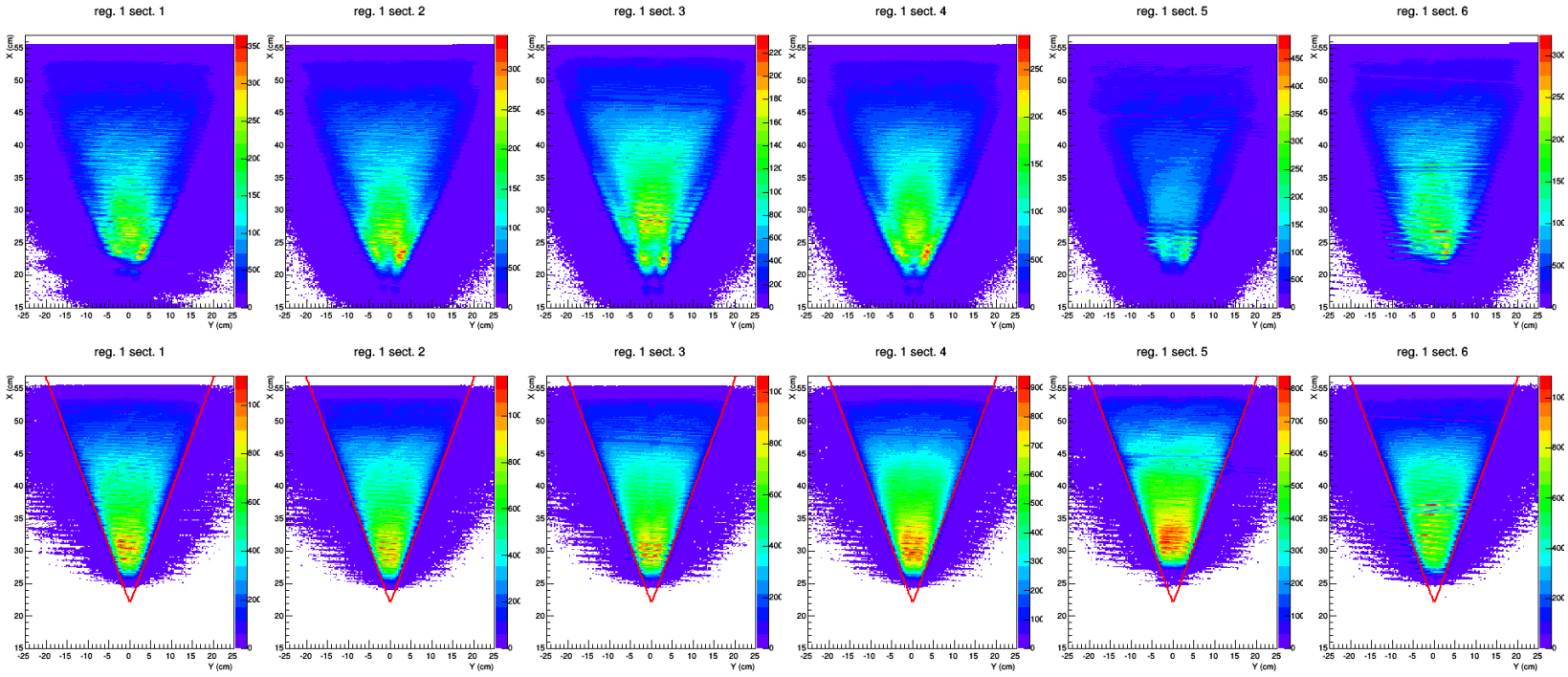

Fig. 3.9: The X vs Y position of tracks in region 1 of the DC for each sector. The top row shows results for all negative tracks and the bottom row shows results with all the other electron ID cuts applied. The cut applied here is shown with red lines.

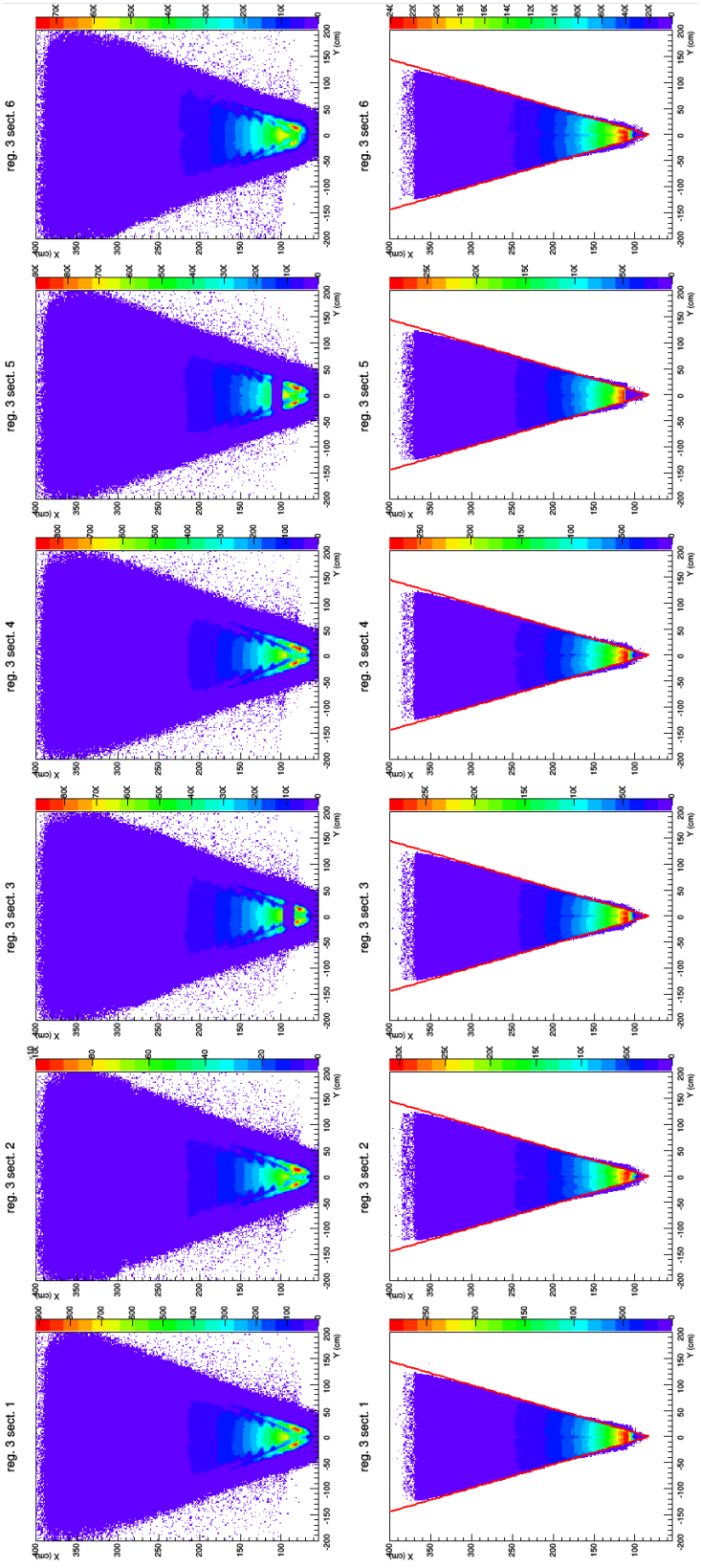

Fig. 3.10: The X vs Y position of tracks in region 3 of the DC for each sector. The top row shows results for all negative tracks and the bottom row shows results with all the other electron ID cuts applied. The cut applied here is shown with red lines.

$(0.15cm, -0.25cm)$.

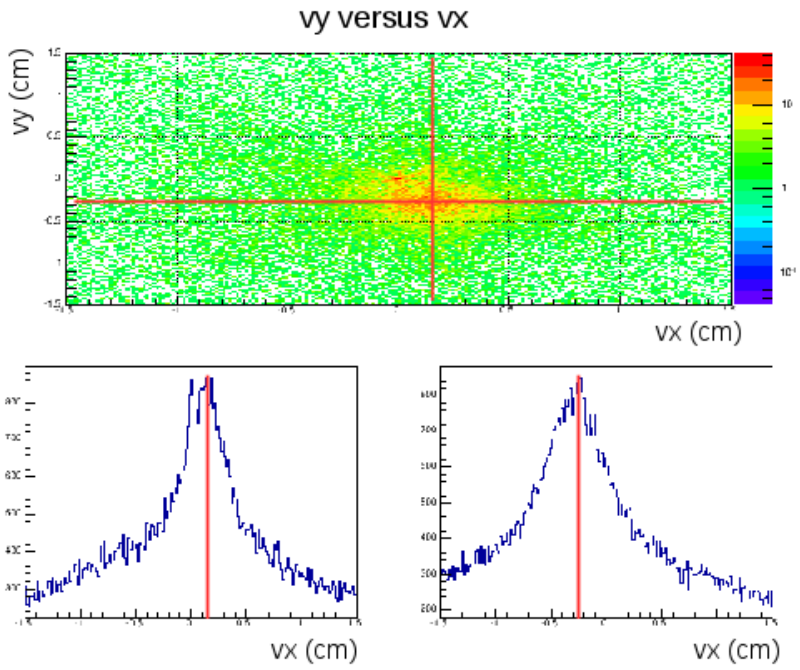

Fig. 3.11: Top: y vs x beam position for the E1-f run. Bottom left: x beam position for the E1-f run. Bottom right: y beam position for the E1-f run. The beam position is located at $x = 0.15cm, y = -0.25cm$ which is indicated by the red lines.

The z vertex is corrected by recalculating the intersection of the tracks with the midplanes after shifting the midplanes so that they contain the correct beam-line $(0.15, -0.25, z)$. The z vertex for electron candidates is plotted in figure 3.12 before and after applying the correction.

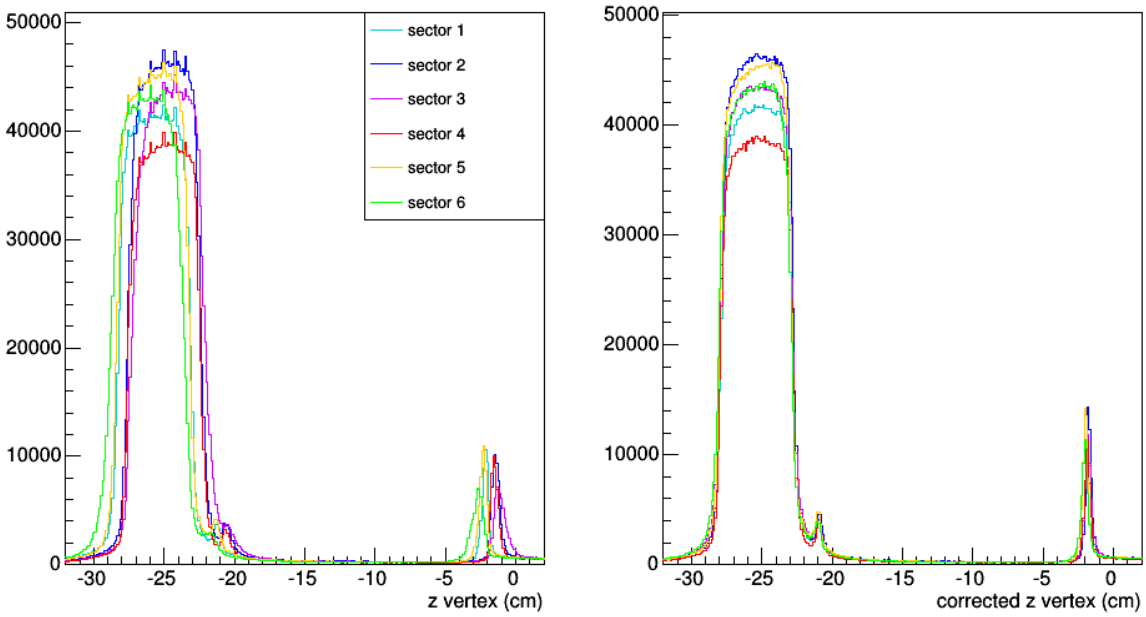

Fig. 3.12: Left: The z vertex for electron candidates for each sector. Right: The corrected z vertex for electron candidates for each sector. The two peaks near $-21cm$ and $-2cm$ are from aluminium foils placed there as reference points.

The E1-f experiment was designed to have a $5cm$ long target centered at $z = -25cm$. To have an even more precise location of the target, empty target runs are used to identify the positions of the target cell's entry and exit window (see figure 3.13). The target cell's entry window was measured to be at $z = -27.7302cm$ and the exit window was measured to be at $z = -22.6864cm$; these values are used for the electron z vertex cut, which is shown in figure 3.14.

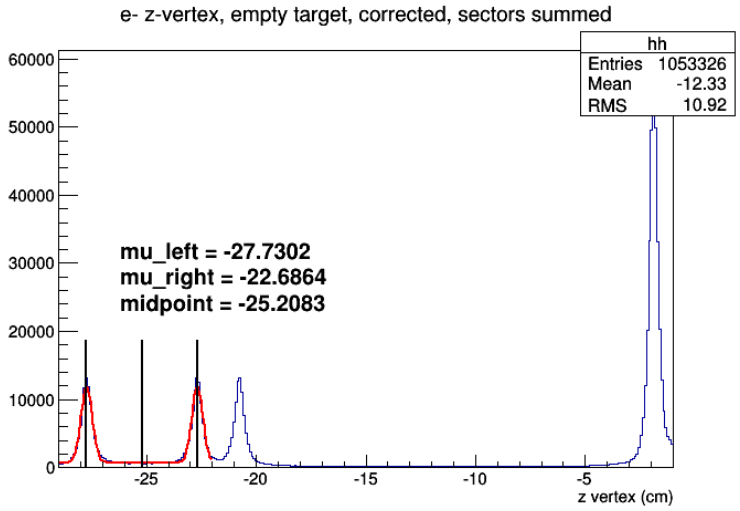

Fig. 3.13: The electron z vertex distribution for empty target runs. This data is used to identify the precise location of the target cell's entry and exit window. The two peaks near $-21cm$ and $-2cm$ are from aluminium foils placed there as reference points.

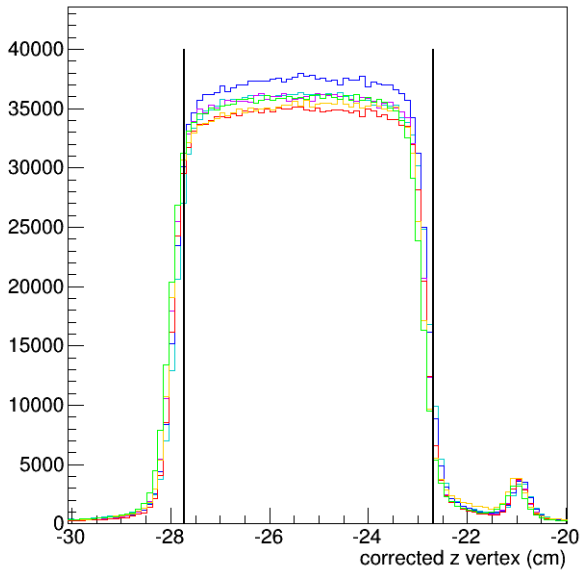

Fig. 3.14: The corrected z vertex distribution for electrons candidates passing all the other electron ID cuts with this cut shown by black vertical lines. The peak near $-21cm$ is from an aluminium foil placed there as a reference point.

3.4 Hadron Identification

3.4.1 π^+ Identification

Positive pions are identified by selecting positive tracks that pass a momentum and sector dependent β cut (where $\beta = v/c$). Additionally, a geometric fiducial cut is applied to region 1 of the DC. A missing mass cut is also applied. Traditionally, missing mass cuts are used for selecting particular kinematic regions, not for particle ID. However, in this situation a missing mass cut significantly improved π^+/proton separation, and since SIDIS event selection requires a missing mass cut anyway, this cut is applied at the particle ID stage.

π^+ Missing Mass Cut

In pion SIDIS events ($ep \rightarrow e\pi X$), the missing mass (M_X) is defined as the invariant mass of the undetected state X. That is, if p, q, and π are the 4-momenta of the initial state proton, the virtual photon, and the detected pion, respectively, then

$$M_X^2 = (p + q - \pi)^2 . \tag{3.1}$$

To calculate this the pion mass is assumed for the candidate pion. Figure 3.15 shows the M_X distribution for candidate $ep \rightarrow e\pi^+ X$ events. Events with $M_X <$ 1.35 GeV are cut. This cut helps to remove proton contamination at high momenta, which can be seen in figure 3.16 and also cuts out exclusive events ($ep \rightarrow$

$e\pi^+n$, the peak near the nucleon mass (0.938 GeV) in figure 3.15) and the delta resonance (the peak near 1.2 GeV in figure 3.15), both of which are not desirable for a SIDIS sample anyway.

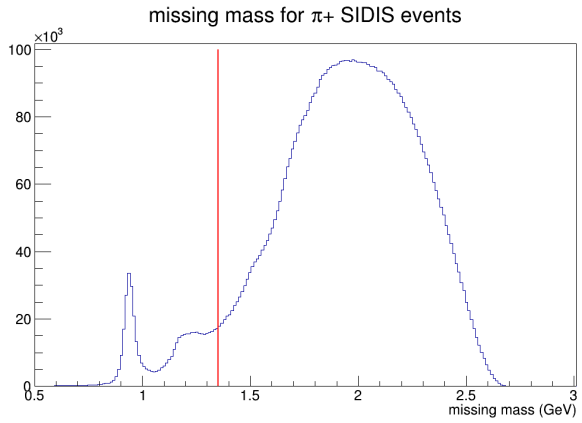

Fig. 3.15: The missing mass distribution for $ep \rightarrow e\pi^+X$ events. The vertical red line shows the cut of 1.35 GeV. Events to the left of this line are removed from the sample.

$\pi^+\beta$ Cut

β is calculated by simply dividing the track's path length by its time of flight and then dividing this quantity by the speed of light. To select positive pions, β for positive tracks is plotted in 70 bins of momentum from 0.2 to 3.75 GeV (with the missing mass cut applied). The pion peak for each bin is then fit with a gaussian. At low momenta, a 3σ cut is used, while at higher momenta a tighter cut, which was estimated by eye, is used. The tightening of the cut at higher momenta is clearly necessary to reduce proton contamination. This is shown (for electron

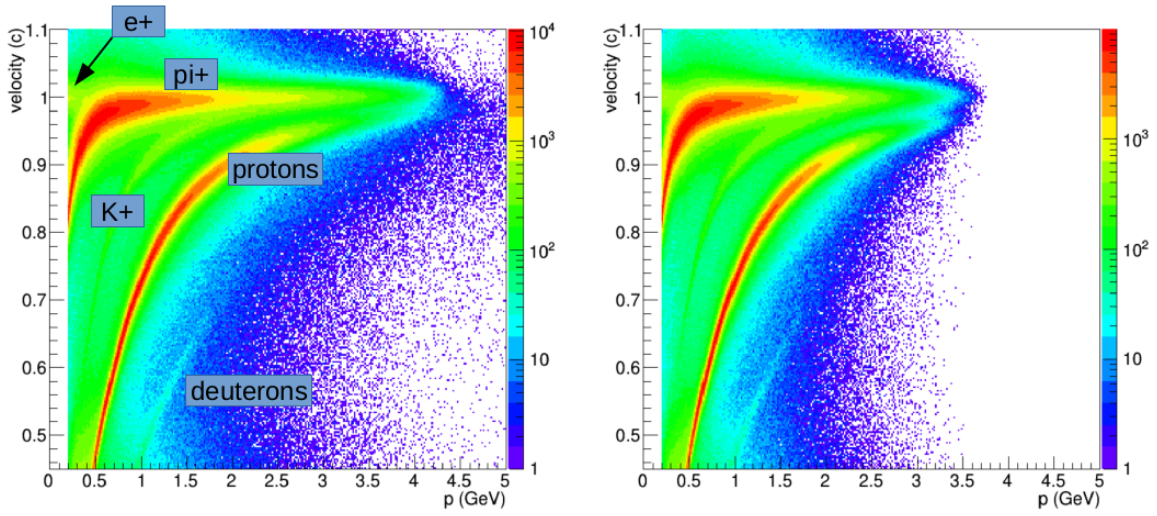

Fig. 3.16: β vs momentum distribution for positive tracks before (left) and after (right) the missing mass cut. The cut removes most tracks above 3.5 GeV, making π^+/proton separation easier. SIDIS samples require a missing mass cut anyway, so it makes sense to apply it here at the particle ID stage.

sector 4) in figure 3.17 - the top left plot is the lowest momentum bin and the bottom right plot highest momentum bin, the red curves show the gaussian fits, the vertical black lines show $\mu \pm 3\sigma$, and the vertical red lines show the actual cut. The two dimensional view of this cut is shown in figure 3.18.

π^+ Fiducial Cut

To improve the data quality, a geometric fiducial cut is applied to region 1 of the DC. The cut is shown with red lines in figure 3.19. The lines are symmetric and form a 60° angle and intersect at $(0, 10)$ cm.

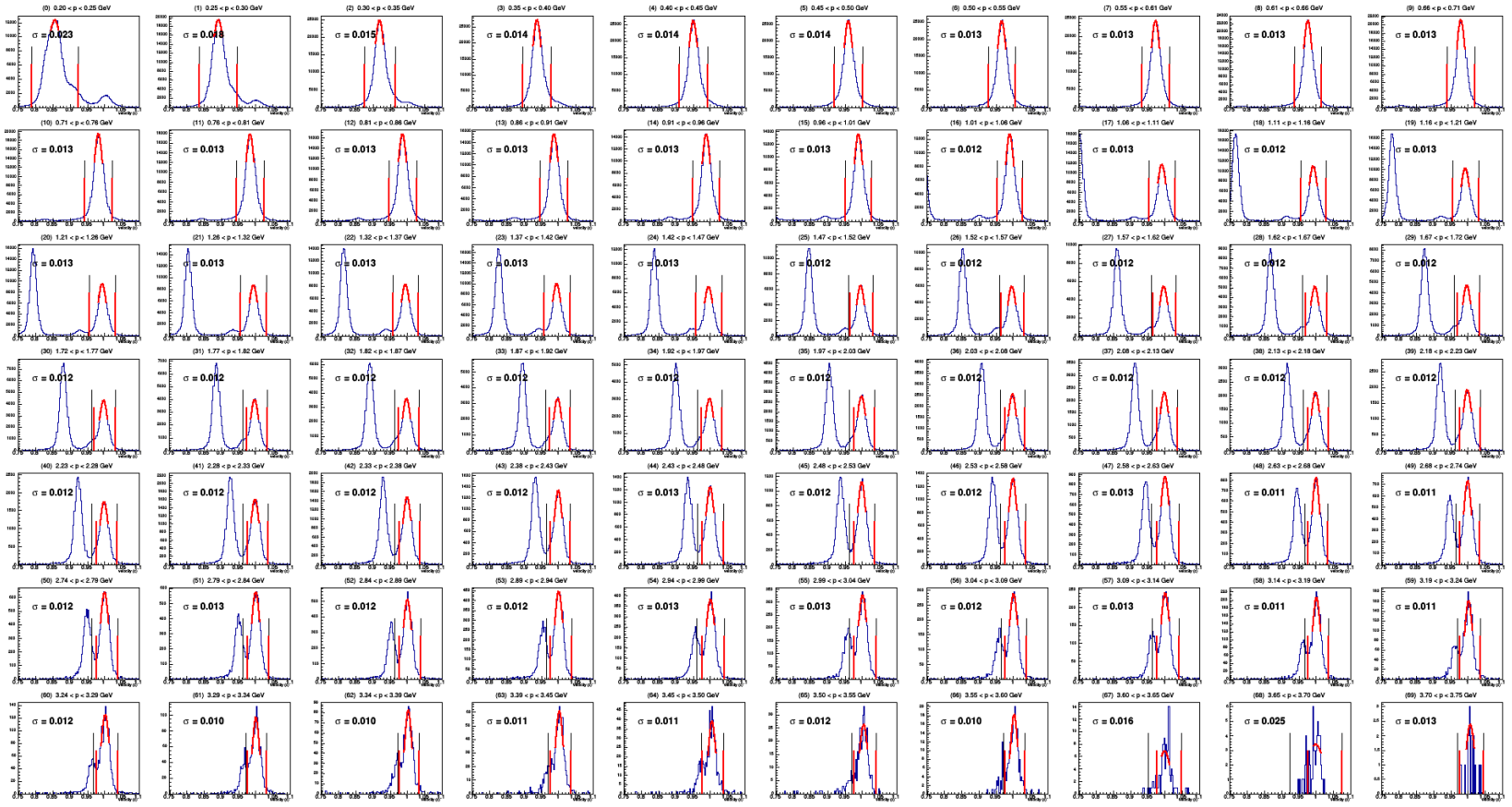

Fig. 3.17: β for positive tracks in bins of momentum when the electron is in sector 4. The top left plot is the lowest momentum bin and the bottom right plot highest momentum bin, the red curves show the gaussian fits, the vertical black lines show $\mu \pm 3\sigma$, and the vertical red lines show the actual cut.

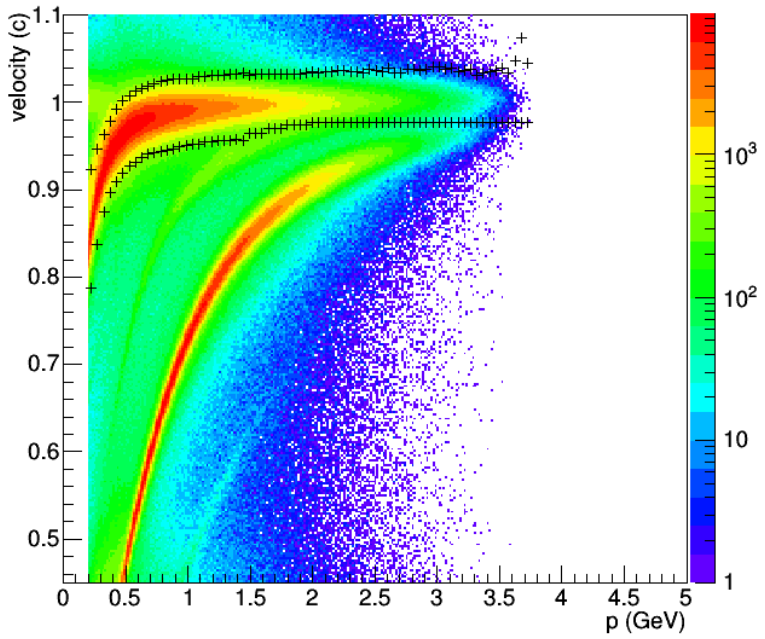

Fig. 3.18: The two dimensional view of the π^+ β cut. The black crosses show the upper and lower cut for each of the 70 momentum bins.

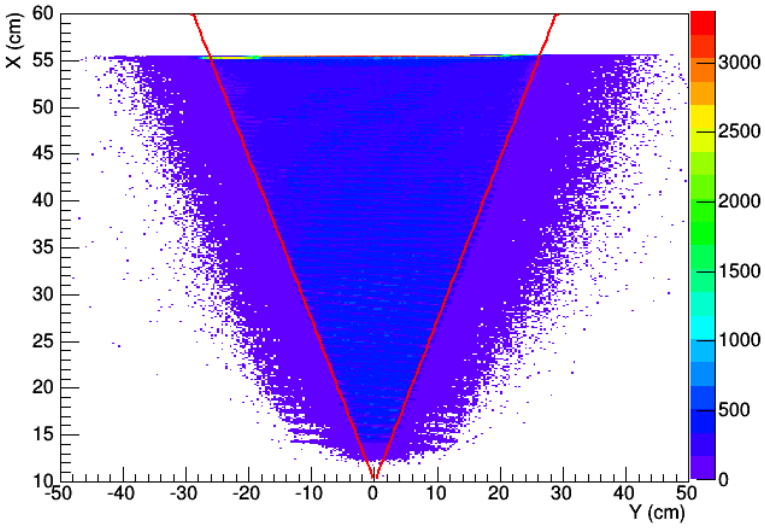

Fig. 3.19: X vs Y in region 1 of the DC for positive tracks. Events inside of the red lines are kept.

3.4.2 π^- Identification

Negative tracks that are not identified as electrons become π^- candidates. Negative pions are then selected using cuts very similar to the π^+ ID.

π^- Missing Mass Cut

Although the π^- channel does not have proton (or anti-proton) contamination, a missing mass cut of 1.35 GeV is applied here as well for consistency. Figure 3.20 shows this cut.

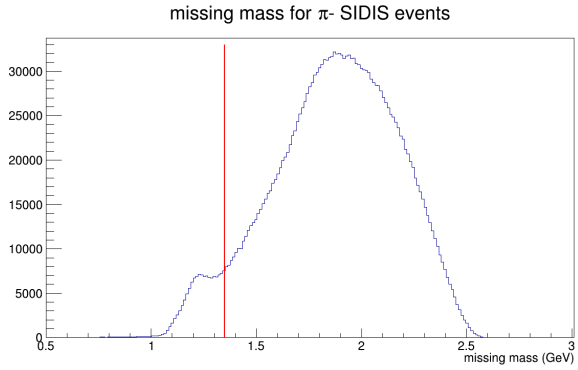

Fig. 3.20: The missing mass distribution for $ep \rightarrow e\pi^- X$ events. The vertical red line shows the cut of 1.35 GeV. Events to the left of this line are removed from the sample.

$\pi^-\beta$ Cut

The π^- β cut is done in exactly the same way as π^+ β cut. The results can be seen in figures 3.21 and 3.22.

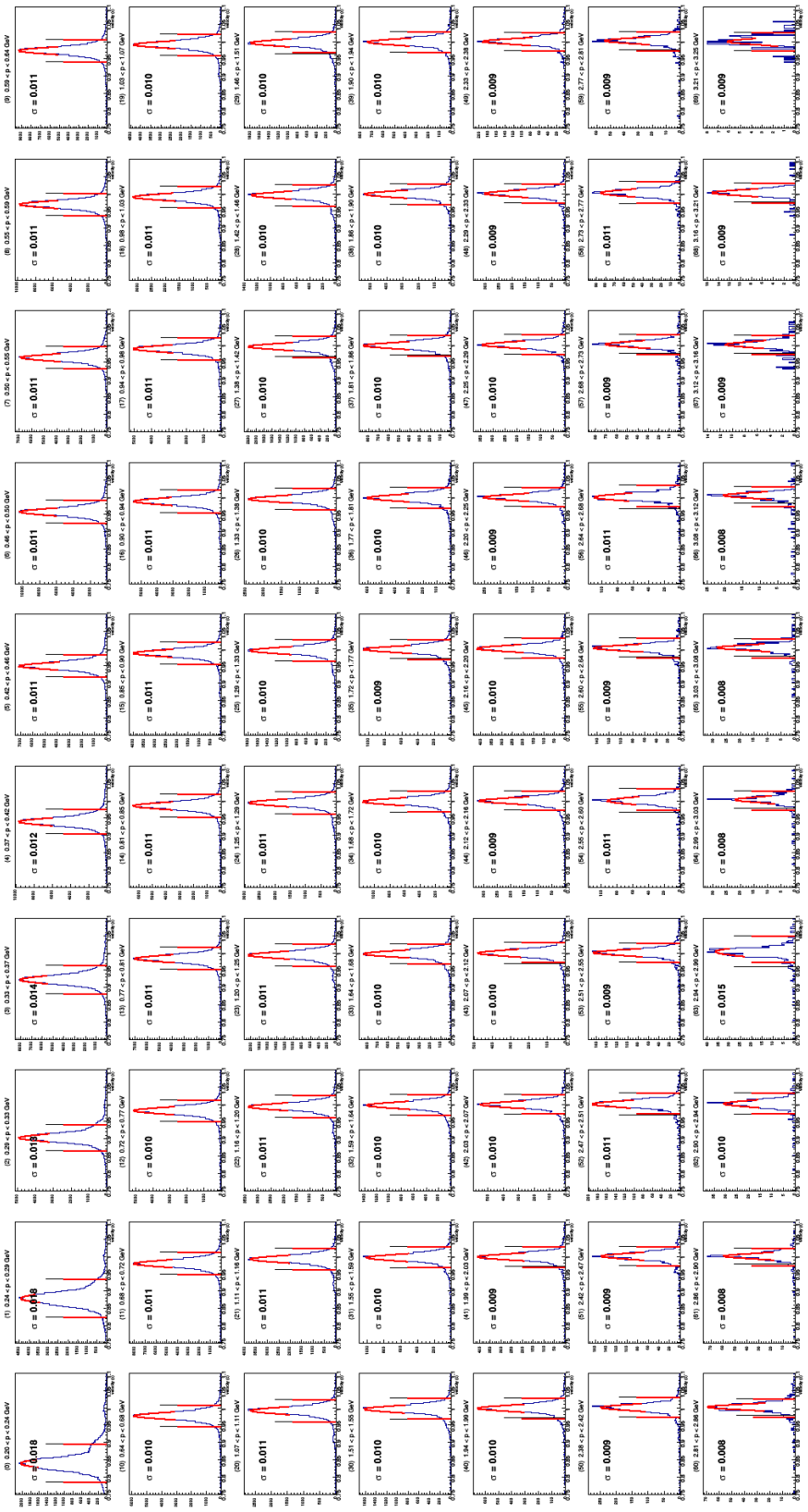

Fig. 3.21: β for negative tracks in bins of momentum when the electron is in sector 3. The top left plot is the lowest momentum bin and the bottom right plot highest momentum bin, the red curves show the gaussian fits, the vertical black lines show $\mu \pm 3\sigma$, and the vertical red lines show the actual cut.

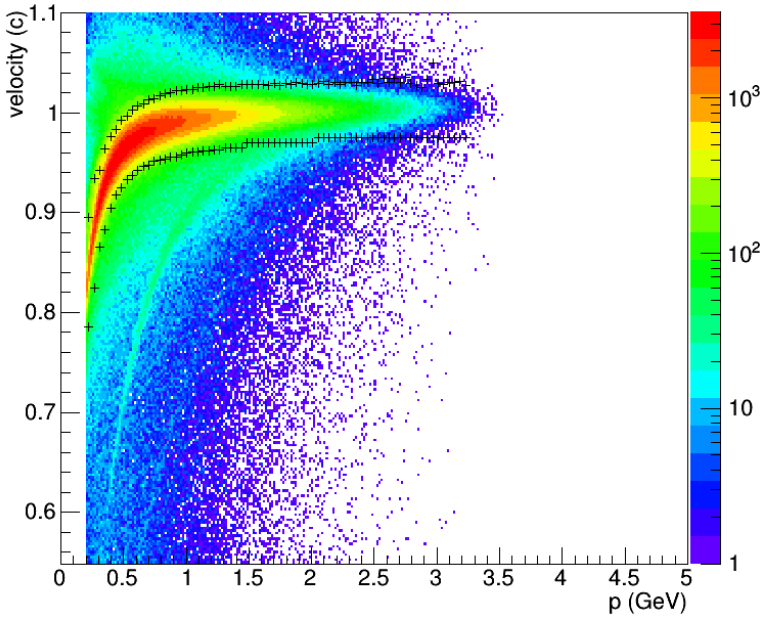

Fig. 3.22: The two dimensional view of the π^- β cut. The black crosses show the upper and lower cut for each of the 70 momentum bins.

π^- Fiducial Cut

To improve the data quality, a geometric fiducial cut is applied to region 1 of the DC. The cut is shown with red lines in figure 3.23. The diagonal lines are symmetric and form an 80° angle and intersect at $(0, 20)$ cm. The horizontal line is at X = 24 cm.

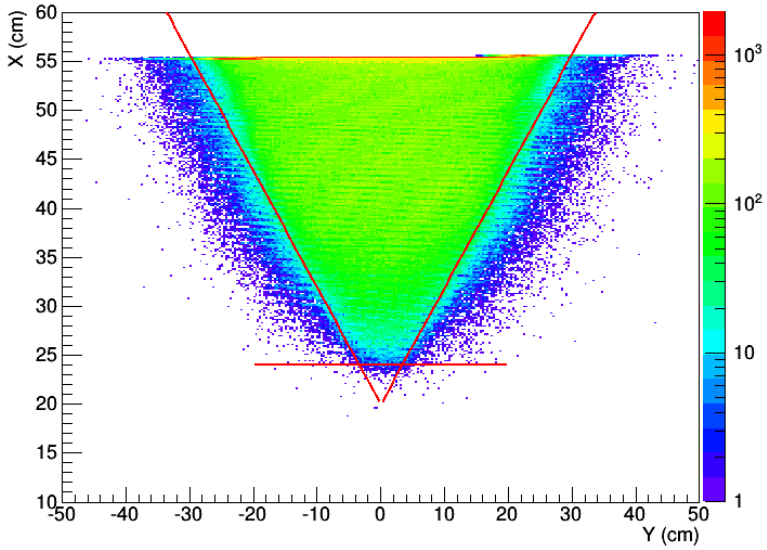

Fig. 3.23: X vs Y in region 1 of the DC for negative tracks. Events inside of the red lines are kept.

3.5 Momentum Corrections

The CLAS detector may have some small misalignments and imperfections in the magnetic field that can cause a particle's reconstructed momentum to be slightly off. This effect can be corrected by studying well known processes, such as elastic events ($ep \rightarrow ep$), Bethe-Heitler events ($ep \rightarrow ep\gamma$), and exclusive events such as $ep \rightarrow e\pi^+ n$. The correction functions used for this analysis were developed by Marco Mirazita [36]. The following subsections show results with and without the corrections to demonstrate their efficacy.

3.5.1 Electron Momentum Corrections

A first step in checking the efficacy of electron momentum corrections is to look at the missing mass distribution of $ep \rightarrow eX$ events near the proton mass, which are elastic events (missing mass is the same as W in this context). As seen in figures 3.24 and 3.25, the momentum corrections produce an improvement in the mean value (bringing it closer to the proton mass) and in the width (making it narrower) of the elastic peak. When W is plotted as a function of $\phi_{e^-}^{lab}$, a visible improvement in the symmetry of the distribution is present (see figures 3.26 and 3.27).

Although the momentum corrections produce an improvement in the W distributions of elastic events, the overlap in phase space coverage between elastic events and SIDIS events is small. In order to have greater confidence in the

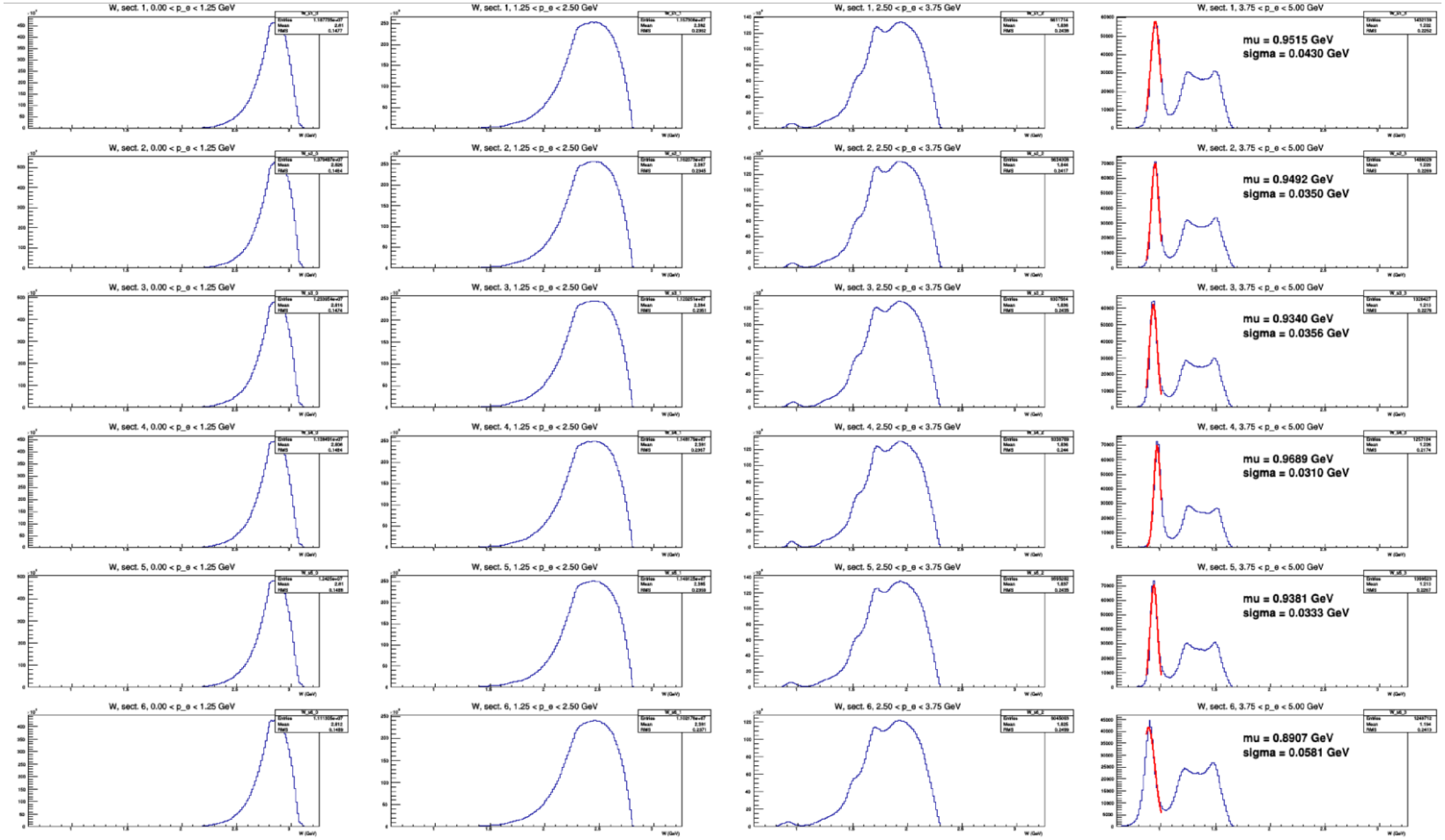

Fig. 3.24: Plots of W for $ep \rightarrow eX$ events without momentum corrections. The top row is sector 1, the second row is sector 2, etc. The columns are bins of electron momentum (4 bins from 0 - 5 GeV). The elastic peak becomes visible at higher momenta and is fit with a Gaussian.

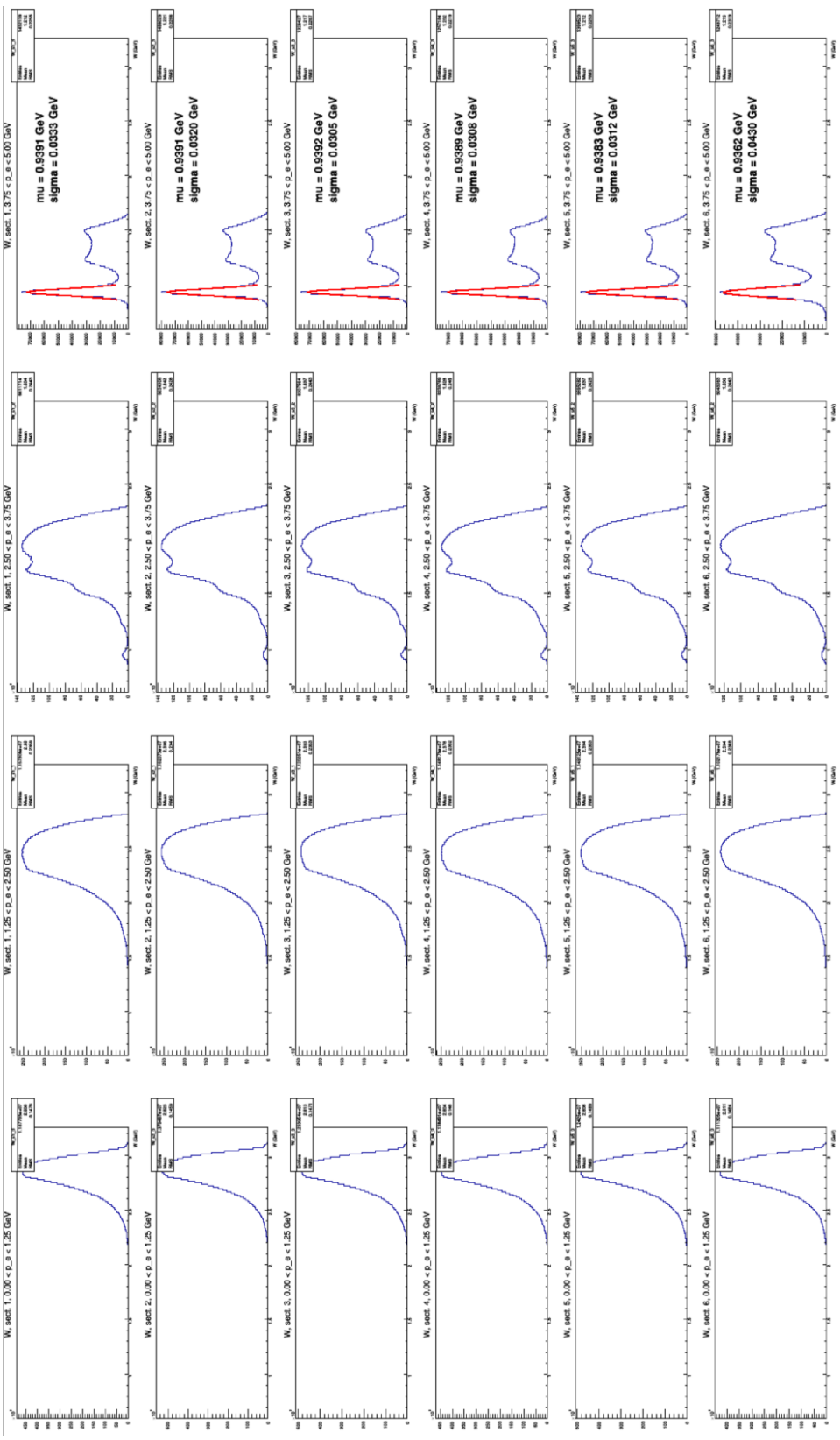

Fig. 3.25: The same plots as in figure 3.24 but with momentum corrections. The mean value (mu) and width (sigma) are both improved for each sector.

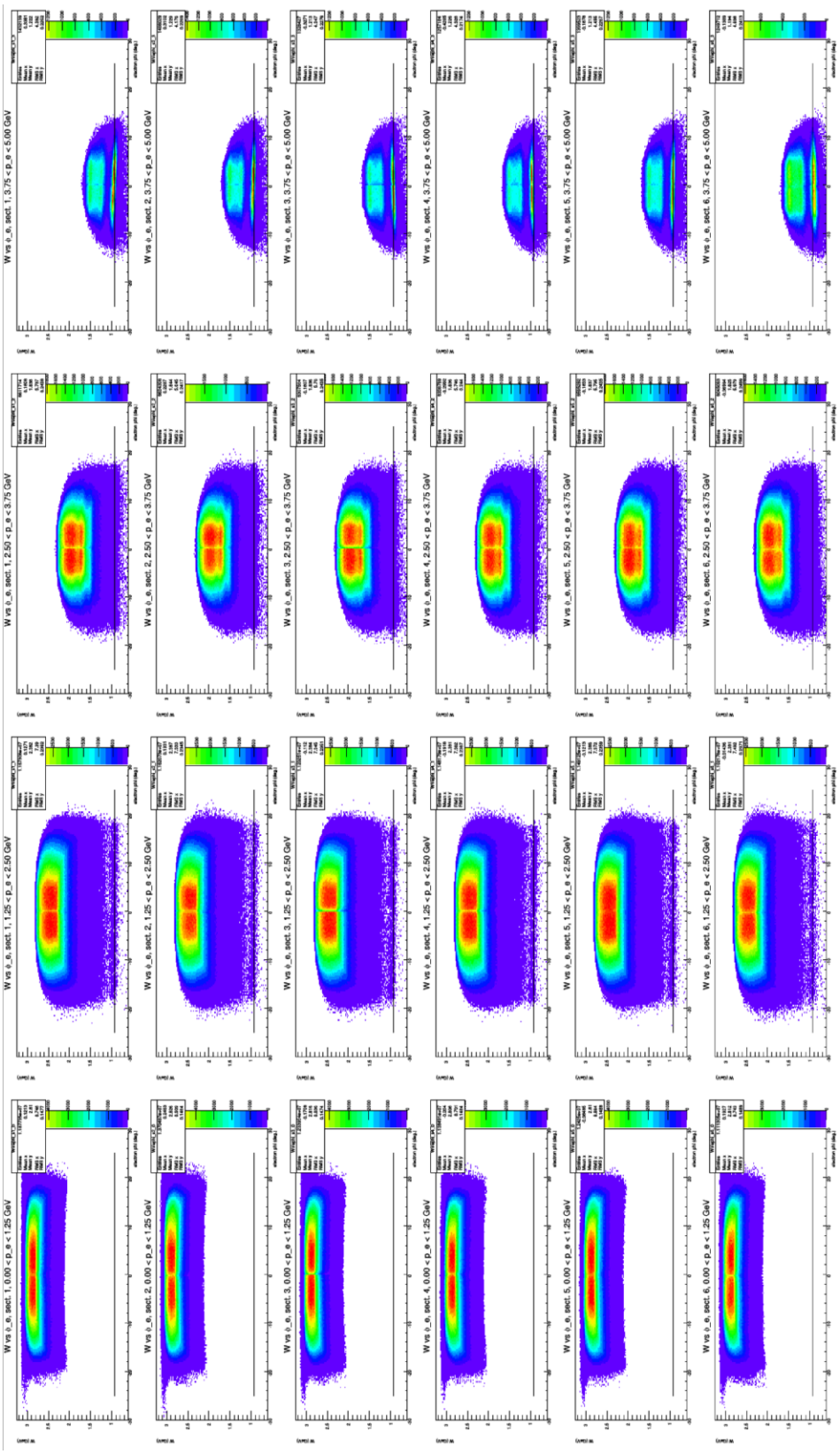

Fig. 3.26: Plots of W vs $\phi_{e^-}^{lab}$ (relative to the center of the sector) for $ep \to eX$ events without momentum corrections. The top row is sector 1, the second row is sector 2, etc. The columns are bins of electron momentum (4 bins from 0 - 5 GeV). The elastic peak becomes visible at higher momenta, the black horizontal line shows the location of the proton mass.

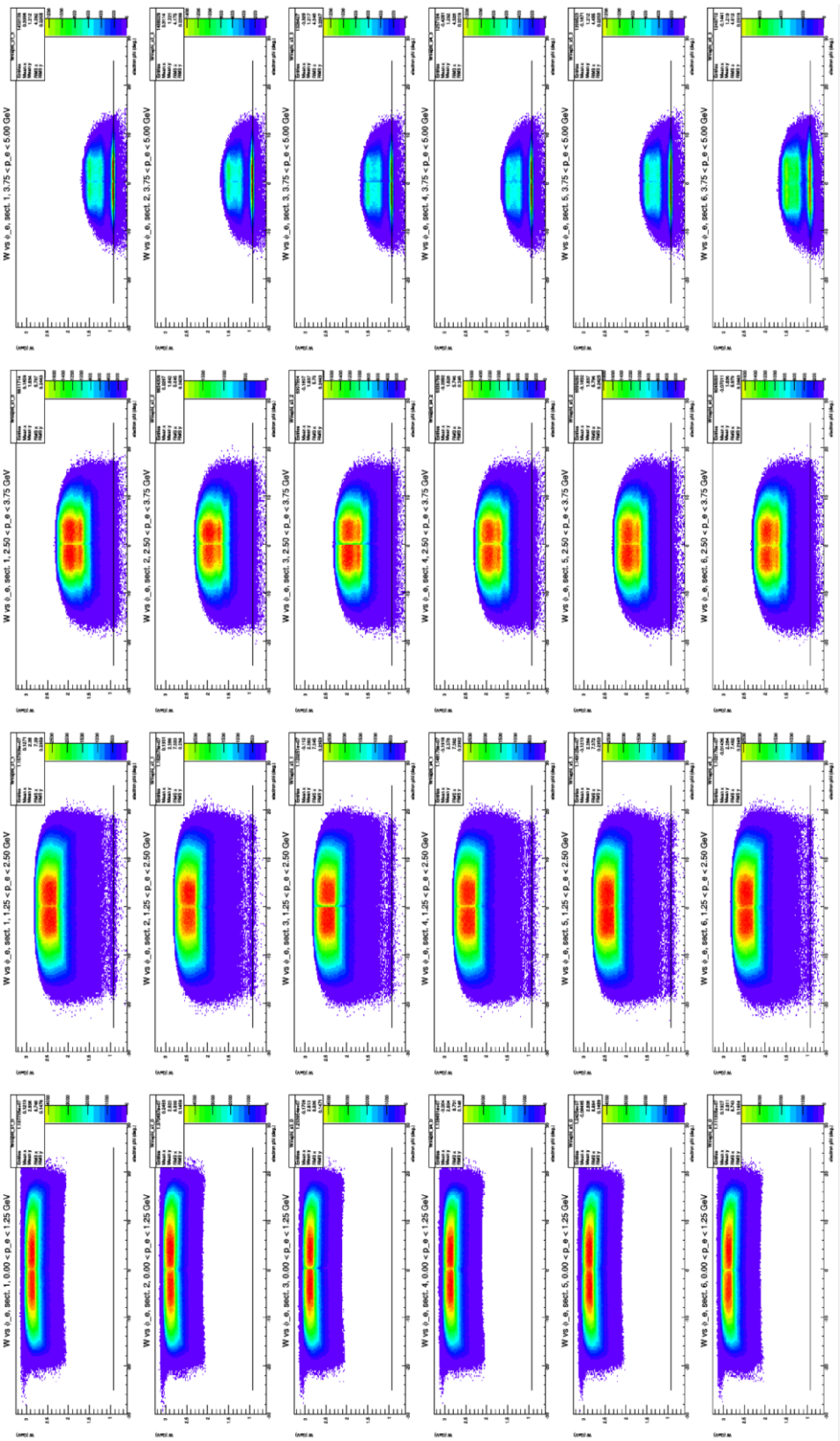

Fig. 3.27: The same plots as in figure 3.26 but with momentum corrections. The symmetry of the distribution is improved for each sector.

momentum corrections, a process with a phase space coverage similar to that of SIDIS events must be studied. This is done using Bethe-Heitler events. Bethe-Heitler events are selected using the following criteria: an electron and a proton must be reconstructed, the missing mass squared must be near zero (the photon mass), and the direction of X must be close to either the incoming or outgoing electron direction (since the radiated photon tends to travel in a direction close to that of the electron which radiated it, as shown in figure 3.28). Since we are looking for events with a phase space coverage similar to that of SIDIS, the additional requirement $W > 2GeV$ is also added.

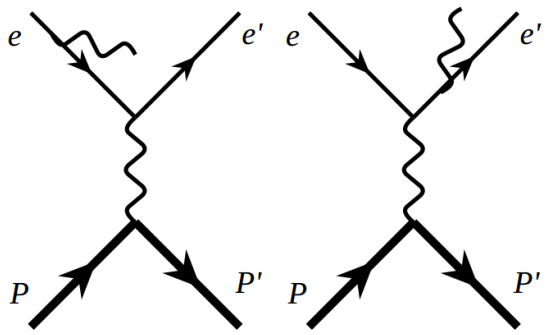

Fig. 3.28: Left: Pre-radiated Bethe-Heitler process. Right: Post-radiative Bethe-Heitler process. The radiated photon tends to travel in a direction close to that of the electron which radiated it.

Figure 3.29 shows the missing mass squared distribution for $ep \rightarrow epX$ events with $W > 2GeV$; a cut $-0.05 < M_X^2 < 0.05GeV^2$ is applied to this quantity to select Bethe-Heitler events. Furthermore, figure 3.30 shows the angle

between X and the incoming electron ($\Delta\theta_{incoming}$) (left) and the angle between X and the outgoing electron ($\Delta\theta_{outgoing}$) (right) for Bethe-Heitler candidate events. Events with $\Delta\theta_{incoming} < 0.5$ degrees or $\Delta\theta_{outgoing} < 2$ degrees are kept.

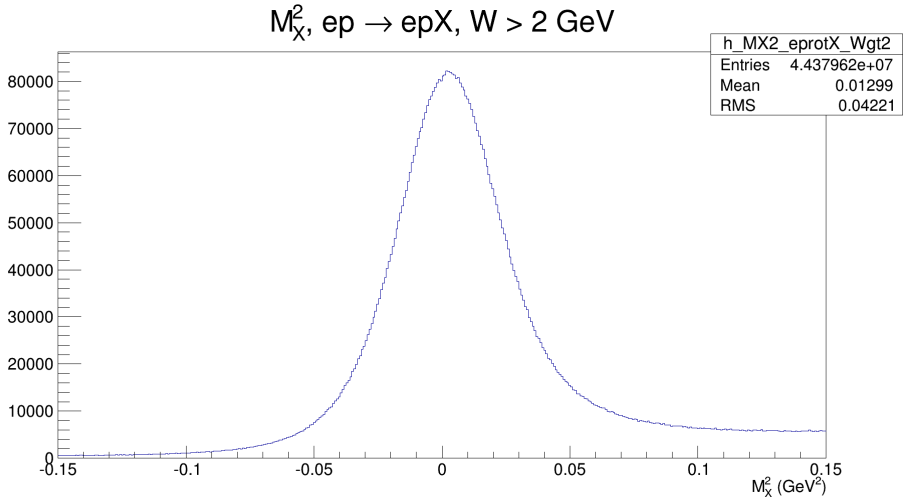

Fig. 3.29: The missing mass squared distribution for $ep \rightarrow epX$ events with $W > 2GeV$.

Returning to the missing mass squared distribution after applying the $\Delta\theta_{incoming}$ and $\Delta\theta_{outgoing}$ cuts (figure 3.31), it can be seen that the momentum corrections produce a small improvement in the peak position (bringing it closer to zero) while the width does not change significantly. Likewise, when the missing mass squared is plotted as a function of ϕ_{e-}^{lab} (relative to the center of the sector), a visible improvement is noticeable in the symmetry of the distributions after momentum corrections are applied (see figure 3.32).

The $Q^2 - x$ space for Bethe-Heitler events with $W > 2GeV$ is plotted in

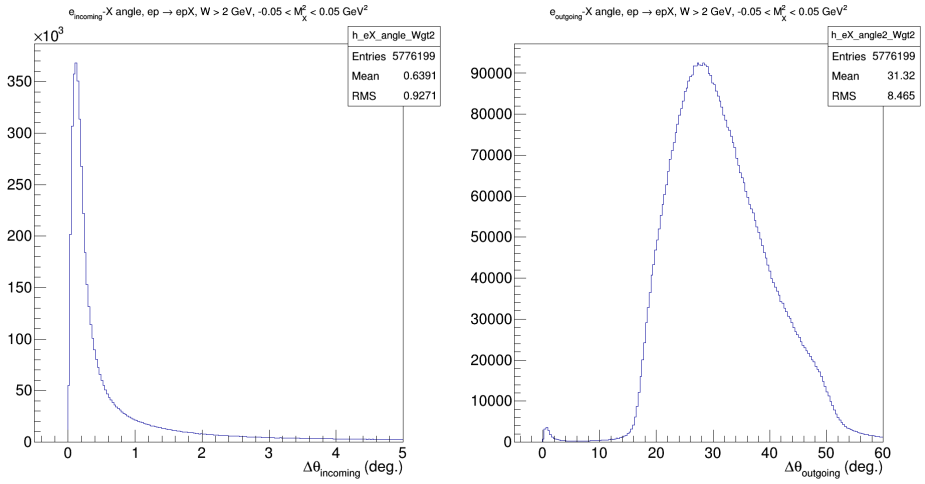

Fig. 3.30: Left: $\Delta\theta_{incoming}$ and right: $\Delta\theta_{outgoing}$ for $ep \rightarrow epX$ events with $W > 2GeV$ and $-0.05 < M_X^2 < 0.05GeV^2$.

figure 3.33 to confirm that the phase space coverage of these events is similar to that of SIDIS events.

The electron momentum correction functions studied here have been shown to improve the kinematic distributions of well know processes with similar phase space coverage as SIDIS events, making them suitable for this analysis.

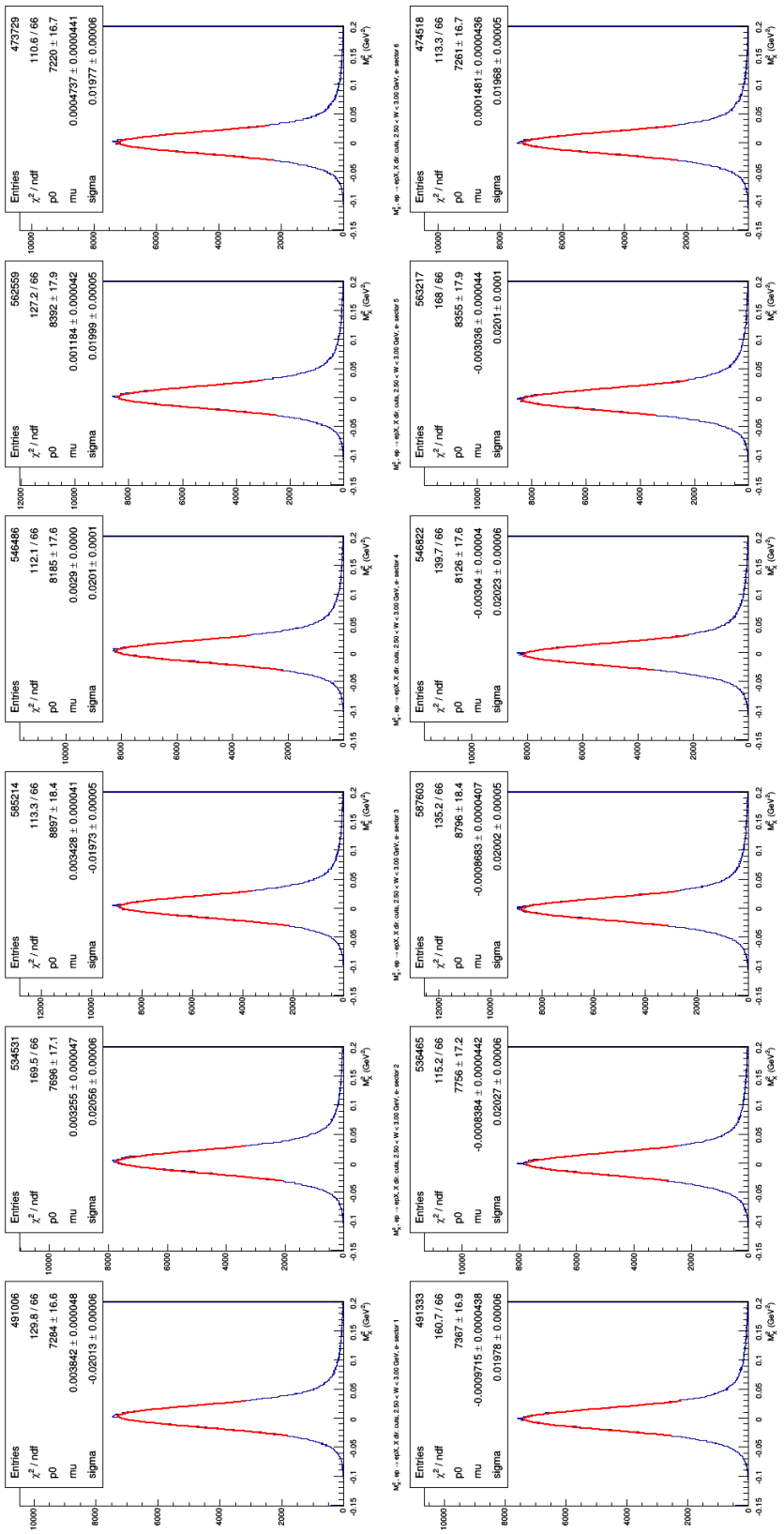

Fig. 3.31: The missing mass squared distribution for Bethe-Heitler events. The first column is for events with the electron in sector 1, second column sector 2, etc. The top row is without momentum corrections and the bottom row is with the corrections.

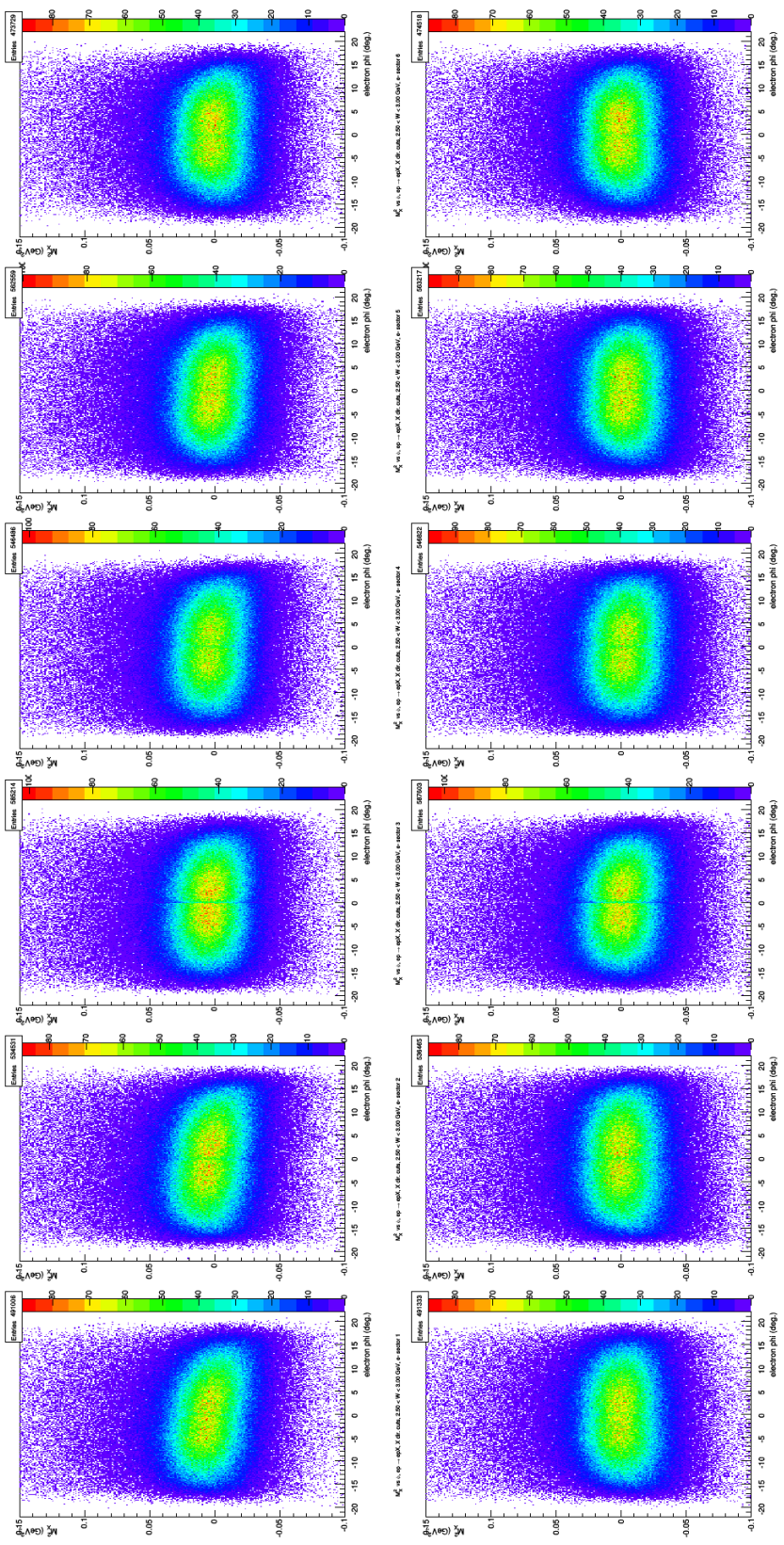

Fig. 3.32: The missing mass squared vs $\phi_{e^-}^{lab}$ (relative to the center of the sector) distribution for Bethe-Heitler events. The first column is for events with the electron in sector 1, second column sector 2, etc. The top row is without momentum corrections and the bottom row is with the corrections.

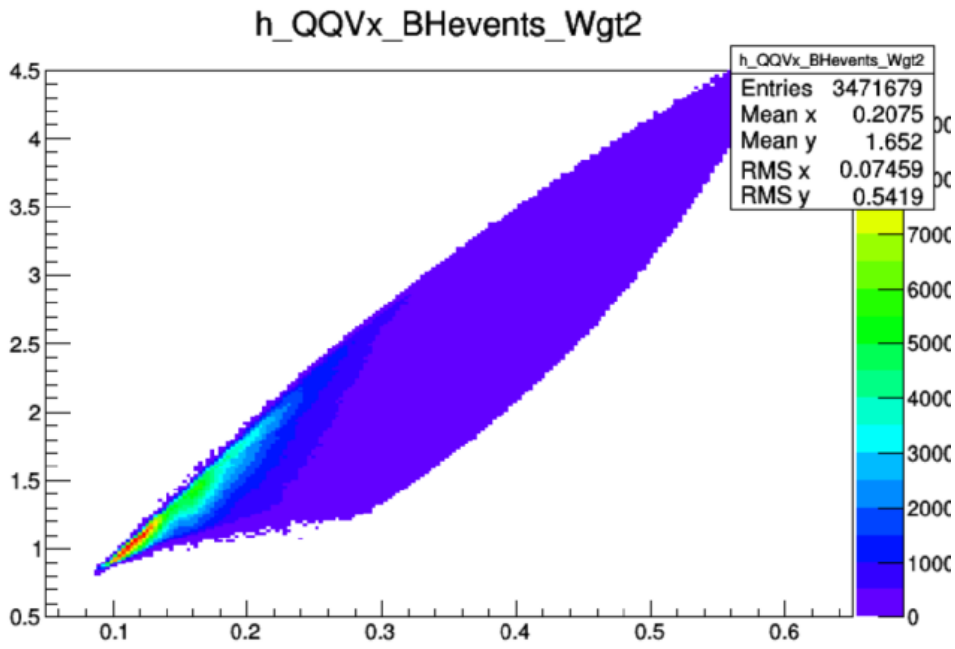

Fig. 3.33: The $Q^2 - x$ space for Bethe-Heitler events with $W > 2GeV$. This coverage is similar to that of SIDIS events which makes Bethe-Heitler events useful for studying momentum corrections in a SIDIS analysis such as this one.

3.6 Kinematic Cuts

Once $ep \to e\pi^{\pm}X$ events have been identified, kinematic cuts must be imposed to ensure that they are within the SIDIS kinematic regions. To select deeply inelastic events, events with $W < 2.05$ GeV and $Q^2 < 1.0$ GeV^2 are cut. The Q^2-W space for inclusive electron events ($ep \to eX$) is shown in figure 3.34 with the Q^2 and W cuts shown. Events with $y > 0.85$ are also cut to eliminate regions where radiative effects are large and poorly understood.

Traditionally, events with $z < 0.4$ or $z > 0.7$ are cut to eliminate target fragmentation events and exclusive events, respectively. However, the full range of z will be analyzed here. Since the results are binned in z these cuts are not necessary.

A missing mass cut has already been applied at the particle ID stage to reduce contamination (see section 3.4). No additional missing mass conditions are applied here. A constant value of M_X creates a contour in the $P_{h\perp}^2$-z space which can be seen in figure 3.35. Therefore, if a tighter M_X cut is desired, one can simply only consider $P_{h\perp}^2$-z bins below these contours.

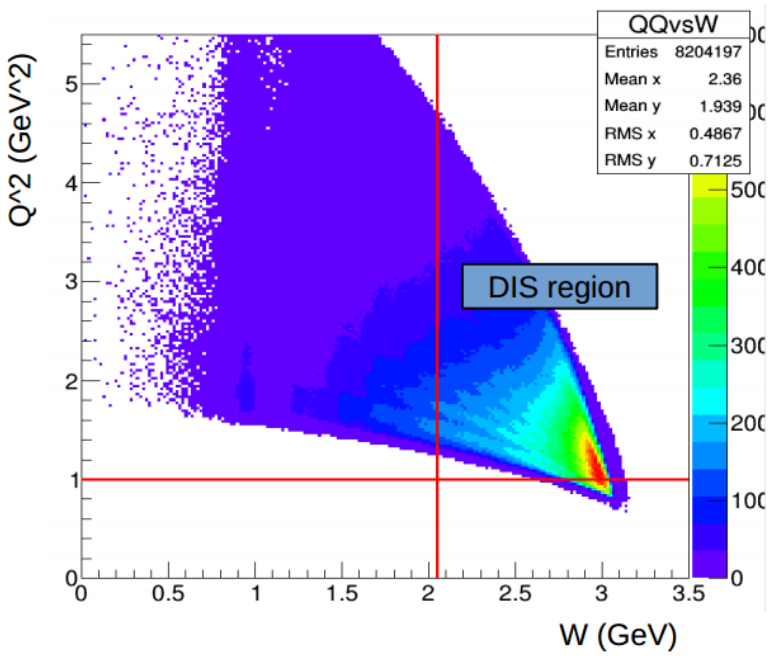

Fig. 3.34: The Q^2-W space for inclusive electron events ($ep \rightarrow eX$). $W > 2.05$ GeV and $Q^2 > 1.0$ GeV^2 define the DIS region. The cuts are shown with red lines.

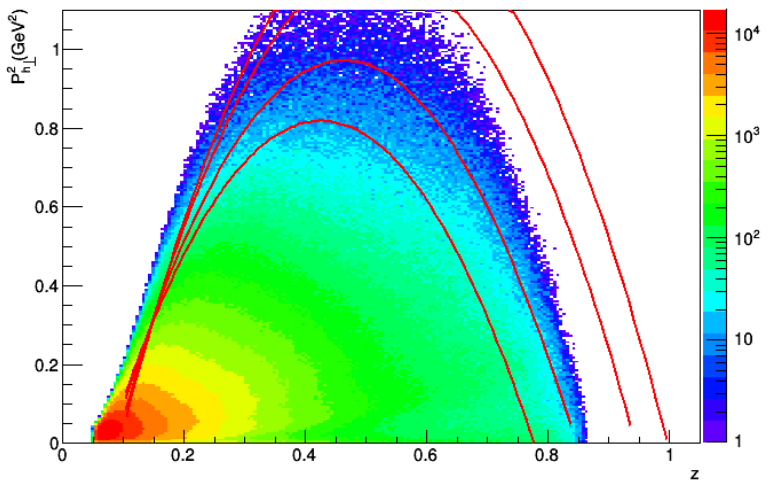

Fig. 3.35: $P_{h\perp}^2$-z space for π^+ SIDIS events for $0.1 < x < 0.2$ and $1.0 < Q^2 < 1.3$ GeV^2 with four lines of constant M_X. The M_X values, from outermost line to innermost line, are M_p, 1.1 GeV, 1.35 GeV, and 1.5 GeV.

3.7 ϕ_h Fiducial Cuts

Certain regions of x-Q^2-z-$P_{h\perp}^2$ space have limited ϕ_h coverage (due to acceptance). The "holes" in the ϕ_h distribution occur around $\phi_h = 0$ a vast majority of the time. As the edge of a hole is approached, the number of events begins to drop sharply. This "edge effect" is difficult to describe realistically with simulations (simulations and acceptance studies are discussed in chapters 4 and 5), therefore a cut is applied to eliminate these regions.

For example, figure 3.36 shows the π^+ ϕ_h distribution for $0.4 < x < 0.5$, $2.2 < Q^2 < 2.8\text{GeV}^2$, $0.35 < z < 0.4$, and $0.05 < P_{h\perp}^2 < 0.1$. It can be seen that just inside of $\pm 50^\circ$ the number of events begins to drop off to zero. In this example, events with $-50^\circ < \phi_h < 50^\circ$ are cut to eliminate the edges. Every x-Q^2-z-$P_{h\perp}^2$ bin has a different ϕ_h fiducial cut (if a cut is necessary) which was determined by eye, placing the cut at the location in ϕ_h where the distribution starts dropping off to zero.

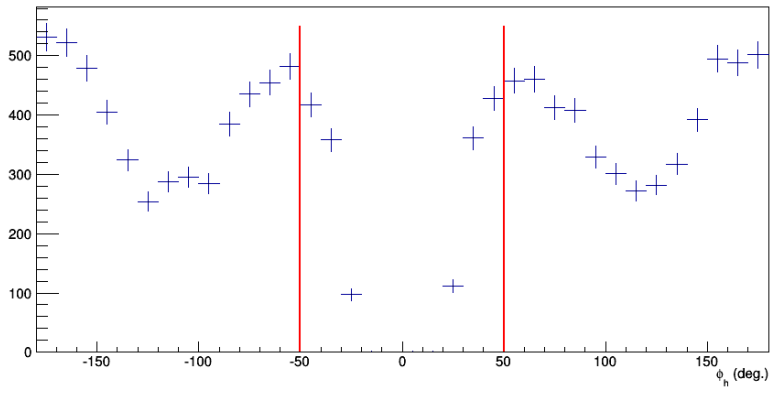

Fig. 3.36: The π^+ ϕ_h distribution for $0.4 < x < 0.5$, $2.2 < Q^2 < 2.8\text{GeV}^2$, $0.35 < z < 0.4$, and $0.05 < P_{h\perp}^2 < 0.1$. The vertical red lines show the ϕ_h fiducial cut for this particular bin; events inside of the lines are cut to eliminate edge effects.

Chapter 4

Simulation

ϕ_h distributions at CLAS are highly dependent on acceptance. Here, acceptance refers to both geometrical acceptance (the location of active detector elements) and the efficiency in the active regions. The $cos\phi_h$ and $cos2\phi_h$ moments, therefore, cannot be extracted without acceptance corrections. This is done using Monte Carlo simulations. An event generator is used to create a realistic large set of events (several iterations may be required before the set is "realistic") which are passed through a GEANT based simulation of the CLAS detector. For a given kinematic space, the acceptance is equal to the number of reconstructed events divided by the number of generated events. The number of events in the E1-f data is then divided by the acceptance to get a corrected value for the number of events.

4.1 Simulation

Below is a general outline for how the simulations are performed. The details for each step will be discussed in the subsequent subsections.

- clasDIS is a program that generates electron-proton scattering events.
- GSim is a program that attempts recreate how CLAS would reconstruct the generated events.
- GPP (GSim Post Processing) is a program that smears and introduces additional inefficiencies to the GSim results to make the resolutions and acceptance more realistic.
- the RECSIS software cooks and formats the raw data using the same procedure as in the E1-f cooking and formatting.
- the same particle ID and fiducial cuts used in the E1-f data are used on the simulation.

4.1.1 Event Generation

The first step in doing Monte Carlo simulations is event generation. The distribution of events created by the generator should resemble nature as closely as possible. Since the $cos\phi_h$ and $cos2\phi_h$ moments are not known a priori, this is accomplished in an iterative way, starting with a flat ϕ_h distribution (i.e. $A_{UU}^{cos\phi_h} = A_{UU}^{cos2\phi_h} = 0$). The program used to do this is clasDIS, which is based on the PYTHIA generator and has been modified to be compatible with the kinematics at CLAS. The control options used with clasDIS for this analysis are summarized in table 4.1. Approximately one billion events were generated in order

to minimize the statistical error of the acceptance calculations.

Option	**Description**
–trig N	Tells the generator to process N events.
–datf	Tells the generator to output a data file.
–outform 2	Tells the generator to format the output for GSim.
–beam 5498	Sets the beam energy to 5.498 GeV.
–zpos -250	Sets the z-position at -250 mm.
–zwidth 25	Sets the target half-width to 25 mm.
–t 5 60	Sets the range of acceptable θ in degrees.
–parl3 0.7	Sets the mean of the k_T distribution, which is tuned such that the output $P_{h\perp}$ matches E1-f.
–lst15 145	Defines the set of parton distribution functions used in the simulation.
–parj33 0.3	Defines the remaining energy below which the fragmentation of a parton system is stopped and two hadrons are formed.

Table 4.1: Control options for the clasDIS event generator.

4.1.2 Detector Simulation

The software package used to simulate the CLAS detector is GSim. GSim is a GEANT based Monte Carlo simulation that simulates the passage of particles

through matter. The functionality includes detector geometry, physics models, and particle tracking and hits. Each event generated with clasDIS is passed to GSim; GSim then produces a realistic reconstruction of how the CLAS detector would reconstruct those events. Figure 4.1 shows an example of this. Both the generated information and the reconstructed information of the event are saved in the GSim output data file, the reconstructed portion being identical in format to the E1-f raw data files.

Each experimental run at Jefferson Lab uses slightly different conditions (magnetic field strength, target type/polarization, etc.). To customize GSim to be compatible with a particular run, a file called ffread.in must included in the GSim options. The ffread.in file for the E1-f run is summarized in table 4.2

Table 4.2: The information contained in the ffread.in file, customized for the E1-f run.

Input	**Description**
GEOM 'ALL'	Includes all CLAS geometry.
NOGEOM 'PTG''ST''IC'	Excludes geometry not present in E1-f.
MAGTYPE 3	Sets magnetic field type to "torus + mini from lookup table."
CUTS 5.e-3 5.e-3 5.e-3 5.e-3	Kinetic energy cuts in GeV.
CCCUTS 1.e-3 1.e-3 1.e-3 1.e-3	Cuts for the Čerenkov counter.

Continued on next page

Table 4.2 – *Continued from previous page*

Input	**Description**
DCCUTS 1.e-4 1.e-4 1.e-4 1.e-4	Cuts for the drift chamber.
ECCUTS 1.e-4 1.e-4 1.e-4 1.e-4	Cuts for the electromagnetic calorimeter.
SCCUTS 1.e-4 1.e-4 1.e-4 1.e-4	Cuts for the time-of-flight detector.
NTARGET 2	Sets the target type to liquid hydrogen.
MAGSCALE 0.5829 0.7495	Sets the scale of the magnetic fields.
RUNG 10	Default setting.
TARGET 'e1e'	Defines the target geometry (e1e is compatible with e1f).
TGMATE 'PROT''ALU'	Sets the target and target cell materials.
TGPOS 0.00 0.00 -25.0	Defines the target position.
NOMCDATA 'ALL'	Default setting to turn off additional GEANT hit information.
SAVE 'ALL''LEVL'10	Save all secondaries up to cascade level 10.
KINE 5	Setting for LUND event generator.
AUTO 1	Automatic computation of the tracking medium parameters.
STOP	GEANT command to end the ffread file.

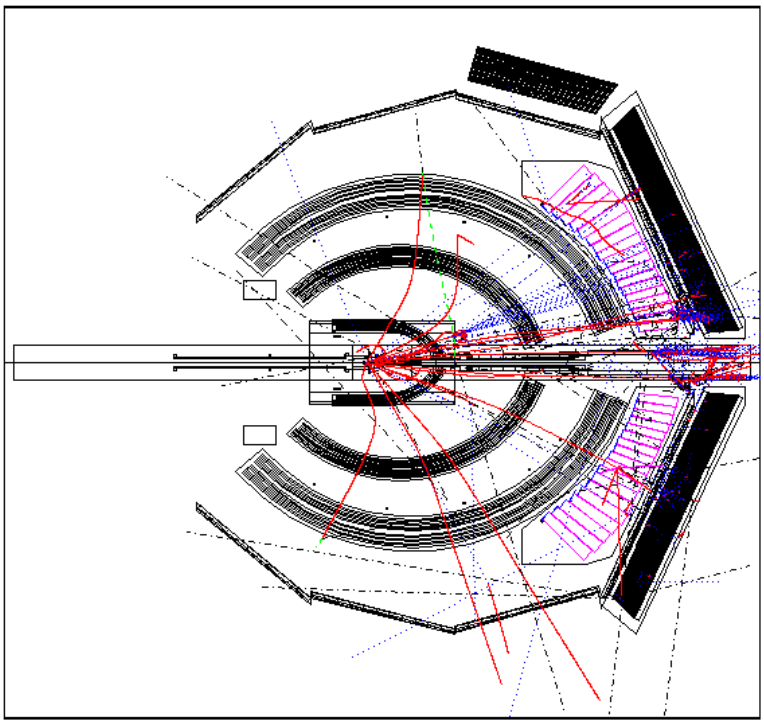

Fig. 4.1: A GSim reconstruction of five simulated events. The red tracks represent charged particles while gray tracks represent neutral particles.

4.1.3 Resolution Matching

Since GSim significantly over estimates the detector resolution, the GPP program is used to smear the DC and TOF values. To determine the amount of DC smearing necessary, studies were done using the reaction $ep \rightarrow e\pi^+\pi^- p$ in the experimental data and in the Monte Carlo. After selecting these events, the following resolutions are defined

$$\begin{aligned} \Delta p_{\pi^+} &= p_{\pi^+,calc} - p_{\pi^+,rec} \\ \Delta\theta_{\pi^+} &= \theta_{\pi^+,calc} - \theta_{\pi^+,rec} \\ \Delta\phi_{\pi^+} &= \phi_{\pi^+,calc} - \phi_{\pi^+,rec} \end{aligned} \tag{4.1}$$

where p, θ, and ϕ are the momentum, θ, and ϕ in the lab frame and the π^+, rec subscript refers to the actual reconstructed value of the π^+ while $\pi^+, calc$ is the value calculated based on the momenta of the other three particle and momentum conservation. These resolutions can be compared for data and simulation and the simulation can be tuned with GPP until the resolutions match. This tuning is done with three parameters called "a", "b", and "c." The optimum values for this analysis were found to be $a = b = c = 2.5$. Comparison between the data and the Monte Carlo with these parameters can be seen in figures 4.2, 4.3, and 4.4.

GPP also smears the TOF values via a parameter "f." The f parameter can be tuned by comparing the widths of the β distributions (in bins of momentum) for data and Monte Carlo. It was found that $f = 0.85$ is the best value for this analysis. Figure 4.5 compares π^+ β for data and Monte Carlo with $f = 0.85$.

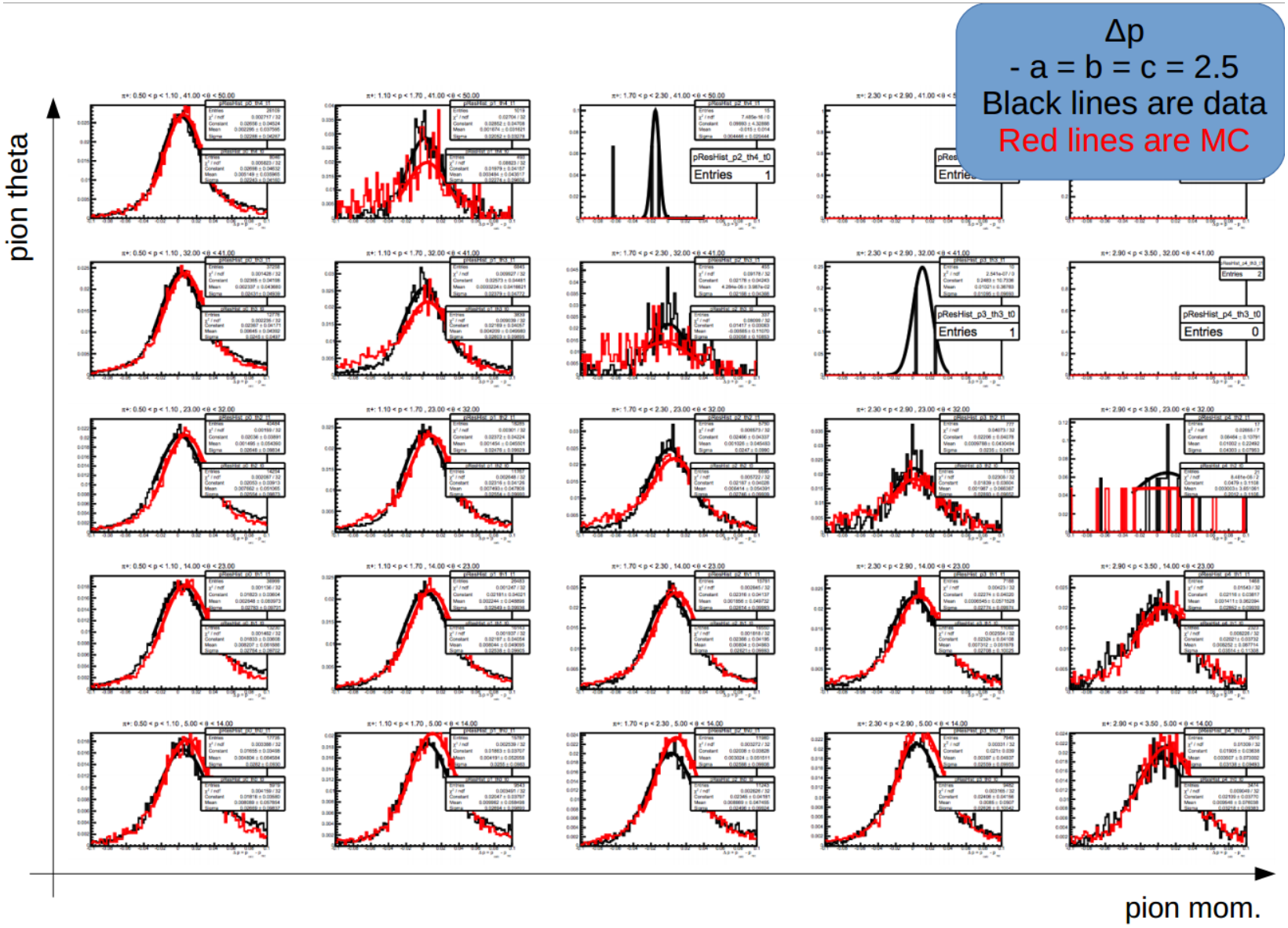

Fig. 4.2: Δp_{π^+} in bins of π^+ θ and ϕ for data (black) and Monte Carlo with GPP parameters $a = b = c = 2.5$ (red). It is clear that the agreement in resolution is good between the data and Monte Carlo.

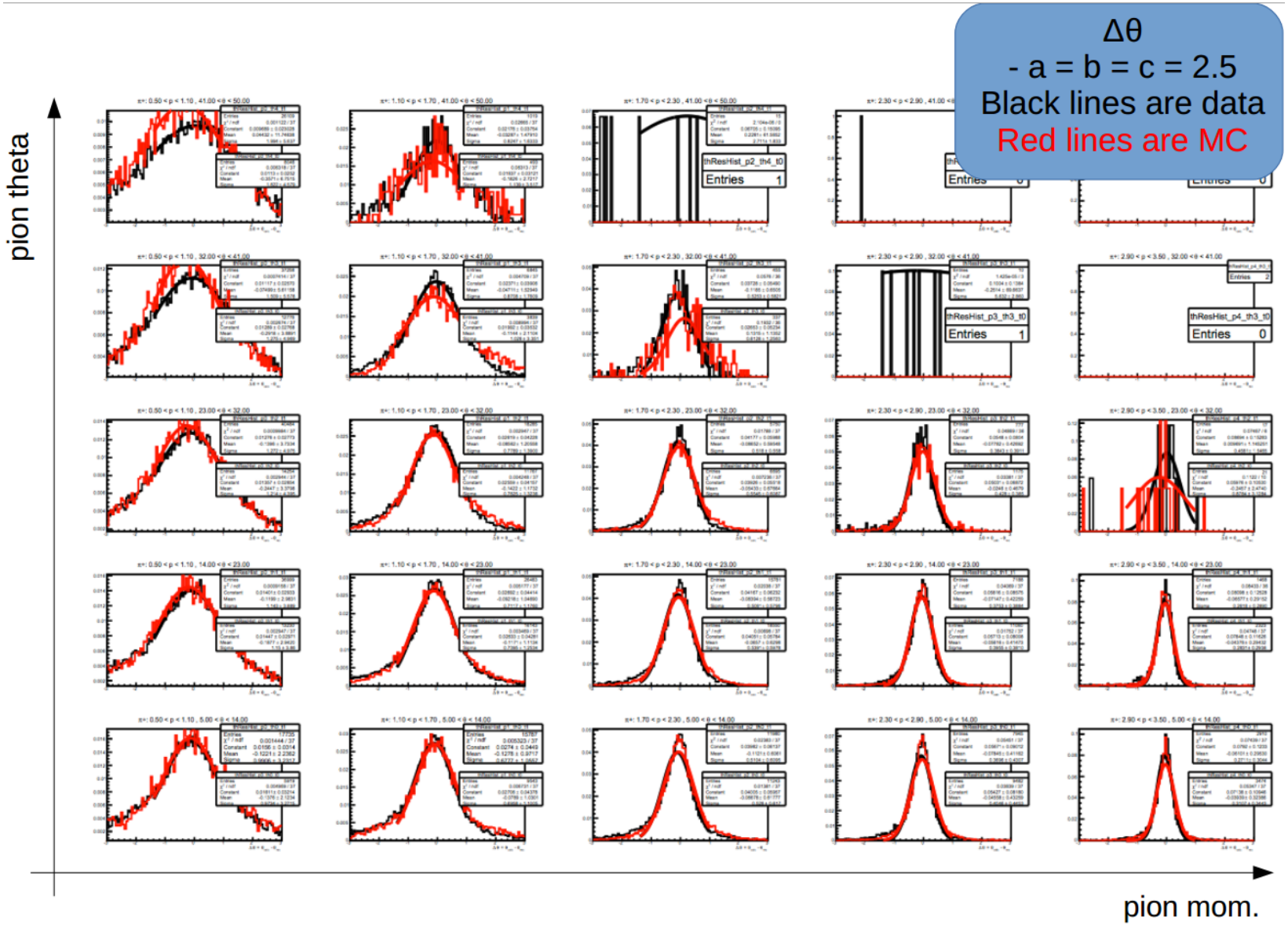

Fig. 4.3: $\Delta\theta_{\pi^+}$ in bins of π^+ θ and ϕ for data (black) and Monte Carlo with GPP parameters $a = b = c = 2.5$ (red). It is clear that the agreement in resolution is good between the data and Monte Carlo.

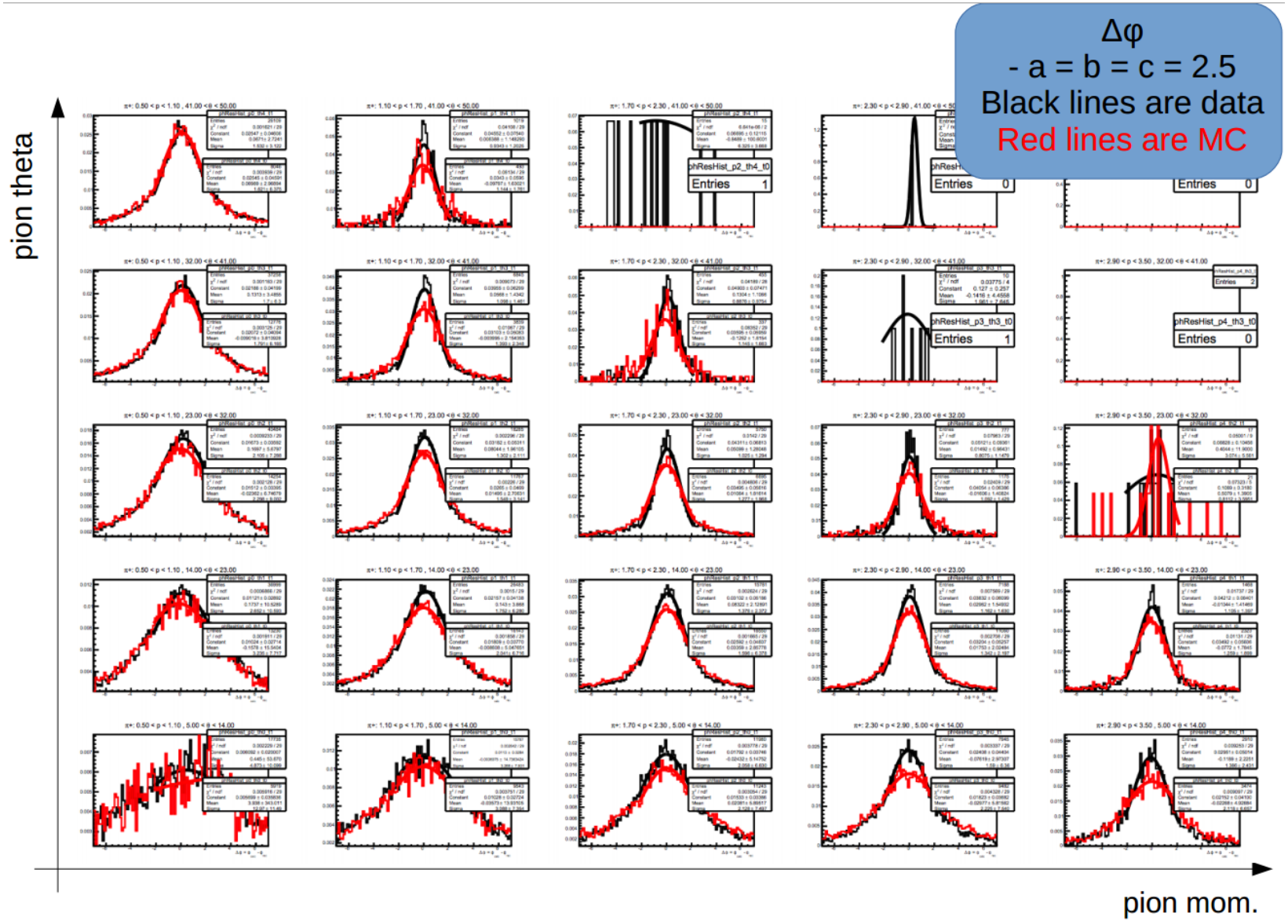

Fig. 4.4: $\Delta\phi_{\pi^+}$ in bins of π^+ θ and ϕ for data (black) and Monte Carlo with GPP parameters $a = b = c = 2.5$ (red). It is clear that the agreement in resolution is good between the data and Monte Carlo.

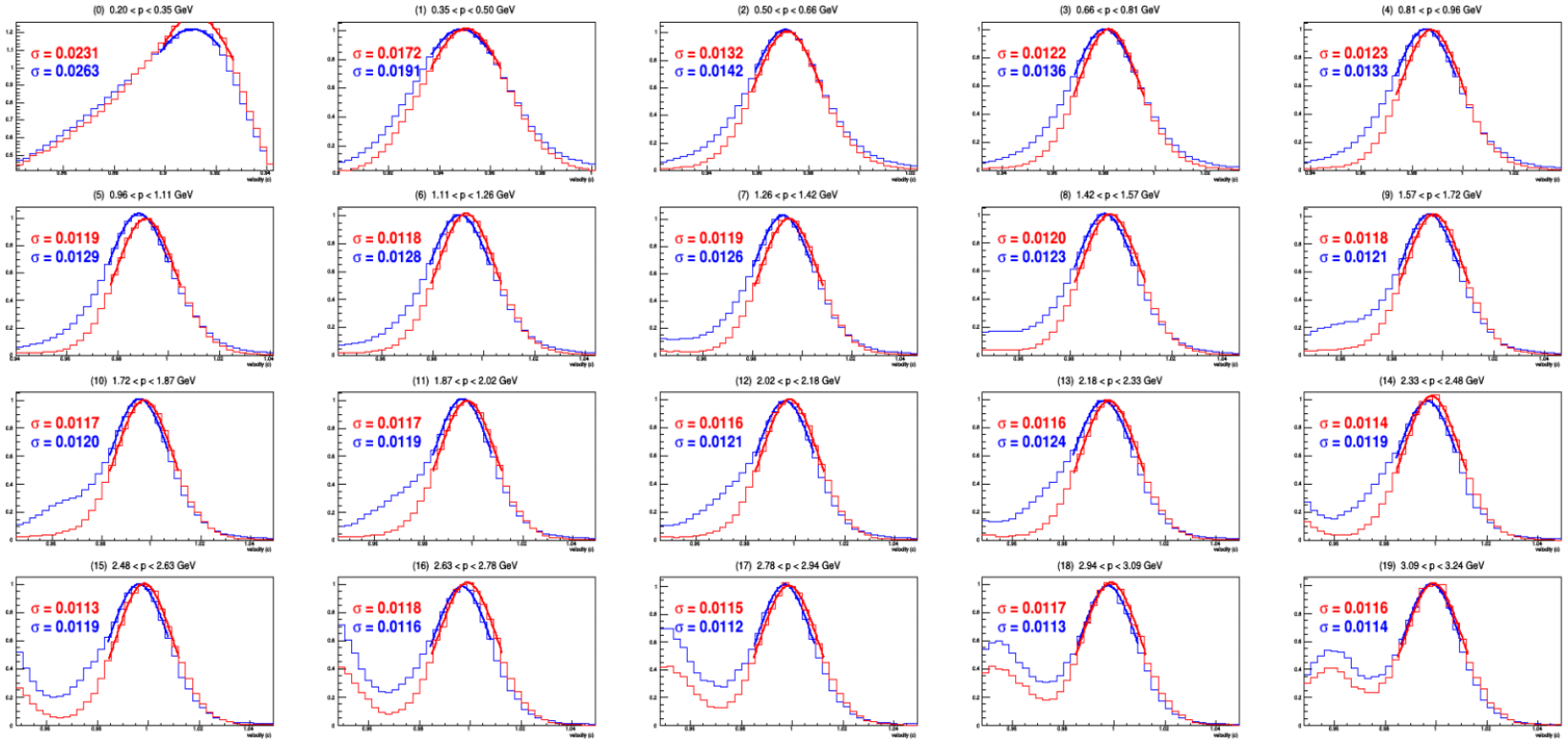

Fig. 4.5: π^+ β distributions in bins of momentum for data (blue) and Monte Carlo with $f = 0.85$ (red). The top left plot is the lowest momentum bin and the bottom right plot is the highest momentum bin. Each peak is fit with a gaussian and σ is printed on the plot (MC on top, data on bottom). This shows the good agreement in TOF resolution between the data and Monte Carlo.

The second purpose of GPP is to cut or introduce inefficiencies to certain DC wires in the simulation so that it matches the data. To check that this worked properly a wire map of the DC occupancy is made for the data and simulation (after using GPP). This is shown in figure 4.6 which confirms the efficacy of this feature of GPP.

4.1.4 Monte Carlo Reconstruction and Event Selection

After the generated data has been passed through GSim and after the GSim output has been modified by GPP, this data is then cooked with RECSIS in the same was as the experimental data as described in section 3.1. This produces an ntuple file where each event has a generated part and (possibly) a reconstructed part, the reconstructed part being identical in format to the cooked E1-F data files. The reconstructed part is put through the same set of particle ID and fiducial cuts as the experimental data. The cuts used here are not necessarily exactly identical to the experimental cuts, but they are the same kind of cuts; for example a $\mu \pm 3\sigma$ cut could produce slightly different cut values if μ and σ are slightly different in the data and simulation. Figure 4.7 shows, as an example, the momentum dependent β cut for π^+ ID for the reconstructed Monte Carlo; this should be compared to the experimental data version in figure 3.18. Finally, both the generated and reconstructed Monte Carlo data is orgainzed into bins of x, Q^2, z, $P_{h\perp}^2$, and ϕ_h in the same way the data is.

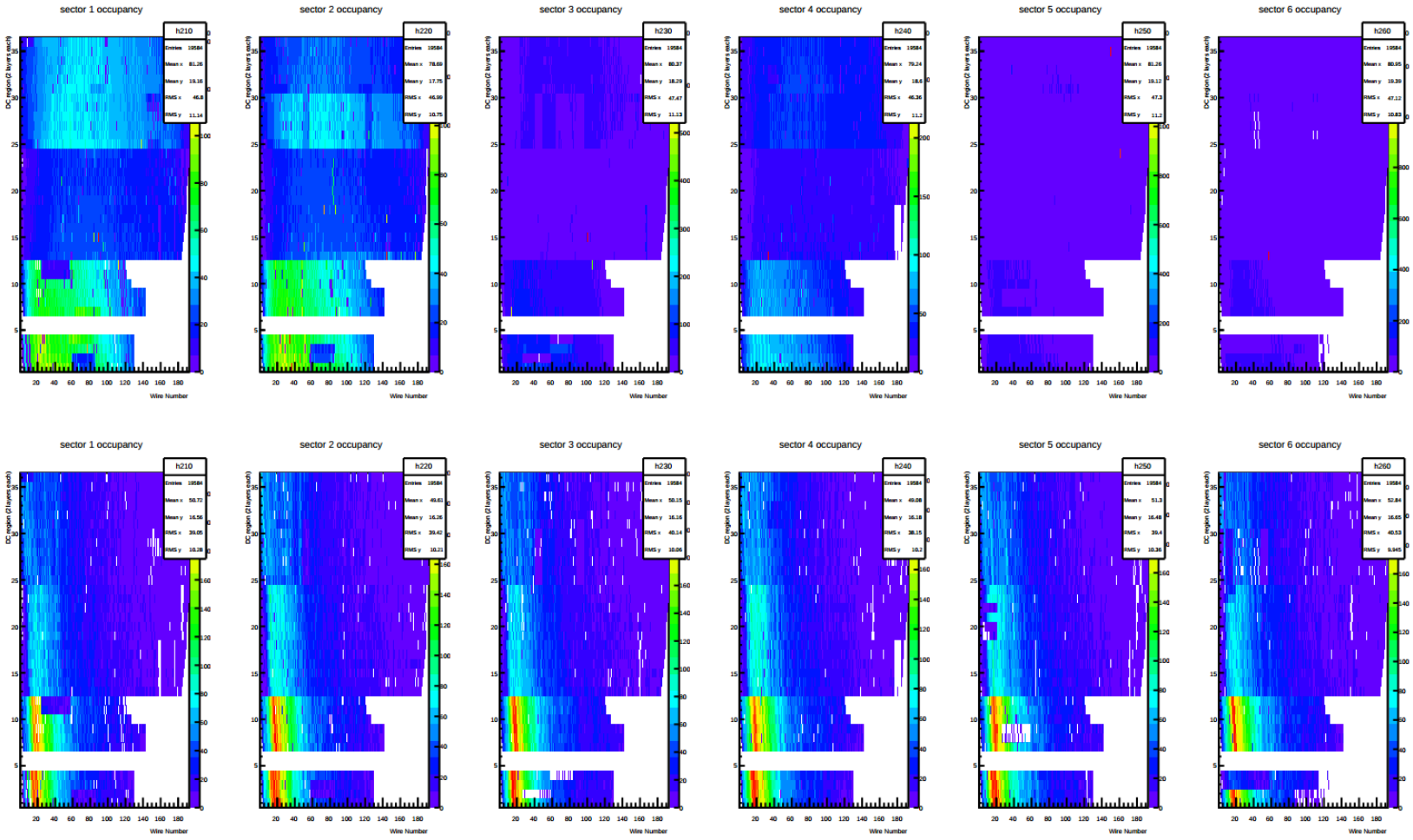

Fig. 4.6: A wire map of the DC occupancy for data (top row) and Monte Carlo (bottom row) for each sector (column 1 is sector 1, column 2 is sector 2, etc.). The holes are consistent between data and Monte Carlo confirming the efficacy of GPP.

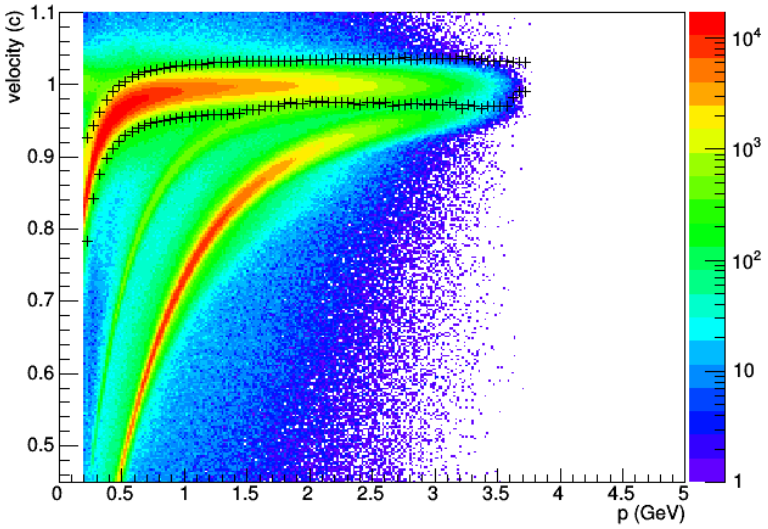

Fig. 4.7: The two dimensional view of the momentum dependent π^+ β cut for the reconstructed Monte Carlo. This should be compared to the experimental data version in figure 3.18.

4.2 Minimum ϕ_h Coverage for Reliable Fitting

There are certain regions of phase space where the CLAS acceptance is zero. These regions commonly occur around $\phi_h = 0$, potentially creating an occasion for unreliable results when fitting a particular ϕ_h distribution. A study is therefore needed to check what is the minimum allowable coverage in ϕ_h for which A_0, $A_{UU}^{\cos\phi_h}$, and $A_{UU}^{\cos 2\phi_h}$ can be reliably extracted. The criteria for A_0 will be different than the criteria for $A_{UU}^{\cos\phi_h}$ and $A_{UU}^{\cos 2\phi_h}$ since A_0 is a much more stable quantity.

This study consisted of generating ϕ_h distributions with three options: the number of events to generate, the value of the $\cos\phi_h$ moment, and the value of the $\cos 2\phi_h$ moment. The generated values of $A_{UU}^{\cos\phi_h}$ were -0.3, -0.2, -0.1, 0.0, 0.1, 0.2, and 0.3 (7 values). Similarly, the generated values of $A_{UU}^{\cos 2\phi_h}$ were -0.3, -0.2, -0.1, 0.0, 0.1, 0.2, and 0.3 (7 values). Finally, the number of generated events were 500, 1000, 2000, 5000, 10000, 20000, 50000, 100000, and 1000000 (9 values). All $7 \times 7 \times 9 = 441$ combinations were produced. Each distribution is then fit several times; each time a different range of ϕ_h around 0 was first cut out. An example of this can be seen in figure 4.8 which shows 5000 generated ϕ_h events with $A_{UU}^{\cos\phi_h} = -0.2$ and $A_{UU}^{\cos 2\phi_h} = 0.1$ and fit results; with each successive plot a larger range of ϕ_h around 0 is cut out before fitting.

As expected, higher statistics distributions produce more stable fit results. Within common sense limitations, a worst-case-scenario should be used as the criteria; anything less conservative could produce unreliable results. Furthermore,

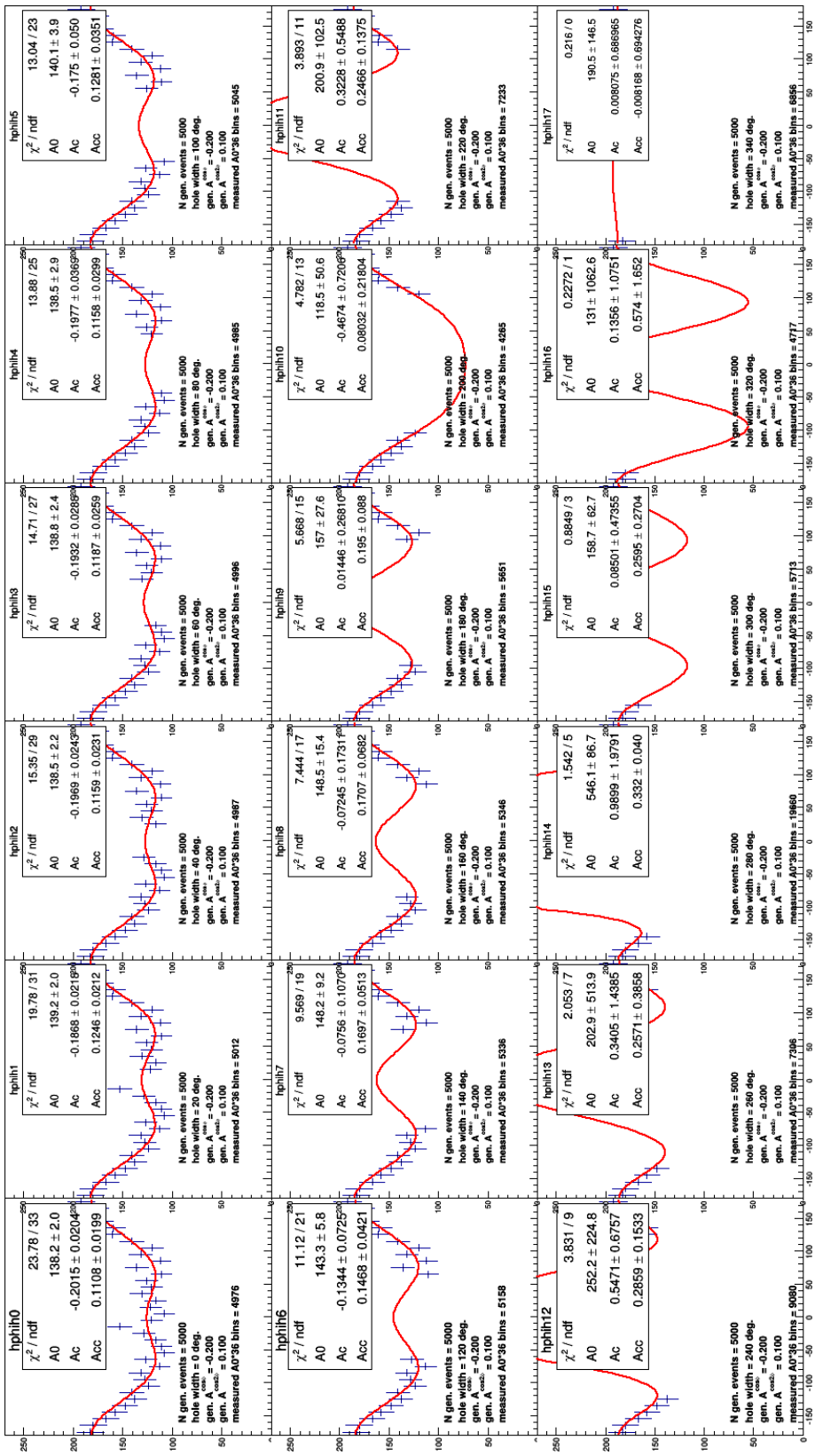

Fig. 4.8: Generated ϕ_h distributions with fit results with different ranges of ϕ_h cut out around 0. The top left plot has full 360° coverage while the bottom right plot has only 10° of coverage on each side. In this example 5000 events were generated with $A_{UU}^{\cos\phi_h} = -0.2$ and $A_{UU}^{\cos 2\phi_h} = 0.1$.

generated distributions are always much more ideal than experimental results. The case of 2000 generated events with $A_{UU}^{\cos\phi_h} = -0.2$ and $A_{UU}^{\cos 2\phi_h} = 0.0$ is used as a representative example. The results for this case are summarized in figure 4.9. It is clear that the fit results become very volatile with a hole width greater than 60° (i.e. events between −30° and 30° are cut).

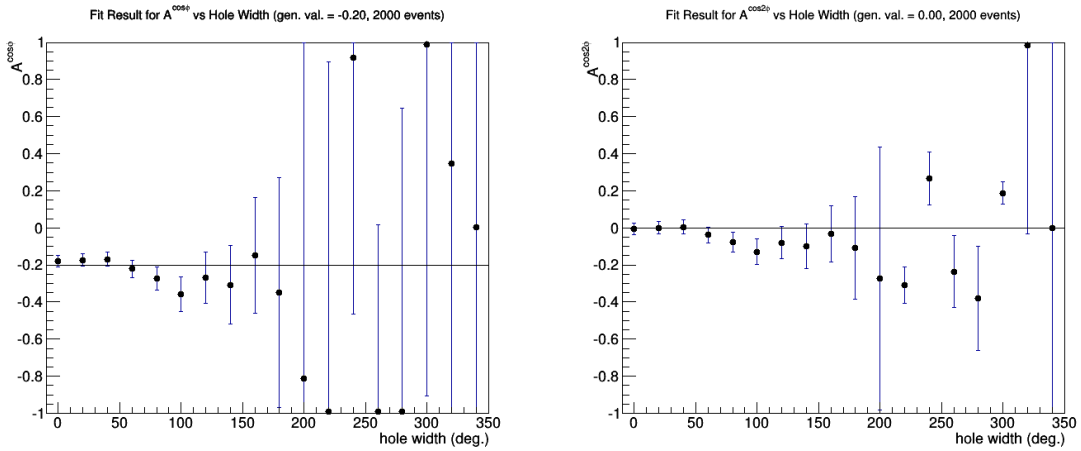

Fig. 4.9: $A_{UU}^{\cos\phi_h}$ (left) and $A_{UU}^{\cos 2\phi_h}$ (right) extracted from the fit of the generated ϕ_h distribution as a function of the width of the zero acceptance hole. The black horizontal lines show the generated values.

As a result of this study, $A_{UU}^{\cos\phi_h}$ and $A_{UU}^{\cos 2\phi_h}$ are not measured in bins where there is an acceptance hole in ϕ_h greater than 60° in width. For measuring A_0, at least 100° of coverage is required.

Chapter 5

Results

5.1 Binning

The binning schemes used for the π^+ channel and the π^- channel are the same. x is divided into 5 equally spaced bins from 0.1 to 0.6. Each x bin is divided into two Q^2 bins, a "low Q^2 bin" and a "high Q^2 bin," except for the highest x bin which has only one Q^2 bin. The upper limit of the high Q^2 bin is defined by the y cut of 0.85 and the lower limit of the low Q^2 bin is defined by the cuts on W and Q^2 of 2.05 GeV and 1.0 GeV^2, respectively. The Q^2 values that divide the low Q^2 bin and the high Q^2 bin for the first four x bins are 1.3, 1.7, 2.2, and 2.9 GeV^2. This is all summarized in figure 5.1, which shows results for π^+ and π^-, E1-f data and Monte Carlo.

For the hadronic variables, z is divided into 18 equally spaced bins from 0.0 to 0.9 and $P_{h\perp}^2$ is divided into 20 equally spaced bins from 0.0 to 1.0 GeV^2. The $P_{h\perp}^2$ vs z distributions with binning scheme and lines of constant missing mass for each of the 9 x-Q^2 bins are plotted in figures 5.2, 5.3, 5.4, and 5.5 for π^+ E1-f,

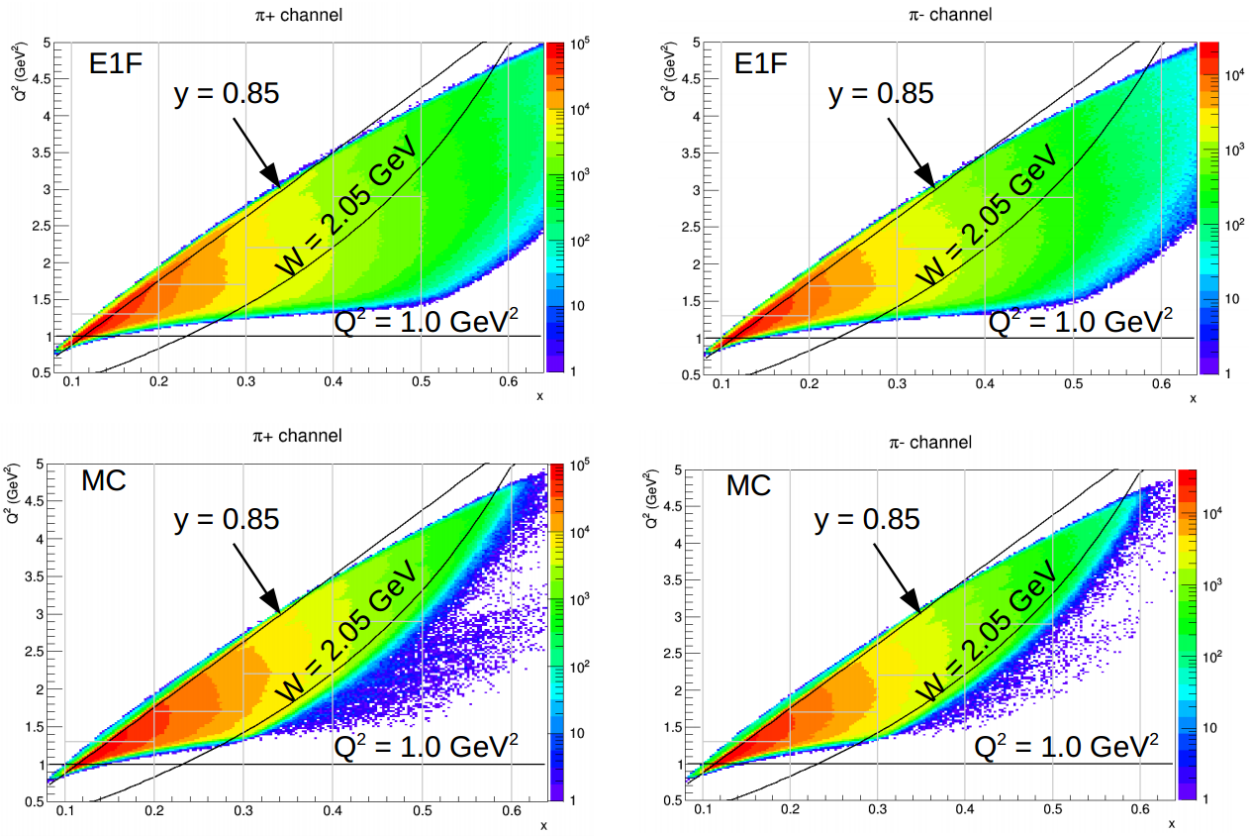

Fig. 5.1: The x-Q^2 binning scheme for both pion channels for data and MC (top row is data, bottom row is MC, left column is π^+, right column is π^-). The gray lines show the bin limits and the black lines show the y, W, and Q^2 cuts. Although there are no low W events in the Monte Carlo, this has little to no impact because of the W cut at 2.05 GeV.

π^- E1-f, π^+ Monte Carlo, and π^- Monte Carlo, respectively. ϕ_h is divided into 36 equally spaced bins from $-180°$ to $180°$.

As described in sections 3.7 and 4.2, certain x-Q^2-z-$P_{h\perp}^2$ bins have acceptance holes around $\phi_h = 0$. If the hole has a width of greater than $60°$, then $A_{UU}^{cos\phi_h}$ and $A_{UU}^{cos2\phi_h}$ cannot be reliably extracted for that bin. Figures 5.6 and 5.7 show the z-$P_{h\perp}^2$ phase space coverage for π^+ and π^- (E1-f data), respectively, for events with $-30° < \phi_h < 30°$. From these plots, the x-Q^2-z-$P_{h\perp}^2$ bins for which $A_{UU}^{cos\phi_h}$ and $A_{UU}^{cos2\phi_h}$ can be extracted can be seen.

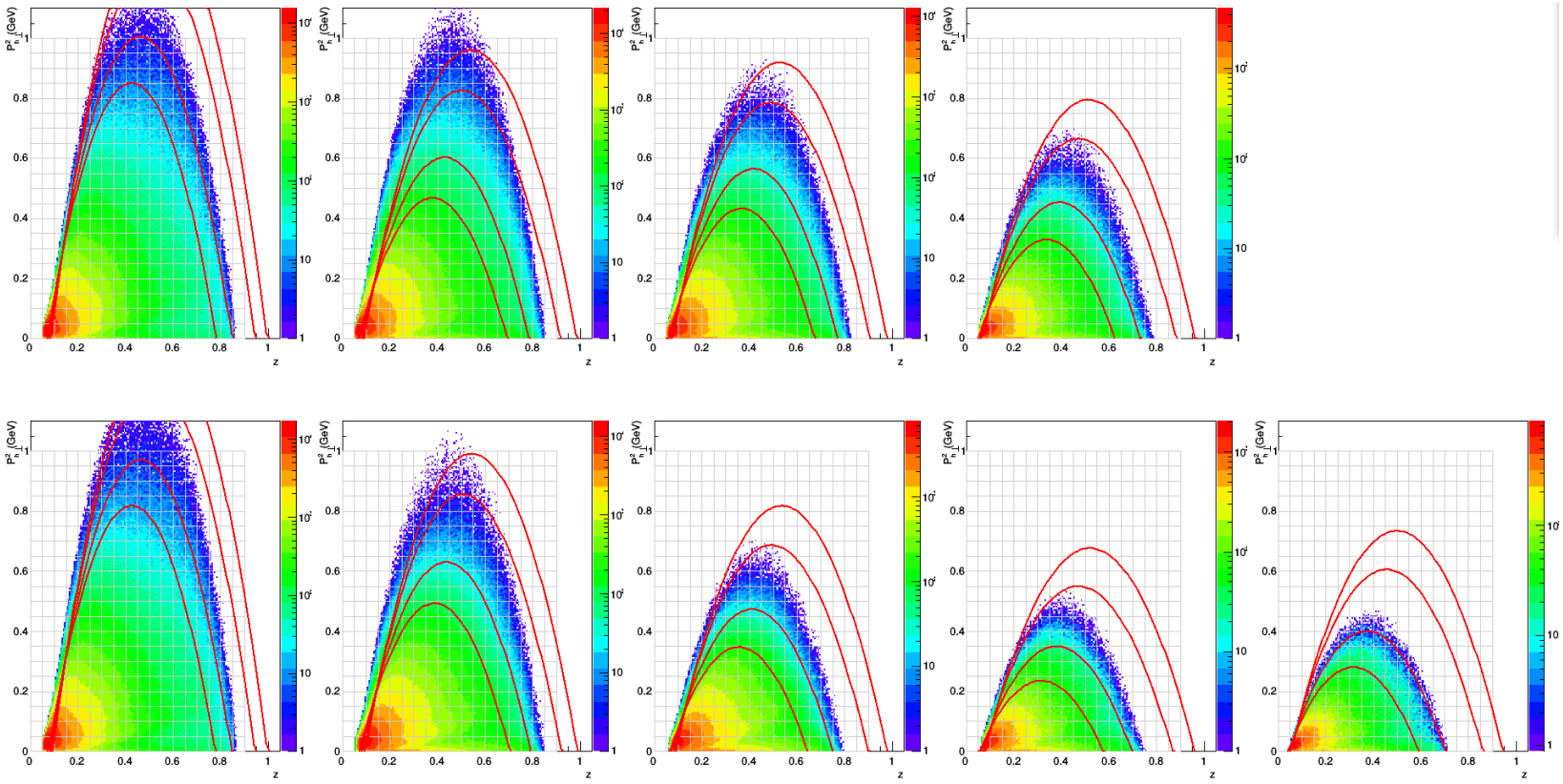

Fig. 5.2: The z-$P_{h\perp}^2$ phase space coverage for π^+ for each x-Q^2 bin for E1-f data. Column 1 is the first x bin, column 2 is the second x bin, etc. and the bottom row is the low Q^2 bin and the top row is the high Q^2 bin. The red lines are lines of constant missing mass of (from outermost to innermost) M_P, 1.1, 1.35, and 1.5 GeV. The lines are approximate since they depend on x and Q^2. The binning scheme is shown with gray lines.

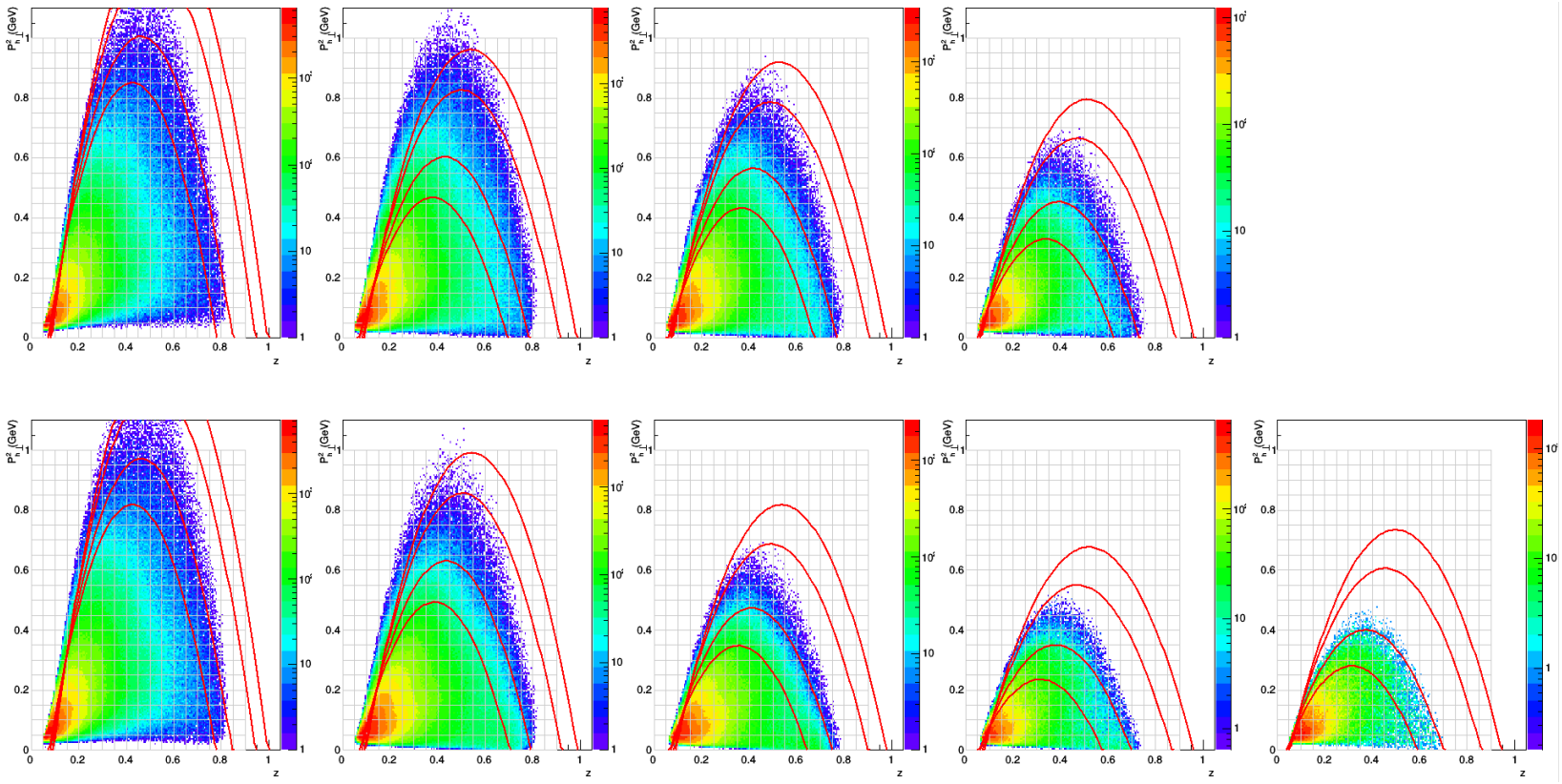

Fig. 5.3: The z-$P_{h\perp}^2$ phase space coverage for π^- for each x-Q^2 bin for E1-f data. Column 1 is the first x bin, column 2 is the second x bin, etc. and the bottom row is the low Q^2 bin and the top row is the high Q^2 bin. The red lines are lines of constant missing mass of (from outermost to innermost) M_P, 1.1, 1.35, and 1.5 GeV. The lines are approximate since they depend on x and Q^2. The binning scheme is shown with gray lines.

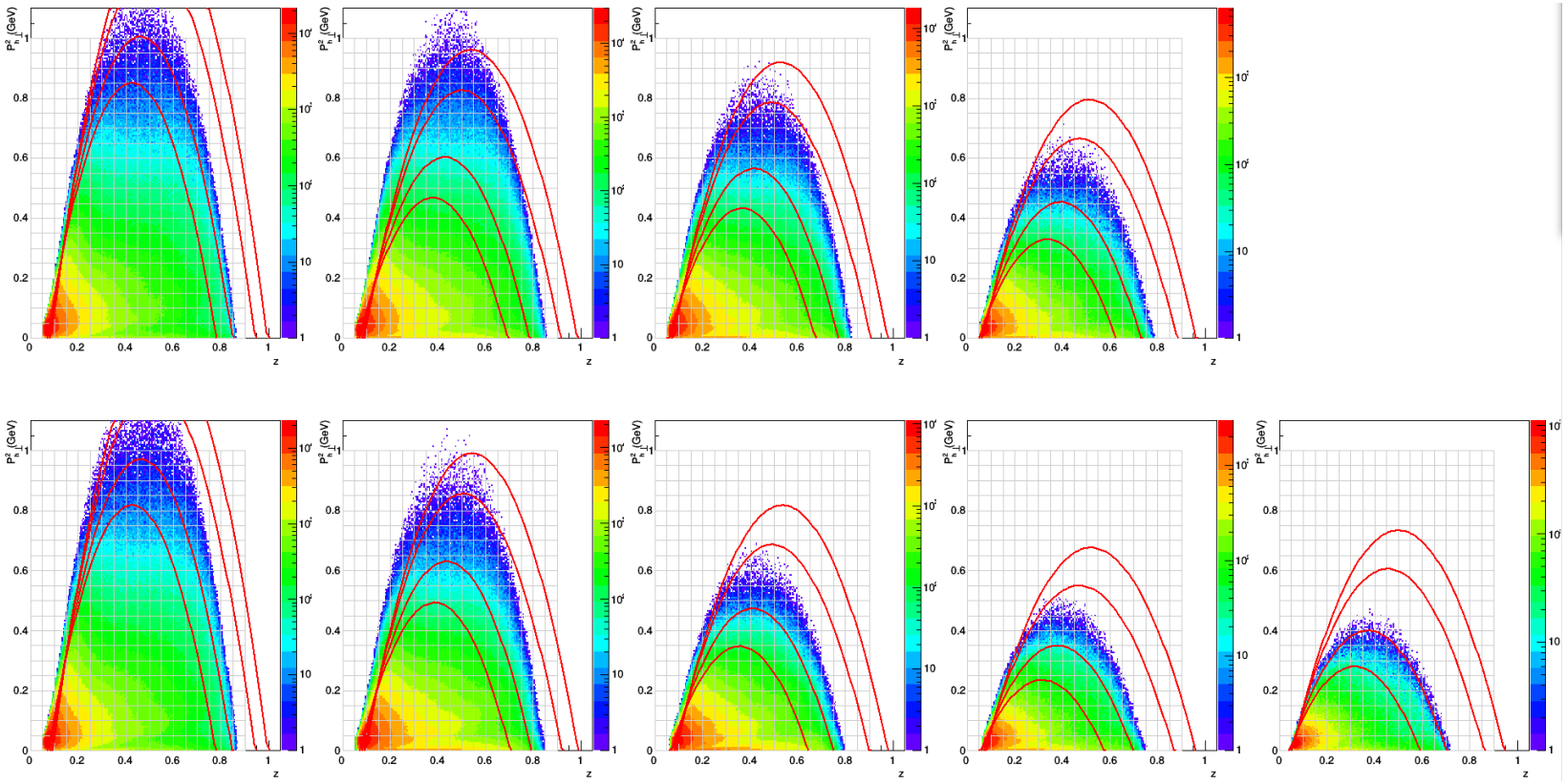

Fig. 5.4: The z-$P_{h\perp}^2$ phase space coverage for π^+ for each x-Q^2 bin for reconstructed Monte Carlo. Column 1 is the first x bin, column 2 is the second x bin, etc. and the bottom row is the low Q^2 bin and the top row is the high Q^2 bin. The red lines are lines of constant missing mass of (from outermost to innermost) M_P, 1.1, 1.35, and 1.5 GeV. The lines are approximate since they depend on x and Q^2. The binning scheme is shown with gray lines.

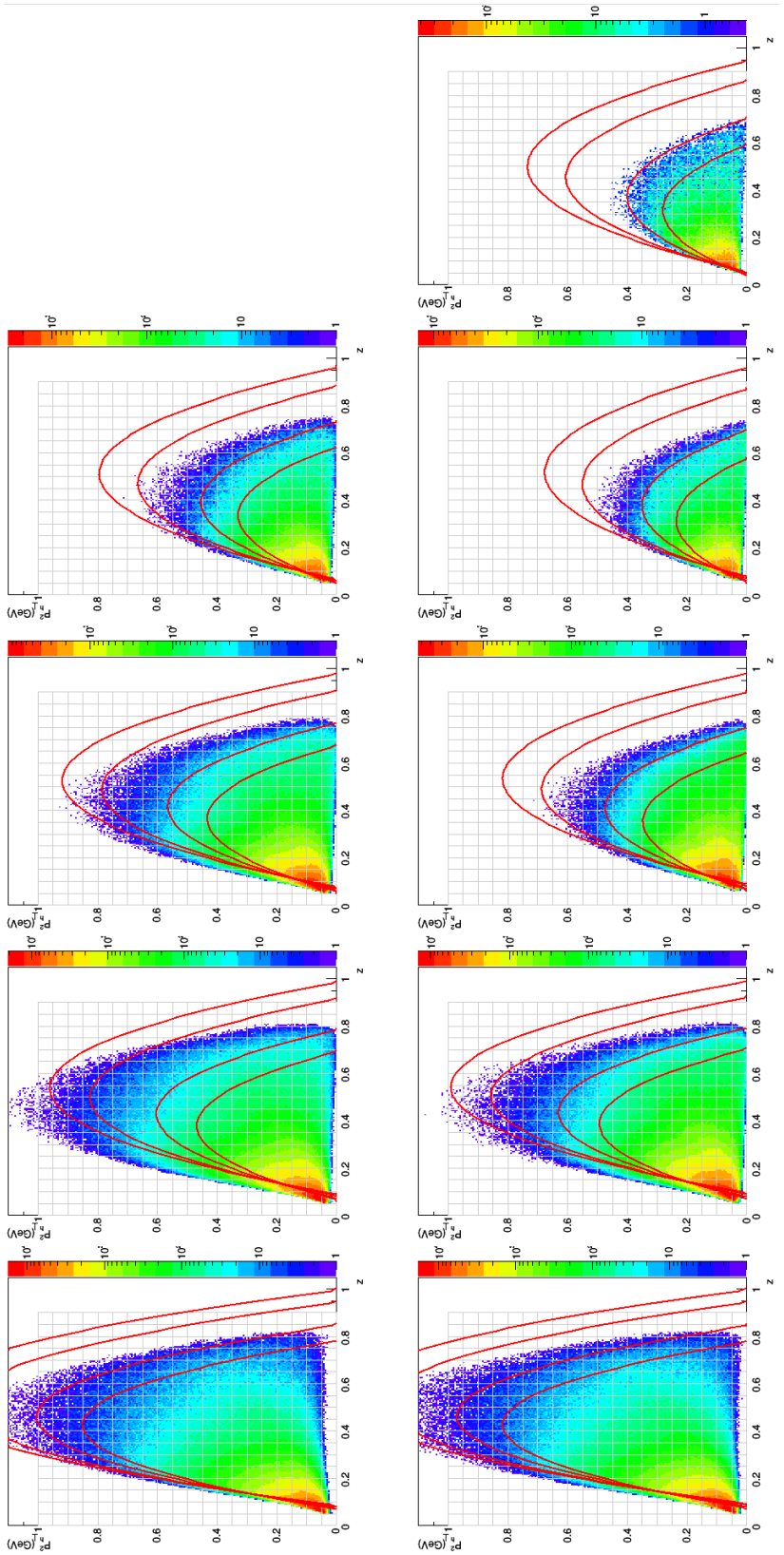

Fig. 5.5: The z-$P_{h\perp}^2$ phase space coverage for π^- for each x-Q^2 bin for reconstructed Monte Carlo. Column 1 is the first x bin, column 2 is the second x bin, etc. and the bottom row is the low Q^2 bin and the top row is the high Q^2 bin. The red lines are lines of constant missing mass of (from outermost to innermost) M_P, 1.1, 1.35, and 1.5 GeV. The lines are approximate since they depend on x and Q^2. The binning scheme is shown with gray lines.

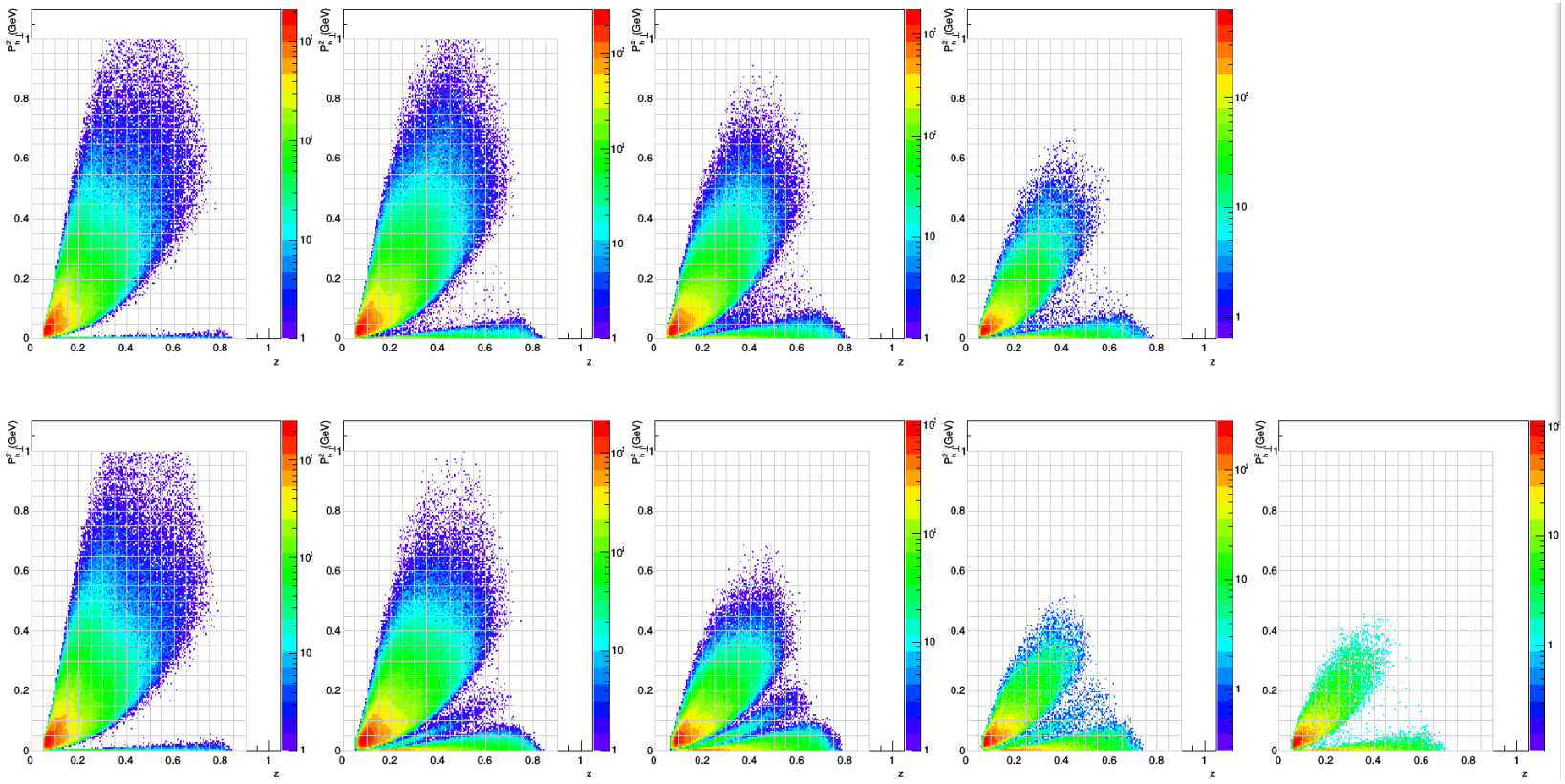

Fig. 5.6: The z-$P_{h\perp}^2$ phase space coverage for events with $-30° < \phi_h < 30°$ for π^+ for each x-Q^2 bin for E1-f data. Column 1 is the first x bin, column 2 is the second x bin, etc. and the bottom row is the low Q^2 bin and the top row is the high Q^2 bin. The empty or nearly empty bins have ϕ_h holes with a width greater than 60° and therefore $A_{UU}^{cos\phi_h}$ and $A_{UU}^{cos2\phi_h}$ cannot be reliably extracted from them.

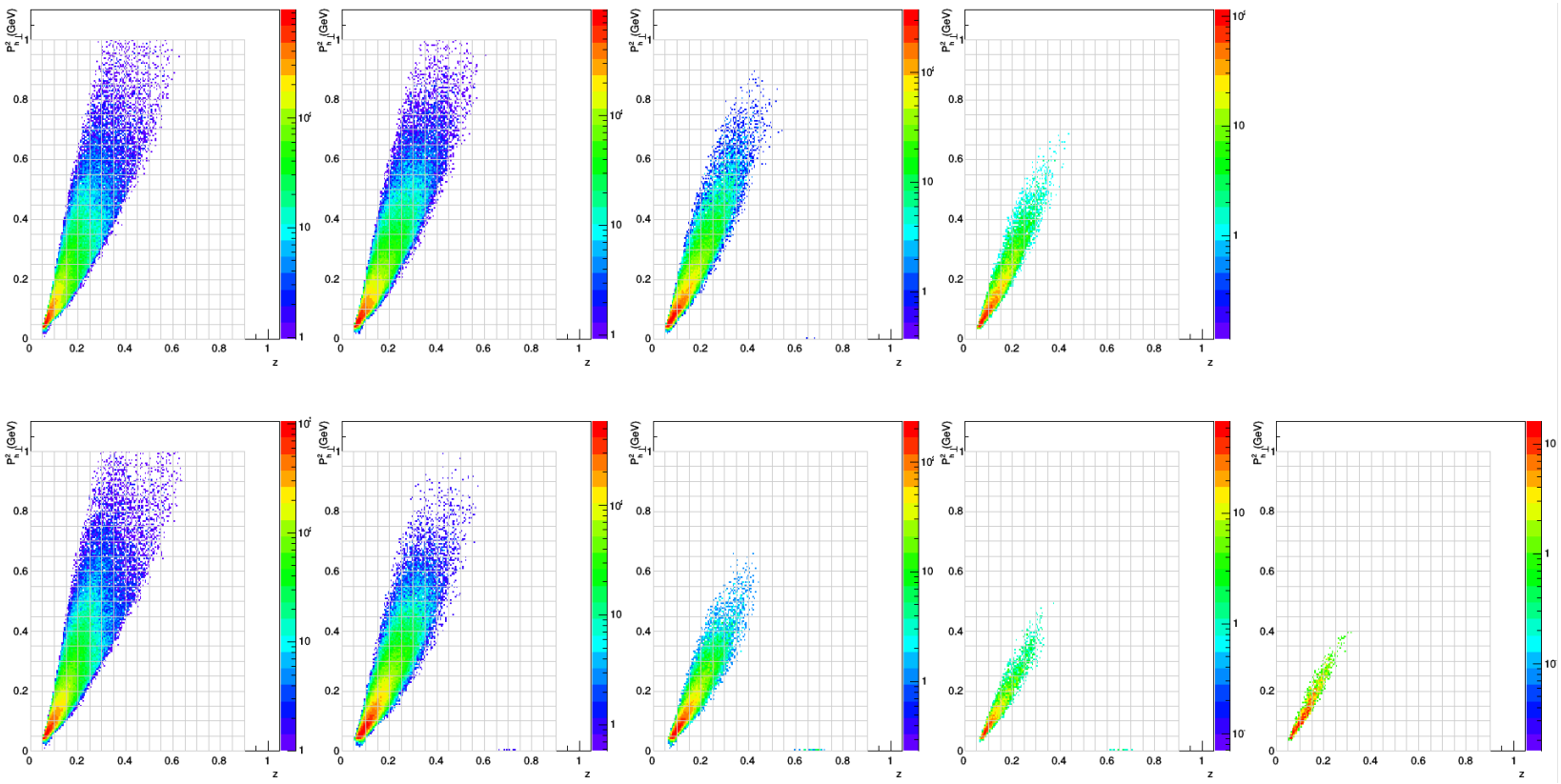

Fig. 5.7: The z-$P_{h\perp}^2$ phase space coverage for events with $-30^\circ < \phi_h < 30^\circ$ for π^- for each x-Q^2 bin for E1-f data. Column 1 is the first x bin, column 2 is the second x bin, etc. and the bottom row is the low Q^2 bin and the top row is the high Q^2 bin. The empty or nearly empty bins have ϕ_h holes with a width greater than 60° and therefore $A_{UU}^{cos\phi_h}$ and $A_{UU}^{cos2\phi_h}$ cannot be reliably extracted from them.

5.2 Corrections

5.2.1 Acceptance Corrections

Acceptance, for a given range of phase space, is equal to the number of reconstructed Monte Carlo Events in that range divided by the number of generated Monte Carlo Events in that range:

$$Acceptance = \frac{N_{rec}}{N_{gen}}. \tag{5.1}$$

The acceptance corrected number of events in the experimental data is then simply the number of events in the data divided by the acceptance:

$$corrected\ value = \frac{N_{data}}{Acceptance}. \tag{5.2}$$

Because of detector resolution and non-zero bin widths, the acceptance calculations show some dependence on the model used in the event generator. For this analysis, it is assumed that the event generator has a realistic model except for the ϕ_h modulation; a fairly safe assumption. To minimize the effects of ϕ_h model dependence, an iterative procedure is used, where the zeroth iteration assumes a flat ϕ_h distribution (i.e. $A_{UU}^{\cos\phi_h} = A_{UU}^{\cos 2\phi_h} = 0$) and each successive iteration uses a model based on the physics extracted from the data using the previous model. Figure 5.8 shows a conceptual example of this process for a particular x-Q^2-z-$P_{h\perp}^2$ bin. The data, Monte Carlo, and corrected data ϕ_h distributions for this bin are plotted for 4 iterations. The results for the last and second-to-last iterations are within error bars, so the procedure converges.

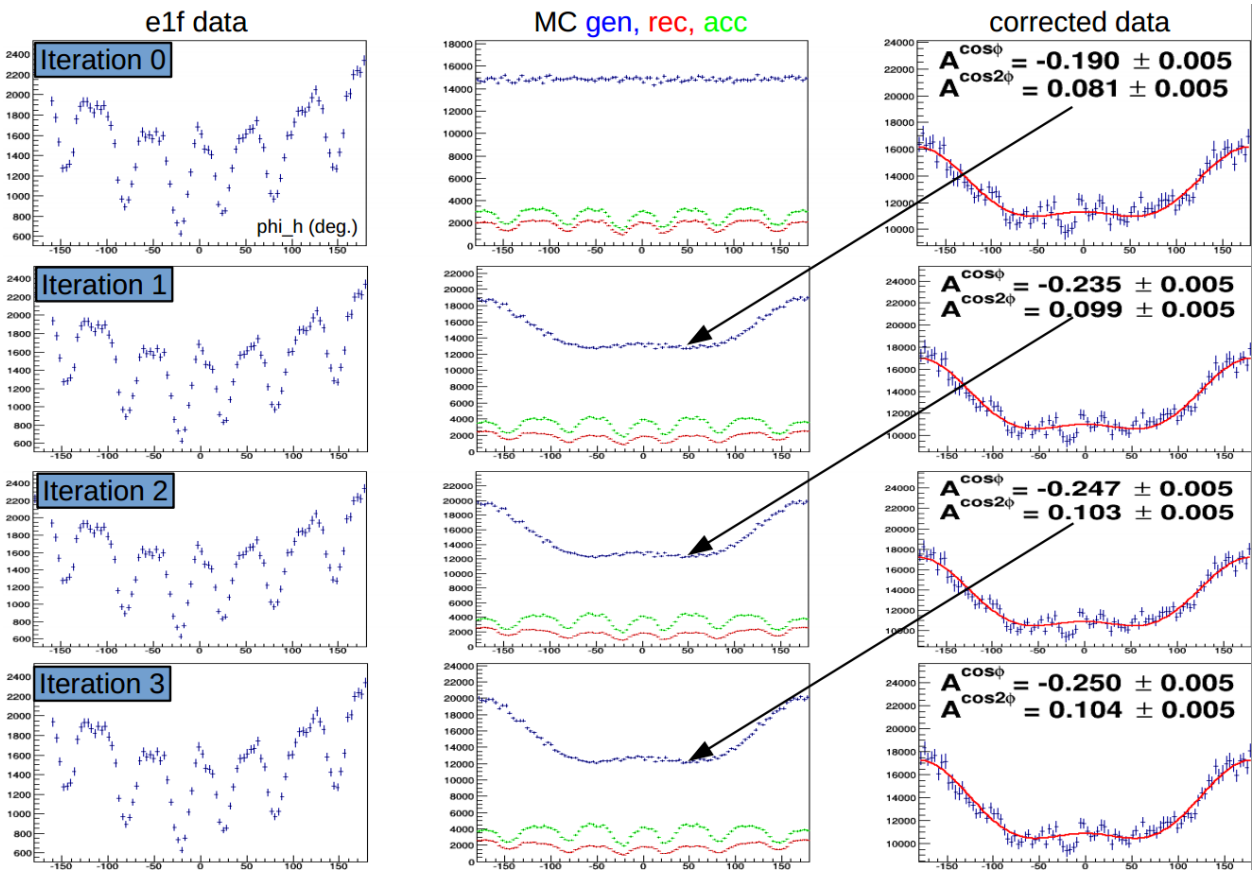

Fig. 5.8: A conceptual example of the iterative procedure used for acceptance calculations. The top row shows the zeroth iteration (flat generated ϕ_h distribution), the second row shows the first iteration, etc. For a given row, the E1-f ϕ_h distribution is plotted on the left; in the middle, the Monte Carlo generated (blue), reconstructed (red), and acceptance (green) ϕ_h distributions are plotted; and on the right is the acceptance corrected data with a best fit to extract the $\cos\phi$ and $\cos 2\phi$ moments. The vertical scale for the acceptance goes from 0 at the bottom of the plot to 1 at the top of the plot. The moments extracted from iteration 0 are used in the generator of iteration 1 and so on. By iteration 3 the results converge.

At first, a bin-by-bin technique was tried, where the procedure shown in figure 5.8 was applied for each bin individually. This, however, proved to be an unsafe strategy since it produced models that were very discontinuous (and therefore unrealistic), especially in regions of low or zero acceptance. Iterating this procedure only exacerbated the problem. A new strategy is therefore adopted and three (continuous) models are tested. The aforementioned "flat" model is used as the zeroth iteration. A default model that came built into HAPRAD (see section 5.2.2) is used as iteration 1 after it was shown to have reasonable agreement with the results of this analysis. Finally, iteration 2 is an improved version of the HAPRAD default model that is modified to have better agreement with experimental results. Studying multiple models is important for understanding systematic uncertainties (see section 5.4). The systematic uncertainty from this part of the analysis will be based on the difference in the final results between iteration 1 and iteration 2. Figure 5.9 shows a representative example of acceptance model dependence on A_0, $A_{UU}^{\cos\phi_h}$, and $A_{UU}^{\cos 2\phi_h}$ in bins of $P_{h\perp}^2$ for π^+ and π^-. The Monte Carlo generated, reconstructed, and acceptance for iteration 2 are plotted vs ϕ_h in figure 5.10 for π^+ and in figure 5.11 for π^- for several z-$P_{h\perp}^2$ bins for the lowest x-Q^2 bin.

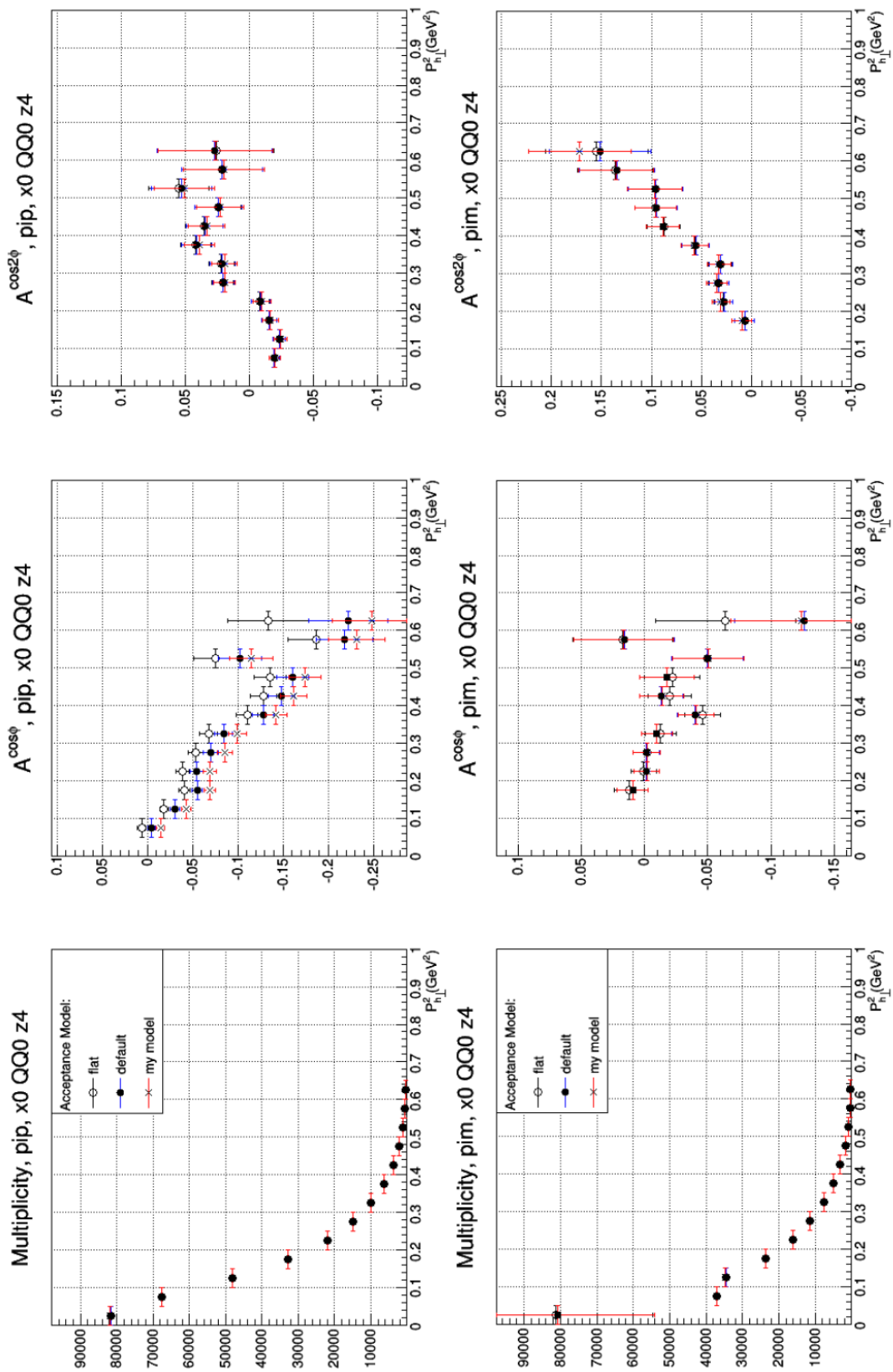

Fig. 5.9: A_0 (left), $A_{UU}^{\cos\phi_h}$ (middle), and $A_{UU}^{\cos 2\phi_h}$ (right) vs $P_{h\perp}^2$ for π^+ (top) and π^- (bottom) for the three different event generator models discussed in the text. These results are for the low Q^2 bin of $0.1 < x < 0.2$, and $0.2 < z < 0.25$.

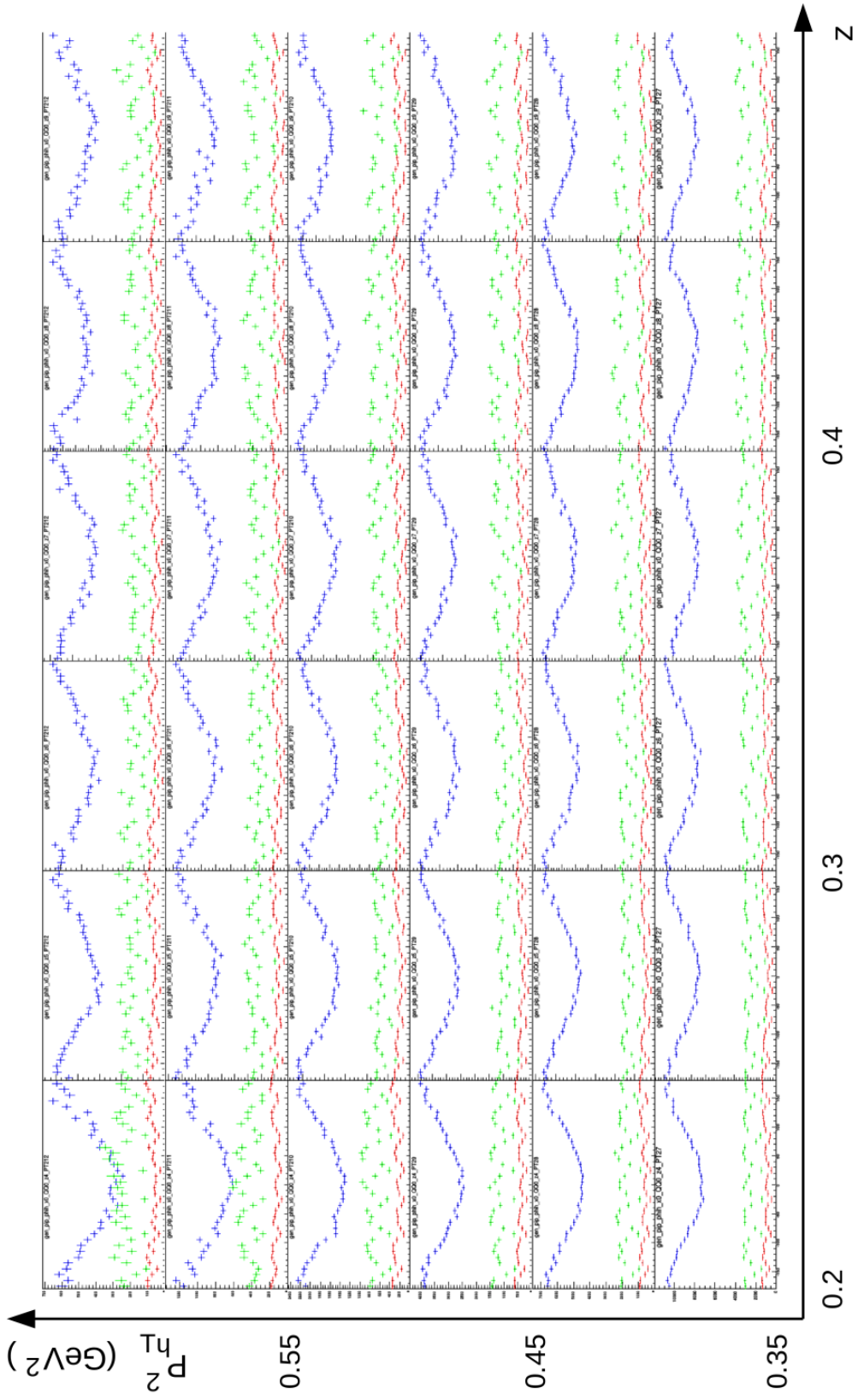

Fig. 5.10: π^+ Monte Carlo generated (blue), reconstructed (red), and acceptance (green) vs ϕ_h for iteration 2 in bins of z and $P_{h\perp}^2$ for the lowest x-Q^2 bin.

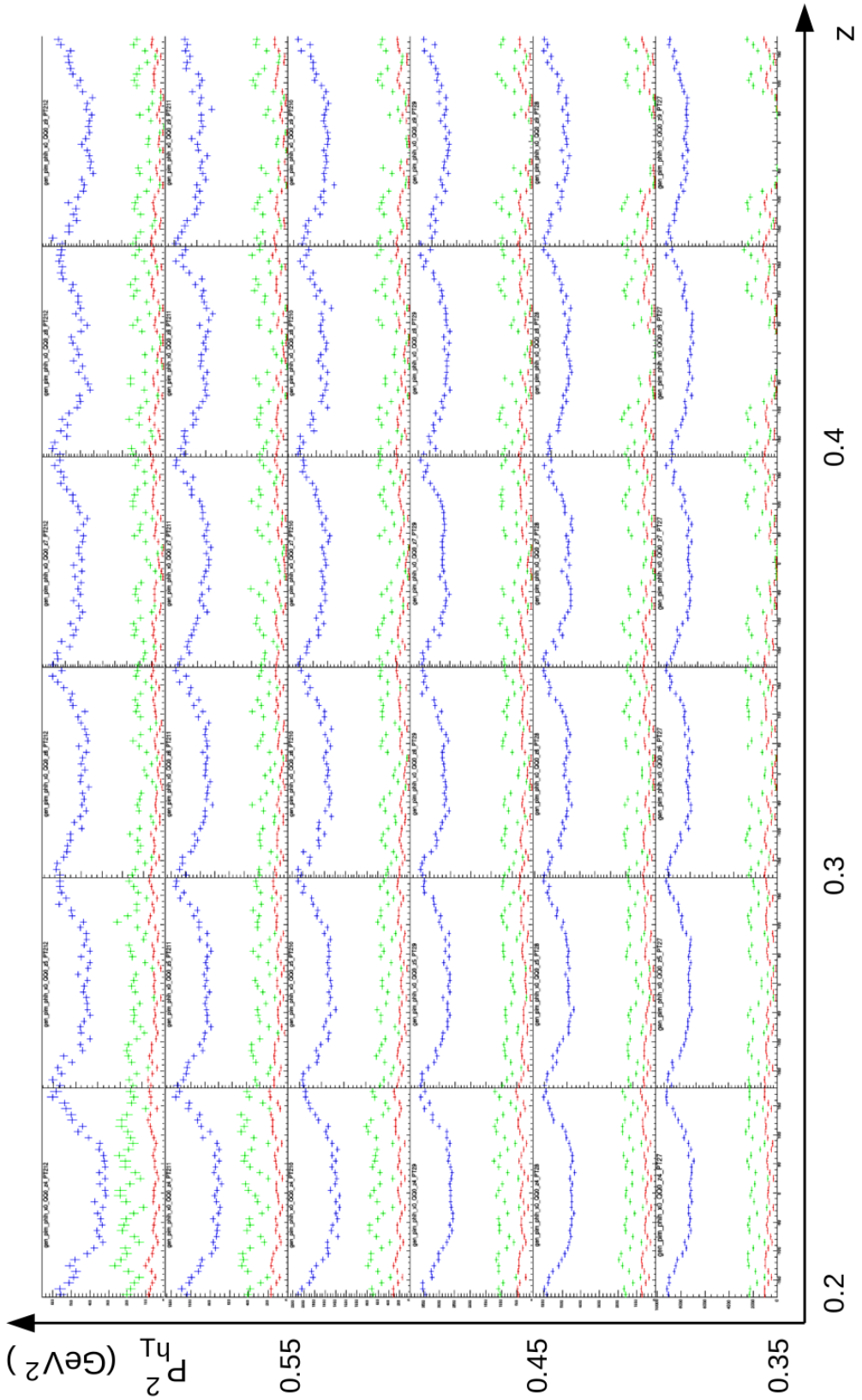

Fig. 5.11: π^- Monte Carlo generated (blue), reconstructed (red), and acceptance (green) vs ϕ_h for iteration 2 in bins of z and $P_{h\perp}^2$ for the lowest x-Q^2 bin.

5.2.2 Radiative Corrections

It is possible that either the incoming or the scattered electron can radiate a photon, thus changing the kinematics of the entire event. This effect can be non-negligible for SIDIS events. Furthermore, exclusive events which are outside of the kinematics of interest can come into the SIDIS sample because of radiative effects (this is called the "exclusive tail"). Exclusive events refers to $ep \to e\pi^+ n$ events; there is no analogous reaction for the π^- channel so this effect only affects the π^+ channel. The measured cross-section, then, is the radiated cross-section, not the Born (un-radiated) cross-section. The goal of this analysis is to measure the Born cross-section, so corrections must be made for radiative effects. This is done with a program called HAPRAD (version 2, which includes contributions from the radiative tail of exclusive reaction), described in [37] and [38].

Like the acceptance corrections, HAPRAD is model dependent, and therefore an iterative approach is used here as well. The same three models described in section 5.2.1 are also used here. For a given $\sigma_{Born}(x, Q^2, z, P_{h\perp}^2, \phi_h)$ (obtained from the model), HAPRAD calculates $\sigma_{rad}(x, Q^2, z, P_{h\perp}^2, \phi_h)$. The correction factor for radiative effects is then simply the ratio

$$RC\ factor = \frac{\sigma_{rad}(x, Q^2, z, P_{h\perp}^2, \phi_h)}{\sigma_{Born}(x, Q^2, z, P_{h\perp}^2, \phi_h)}. \tag{5.3}$$

Figure 5.12 shows a representative example of HAPRAD model dependence on A_0, $A_{UU}^{\cos\phi_h}$, and $A_{UU}^{\cos 2\phi_h}$ in bins of $P_{h\perp}^2$ for π^+ and π^-. The systematic uncertainty

from this part of the analysis will be based on the difference in the final results between iteration 1 and iteration 2. σ_{Born}, σ_{rad}, and σ_{tail} from HAPRAD for iteration 2 are plotted vs ϕ_h in figure 5.13 for π^+ and in figure 5.14 for π^- for several z-$P_{h\perp}^2$ bins for the lowest x-Q^2 bin.

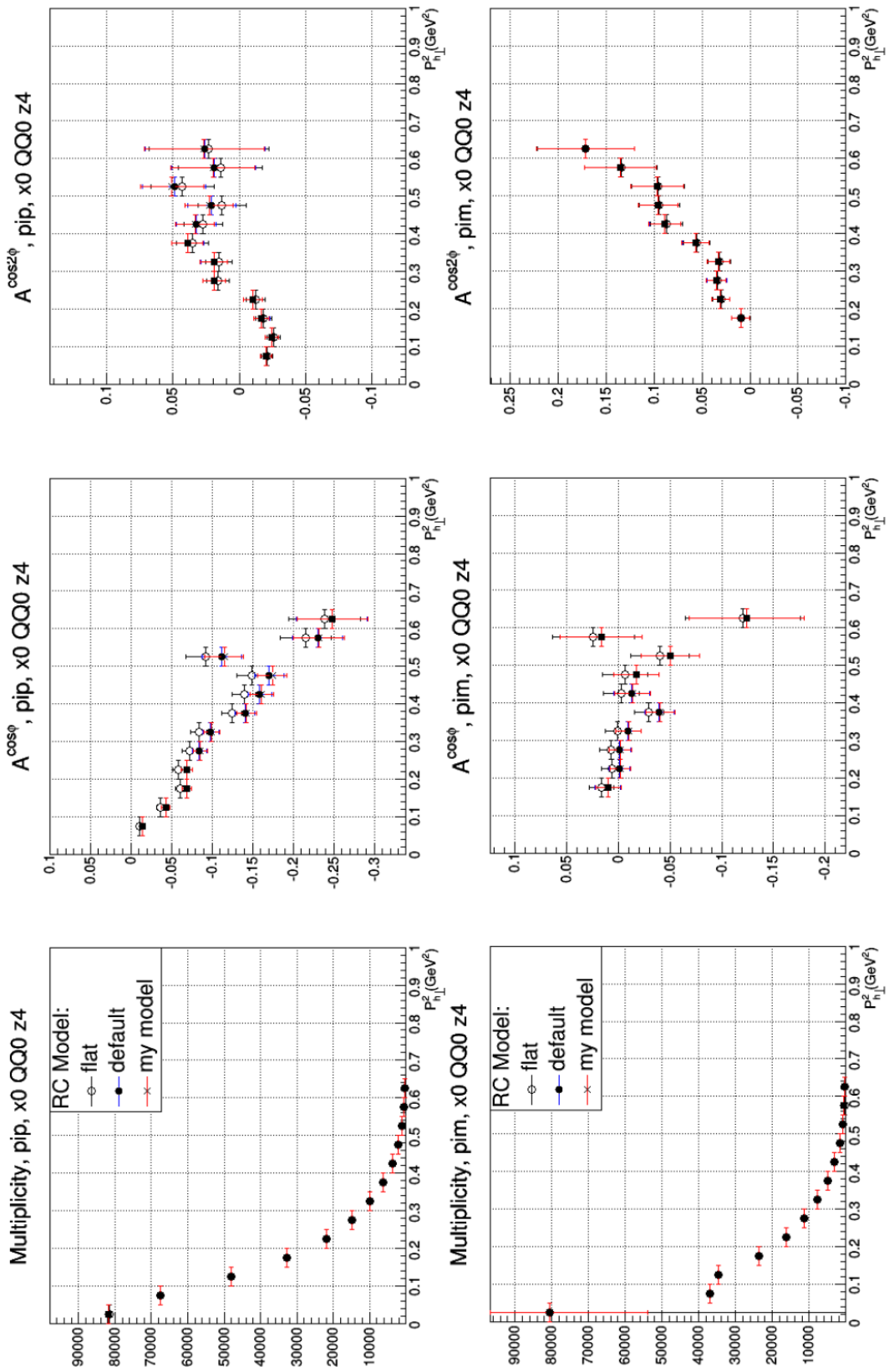

Fig. 5.12: A_0 (left), $A_{UU}^{\cos\phi_h}$ (middle), and $A_{UU}^{\cos 2\phi_h}$ (right) vs $P_{h\perp}^2$ for π^+ (top) and π^- (bottom) for the three different HAPRAD models discussed in the text. These results are for the low Q^2 bin of $0.1 < x < 0.2$, and $0.2 < z < 0.25$.

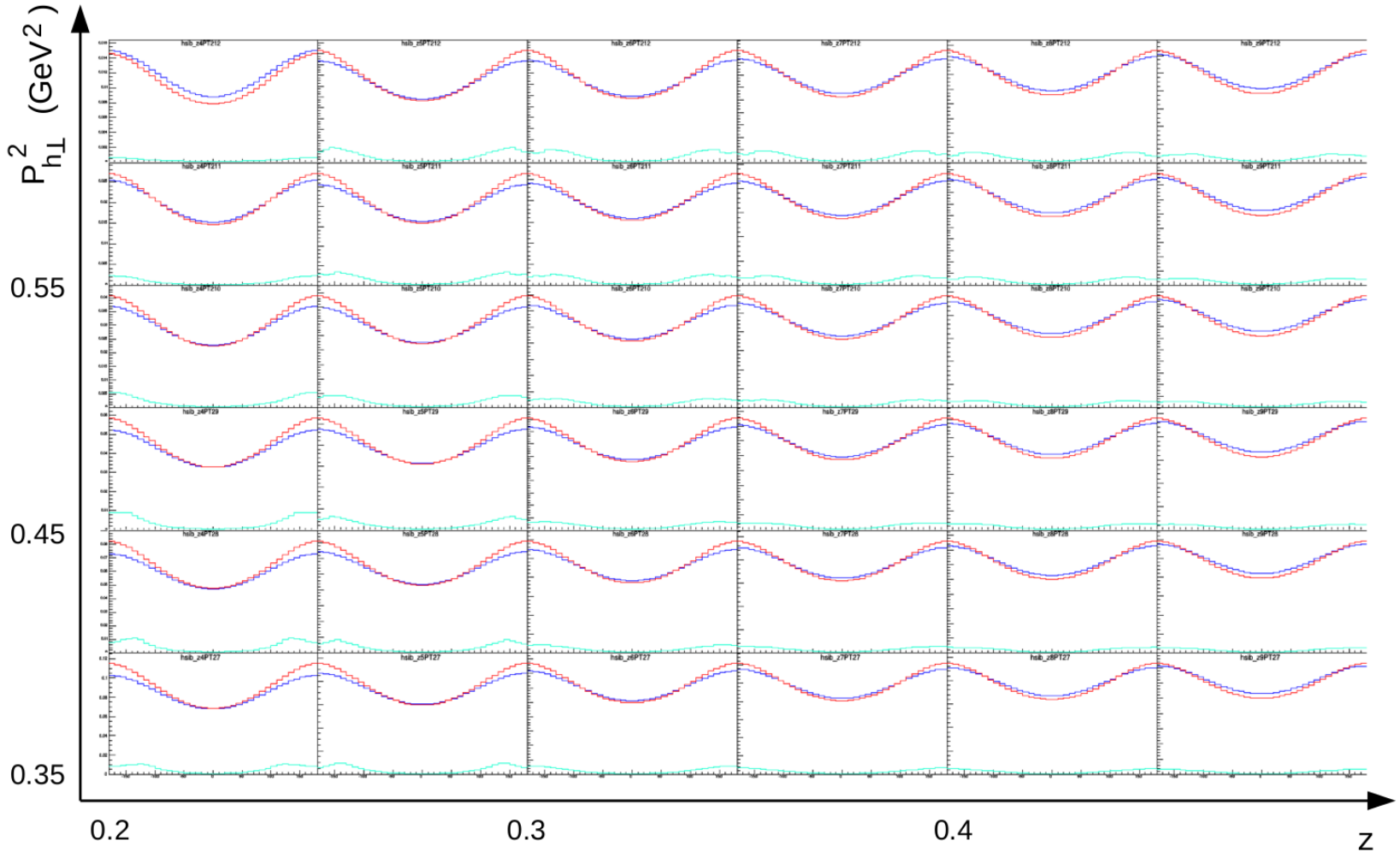

Fig. 5.13: π^+ σ_{Born} (blue), σ_{rad} (red), and σ_{tail} (teal) vs ϕ_h from HAPRAD for iteration 2 in bins of z and $P_{h\perp}^2$ for the lowest x-Q^2 bin.

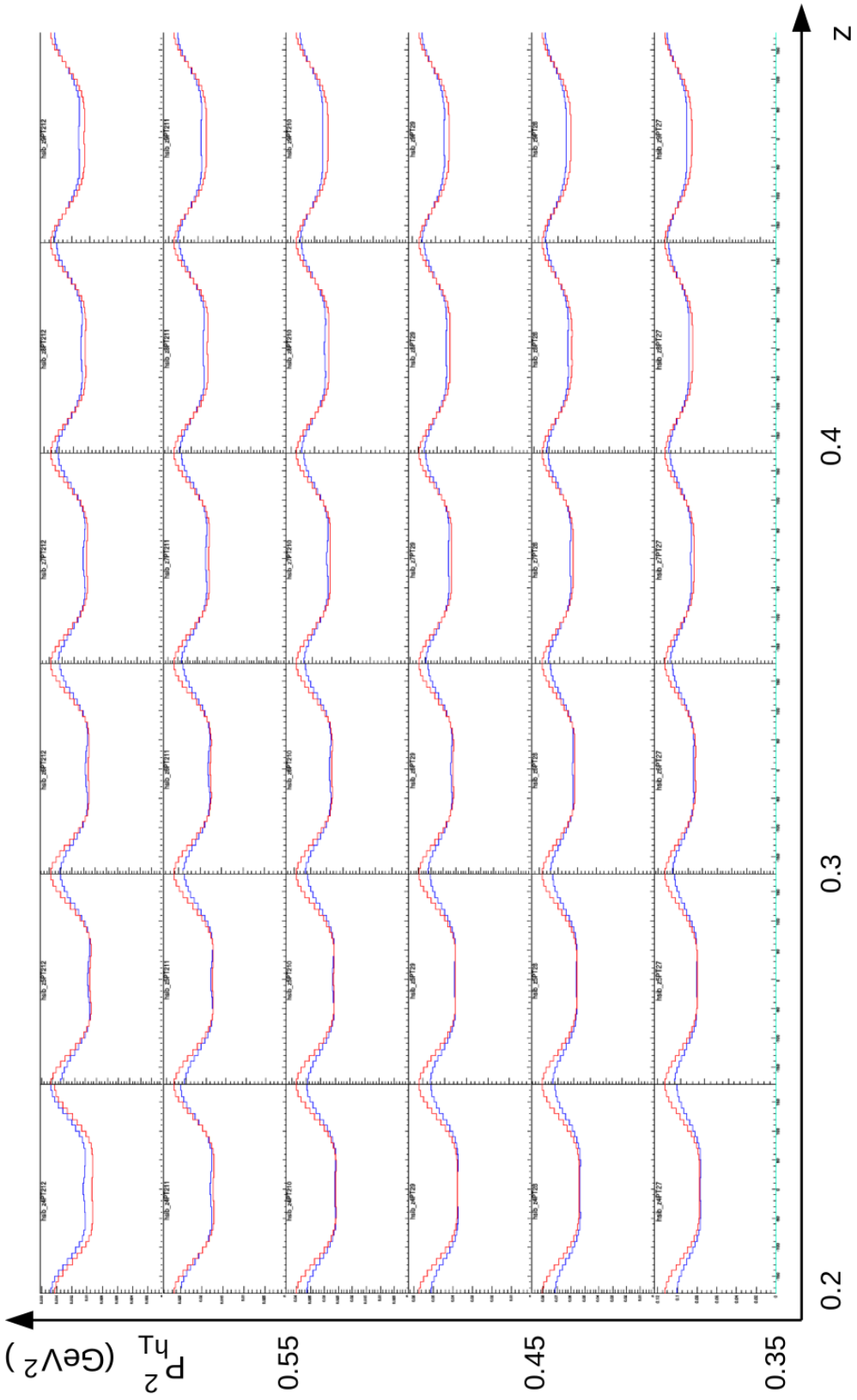

Fig. 5.14: π^- σ_{Born} (blue), σ_{rad} (red), and σ_{tail} (teal) vs ϕ_h from HAPRAD for iteration 2 in bins of z and $P_{h\perp}^2$ for the lowest x-Q^2 bin. For π^-, $\sigma_{tail} = 0$.

5.3 Fitting

The fitting of the ϕ_h distributions to extract A_0, $A_{UU}^{\cos\phi_h}$, and $A_{UU}^{\cos 2\phi_h}$ is done via MINUIT [39] χ^2 minimization algorithms. χ^2 is defined as

$$\chi^2 = \sum_{i,j} (x_i - y_i(a))\, V_{ij}\, (x_j - y_j(a)) \tag{5.4}$$

where V_{ij} is the inverse of the error matrix. If V_{ij} is diagonal, this simplifies to the familiar expression

$$\chi^2 = \sum_i \frac{(x_i - y_i(a))^2}{\sigma_i^2} \tag{5.5}$$

where σ_i^2 is the inverse of the i^{th} diagonal element of V and can be interpreted as the error on the corresponding value of x. The statistical errors quoted in this analysis are those provided by MINUIT.

5.4 Systematic Uncertainties

Since it is not always possible to determine the ideal set of values for a particular analytical technique, estimates of systematic errors are performed here. This is done by making small variations to a particular value, while holding the rest constant, and looking at how the end results change. 13 sources of systematic errors are studied (labeled 0-12), they are given in table 5.1 along with the number of variations and description for each source.

The systematic error on the final result due to a given source is the RMS of the deviations of the modified result from the original, i.e. the error from source i is

$$\Delta^i_{RMS} = \frac{\sqrt{\sum_j^{N_v^i} \Delta_j^2}}{\sqrt{N_v^i}} \tag{5.6}$$

where Δ_j is the difference between the final result with the nominal value and the final result with variation j, and N_v^i is the number of variations for source i. "Final result" refers to the values of A_0, $A_{UU}^{\cos\phi_h}$, and $A_{UU}^{\cos 2\phi_h}$ for each kinematic bin (systematic errors are calculated for each quantity). The sources of systematic error are assumed to be uncorrelated and therefore are added in quadrature to get the total systematic error. In the case of a cut value, there are two variations: a looser cut and a tighter cut. In the case of model dependence, there is one variation: the second to last iteration. Figure 5.17 shows the systematic error contribution of each source on A_0, $A_{UU}^{\cos\phi_h}$, and $A_{UU}^{\cos 2\phi_h}$ for a representitive bin.

Label	**Source**	**# of variations**	**Description**
0	e- z-vertex cut	2	cut value is loosened or tightened by 0.2 cm on each side
1	e- EC sampling cut	2	see figure 5.15
2	e- EC outer vs inner cut	2	cut value is loosened or tightened by 0.005 GeV
3	e- EC geometric cut	2	see figure 5.15
4	e- CC θ matching cut	2	see figure 5.15
5	e- region 1 fiducial cut	2	see figure 5.15
6	e- region 3 fiducial cut	2	see figure 5.15
7	e- CC fiducial cut	2	see figure 5.15
8	pion β cut	2	cut is loosened or tightened by 0.25σ on both the low and high side
9	pion region 1 fiducial cut	2	see figure 5.16
10	ϕ_h fiducial cut	2	a bin (10°) on each side is added or removed
11	acceptance model dependence	1	the second to last iteration is used
12	radiative correction model dependence	1	the second to last iteration is used

Table 5.1: Sources of systematic error studied.

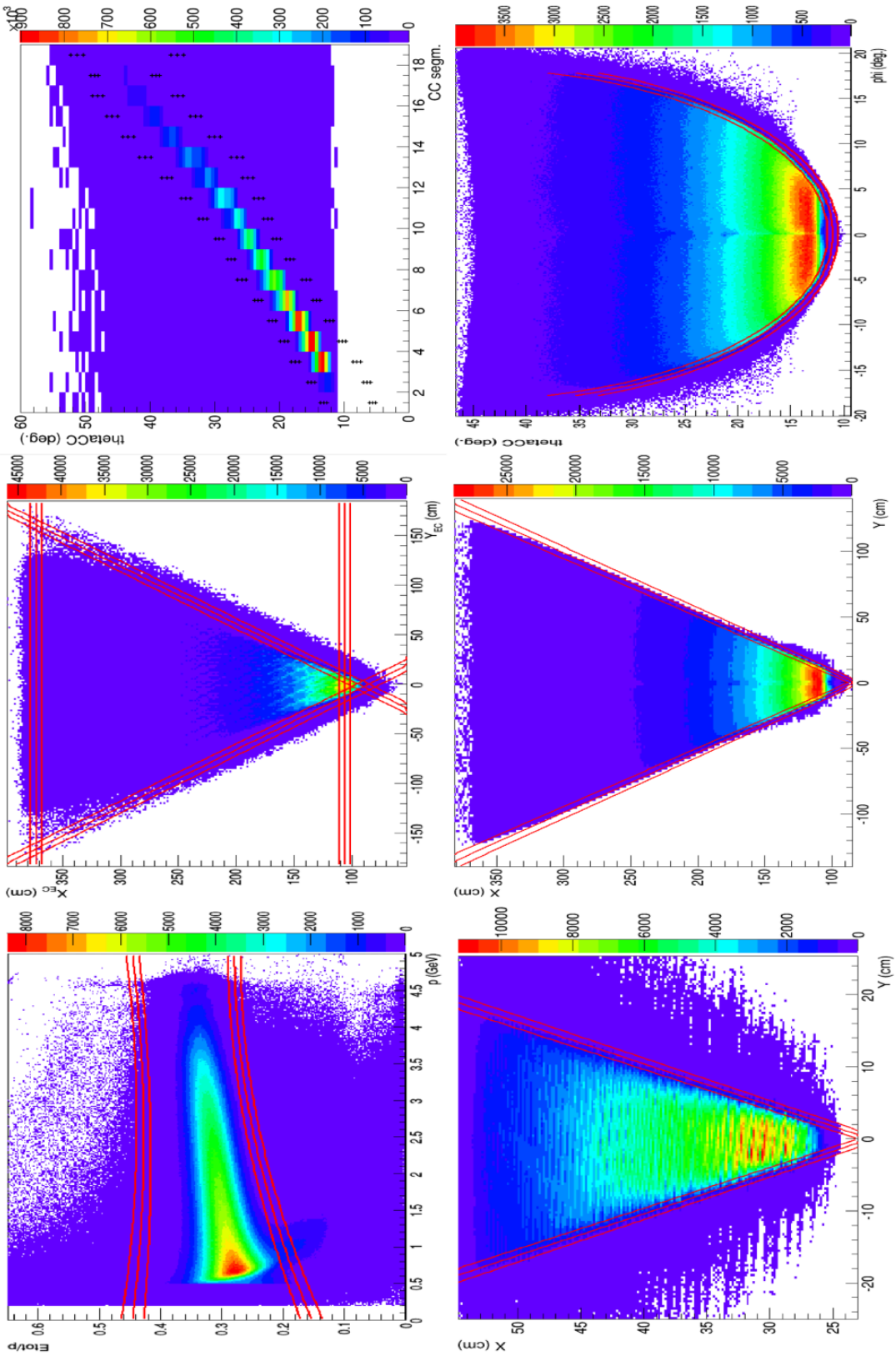

Fig. 5.15: The loose, nominal, and tight cuts for six electron ID plots used for calculating systematic errors.

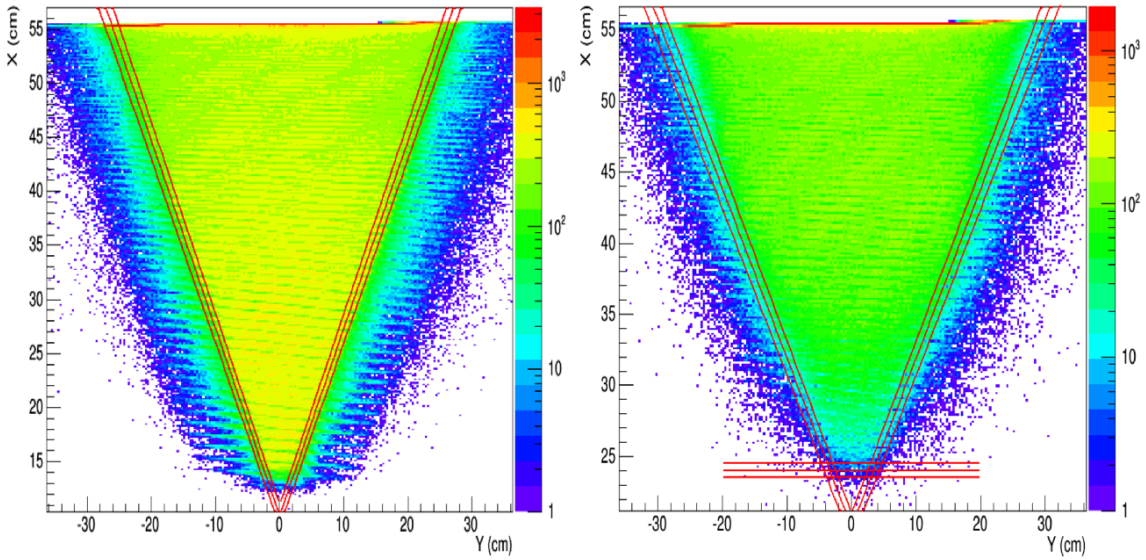

Fig. 5.16: The loose, nominal, and tight cuts for the region 1 fiducial cut for π^+ (left) and π^- (right) used for calculating systematic errors.

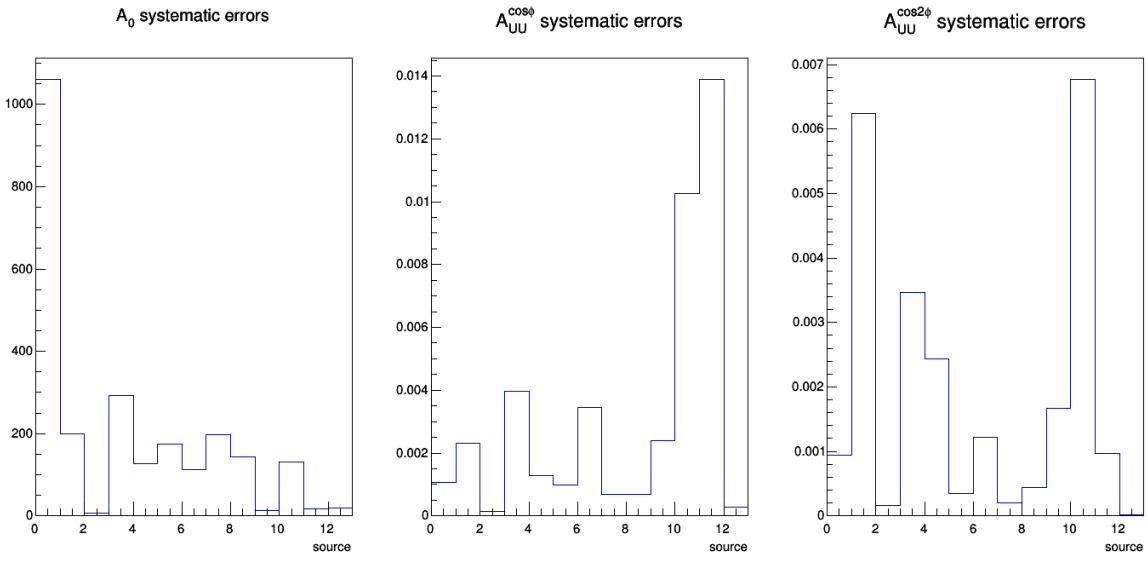

Fig. 5.17: Systematic errors on A_0, $A_{UU}^{\cos\phi_h}$, and $A_{UU}^{\cos 2\phi_h}$ for each source for a representitive bin.

5.5 A_0, $A_{UU}^{\cos\phi_h}$, and $A_{UU}^{\cos 2\phi_h}$

A complete table of results can be found in appendix B. Several representitive plots are shown here in figure 5.18, which shows A_0, $A_{UU}^{\cos\phi_h}$, and $A_{UU}^{\cos 2\phi_h}$ vs $P_{h\perp}^2$ for several z bins for both pion channels.

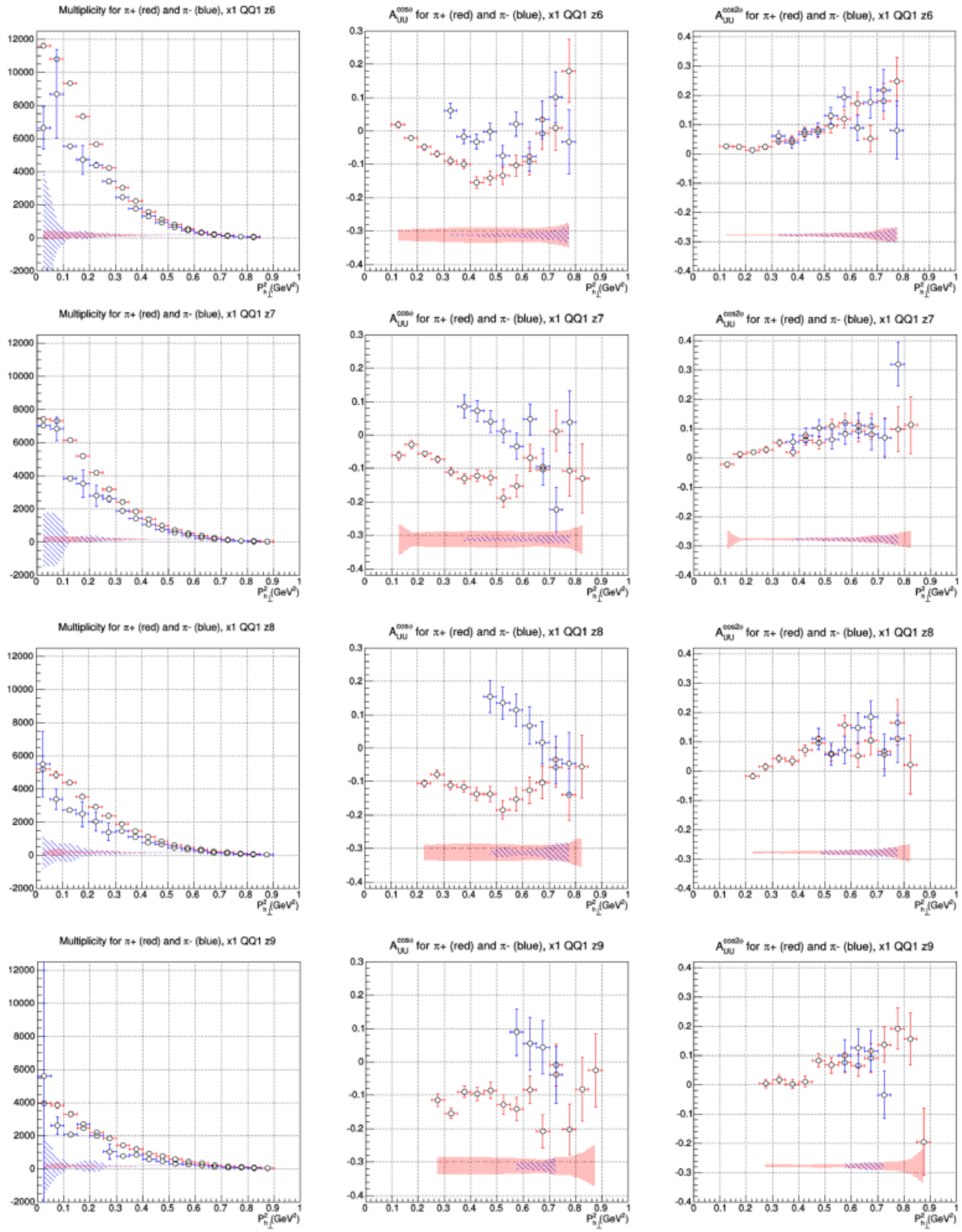

Fig. 5.18: A_0 (left column), $A_{UU}^{\cos\phi_h}$ (right column), and $A_{UU}^{\cos 2\phi_h}$ (right column) vs $P_{h\perp}^2$ for both pion channels. The x-Q^2 bin is fixed (the high Q^2 of $0.2 < x < 0.3$). Several z bins are shown: $0.30 < z < 0.35$ (top row), $0.35 < z < 0.40$ (second row), $0.40 < z < 0.45$ (third row), $0.45 < z < 0.50$ (bottom row).

Chapter 6

Physics Analysis

6.1 Comparison to Other Data

A similar measurement has been published by the CLAS Collaboration using E1-6 data [40]. However, it only measures the π^+ channel and has a more limited kinematic range. A comparison for the π^+ channel in overlapping kinematic ranges is done here (see figure 6.1). [40] uses an alternative definition for the cross-section:

$$\frac{d^5\sigma}{dxdQ^2dzdp_T^2d\phi} = \frac{2\pi\alpha^2}{xQ^4}\frac{E_h}{|p_\parallel|}\xi\left[\epsilon\mathcal{H}_1 + \mathcal{H}_2 + 2(2-y)\sqrt{\frac{\kappa}{\xi}}\cos\phi\mathcal{H}_3 + 2\kappa\cos 2\phi\mathcal{H}_4\right] \tag{6.1}$$

where $\xi = 1 - y - \frac{1}{4}\gamma^2y^2$ and $\kappa = \frac{1}{1+\gamma^2}$; and reports the values of $\mathcal{H}_3/(\mathcal{H}_2 + \epsilon\mathcal{H}_1)$ and $\mathcal{H}_4/(\mathcal{H}_2 + \epsilon\mathcal{H}_1)$. To have a meaningful comparison, then, $\mathcal{H}_3/(\mathcal{H}_2 + \epsilon\mathcal{H}_1)$ and $\mathcal{H}_4/(\mathcal{H}_2 + \epsilon\mathcal{H}_1)$ are multiplied by $2(2-y)\sqrt{\frac{\kappa}{\xi}}$ and 2κ, respectively, to convert them to $A_{UU}^{\cos\phi_h}$ and $A_{UU}^{\cos 2\phi_h}$.[1]

[1] The notation in this paragraph is that of [40], which differs slightly from mine. The correspondence is $p_T^2 \to P_{h\perp}^2$ and $\phi \to \phi_h$.

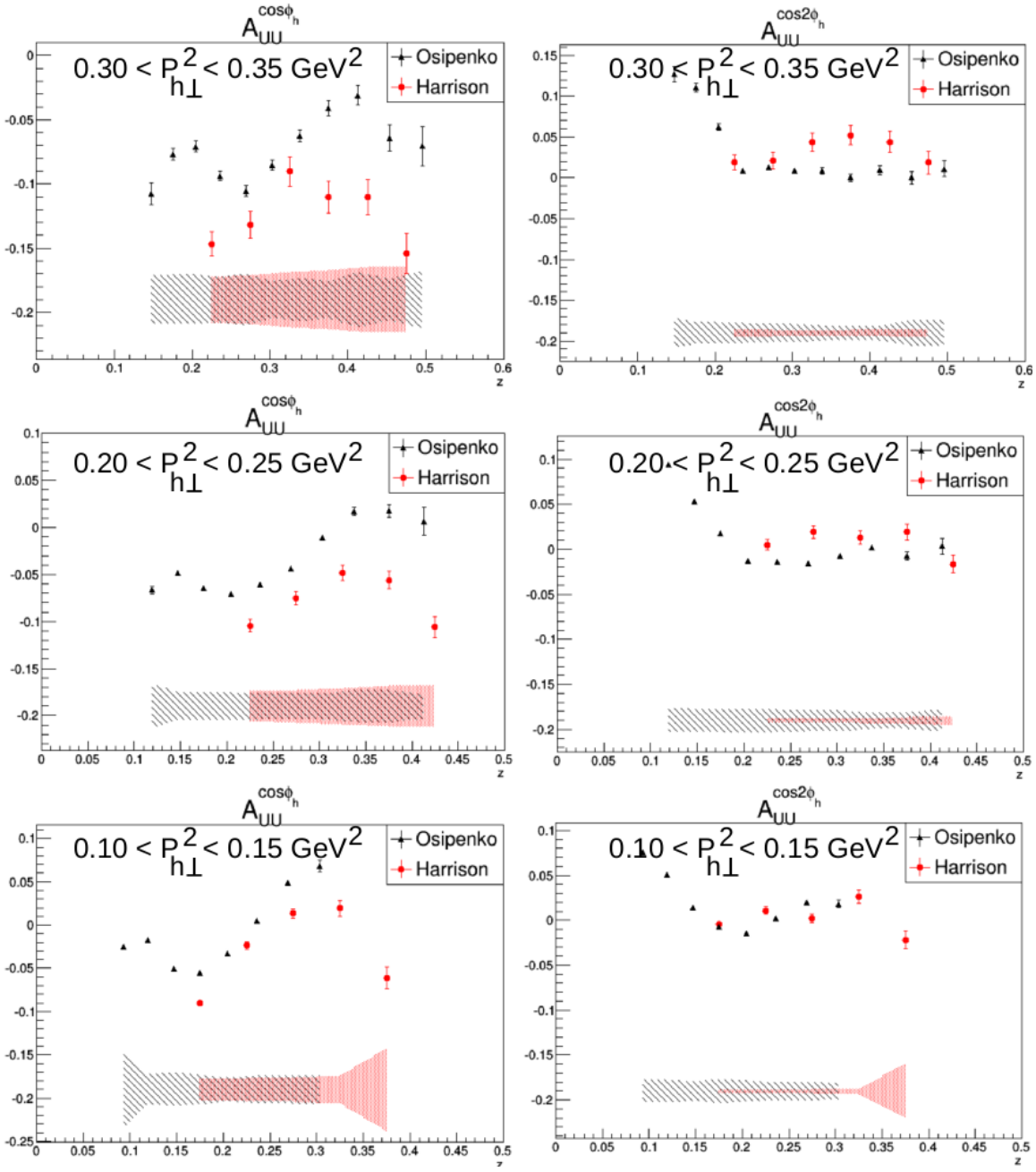

Fig. 6.1: A comparison between π^+ results in this analysis and a previous CLAS analysis. The x-Q^2 bin here is the high Q^2 bin for $0.2 < x < 0.3$.

6.2 Conclusion

The multiplicity, $\cos\phi_h$ moment, and $\cos 2\phi_h$ moment of the unpolarized SIDIS cross-section have been measured for both charged pion channels in a fully differential way with good statistics over a wide kinematic range ($0.1 < x < 0.6$, $1.0 < Q^2 < 4.7$ GeV^2, $0.0 < z < 0.9$, $0.0 < P_{h\perp}^2 < 1.0$ GeV^2, $-180^\circ < \phi_h < 180^\circ$) in conjunction with the CLAS Collaboration. The $\cos\phi_h$ and $\cos 2\phi_h$ modulations show a clear dependence on flavor which hints at a non-zero Boer-Mulders effect [41] [42] [43] [44] and could give insights into the quark orbital angular momentum (L_q) contribution of the proton spin; but more intensive theoretical comparisons, which are currently in progress, are needed first. Results show a reasonable agreement with a previous CLAS measurement in overlapping kinematics with some discrepancies that may be the result of different kinematic cuts. For example, [40] does not have a cut on y to reduce events with potentially problematic radiative effects. Also, [40] uses a missing mass cut of 1.04 GeV (vs the 1.35 GeV cut used here) and could therefore have a significant contribution from Δs.

The study of nucleon structure via the accessing of TMDs is a major thrust of up-and-coming nuclear physics projects such as CLAS12 [45] and the proposed Electron-Ion Collider (EIC) [46]. A CLAS Collaboration proposal to continue studies of the Boer-Mulders function at higher energies at CLAS12 has been given the highest priority rating by PAC 30 [47]. Many of the challenges associated with precision measurements of this type have been addressed here. Furthermore,

the two experiments (this one and the future one at CLAS12) will have some overlapping kinematics and some unique kinematics, and therefore this analysis will be valuable both in its own right and for comparison purposes. In conclusion, the work described in this dissertation has improved our understanding of this field and provided a solid foundation for future advancements.

Bibliography

[1] R.W. McAllister and R. Hofstader, Phys. Rev. **102**, 851 (1956).

[2] M.R. Yearian and R. Hofstader, Phys. Rev. **110**, 552 (1958).

[3] M. Gell-Mann, "The Eightfold Way: A Theory of Strong Interaction Symmetry," Caltech Synchrotron Laboratory Report No. CTSL-20 (1961).

[4] Y. Ne'eman, Nucl. Phys. **26**, 222 (1961).

[5] M. Gell-Mann, Phys. Lett. **8**, 214 (1964).

[6] G. Zweig, "An SU_3 Model for Strong Interaction Symmetry and Its Breaking," CERN Report No. TH 412 (Geneva, 1964).

[7] G. Zweig, "Fractionally Charged Particles and SU_6," Symmetries in Elementary Particle Physics (Academic Press, New York, 1965), p. 192.

[8] SLAC-MIT-CIT Collaboration, "Proposals for Initial Electron Scattering Experiments Using the SLAC Spectrometer Facilities," Stanford Linear Accelerator Center Proposal No.4 (January 1966)

[9] J.D. Bjorken and E.A. Paschos, "Inelastic Electron Proton and gamma Proton Scattering, and the Structure of the Nucleon," Phys. Rev. **185**, 1975 (1969).

[10] R.P. Feynman, "Very High-Energy Collision of Hadrons," Phys. Rev. Lett. **23**, 1415 (1969).

[11] C. S. Deans, "Progress in the NNPDF Global Analysis," hep-ph/1304.2781 (2013).

[12] European Muon Collaboration, "A measurement of the spin asymmetry and determination of the structure function g_1 in deep inelastic muon-proton scattering," Phys. Rev. B, Vol. 206, Issue 2, 364-370 (1988).

[13] J. C. Collins, "Leading twist single transverse-spin asymmetries: Drell-Yan and deep inelastic scattering," Phys. Lett. B536 43-48, (2002).

[14] B. Pasquini, "Sivers and Boer-Mulders functions in Light-Cone Quark Models," Phys. Rev. D81 114013, (2010).

[15] R.L. Jaffe, "Spin, Twist and Hadron Structure in Deep Inelastic Processes," hep-ph/9602236 (1996).

[16] D. Boer and P.J. Mulders, Phys. Rev. **D57**, 5780 (1998), hep-ph/9711485.

[17] A. Bacchetta, U. D'Alesio, M. Diehl, and C. A. Miller, Phys. Rev. **D70**, 117504 (2004), hep-ph/0410050.

[18] A. Bacchetta *et al.*, JHEP 0702:093 (2007), hep-ph/0611265v2.

[19] J. C. Collins, D. E. Soper, and G. Sterman, "Factorization of Hard Processes in QCD," Adv. Ser. Direct. High Energy Phys., 5:1-91, (1988).

[20] G. Sterman *et al.*, "Handbook of perturbative QCD," Rev. Mod. Phys., 67(1):157-248, (1995).

[21] A. Airapetian *et al.*, Phys. Rev. Lett. 94 012002 (2005).

[22] G. A. Miller, Phys. Rev. C 76 065209 (2007).

[23] R. Jacob, P. J. Mulders, and J. Rodrigues, Nucl. Phys. **A626**, 937 (1997).

[24] B. Pasquini, S. Cazzaniga, and S. Boffi, Phys. Rev. **D78**, 034025 (2008).

[25] A. Bacchetta, F. Conti, and M. Radici, Phys. Rev. **D78**, 074010 (2008).

[26] H. Avakian, A. V. Efremov, P. Schweitzer, and F. Yuan, Phys. Rev. **D81**, 074035 (2010).

[27] M. Hirai, S. Kumano, T. H. Nagai, and K. Sudoh, Phys. Rev. **D75**, 094009 (2007).

[28] S. Nam, C. Kao, and B. Yu, Few Body Syst. 54 251-254 (2013).

[29] R. Cahn, "Azimuthal dependence in leptoproduction: A simple parton model calculation," Phys. Lett. B 78(2-3), 269-273, (1978).

[30] CLAS Collaboration, B. Mecking *et al.*, Nucl.Instrum.Meth. **A503**, 513 (2003).

[31] M. Mestayer *et al.*, Nucl.Instrum.Meth. **A449**, 81 (2000).

[32] G. Adams, V. Burkert *et al.*, Nucl.Instrum.Meth. **A465**, 414 (2001).

[33] E.S. Smith, T. Carstens *et al.*, Nucl.Instrum.Meth. **A432**, 265 (1999).

[34] M. Amarian *et al.*, Nucl.Instrum.Meth. **A460**, 239 (2001).

[35] W. Gohn *et al.*, Phys. Rev. D89 (2014) 072011.

[36] M. Mirazita, https://www.jlab.org/Hall-B/secure/e1f/mirazita/momcorr/note_momcorr.pdf

[37] I. Akushevich, N. Shumeiko, and A. Soroko, Eur. Phys. J **C10** (1999) 681.

[38] I. Akushevich *et al.*, Phys. Lett. B672 (2009) 35-44.

[39] F. James, "MINUIT Reference Manual," CERN Program Library Writeup D506.

[40] M. Osipenko *et al.*, Phys. Rev. D80 032004 (2009).

[41] L. P. Gamberg, G. R. Goldstein, and M. Schlegel, Phys. Rev. D77 094016 (2008).

[42] V. Barone, A. Prokudin, and B. Ma, Phys. Rev. D78 045022 (2008).

[43] B. Zhang, Z. Lu, B. Ma, and I. Schmidt, Phys. Rev. D78 094035 (2008).

[44] V. Barone, A. Prokudin, and S. Melis, Phys. Rev. D81 114026 (2010).

[45] V. D. Burkert, "CLAS12 and its initial Science Program at the Jefferson Lab Upgrade," *arxiv:* 0810:4718 (2008).

[46] D. Boer *et al.*, "A report on the joint BNL/INT/JLab program on the science case for an Electron-Ion Collider," Institute for Nuclear Theory, Seattle (2011).

[47] H. Avakian *et al.*, "Probing the Proton's Quark Dynamics in SIDIS at 12 GeV," JLab Experiment E12-06-112 (2006).

Appendix A

Good Run List

37658 37659 37661 37662 37664 37665 37666 37667 37670 37672 37673 37674 37675

37677 37678 37679 37680 37681 37683 37684 37685 37686 37687 37688 37689 37690

37691 37692 37693 37694 37698 37699 37700 37701 37702 37703 37704 37705 37706

37707 37708 37709 37710 37711 37712 37713 37714 37715 37716 37717 37719 37721

37722 37723 37724 37725 37726 37740 37744 37745 37746 37747 37748 37750 37753

37762 37763 37766 37767 37769 37770 37772 37773 37775 37776 37778 37780 37781

37782 37783 37784 37785 37788 37789 37790 37801 37802 37803 37804 37805 37806

37807 37808 37809 37810 37811 37812 37813 37814 37815 37816 37817 37818 37819

37820 37822 37823 37824 37825 37828 37831 37832 37833 37844 37845 37846 37847

37848 37849 37850 37851 37852 38046 38047 38048 38049 38050 38051 38052 38053

38070 38071 38072 38074 38075 38076 38077 38078 38079 38080 38081 38082 38083

38084 38085 38086 38089 38090 38091 38092 38093 38094 38095 38096 38097 38098

38099 38100 38114 38117 38118 38119 38120 38121 38122 38131 38132 38133 38134

38135 38136 38137 38138 38139 38140 38141 38142 38143 38144 38146 38172 38173

38174 38175 38176 38177 38182 38183 38184 38185 38186 38187 38188 38189 38190

38191 38192 38194 38195 38196 38197 38198 38199 38200 38201 38203 38204 38205

38206 38207 38208 38209 38210 38211 38212 38213 38214 38215 38216 38217 38218

38219 38220 38221 38222 38223 38225 38226 38265 38266 38268 38271 38272 38273

38274 38275 38276 38277 38278 38283 38284 38285 38286 38288 38289 38290 38300

38301 38302 38304 38305 38306 38307 38309 38310 38312 38313 38314 38315 38317

38318 38320 38322 38328 38331 38337 38338 38341 38342 38344 38346 38347 38350

38351 38353 38354 38355 38356 38359 38360 38364 38365 38378 38379 38380 38381

38382 38383 38384 38385 38387 38388 38389 38390 38391 38392 38393 38394 38395

38396 38397 38398 38399 38400 38401 38402 38403 38404 38405 38408 38409 38410

38411 38412 38415 38417 38418 38419 38420 38421 38422 38423 38430 38431 38432

38433 38434 38435 38436 38437 38438 38440 38441 38443 38446 38447 38449 38450

38451 38452 38453 38454 38455 38456 38457 38458 38459 38460 38461 38462 38463

38464 38465 38466 38467 38468 38469 38470 38471 38472 38473 38474 38475 38476

38477 38479 38480 38483 38484 38485 38486 38487 38488 38489 38490 38491 38492

38493 38494 38495 38497 38498 38499 38500 38501 38507 38508 38509 38510 38511

38512 38513 38514 38515 38516 38517 38518 38519 38520 38521 38522 38523 38524

38525 38526 38527 38528 38529 38530 38531 38534 38536 38537 38538 38539 38540

38541 38542 38543 38544 38545 38548 38549 38550 38551 38552 38553 38554 38558

38559 38560 38561 38562 38563 38568 38571 38572 38573 38574 38575 38576 38577

38578 38579 38580 38581 38582 38583 38584 38585 38596 38597 38598 38600 38601

38602 38603 38604 38606 38607 38608 38609 38610 38611 38612 38613 38614 38616

38617 38618 38619 38620 38621 38622 38623 38624 38625 38626 38627 38628 38629

38630 38631 38632 38633 38634 38635 38636 38637 38638 38639 38640 38641 38642

38645 38646 38647 38648 38649 38650 38651 38652 38653 38654 38655 38656 38670

38671 38672 38673 38674 38675 38676 38677 38681 38682 38684 38685 38686 38687

38689 38690 38691 38692 38693 38694 38696 38697 38698 38699 38700 38701 38702

38703 38704 38705 38706 38707 38708 38709 38710 38711 38712 38713 38714 38715

38716 38717 38719 38720 38721 38722 38723 38724 38725 38727 38728 38729 38730

38731 38732 38733 38734 38735 38737 38738 38739 38740 38743 38744 38745 38746

38748 38749 38750 38751

Appendix B

Tables of Results

Table B.1: Table of results for π^+. The Δ quantities are statistical uncertainty and the δ quantities are systematic uncertainty. The x, Q^2, z, and $P_{h\perp}^2$ values refer to the bin number (starting with 0), not the value. Bins where nothing is measure are omitted; in bins where only the multiplicity is measured, the moments have a value of "n.m." for no measurement.

x	Q^2	z	$P_{h\perp}^2$	A_0	ΔA_0	δA_0	$A_{UU}^{\cos\phi_h}$	$\Delta A_{UU}^{\cos\phi_h}$	$\delta A_{UU}^{\cos\phi_h}$	$A_{UU}^{\cos 2\phi_h}$	$\Delta A_{UU}^{\cos 2\phi_h}$	$\delta A_{UU}^{\cos 2\phi_h}$
0	0	1	0	516500.0	812.8	29471.1	-0.1522	0.0025	0.0163	-0.0162	0.0024	0.0025
0	0	2	0	224535.0	479.8	12355.3	-0.0863	0.0034	0.0163	0.0265	0.0031	0.0065
0	0	2	1	164948.0	349.6	9236.6	-0.1937	0.0033	0.0172	-0.0010	0.0033	0.0051
0	0	2	2	82805.3	224.0	4651.4	-0.2201	0.0042	0.0168	-0.0183	0.0043	0.0056
0	0	2	3	32766.6	111.3	1835.8	-0.2576	0.0047	0.0196	-0.0022	0.0047	0.0037
0	0	3	0	138155.0	457.5	7418.4	-0.0198	0.0055	0.0245	0.0454	0.0043	0.0098
0	0	3	1	101719.0	281.1	5511.7	-0.0910	0.0044	0.0168	-0.0031	0.0041	0.0040
0	0	3	2	63829.7	208.7	3395.1	-0.1210	0.0052	0.0158	-0.0404	0.0050	0.0090
0	0	3	3	40287.9	159.4	2133.7	-0.1429	0.0062	0.0166	-0.0342	0.0062	0.0078
0	0	3	4	24624.8	105.5	1401.4	-0.1386	0.0061	0.0168	0.0082	0.0061	0.0064

Continued on next page

Table B.1 – *Continued from previous page*

x	Q^2	z	$P_{h\perp}^2$	A_0	ΔA_0	δA_0	$A_{UU}^{\cos\phi_h}$	$\Delta A_{UU}^{\cos\phi_h}$	$\delta A_{UU}^{\cos\phi_h}$	$A_{UU}^{\cos 2\phi_h}$	$\Delta A_{UU}^{\cos 2\phi_h}$	$\delta A_{UU}^{\cos 2\phi_h}$
0	0	3	5	13252.5	70.5	754.8	-0.1815	0.0075	0.0169	0.0014	0.0076	0.0058
0	0	3	6	6700.8	46.1	400.9	-0.1993	0.0097	0.0181	0.0286	0.0097	0.0054
0	0	3	7	3272.1	30.3	187.3	-0.2209	0.0128	0.0171	-0.0083	0.0132	0.0067
0	0	3	8	1734.4	23.1	95.3	-0.3435	0.0183	0.0283	0.0559	0.0183	0.0075
0	0	4	0	81760.7	798.0	4779.5	n.m.	n.m.	n.m.	n.m.	n.m.	n.m.
0	0	4	1	67563.7	213.7	3594.1	-0.0146	0.0046	0.0154	-0.0200	0.0042	0.0047
0	0	4	2	48078.3	170.4	2470.1	-0.0430	0.0050	0.0142	-0.0243	0.0050	0.0064
0	0	4	3	32844.7	137.9	1691.0	-0.0690	0.0060	0.0164	-0.0166	0.0060	0.0070
0	0	4	4	21990.9	109.7	1160.6	-0.0692	0.0071	0.0155	-0.0099	0.0072	0.0051
0	0	4	5	14947.0	88.3	811.8	-0.0855	0.0085	0.0172	0.0192	0.0085	0.0078
0	0	4	6	9919.2	69.4	549.8	-0.0995	0.0100	0.0184	0.0193	0.0100	0.0053
0	0	4	7	6258.5	52.3	346.7	-0.1424	0.0120	0.0177	0.0392	0.0119	0.0111
0	0	4	8	3760.0	38.4	202.1	-0.1614	0.0146	0.0161	0.0334	0.0146	0.0085
0	0	4	9	2178.9	27.9	122.2	-0.1743	0.0180	0.0190	0.0228	0.0183	0.0077
0	0	4	10	1219.2	20.3	64.6	-0.1152	0.0239	0.0172	0.0507	0.0236	0.0144
0	0	4	11	710.1	15.8	41.2	-0.2319	0.0311	0.0192	0.0198	0.0317	0.0167
0	0	4	12	377.5	12.0	22.4	-0.2486	0.0440	0.0358	0.0265	0.0451	0.0194
0	0	5	0	67604.1	431.5	6307.5	n.m.	n.m.	n.m.	n.m.	n.m.	n.m.
0	0	5	1	43831.4	214.3	2435.0	-0.0118	0.0081	0.0331	-0.0434	0.0066	0.0204
0	0	5	2	33937.8	143.4	1701.9	-0.0304	0.0060	0.0142	-0.0371	0.0057	0.0064
0	0	5	3	25218.9	121.9	1285.7	-0.0364	0.0069	0.0154	-0.0283	0.0067	0.0075
0	0	5	4	17737.3	101.3	886.6	-0.0721	0.0081	0.0166	-0.0140	0.0080	0.0052
0	0	5	5	12524.0	84.9	637.8	-0.0844	0.0098	0.0178	0.0199	0.0096	0.0057
0	0	5	6	8724.9	70.0	443.3	-0.0705	0.0115	0.0179	0.0002	0.0115	0.0069
0	0	5	7	6081.0	57.7	321.8	-0.0772	0.0136	0.0186	0.0086	0.0137	0.0085
0	0	5	8	4318.5	47.7	220.9	-0.1170	0.0158	0.0183	0.0193	0.0160	0.0082
0	0	5	9	3001.7	38.9	168.5	-0.0963	0.0188	0.0231	0.0553	0.0186	0.0093
0	0	5	10	1960.1	30.6	102.6	-0.0931	0.0224	0.0191	0.0244	0.0223	0.0120
0	0	5	11	1243.8	23.6	71.2	-0.1044	0.0277	0.0173	0.0855	0.0265	0.0107
0	0	5	12	762.3	18.2	40.7	-0.0934	0.0346	0.0196	0.0610	0.0338	0.0336
0	0	5	13	465.3	14.0	25.9	-0.0888	0.0438	0.0265	0.0598	0.0420	0.0319
0	0	5	14	260.7	10.5	14.4	-0.1001	0.0578	0.0482	0.0261	0.0584	0.0353
0	0	5	15	156.1	8.5	10.3	-0.0800	0.0783	0.0339	0.0710	0.0768	0.0417
0	0	5	16	85.4	7.3	9.6	n.m.	n.m.	n.m.	n.m.	n.m.	n.m.
0	0	6	0	42046.4	348.8	2608.4	n.m.	n.m.	n.m.	n.m.	n.m.	n.m.
0	0	6	1	28722.3	3467.8	3501.0	n.m.	n.m.	n.m.	n.m.	n.m.	n.m.
0	0	6	2	23477.8	140.7	1176.9	-0.0010	0.0096	0.0185	-0.0251	0.0082	0.0104
0	0	6	3	17977.9	100.9	894.6	-0.0241	0.0081	0.0165	-0.0187	0.0077	0.0050
0	0	6	4	13387.1	85.9	667.6	-0.0662	0.0091	0.0171	-0.0265	0.0089	0.0037

Continued on next page

Table B.1 – *Continued from previous page*

x	Q^2	z	$P_{h\perp}^2$	A_0	ΔA_0	δA_0	$A_{UU}^{\cos\phi_h}$	$\Delta A_{UU}^{\cos\phi_h}$	$\delta A_{UU}^{\cos\phi_h}$	$A_{UU}^{\cos 2\phi_h}$	$\Delta A_{UU}^{\cos 2\phi_h}$	$\delta A_{UU}^{\cos 2\phi_h}$
0	0	6	5	9832.5	73.8	484.1	-0.0913	0.0108	0.0192	0.0065	0.0105	0.0075
0	0	6	6	7194.2	64.1	358.8	-0.1001	0.0129	0.0193	0.0092	0.0124	0.0056
0	0	6	7	5142.1	54.0	253.8	-0.1236	0.0151	0.0190	0.0082	0.0150	0.0107
0	0	6	8	3598.0	44.7	179.5	-0.1201	0.0179	0.0198	0.0100	0.0178	0.0072
0	0	6	9	2699.3	39.1	133.5	-0.1465	0.0209	0.0191	0.0301	0.0214	0.0140
0	0	6	10	2040.7	34.7	112.3	-0.1664	0.0252	0.0258	0.1072	0.0240	0.0108
0	0	6	11	1391.2	27.7	70.2	-0.0928	0.0295	0.0187	0.0994	0.0281	0.0211
0	0	6	12	949.5	22.7	51.5	-0.0587	0.0357	0.0382	0.1130	0.0343	0.0189
0	0	6	13	661.7	18.7	37.5	-0.1291	0.0419	0.0325	0.0973	0.0406	0.0193
0	0	6	14	378.1	13.2	21.0	-0.0361	0.0512	0.0301	0.0644	0.0513	0.0350
0	0	6	15	241.3	10.7	14.6	0.0209	0.0653	0.0368	0.0912	0.0610	0.0296
0	0	6	16	170.4	9.9	10.2	-0.0728	0.0857	0.1194	0.0983	0.0807	0.0570
0	0	6	17	99.6	7.9	7.7	-0.2200	0.1153	0.0620	0.1311	0.1166	0.1025
0	0	6	18	70.8	8.3	8.5	n.m.	n.m.	n.m.	n.m.	n.m.	n.m.
0	0	7	0	26551.0	277.6	6696.5	n.m.	n.m.	n.m.	n.m.	n.m.	n.m.
0	0	7	1	24096.5	208.9	1646.7	n.m.	n.m.	n.m.	n.m.	n.m.	n.m.
0	0	7	2	15603.6	313.0	921.3	n.m.	n.m.	n.m.	n.m.	n.m.	n.m.
0	0	7	3	12741.1	98.6	611.8	0.0159	0.0123	0.0276	0.0148	0.0103	0.0143
0	0	7	4	9421.8	69.0	473.0	-0.0562	0.0107	0.0203	0.0009	0.0100	0.0076
0	0	7	5	7089.3	59.2	360.2	-0.0942	0.0119	0.0200	-0.0204	0.0116	0.0050
0	0	7	6	5383.3	52.3	255.1	-0.0942	0.0139	0.0219	-0.0030	0.0135	0.0082
0	0	7	7	3917.9	44.7	195.8	-0.1440	0.0161	0.0207	-0.0307	0.0160	0.0059
0	0	7	8	2925.3	39.0	148.4	-0.1531	0.0189	0.0213	-0.0237	0.0190	0.0204
0	0	7	9	2173.3	34.3	112.6	-0.1180	0.0230	0.0252	0.0277	0.0228	0.0138
0	0	7	10	1591.5	29.5	82.4	-0.1414	0.0272	0.0256	0.0441	0.0263	0.0146
0	0	7	11	1206.8	26.2	66.8	-0.1028	0.0324	0.0216	0.1009	0.0306	0.0169
0	0	7	12	890.6	22.6	46.4	-0.1643	0.0369	0.0241	0.0745	0.0358	0.0177
0	0	7	13	643.6	19.1	32.2	-0.0950	0.0432	0.0206	0.0434	0.0422	0.0173
0	0	7	14	463.1	16.7	26.9	-0.2495	0.0534	0.0450	0.0830	0.0525	0.0306
0	0	7	15	297.1	12.8	19.8	-0.0536	0.0635	0.0334	0.0992	0.0641	0.0371
0	0	7	16	218.0	11.9	15.1	-0.1675	0.0801	0.0539	0.0892	0.0849	0.0298
0	0	7	17	136.7	9.6	7.9	-0.1671	0.1074	0.0724	0.2906	0.0906	0.0656
0	0	7	18	84.8	7.6	10.6	n.m.	n.m.	n.m.	n.m.	n.m.	n.m.
0	0	7	19	45.4	7.2	13.0	n.m.	n.m.	n.m.	n.m.	n.m.	n.m.
0	0	8	0	11607.3	140.5	4277.5	n.m.	n.m.	n.m.	n.m.	n.m.	n.m.
0	0	8	1	14067.1	2344.7	2709.5	n.m.	n.m.	n.m.	n.m.	n.m.	n.m.
0	0	8	2	10460.1	1992.1	2250.7	n.m.	n.m.	n.m.	n.m.	n.m.	n.m.
0	0	8	3	8799.1	228.3	484.5	n.m.	n.m.	n.m.	n.m.	n.m.	n.m.
0	0	8	4	6957.5	59.4	337.0	-0.0261	0.0128	0.0228	0.0356	0.0113	0.0090

Continued on next page

Table B.1 – *Continued from previous page*

x	Q^2	z	$P_{h\perp}^2$	A_0	ΔA_0	δA_0	$A_{UU}^{\cos\phi_h}$	$\Delta A_{UU}^{\cos\phi_h}$	$\delta A_{UU}^{\cos\phi_h}$	$A_{UU}^{\cos 2\phi_h}$	$\Delta A_{UU}^{\cos 2\phi_h}$	$\delta A_{UU}^{\cos 2\phi_h}$
0	0	8	5	5247.1	49.6	250.3	-0.0744	0.0138	0.0256	0.0131	0.0128	0.0101
0	0	8	6	4026.6	43.2	197.7	-0.0745	0.0155	0.0270	-0.0094	0.0146	0.0083
0	0	8	7	2958.4	36.8	144.1	-0.1348	0.0179	0.0271	0.0037	0.0172	0.0089
0	0	8	8	2284.0	32.8	113.2	-0.1378	0.0207	0.0255	0.0017	0.0200	0.0082
0	0	8	9	1668.2	27.8	86.7	-0.1899	0.0238	0.0231	-0.0050	0.0232	0.0159
0	0	8	10	1318.0	25.7	69.2	-0.1960	0.0276	0.0231	-0.0337	0.0270	0.0199
0	0	8	11	998.6	22.6	55.6	-0.1615	0.0328	0.0314	0.0223	0.0323	0.0334
0	0	8	12	798.4	21.3	42.4	-0.1571	0.0389	0.0215	0.0616	0.0380	0.0152
0	0	8	13	560.5	17.5	32.9	-0.1827	0.0461	0.0388	0.1135	0.0463	0.0142
0	0	8	14	440.1	16.6	25.0	-0.0922	0.0563	0.0371	0.1239	0.0532	0.0216
0	0	8	15	331.1	14.9	21.1	-0.3018	0.0655	0.0653	0.1136	0.0610	0.0404
0	0	8	16	220.4	12.0	14.0	0.0036	0.0817	0.0627	0.1240	0.0838	0.0612
0	0	8	17	161.3	10.9	13.6	-0.2350	0.1001	0.0622	0.1018	0.0909	0.0705
0	0	8	18	106.6	9.7	10.6	n.m.	n.m.	n.m.	n.m.	n.m.	n.m.
0	0	8	19	75.7	11.0	33.8	n.m.	n.m.	n.m.	n.m.	n.m.	n.m.
0	0	9	0	8563.1	88.5	451.2	n.m.	n.m.	n.m.	n.m.	n.m.	n.m.
0	0	9	1	9830.6	2042.3	2554.2	n.m.	n.m.	n.m.	n.m.	n.m.	n.m.
0	0	9	2	8894.7	1672.3	1687.6	n.m.	n.m.	n.m.	n.m.	n.m.	n.m.
0	0	9	3	5587.7	68.7	310.3	n.m.	n.m.	n.m.	n.m.	n.m.	n.m.
0	0	9	4	4927.5	49.6	241.3	-0.1300	0.0154	0.0251	-0.0207	0.0132	0.0075
0	0	9	5	3963.5	43.3	185.6	-0.0634	0.0164	0.0234	0.0115	0.0146	0.0077
0	0	9	6	3127.6	37.6	154.6	-0.0849	0.0178	0.0272	0.0099	0.0165	0.0078
0	0	9	7	2443.4	33.2	126.8	-0.1003	0.0199	0.0277	0.0179	0.0185	0.0192
0	0	9	8	1898.9	29.3	96.4	-0.1265	0.0223	0.0295	0.0033	0.0212	0.0124
0	0	9	9	1357.4	24.2	76.6	-0.1727	0.0260	0.0264	0.0276	0.0243	0.0097
0	0	9	10	1105.8	22.9	59.8	-0.1242	0.0297	0.0233	-0.0036	0.0285	0.0220
0	0	9	11	843.9	20.0	45.9	-0.2055	0.0338	0.0255	-0.0179	0.0325	0.0236
0	0	9	12	663.4	18.7	39.4	-0.1804	0.0421	0.0515	0.0908	0.0404	0.0263
0	0	9	13	557.1	17.8	31.5	-0.2551	0.0456	0.0303	0.0209	0.0454	0.0301
0	0	9	14	418.6	16.0	21.2	-0.1601	0.0564	0.0358	0.0418	0.0561	0.0408
0	0	9	15	295.3	13.4	21.6	-0.1216	0.0677	0.0488	0.0910	0.0626	0.0221
0	0	9	16	196.6	11.0	13.1	-0.1526	0.0845	0.0431	0.1380	0.0803	0.0552
0	0	9	17	159.0	10.9	11.9	-0.2307	0.1064	0.0706	0.2142	0.0933	0.0755
0	0	9	18	102.8	9.9	9.9	n.m.	n.m.	n.m.	n.m.	n.m.	n.m.
0	0	9	19	89.9	13.6	9.2	n.m.	n.m.	n.m.	n.m.	n.m.	n.m.
0	0	10	0	6664.5	187.6	371.4	n.m.	n.m.	n.m.	n.m.	n.m.	n.m.
0	0	10	1	8903.8	1798.2	2604.2	n.m.	n.m.	n.m.	n.m.	n.m.	n.m.
0	0	10	2	5764.1	147.4	338.3	n.m.	n.m.	n.m.	n.m.	n.m.	n.m.
0	0	10	3	4410.6	50.7	318.8	n.m.	n.m.	n.m.	n.m.	n.m.	n.m.

Continued on next page

Table B.1 – *Continued from previous page*

x	Q^2	z	$P_{h\perp}^2$	A_0	ΔA_0	δA_0	$A_{UU}^{\cos\phi_h}$	$\Delta A_{UU}^{\cos\phi_h}$	$\delta A_{UU}^{\cos\phi_h}$	$A_{UU}^{\cos 2\phi_h}$	$\Delta A_{UU}^{\cos 2\phi_h}$	$\delta A_{UU}^{\cos 2\phi_h}$
0	0	10	4	3602.9	303.2	298.0	n.m.	n.m.	n.m.	n.m.	n.m.	n.m.
0	0	10	5	3071.9	38.5	152.6	-0.1415	0.0190	0.0265	-0.0245	0.0164	0.0130
0	0	10	6	2557.4	34.6	125.3	-0.0929	0.0205	0.0274	0.0125	0.0182	0.0108
0	0	10	7	2007.7	30.1	99.5	-0.1404	0.0221	0.0262	-0.0404	0.0210	0.0148
0	0	10	8	1519.9	25.8	83.1	-0.1048	0.0251	0.0308	0.0215	0.0233	0.0131
0	0	10	9	1227.5	23.4	59.1	-0.1469	0.0277	0.0327	-0.0081	0.0259	0.0144
0	0	10	10	978.5	21.2	55.6	-0.1665	0.0319	0.0290	0.0232	0.0300	0.0235
0	0	10	11	759.8	18.7	42.8	-0.2057	0.0358	0.0326	0.0311	0.0342	0.0209
0	0	10	12	616.0	17.5	30.3	-0.2831	0.0392	0.0294	-0.0296	0.0394	0.0314
0	0	10	13	456.3	15.2	21.3	-0.1623	0.0479	0.0319	0.0045	0.0478	0.0386
0	0	10	14	363.6	14.5	20.4	-0.1622	0.0596	0.0403	0.0996	0.0550	0.0326
0	0	10	15	279.6	13.0	18.6	-0.2509	0.0692	0.0450	0.1241	0.0649	0.0263
0	0	10	16	219.1	12.1	10.7	-0.2788	0.0793	0.0784	-0.0141	0.0789	0.0417
0	0	10	17	152.9	10.7	12.2	n.m.	n.m.	n.m.	n.m.	n.m.	n.m.
0	0	10	18	115.3	11.1	10.4	n.m.	n.m.	n.m.	n.m.	n.m.	n.m.
0	0	10	19	99.4	28.3	14.4	n.m.	n.m.	n.m.	n.m.	n.m.	n.m.
0	0	11	0	5583.0	96.8	340.5	n.m.	n.m.	n.m.	n.m.	n.m.	n.m.
0	0	11	1	5515.6	9116.3	4131.0	n.m.	n.m.	n.m.	n.m.	n.m.	n.m.
0	0	11	2	5182.3	388.1	627.7	n.m.	n.m.	n.m.	n.m.	n.m.	n.m.
0	0	11	3	3956.3	321.1	308.0	n.m.	n.m.	n.m.	n.m.	n.m.	n.m.
0	0	11	4	3083.4	42.5	184.0	n.m.	n.m.	n.m.	n.m.	n.m.	n.m.
0	0	11	5	2469.3	37.8	230.4	n.m.	n.m.	n.m.	n.m.	n.m.	n.m.
0	0	11	6	2078.7	32.3	103.9	-0.1655	0.0238	0.0284	-0.0545	0.0207	0.0115
0	0	11	7	1736.4	28.8	89.8	-0.1376	0.0249	0.0269	-0.0465	0.0227	0.0174
0	0	11	8	1395.1	26.2	77.8	-0.1270	0.0283	0.0290	0.0013	0.0252	0.0187
0	0	11	9	1137.2	23.3	63.2	-0.1514	0.0305	0.0377	0.0294	0.0281	0.0160
0	0	11	10	920.2	21.3	42.0	-0.0734	0.0345	0.0312	0.0192	0.0316	0.0277
0	0	11	11	733.5	19.3	40.5	-0.1360	0.0393	0.0365	0.0604	0.0364	0.0163
0	0	11	12	582.7	17.7	31.0	-0.1109	0.0458	0.0467	0.1033	0.0408	0.0238
0	0	11	13	460.5	16.0	23.4	-0.1225	0.0508	0.0353	0.0035	0.0487	0.0268
0	0	11	14	345.8	13.9	22.1	-0.1495	0.0567	0.0298	-0.0679	0.0559	0.0343
0	0	11	15	233.8	11.9	14.9	-0.1033	0.0771	0.0493	0.1468	0.0701	0.0463
0	0	11	16	214.0	13.0	11.6	-0.1780	0.0911	0.0752	0.0317	0.0889	0.0545
0	0	11	17	134.2	10.8	14.9	n.m.	n.m.	n.m.	n.m.	n.m.	n.m.
0	0	11	18	137.7	23.9	15.7	n.m.	n.m.	n.m.	n.m.	n.m.	n.m.
0	0	11	19	100.6	25.0	45.1	n.m.	n.m.	n.m.	n.m.	n.m.	n.m.
0	0	12	0	4886.2	91.3	298.6	n.m.	n.m.	n.m.	n.m.	n.m.	n.m.
0	0	12	1	4262.2	229.7	2908.5	n.m.	n.m.	n.m.	n.m.	n.m.	n.m.
0	0	12	2	6557.2	279.1	1774.8	n.m.	n.m.	n.m.	n.m.	n.m.	n.m.

Continued on next page

Table B.1 – *Continued from previous page*

x	Q^2	z	$P_{h\perp}^2$	A_0	ΔA_0	δA_0	$A_{UU}^{\cos\phi_h}$	$\Delta A_{UU}^{\cos\phi_h}$	$\delta A_{UU}^{\cos\phi_h}$	$A_{UU}^{\cos 2\phi_h}$	$\Delta A_{UU}^{\cos 2\phi_h}$	$\delta A_{UU}^{\cos 2\phi_h}$
0	0	12	3	3609.0	313.0	291.8	n.m.	n.m.	n.m.	n.m.	n.m.	n.m.
0	0	12	4	2916.5	260.5	249.1	n.m.	n.m.	n.m.	n.m.	n.m.	n.m.
0	0	12	5	2265.9	37.9	122.5	n.m.	n.m.	n.m.	n.m.	n.m.	n.m.
0	0	12	6	1856.8	34.0	90.2	n.m.	n.m.	n.m.	n.m.	n.m.	n.m.
0	0	12	7	1509.9	31.4	137.1	n.m.	n.m.	n.m.	n.m.	n.m.	n.m.
0	0	12	8	1333.0	27.4	63.3	-0.1713	0.0310	0.0254	-0.0469	0.0278	0.0150
0	0	12	9	1109.2	25.3	54.0	-0.0299	0.0343	0.0424	-0.0124	0.0302	0.0267
0	0	12	10	877.9	22.4	46.8	-0.1123	0.0386	0.0276	0.0199	0.0352	0.0190
0	0	12	11	710.6	20.5	35.1	-0.1126	0.0431	0.0298	0.0121	0.0404	0.0271
0	0	12	12	495.6	16.5	29.8	-0.0839	0.0506	0.0373	0.0101	0.0474	0.0266
0	0	12	13	414.8	16.2	24.2	-0.0937	0.0577	0.0572	0.0099	0.0545	0.0266
0	0	12	14	290.6	13.9	19.4	-0.0799	0.0725	0.0638	0.0436	0.0681	0.0331
0	0	12	15	229.3	12.8	19.4	-0.2177	0.0844	0.0627	0.1032	0.0788	0.0666
0	0	12	16	151.0	10.6	9.5	n.m.	n.m.	n.m.	n.m.	n.m.	n.m.
0	0	12	17	129.8	13.1	8.4	n.m.	n.m.	n.m.	n.m.	n.m.	n.m.
0	0	12	18	132.8	31.2	17.7	n.m.	n.m.	n.m.	n.m.	n.m.	n.m.
0	0	13	0	4791.2	92.7	306.2	n.m.	n.m.	n.m.	n.m.	n.m.	n.m.
0	0	13	1	3944.8	81.2	192.9	n.m.	n.m.	n.m.	n.m.	n.m.	n.m.
0	0	13	2	3488.2	85.9	418.6	n.m.	n.m.	n.m.	n.m.	n.m.	n.m.
0	0	13	3	3698.2	1284.2	1102.7	n.m.	n.m.	n.m.	n.m.	n.m.	n.m.
0	0	13	4	2810.4	285.6	440.7	n.m.	n.m.	n.m.	n.m.	n.m.	n.m.
0	0	13	5	2274.6	262.4	343.9	n.m.	n.m.	n.m.	n.m.	n.m.	n.m.
0	0	13	6	1582.2	32.6	120.3	n.m.	n.m.	n.m.	n.m.	n.m.	n.m.
0	0	13	7	1438.4	202.9	198.8	n.m.	n.m.	n.m.	n.m.	n.m.	n.m.
0	0	13	8	1242.0	172.7	287.3	n.m.	n.m.	n.m.	n.m.	n.m.	n.m.
0	0	13	9	895.4	25.9	48.1	n.m.	n.m.	n.m.	n.m.	n.m.	n.m.
0	0	13	10	776.2	23.0	48.8	-0.0988	0.0453	0.0446	-0.0140	0.0387	0.0324
0	0	13	11	638.2	22.5	34.6	0.0404	0.0526	0.0306	-0.0505	0.0481	0.0186
0	0	13	12	501.3	19.7	25.1	-0.0770	0.0599	0.0850	0.0651	0.0552	0.0428
0	0	13	13	353.2	17.1	17.8	0.1283	0.0710	0.0389	0.0222	0.0623	0.0392
0	0	13	14	257.7	17.0	35.2	n.m.	n.m.	n.m.	n.m.	n.m.	n.m.
0	0	13	15	177.3	14.6	61.2	n.m.	n.m.	n.m.	n.m.	n.m.	n.m.
0	0	13	16	153.6	19.9	42.5	n.m.	n.m.	n.m.	n.m.	n.m.	n.m.
0	0	14	0	4315.7	86.3	271.3	n.m.	n.m.	n.m.	n.m.	n.m.	n.m.
0	0	14	1	3821.2	111.8	1317.7	n.m.	n.m.	n.m.	n.m.	n.m.	n.m.
0	0	14	2	2998.5	93.1	176.2	n.m.	n.m.	n.m.	n.m.	n.m.	n.m.
0	0	14	3	2612.7	72.3	423.9	n.m.	n.m.	n.m.	n.m.	n.m.	n.m.
0	0	14	4	2454.4	305.4	311.5	n.m.	n.m.	n.m.	n.m.	n.m.	n.m.
0	0	14	5	1736.5	37.2	273.7	n.m.	n.m.	n.m.	n.m.	n.m.	n.m.

Continued on next page

Table B.1 – *Continued from previous page*

x	Q^2	z	$P_{h\perp}^2$	A_0	ΔA_0	δA_0	$A_{UU}^{\cos\phi_h}$	$\Delta A_{UU}^{\cos\phi_h}$	$\delta A_{UU}^{\cos\phi_h}$	$A_{UU}^{\cos 2\phi_h}$	$\Delta A_{UU}^{\cos 2\phi_h}$	$\delta A_{UU}^{\cos 2\phi_h}$
0	0	14	6	1437.1	34.1	159.1	n.m.	n.m.	n.m.	n.m.	n.m.	n.m.
0	0	14	7	1183.8	249.0	99.8	n.m.	n.m.	n.m.	n.m.	n.m.	n.m.
0	0	14	8	1089.5	187.6	154.5	n.m.	n.m.	n.m.	n.m.	n.m.	n.m.
0	0	14	9	721.4	26.2	212.2	n.m.	n.m.	n.m.	n.m.	n.m.	n.m.
0	0	14	10	576.8	25.0	33.2	-0.1161	0.0692	0.0768	-0.0558	0.0590	0.0527
0	0	14	11	518.1	26.5	27.8	n.m.	n.m.	n.m.	n.m.	n.m.	n.m.
0	0	14	12	386.6	24.9	21.5	n.m.	n.m.	n.m.	n.m.	n.m.	n.m.
0	0	14	13	259.2	24.9	19.3	n.m.	n.m.	n.m.	n.m.	n.m.	n.m.
0	0	15	0	4227.1	93.9	251.3	n.m.	n.m.	n.m.	n.m.	n.m.	n.m.
0	0	15	1	5178.5	251.0	1474.4	n.m.	n.m.	n.m.	n.m.	n.m.	n.m.
0	0	15	2	4381.4	259.4	1734.0	n.m.	n.m.	n.m.	n.m.	n.m.	n.m.
0	0	15	3	2192.3	80.9	138.4	n.m.	n.m.	n.m.	n.m.	n.m.	n.m.
0	0	15	4	2769.0	101.2	1366.9	n.m.	n.m.	n.m.	n.m.	n.m.	n.m.
0	0	15	5	2185.6	84.9	858.6	n.m.	n.m.	n.m.	n.m.	n.m.	n.m.
0	0	15	6	1672.3	1003.3	784.7	n.m.	n.m.	n.m.	n.m.	n.m.	n.m.
0	0	15	7	1327.1	66.9	193.1	n.m.	n.m.	n.m.	n.m.	n.m.	n.m.
0	0	15	8	760.6	48.2	361.3	n.m.	n.m.	n.m.	n.m.	n.m.	n.m.
0	0	15	9	541.8	44.7	223.4	n.m.	n.m.	n.m.	n.m.	n.m.	n.m.
0	0	16	0	3491.8	82.5	226.7	n.m.	n.m.	n.m.	n.m.	n.m.	n.m.
0	0	16	1	4087.1	308.5	1253.2	n.m.	n.m.	n.m.	n.m.	n.m.	n.m.
0	0	16	2	3491.4	371.9	455.3	n.m.	n.m.	n.m.	n.m.	n.m.	n.m.
0	0	16	3	2631.1	848.4	1609.8	n.m.	n.m.	n.m.	n.m.	n.m.	n.m.
0	0	16	4	1070.1	72.9	469.5	n.m.	n.m.	n.m.	n.m.	n.m.	n.m.
0	1	1	0	140022.0	217.1	8123.1	-0.1511	0.0022	0.0199	-0.0194	0.0022	0.0023
0	1	1	1	46892.6	105.7	2807.1	-0.3270	0.0030	0.0357	0.0256	0.0031	0.0038
0	1	2	0	63506.0	137.3	3535.5	-0.1211	0.0032	0.0157	0.0268	0.0030	0.0041
0	1	2	1	41992.3	95.5	2307.8	-0.1992	0.0034	0.0305	-0.0172	0.0034	0.0249
0	1	2	2	22983.1	65.5	1247.1	-0.2426	0.0041	0.0327	0.0072	0.0042	0.0262
0	1	2	3	11618.6	43.3	630.2	-0.2521	0.0052	0.0280	0.0238	0.0052	0.0057
0	1	2	4	4817.6	27.1	266.3	-0.3140	0.0077	0.0319	0.0211	0.0077	0.0072
0	1	2	5	1699.8	15.8	95.7	-0.3562	0.0126	0.0378	0.0555	0.0125	0.0112
0	1	2	6	528.8	9.0	31.5	-0.3473	0.0233	0.0480	0.0410	0.0231	0.0122
0	1	3	0	37839.8	339.7	2070.6	n.m.	n.m.	n.m.	n.m.	n.m.	n.m.
0	1	3	1	27494.3	78.1	1458.0	-0.0805	0.0040	0.0175	-0.0180	0.0040	0.0052
0	1	3	2	17366.1	60.7	900.8	-0.1249	0.0052	0.0254	-0.0397	0.0052	0.0169
0	1	3	3	10847.5	45.6	582.2	-0.1655	0.0062	0.0338	-0.0365	0.0063	0.0270
0	1	3	4	6788.9	34.5	360.4	-0.2210	0.0074	0.0327	-0.0244	0.0076	0.0242
0	1	3	5	4208.4	25.2	225.6	-0.2353	0.0084	0.0245	0.0333	0.0085	0.0063
0	1	3	6	2424.5	18.5	124.5	-0.2555	0.0108	0.0292	0.0708	0.0107	0.0062

Continued on next page

Table B.1 – *Continued from previous page*

x	Q^2	z	$P_{h\perp}^2$	A_0	ΔA_0	δA_0	$A_{UU}^{\cos\phi_h}$	$\Delta A_{UU}^{\cos\phi_h}$	$\delta A_{UU}^{\cos\phi_h}$	$A_{UU}^{\cos 2\phi_h}$	$\Delta A_{UU}^{\cos 2\phi_h}$	$\delta A_{UU}^{\cos 2\phi_h}$
0	1	3	7	1314.2	13.4	70.9	-0.2591	0.0144	0.0303	0.0458	0.0141	0.0094
0	1	3	8	649.4	9.4	37.0	-0.2446	0.0204	0.0304	0.0583	0.0202	0.0115
0	1	3	9	311.2	7.0	18.3	-0.3109	0.0316	0.0340	0.0790	0.0313	0.0186
0	1	3	10	113.0	4.4	6.5	-0.1658	0.0560	0.0408	0.1279	0.0524	0.0556
0	1	4	0	21582.1	99.9	1199.4	n.m.	n.m.	n.m.	n.m.	n.m.	n.m.
0	1	4	1	17817.6	64.6	921.0	-0.0156	0.0052	0.0168	-0.0489	0.0049	0.0077
0	1	4	2	12815.3	51.7	652.9	-0.0542	0.0057	0.0192	-0.0166	0.0056	0.0051
0	1	4	3	8809.9	42.0	441.1	-0.1111	0.0067	0.0214	-0.0265	0.0067	0.0044
0	1	4	4	6123.0	35.1	305.9	-0.1267	0.0082	0.0230	-0.0173	0.0083	0.0044
0	1	4	5	4116.2	28.0	208.7	-0.1156	0.0097	0.0251	-0.0132	0.0099	0.0071
0	1	4	6	2810.2	22.7	143.8	-0.1472	0.0116	0.0275	0.0313	0.0116	0.0082
0	1	4	7	1892.3	18.2	97.7	-0.2095	0.0136	0.0268	0.0299	0.0137	0.0076
0	1	4	8	1263.2	14.8	66.7	-0.2398	0.0166	0.0287	0.0599	0.0165	0.0081
0	1	4	9	800.8	11.6	43.9	-0.2295	0.0204	0.0275	0.0442	0.0205	0.0118
0	1	4	10	499.6	9.3	26.4	-0.1941	0.0268	0.0256	0.0786	0.0268	0.0097
0	1	4	11	277.0	6.8	15.5	-0.2413	0.0362	0.0293	0.1529	0.0337	0.0179
0	1	4	12	161.8	5.8	9.5	-0.1471	0.0516	0.0306	0.0799	0.0512	0.0192
0	1	4	13	82.3	4.5	4.6	-0.0742	0.0804	0.0358	0.0759	0.0740	0.0365
0	1	5	0	15044.2	485.1	1115.6	n.m.	n.m.	n.m.	n.m.	n.m.	n.m.
0	1	5	1	11485.3	65.4	585.8	-0.0107	0.0094	0.0286	-0.0577	0.0078	0.0180
0	1	5	2	9033.9	43.4	447.6	-0.0293	0.0068	0.0215	-0.0283	0.0065	0.0042
0	1	5	3	6689.2	36.7	328.2	-0.0744	0.0078	0.0240	-0.0049	0.0076	0.0044
0	1	5	4	4960.6	32.1	245.1	-0.1080	0.0091	0.0252	-0.0233	0.0090	0.0031
0	1	5	5	3577.8	27.8	177.4	-0.1494	0.0109	0.0260	-0.0155	0.0109	0.0038
0	1	5	6	2556.7	23.7	124.4	-0.1334	0.0131	0.0268	-0.0171	0.0131	0.0080
0	1	5	7	1780.3	19.5	89.6	-0.1737	0.0156	0.0285	-0.0016	0.0159	0.0078
0	1	5	8	1280.2	16.5	65.5	-0.2233	0.0184	0.0302	0.0360	0.0184	0.0105
0	1	5	9	913.2	13.9	47.1	-0.2009	0.0224	0.0295	0.1111	0.0211	0.0140
0	1	5	10	637.6	11.5	32.3	-0.1722	0.0264	0.0267	0.0929	0.0260	0.0094
0	1	5	11	440.2	9.6	23.2	-0.2318	0.0312	0.0311	0.0688	0.0315	0.0142
0	1	5	12	282.0	7.6	14.3	-0.1174	0.0385	0.0312	0.0334	0.0393	0.0164
0	1	5	13	187.1	6.5	10.0	-0.2296	0.0507	0.0328	0.0839	0.0469	0.0263
0	1	5	14	113.7	5.2	7.4	0.1019	0.0657	0.0415	0.0593	0.0712	0.0276
0	1	5	15	68.4	4.3	4.1	-0.1048	0.0979	0.0476	0.2586	0.0820	0.0347
0	1	6	0	10401.0	72.0	631.5	n.m.	n.m.	n.m.	n.m.	n.m.	n.m.
0	1	6	1	7216.5	273.7	473.3	n.m.	n.m.	n.m.	n.m.	n.m.	n.m.
0	1	6	2	6032.3	35.2	301.7	-0.0377	0.0086	0.0260	-0.0211	0.0078	0.0067
0	1	6	3	4801.7	30.4	233.8	-0.0683	0.0091	0.0278	-0.0022	0.0087	0.0038
0	1	6	4	3612.6	26.3	178.7	-0.1038	0.0104	0.0295	0.0110	0.0101	0.0052

Continued on next page

Table B.1 – *Continued from previous page*

x	Q^2	z	$P_{h\perp}^2$	A_0	ΔA_0	δA_0	$A_{UU}^{\cos\phi_h}$	$\Delta A_{UU}^{\cos\phi_h}$	$\delta A_{UU}^{\cos\phi_h}$	$A_{UU}^{\cos 2\phi_h}$	$\Delta A_{UU}^{\cos 2\phi_h}$	$\delta A_{UU}^{\cos 2\phi_h}$
0	1	6	5	2776.8	23.8	133.7	-0.1493	0.0121	0.0315	-0.0045	0.0118	0.0062
0	1	6	6	2088.4	21.2	99.3	-0.1637	0.0144	0.0312	0.0168	0.0143	0.0058
0	1	6	7	1554.3	18.8	76.8	-0.1541	0.0173	0.0323	0.0323	0.0170	0.0071
0	1	6	8	1129.8	16.2	55.9	-0.1676	0.0205	0.0338	0.0245	0.0202	0.0075
0	1	6	9	806.7	13.5	40.1	-0.1662	0.0242	0.0333	0.0342	0.0240	0.0094
0	1	6	10	612.1	12.1	31.0	-0.1364	0.0291	0.0322	0.0627	0.0280	0.0083
0	1	6	11	440.6	10.4	22.6	-0.2030	0.0340	0.0260	0.0524	0.0352	0.0123
0	1	6	12	316.0	8.7	16.0	-0.2140	0.0404	0.0328	0.0761	0.0380	0.0251
0	1	6	13	231.9	7.6	11.3	-0.0923	0.0488	0.0317	0.1242	0.0457	0.0153
0	1	6	14	146.2	6.0	7.5	-0.1498	0.0607	0.0299	0.1671	0.0619	0.0202
0	1	6	15	98.3	5.0	5.1	-0.2041	0.0757	0.0352	0.1676	0.0724	0.0492
0	1	6	16	68.4	4.6	4.6	-0.2866	0.0995	0.0312	0.2516	0.0952	0.0436
0	1	6	17	47.0	5.1	4.0	n.m.	n.m.	n.m.	n.m.	n.m.	n.m.
0	1	7	0	4407.2	47.7	1128.8	n.m.	n.m.	n.m.	n.m.	n.m.	n.m.
0	1	7	1	4156.2	41.6	740.3	n.m.	n.m.	n.m.	n.m.	n.m.	n.m.
0	1	7	2	3991.1	35.9	249.1	-0.0563	0.0151	0.0793	-0.0078	0.0117	0.0484
0	1	7	3	3298.4	26.9	163.6	-0.0669	0.0128	0.0347	0.0217	0.0111	0.0141
0	1	7	4	2620.9	21.9	127.1	-0.0776	0.0123	0.0337	0.0387	0.0114	0.0055
0	1	7	5	2055.1	19.5	97.5	-0.1160	0.0138	0.0350	0.0369	0.0131	0.0059
0	1	7	6	1570.4	17.3	78.2	-0.1297	0.0159	0.0369	0.0233	0.0152	0.0086
0	1	7	7	1197.8	15.5	60.1	-0.1557	0.0186	0.0360	0.0256	0.0181	0.0078
0	1	7	8	935.7	14.2	45.3	-0.1662	0.0222	0.0365	0.0693	0.0214	0.0104
0	1	7	9	690.3	12.4	34.9	-0.1308	0.0258	0.0352	0.0198	0.0252	0.0111
0	1	7	10	526.0	11.1	26.8	-0.1438	0.0310	0.0354	0.0820	0.0295	0.0117
0	1	7	11	398.5	9.9	19.5	-0.1883	0.0358	0.0340	0.0488	0.0340	0.0095
0	1	7	12	299.2	8.7	14.6	-0.1085	0.0421	0.0316	0.0254	0.0414	0.0179
0	1	7	13	218.8	7.5	11.8	-0.2337	0.0486	0.0317	0.0059	0.0482	0.0225
0	1	7	14	167.3	6.9	10.1	-0.1338	0.0604	0.0349	0.0804	0.0600	0.0277
0	1	7	15	129.1	6.4	7.9	-0.2043	0.0694	0.0375	-0.0289	0.0705	0.0324
0	1	7	16	88.5	5.6	4.4	-0.3749	0.0908	0.0434	0.2015	0.0887	0.0294
0	1	7	17	52.0	4.5	4.0	-0.3303	0.1258	0.0870	0.0807	0.1531	0.0846
0	1	7	18	41.6	9.3	4.6	n.m.	n.m.	n.m.	n.m.	n.m.	n.m.
0	1	8	0	3358.7	734.9	866.7	n.m.	n.m.	n.m.	n.m.	n.m.	n.m.
0	1	8	1	4239.2	51.3	1080.0	n.m.	n.m.	n.m.	n.m.	n.m.	n.m.
0	1	8	2	2622.0	567.2	368.2	n.m.	n.m.	n.m.	n.m.	n.m.	n.m.
0	1	8	3	2148.8	19.9	103.0	-0.1818	0.0141	0.0346	-0.0683	0.0123	0.0090
0	1	8	4	1868.8	18.2	89.0	-0.0630	0.0146	0.0362	0.0280	0.0130	0.0063
0	1	8	5	1472.6	16.0	69.3	-0.0834	0.0161	0.0386	0.0520	0.0148	0.0063
0	1	8	6	1152.0	14.1	59.4	-0.1021	0.0181	0.0410	0.0651	0.0168	0.0067

Continued on next page

Table B.1 – *Continued from previous page*

x	Q^2	z	$P_{h\perp}^2$	A_0	ΔA_0	δA_0	$A_{UU}^{\cos\phi_h}$	$\Delta A_{UU}^{\cos\phi_h}$	$\delta A_{UU}^{\cos\phi_h}$	$A_{UU}^{\cos 2\phi_h}$	$\Delta A_{UU}^{\cos 2\phi_h}$	$\delta A_{UU}^{\cos 2\phi_h}$
0	1	8	7	913.6	12.8	45.3	-0.1036	0.0204	0.0418	0.0457	0.0195	0.0112
0	1	8	8	707.9	11.5	35.1	-0.1533	0.0234	0.0424	0.0471	0.0229	0.0096
0	1	8	9	568.7	10.7	27.1	-0.1711	0.0273	0.0412	0.0450	0.0266	0.0114
0	1	8	10	428.0	9.6	22.1	-0.1977	0.0325	0.0435	0.0717	0.0325	0.0188
0	1	8	11	342.2	9.1	18.3	-0.2003	0.0382	0.0389	0.0712	0.0373	0.0223
0	1	8	12	253.7	7.8	13.6	-0.2634	0.0437	0.0399	0.0863	0.0432	0.0198
0	1	8	13	212.4	7.8	11.7	-0.2359	0.0549	0.0389	0.2160	0.0493	0.0271
0	1	8	14	161.6	7.0	7.8	-0.2882	0.0633	0.0417	0.1256	0.0601	0.0336
0	1	8	15	123.4	6.4	6.6	-0.3731	0.0723	0.0296	0.1123	0.0741	0.0378
0	1	8	16	97.5	6.0	6.5	-0.3610	0.0858	0.0434	0.1538	0.0855	0.0288
0	1	8	17	64.5	4.9	4.8	-0.2245	0.1145	0.0744	0.1274	0.1092	0.0762
0	1	8	18	55.5	6.4	6.1	n.m.	n.m.	n.m.	n.m.	n.m.	n.m.
0	1	9	0	2158.4	23.6	105.2	n.m.	n.m.	n.m.	n.m.	n.m.	n.m.
0	1	9	1	3082.8	45.8	643.3	n.m.	n.m.	n.m.	n.m.	n.m.	n.m.
0	1	9	2	1906.2	125.5	120.7	n.m.	n.m.	n.m.	n.m.	n.m.	n.m.
0	1	9	3	1540.8	114.2	102.3	n.m.	n.m.	n.m.	n.m.	n.m.	n.m.
0	1	9	4	1226.1	16.1	62.0	n.m.	n.m.	n.m.	n.m.	n.m.	n.m.
0	1	9	5	1082.9	15.8	55.4	-0.1145	0.0240	0.0483	0.0410	0.0196	0.0187
0	1	9	6	909.0	12.4	44.7	-0.1087	0.0204	0.0406	0.0358	0.0189	0.0109
0	1	9	7	715.4	11.0	36.0	-0.1333	0.0231	0.0442	0.0738	0.0211	0.0094
0	1	9	8	580.1	10.1	29.0	-0.1177	0.0256	0.0432	0.0445	0.0244	0.0103
0	1	9	9	456.9	9.2	22.7	-0.1334	0.0296	0.0452	0.0777	0.0279	0.0109
0	1	9	10	367.7	8.5	18.8	-0.2217	0.0337	0.0439	0.0797	0.0322	0.0115
0	1	9	11	283.3	7.7	13.7	-0.2105	0.0393	0.0398	0.0633	0.0383	0.0237
0	1	9	12	240.1	7.6	12.1	-0.2482	0.0453	0.0437	0.0548	0.0444	0.0159
0	1	9	13	182.3	6.7	9.8	-0.0903	0.0537	0.0360	0.0327	0.0546	0.0239
0	1	9	14	145.3	6.5	9.5	-0.1269	0.0645	0.0613	-0.0158	0.0660	0.0432
0	1	9	15	124.6	6.3	7.1	-0.2288	0.0719	0.0422	0.0025	0.0726	0.0408
0	1	9	16	83.8	5.4	4.7	-0.3606	0.0953	0.0730	0.2568	0.0797	0.0644
0	1	9	17	67.1	5.4	2.7	-0.3018	0.1188	0.0942	0.1719	0.1138	0.0716
0	1	9	18	47.1	5.6	4.4	n.m.	n.m.	n.m.	n.m.	n.m.	n.m.
0	1	10	0	1594.6	20.2	76.0	n.m.	n.m.	n.m.	n.m.	n.m.	n.m.
0	1	10	1	2341.5	41.9	564.9	n.m.	n.m.	n.m.	n.m.	n.m.	n.m.
0	1	10	2	1557.4	111.8	239.5	n.m.	n.m.	n.m.	n.m.	n.m.	n.m.
0	1	10	3	1211.3	99.9	79.1	n.m.	n.m.	n.m.	n.m.	n.m.	n.m.
0	1	10	4	996.8	14.3	53.0	n.m.	n.m.	n.m.	n.m.	n.m.	n.m.
0	1	10	5	864.3	82.0	58.3	n.m.	n.m.	n.m.	n.m.	n.m.	n.m.
0	1	10	6	687.8	10.6	34.7	-0.1790	0.0234	0.0456	0.0415	0.0205	0.0148
0	1	10	7	576.2	9.7	28.5	-0.1552	0.0253	0.0429	0.0417	0.0232	0.0121

Continued on next page

Table B.1 – *Continued from previous page*

x	Q^2	z	$P_{h\perp}^2$	A_0	ΔA_0	δA_0	$A_{UU}^{\cos\phi_h}$	$\Delta A_{UU}^{\cos\phi_h}$	$\delta A_{UU}^{\cos\phi_h}$	$A_{UU}^{\cos 2\phi_h}$	$\Delta A_{UU}^{\cos 2\phi_h}$	$\delta A_{UU}^{\cos 2\phi_h}$
0	1	10	8	464.6	8.9	23.6	-0.1571	0.0281	0.0437	0.0297	0.0264	0.0099
0	1	10	9	387.6	8.3	20.1	-0.1359	0.0313	0.0483	0.0068	0.0297	0.0139
0	1	10	10	324.8	8.0	16.7	-0.1029	0.0363	0.0458	0.0534	0.0348	0.0130
0	1	10	11	277.6	7.9	14.1	-0.1896	0.0422	0.0413	0.1132	0.0383	0.0182
0	1	10	12	205.2	6.7	10.5	-0.1721	0.0478	0.0392	0.0349	0.0496	0.0248
0	1	10	13	172.6	6.6	9.6	-0.0965	0.0580	0.0374	0.1383	0.0522	0.0234
0	1	10	14	150.6	6.7	8.9	-0.2196	0.0664	0.0469	0.1731	0.0640	0.0254
0	1	10	15	112.4	5.9	7.6	-0.3414	0.0761	0.0356	0.1243	0.0734	0.0256
0	1	10	16	90.6	5.4	4.4	-0.0541	0.0919	0.0436	0.1455	0.0794	0.0487
0	1	10	17	66.7	5.5	4.0	-0.0790	0.1273	0.0826	0.0850	0.1202	0.0686
0	1	10	18	55.2	6.1	7.9	n.m.	n.m.	n.m.	n.m.	n.m.	n.m.
0	1	11	0	1257.2	17.8	62.1	n.m.	n.m.	n.m.	n.m.	n.m.	n.m.
0	1	11	1	1368.0	485.1	469.3	n.m.	n.m.	n.m.	n.m.	n.m.	n.m.
0	1	11	2	1194.7	108.1	87.9	n.m.	n.m.	n.m.	n.m.	n.m.	n.m.
0	1	11	3	990.5	14.3	82.6	n.m.	n.m.	n.m.	n.m.	n.m.	n.m.
0	1	11	4	840.9	13.1	44.7	n.m.	n.m.	n.m.	n.m.	n.m.	n.m.
0	1	11	5	660.9	11.6	35.9	n.m.	n.m.	n.m.	n.m.	n.m.	n.m.
0	1	11	6	579.0	11.6	29.2	-0.2203	0.0341	0.0471	-0.0144	0.0273	0.0177
0	1	11	7	485.6	9.2	23.1	-0.2466	0.0282	0.0419	-0.0398	0.0257	0.0129
0	1	11	8	426.9	8.9	19.6	-0.1449	0.0311	0.0433	-0.0264	0.0286	0.0128
0	1	11	9	358.0	8.5	18.4	-0.1063	0.0354	0.0387	0.0268	0.0326	0.0158
0	1	11	10	291.1	7.8	15.3	-0.2050	0.0398	0.0395	0.0696	0.0362	0.0134
0	1	11	11	238.0	7.1	11.9	-0.1475	0.0426	0.0350	-0.0720	0.0429	0.0180
0	1	11	12	194.3	6.7	9.1	-0.1071	0.0524	0.0435	0.1349	0.0467	0.0239
0	1	11	13	162.5	6.3	10.1	-0.2352	0.0557	0.0402	0.0142	0.0555	0.0180
0	1	11	14	122.8	5.6	6.7	-0.2287	0.0675	0.0562	0.0733	0.0628	0.0428
0	1	11	15	102.7	5.3	7.8	-0.1196	0.0730	0.0765	-0.0149	0.0780	0.0199
0	1	11	16	73.2	4.9	4.3	-0.1598	0.0984	0.0521	0.0160	0.0944	0.0464
0	1	11	17	75.4	7.5	4.9	n.m.	n.m.	n.m.	n.m.	n.m.	n.m.
0	1	11	18	68.6	10.7	18.5	n.m.	n.m.	n.m.	n.m.	n.m.	n.m.
0	1	12	0	1133.7	17.2	55.9	n.m.	n.m.	n.m.	n.m.	n.m.	n.m.
0	1	12	1	1237.6	474.8	440.6	n.m.	n.m.	n.m.	n.m.	n.m.	n.m.
0	1	12	2	1004.3	15.7	78.0	n.m.	n.m.	n.m.	n.m.	n.m.	n.m.
0	1	12	3	1042.4	97.6	163.8	n.m.	n.m.	n.m.	n.m.	n.m.	n.m.
0	1	12	4	746.9	12.9	61.4	n.m.	n.m.	n.m.	n.m.	n.m.	n.m.
0	1	12	5	655.1	12.4	52.1	n.m.	n.m.	n.m.	n.m.	n.m.	n.m.
0	1	12	6	683.3	71.9	94.5	n.m.	n.m.	n.m.	n.m.	n.m.	n.m.
0	1	12	7	457.2	10.3	22.6	n.m.	n.m.	n.m.	n.m.	n.m.	n.m.
0	1	12	8	366.7	9.5	18.1	n.m.	n.m.	n.m.	n.m.	n.m.	n.m.

Continued on next page

Table B.1 – *Continued from previous page*

x	Q^2	z	$P_{h\perp}^2$	A_0	ΔA_0	δA_0	$A_{UU}^{\cos\phi_h}$	$\Delta A_{UU}^{\cos\phi_h}$	$\delta A_{UU}^{\cos\phi_h}$	$A_{UU}^{\cos 2\phi_h}$	$\Delta A_{UU}^{\cos 2\phi_h}$	$\delta A_{UU}^{\cos 2\phi_h}$
0	1	12	9	323.9	8.4	15.9	-0.1548	0.0392	0.0374	0.0090	0.0348	0.0148
0	1	12	10	276.3	7.8	14.0	-0.1685	0.0425	0.0314	-0.0165	0.0386	0.0171
0	1	12	11	221.5	7.1	11.4	-0.1658	0.0485	0.0373	0.0123	0.0459	0.0204
0	1	12	12	177.9	6.4	9.5	-0.1498	0.0542	0.0365	0.0052	0.0517	0.0192
0	1	12	13	146.4	6.4	9.1	-0.0513	0.0661	0.0419	0.0439	0.0654	0.0236
0	1	12	14	128.7	6.6	6.9	-0.0860	0.0793	0.0482	0.0688	0.0721	0.0411
0	1	12	15	88.4	6.0	5.8	-0.1213	0.1069	0.0771	0.1437	0.0911	0.0364
0	1	12	16	79.3	6.3	5.1	n.m.	n.m.	n.m.	n.m.	n.m.	n.m.
0	1	12	17	90.2	10.8	12.8	n.m.	n.m.	n.m.	n.m.	n.m.	n.m.
0	1	13	0	1113.2	24.1	54.0	n.m.	n.m.	n.m.	n.m.	n.m.	n.m.
0	1	13	1	1022.7	29.9	80.9	n.m.	n.m.	n.m.	n.m.	n.m.	n.m.
0	1	13	2	939.1	23.9	118.6	n.m.	n.m.	n.m.	n.m.	n.m.	n.m.
0	1	13	3	951.0	97.1	101.2	n.m.	n.m.	n.m.	n.m.	n.m.	n.m.
0	1	13	4	729.7	88.4	110.3	n.m.	n.m.	n.m.	n.m.	n.m.	n.m.
0	1	13	5	679.0	81.6	91.2	n.m.	n.m.	n.m.	n.m.	n.m.	n.m.
0	1	13	6	470.8	11.1	23.8	n.m.	n.m.	n.m.	n.m.	n.m.	n.m.
0	1	13	7	396.8	9.8	19.1	n.m.	n.m.	n.m.	n.m.	n.m.	n.m.
0	1	13	8	323.0	26.8	21.7	n.m.	n.m.	n.m.	n.m.	n.m.	n.m.
0	1	13	9	291.9	9.9	15.7	-0.1122	0.0567	0.0447	0.0382	0.0433	0.0233
0	1	13	10	252.7	8.1	13.9	-0.1904	0.0472	0.0263	-0.1393	0.0441	0.0225
0	1	13	11	210.4	7.9	11.1	-0.0619	0.0557	0.0281	-0.0928	0.0500	0.0214
0	1	13	12	171.7	7.8	9.5	0.0327	0.0686	0.0355	0.0564	0.0577	0.0254
0	1	13	13	127.9	6.8	5.0	-0.1788	0.0782	0.0536	-0.0397	0.0731	0.0328
0	1	13	14	107.8	7.7	5.9	n.m.	n.m.	n.m.	n.m.	n.m.	n.m.
0	1	13	15	103.5	12.8	6.8	n.m.	n.m.	n.m.	n.m.	n.m.	n.m.
0	1	14	0	1002.8	17.5	50.6	n.m.	n.m.	n.m.	n.m.	n.m.	n.m.
0	1	14	1	1370.0	42.0	76.3	n.m.	n.m.	n.m.	n.m.	n.m.	n.m.
0	1	14	2	992.6	452.9	357.1	n.m.	n.m.	n.m.	n.m.	n.m.	n.m.
0	1	14	3	709.0	20.5	214.4	n.m.	n.m.	n.m.	n.m.	n.m.	n.m.
0	1	14	4	596.7	17.8	77.7	n.m.	n.m.	n.m.	n.m.	n.m.	n.m.
0	1	14	5	717.9	22.5	52.7	n.m.	n.m.	n.m.	n.m.	n.m.	n.m.
0	1	14	6	450.9	72.2	55.1	n.m.	n.m.	n.m.	n.m.	n.m.	n.m.
0	1	14	7	356.3	28.0	32.3	n.m.	n.m.	n.m.	n.m.	n.m.	n.m.
0	1	14	8	285.0	30.5	17.0	n.m.	n.m.	n.m.	n.m.	n.m.	n.m.
0	1	14	9	244.4	11.0	11.8	n.m.	n.m.	n.m.	n.m.	n.m.	n.m.
0	1	14	10	210.0	10.7	15.5	n.m.	n.m.	n.m.	n.m.	n.m.	n.m.
0	1	14	11	177.6	11.9	11.9	n.m.	n.m.	n.m.	n.m.	n.m.	n.m.
0	1	14	12	129.4	14.0	9.8	n.m.	n.m.	n.m.	n.m.	n.m.	n.m.
0	1	15	0	927.3	23.7	46.5	n.m.	n.m.	n.m.	n.m.	n.m.	n.m.

Continued on next page

Table B.1 – *Continued from previous page*

x	Q^2	z	$P_{h\perp}^2$	A_0	ΔA_0	δA_0	$A_{UU}^{\cos\phi_h}$	$\Delta A_{UU}^{\cos\phi_h}$	$\delta A_{UU}^{\cos\phi_h}$	$A_{UU}^{\cos 2\phi_h}$	$\Delta A_{UU}^{\cos 2\phi_h}$	$\delta A_{UU}^{\cos 2\phi_h}$
0	1	15	1	830.4	27.0	44.1	n.m.	n.m.	n.m.	n.m.	n.m.	n.m.
0	1	15	2	677.7	24.7	133.4	n.m.	n.m.	n.m.	n.m.	n.m.	n.m.
0	1	15	3	873.4	32.5	232.4	n.m.	n.m.	n.m.	n.m.	n.m.	n.m.
0	1	15	4	510.7	38.4	74.3	n.m.	n.m.	n.m.	n.m.	n.m.	n.m.
0	1	15	5	502.2	324.1	170.1	n.m.	n.m.	n.m.	n.m.	n.m.	n.m.
0	1	15	6	389.8	88.5	81.3	n.m.	n.m.	n.m.	n.m.	n.m.	n.m.
0	1	15	7	256.2	11.7	17.4	n.m.	n.m.	n.m.	n.m.	n.m.	n.m.
0	1	15	8	301.0	65.8	25.4	n.m.	n.m.	n.m.	n.m.	n.m.	n.m.
0	1	16	0	814.2	19.7	54.5	n.m.	n.m.	n.m.	n.m.	n.m.	n.m.
0	1	16	1	916.4	890.9	556.2	n.m.	n.m.	n.m.	n.m.	n.m.	n.m.
0	1	16	2	966.1	68.5	261.8	n.m.	n.m.	n.m.	n.m.	n.m.	n.m.
0	1	16	3	485.3	37.5	276.2	n.m.	n.m.	n.m.	n.m.	n.m.	n.m.
0	1	16	4	426.7	35.3	296.4	n.m.	n.m.	n.m.	n.m.	n.m.	n.m.
1	0	1	0	492627.0	796.5	24323.5	-0.0918	0.0023	0.0090	-0.0258	0.0023	0.0014
1	0	2	0	301080.0	490.5	14923.9	-0.0275	0.0024	0.0067	-0.0024	0.0022	0.0018
1	0	2	1	198701.0	343.6	9951.5	-0.1300	0.0024	0.0076	-0.0048	0.0024	0.0025
1	0	2	2	56973.8	155.4	2842.9	-0.2281	0.0038	0.0119	0.0248	0.0038	0.0024
1	0	3	0	180692.0	413.8	8898.7	0.0724	0.0035	0.0093	0.0300	0.0031	0.0058
1	0	3	1	133178.0	284.6	6502.1	-0.0269	0.0031	0.0088	0.0050	0.0030	0.0029
1	0	3	2	83370.4	214.8	4097.8	-0.1019	0.0037	0.0113	0.0057	0.0036	0.0036
1	0	3	3	47315.7	155.9	2354.4	-0.1392	0.0047	0.0112	0.0018	0.0046	0.0056
1	0	3	4	20239.7	92.1	1013.2	-0.1710	0.0064	0.0116	0.0099	0.0064	0.0065
1	0	3	5	7103.7	48.4	350.7	-0.2406	0.0096	0.0235	0.0502	0.0095	0.0048
1	0	4	0	114996.0	344.5	5688.3	0.0861	0.0048	0.0172	-0.0001	0.0042	0.0131
1	0	4	1	90204.5	244.0	4374.5	0.0572	0.0040	0.0061	0.0215	0.0036	0.0029
1	0	4	2	60219.8	183.5	2954.1	-0.0253	0.0044	0.0093	0.0142	0.0042	0.0038
1	0	4	3	39556.4	144.4	1938.4	-0.0719	0.0052	0.0107	-0.0063	0.0051	0.0041
1	0	4	4	27892.7	123.8	1374.6	-0.1000	0.0063	0.0129	-0.0108	0.0062	0.0073
1	0	4	5	19055.3	106.6	949.6	-0.1226	0.0080	0.0173	0.0137	0.0080	0.0079
1	0	4	6	9469.7	70.0	482.4	-0.0872	0.0105	0.0198	-0.0055	0.0103	0.0105
1	0	4	7	3914.5	39.7	193.5	-0.1186	0.0144	0.0152	0.0119	0.0144	0.0122
1	0	4	8	1648.0	24.5	87.0	-0.2750	0.0208	0.0489	0.0451	0.0210	0.0079
1	0	5	0	72174.8	291.4	3621.4	0.0820	0.0068	0.0202	-0.0209	0.0060	0.0151
1	0	5	1	60370.6	273.3	2999.2	0.0835	0.0076	0.0117	0.0148	0.0059	0.0077
1	0	5	2	45606.1	176.2	2227.7	0.0340	0.0059	0.0095	0.0075	0.0053	0.0064
1	0	5	3	31843.3	132.1	1569.8	-0.0211	0.0060	0.0086	0.0073	0.0056	0.0039
1	0	5	4	22184.6	110.8	1102.5	-0.0565	0.0072	0.0088	-0.0120	0.0069	0.0052
1	0	5	5	15920.4	95.9	812.3	-0.0722	0.0086	0.0119	-0.0074	0.0085	0.0063
1	0	5	6	13067.5	97.2	645.2	-0.0444	0.0108	0.0167	0.0151	0.0103	0.0089

Continued on next page

Table B.1 – *Continued from previous page*

x	Q^2	z	$P_{h\perp}^2$	A_0	ΔA_0	δA_0	$A_{UU}^{\cos\phi_h}$	$\Delta A_{UU}^{\cos\phi_h}$	$\delta A_{UU}^{\cos\phi_h}$	$A_{UU}^{\cos 2\phi_h}$	$\Delta A_{UU}^{\cos 2\phi_h}$	$\delta A_{UU}^{\cos 2\phi_h}$
1	0	5	7	8917.9	84.3	435.4	-0.0452	0.0136	0.0239	0.0118	0.0132	0.0114
1	0	5	8	4708.0	57.5	231.4	-0.0615	0.0177	0.0270	0.0315	0.0174	0.0130
1	0	5	9	2018.8	33.5	106.2	-0.0422	0.0236	0.0270	0.0009	0.0237	0.0222
1	0	5	10	803.7	18.4	44.9	-0.1870	0.0325	0.0346	0.0399	0.0333	0.0140
1	0	6	0	46520.0	184.5	2317.0	0.0566	0.0058	0.0178	-0.0335	0.0057	0.0113
1	0	6	1	40247.3	211.2	2037.2	0.0648	0.0092	0.0223	-0.0063	0.0074	0.0160
1	0	6	2	32854.8	179.2	1634.7	0.0553	0.0090	0.0133	0.0120	0.0071	0.0088
1	0	6	3	24352.2	113.8	1198.1	-0.0044	0.0067	0.0107	-0.0170	0.0063	0.0039
1	0	6	4	17646.5	96.9	867.8	-0.0340	0.0078	0.0112	-0.0257	0.0075	0.0045
1	0	6	5	12866.7	85.3	646.8	-0.0649	0.0095	0.0118	-0.0131	0.0091	0.0075
1	0	6	6	9583.1	77.4	491.7	-0.0688	0.0117	0.0124	0.0108	0.0112	0.0084
1	0	6	7	7770.1	77.6	390.0	-0.0305	0.0145	0.0135	0.0194	0.0137	0.0102
1	0	6	8	5964.6	74.9	313.9	-0.0229	0.0183	0.0240	0.0394	0.0178	0.0135
1	0	6	9	3657.4	59.1	181.2	-0.0227	0.0237	0.0349	0.0442	0.0230	0.0177
1	0	6	10	1844.3	39.1	110.1	0.0110	0.0308	0.0375	0.0309	0.0304	0.0200
1	0	6	11	787.7	22.2	39.9	0.0169	0.0419	0.0334	0.1145	0.0385	0.0295
1	0	6	12	345.3	12.9	16.2	0.0240	0.0513	0.0498	-0.0659	0.0537	0.0323
1	0	7	0	30765.1	143.4	1583.0	0.0107	0.0065	0.0161	-0.0463	0.0064	0.0102
1	0	7	1	28092.3	149.0	1433.8	0.0739	0.0094	0.0285	-0.0076	0.0081	0.0183
1	0	7	2	22729.2	158.7	1149.2	0.0108	0.0123	0.0165	-0.0277	0.0094	0.0069
1	0	7	3	18044.5	104.0	908.6	0.0219	0.0090	0.0152	-0.0020	0.0077	0.0061
1	0	7	4	13750.2	83.3	695.9	-0.0313	0.0088	0.0146	-0.0107	0.0081	0.0049
1	0	7	5	10243.5	73.2	518.1	-0.0476	0.0103	0.0134	-0.0132	0.0097	0.0056
1	0	7	6	7726.3	66.5	393.6	-0.0797	0.0125	0.0159	0.0015	0.0118	0.0089
1	0	7	7	5767.3	61.1	309.9	-0.0689	0.0155	0.0125	0.0295	0.0149	0.0086
1	0	7	8	4652.1	61.9	243.2	-0.0562	0.0193	0.0152	0.0164	0.0185	0.0116
1	0	7	9	3441.6	57.9	182.8	-0.0622	0.0246	0.0231	0.0414	0.0234	0.0194
1	0	7	10	2079.9	45.1	115.1	-0.0401	0.0313	0.0346	-0.0003	0.0313	0.0198
1	0	7	11	1134.6	33.0	63.9	0.0428	0.0433	0.0332	0.0925	0.0397	0.0251
1	0	7	12	547.9	19.9	26.7	0.0612	0.0530	0.0355	0.0627	0.0487	0.0343
1	0	7	13	229.7	11.3	15.5	0.1120	0.0697	0.0454	0.0273	0.0729	0.0335
1	0	7	14	77.4	5.3	3.9	-0.0304	0.1050	0.1037	0.0846	0.0991	0.0762
1	0	8	0	21705.3	115.6	1189.7	0.0050	0.0072	0.0153	-0.0311	0.0072	0.0100
1	0	8	1	19362.8	107.4	1039.8	0.0083	0.0098	0.0294	-0.0506	0.0093	0.0208
1	0	8	2	16400.9	126.1	973.0	0.0176	0.0139	0.0601	0.0015	0.0108	0.0412
1	0	8	3	12954.5	110.8	702.4	-0.0404	0.0150	0.0264	-0.0199	0.0114	0.0136
1	0	8	4	10469.3	71.9	550.5	-0.0572	0.0103	0.0181	-0.0159	0.0090	0.0064
1	0	8	5	8144.5	63.9	420.5	-0.0436	0.0115	0.0171	-0.0133	0.0105	0.0062
1	0	8	6	6104.4	56.7	320.8	-0.0692	0.0135	0.0186	-0.0139	0.0127	0.0078

Continued on next page

Table B.1 – *Continued from previous page*

x	Q^2	z	$P_{h\perp}^2$	A_0	ΔA_0	δA_0	$A_{UU}^{\cos\phi_h}$	$\Delta A_{UU}^{\cos\phi_h}$	$\delta A_{UU}^{\cos\phi_h}$	$A_{UU}^{\cos 2\phi_h}$	$\Delta A_{UU}^{\cos 2\phi_h}$	$\delta A_{UU}^{\cos 2\phi_h}$
1	0	8	7	4488.9	50.1	246.6	-0.0622	0.0159	0.0143	-0.0362	0.0152	0.0101
1	0	8	8	3589.4	50.1	195.2	-0.0594	0.0203	0.0218	-0.0004	0.0190	0.0114
1	0	8	9	2746.8	48.4	142.8	-0.0788	0.0261	0.0191	0.0579	0.0241	0.0131
1	0	8	10	1843.5	41.6	101.6	-0.0096	0.0338	0.0298	0.0767	0.0309	0.0157
1	0	8	11	1049.8	29.8	65.5	-0.0747	0.0417	0.0320	0.0626	0.0422	0.0220
1	0	8	12	574.9	21.2	33.9	-0.0812	0.0539	0.0452	0.0383	0.0546	0.0246
1	0	8	13	283.4	13.9	18.0	-0.0964	0.0721	0.0462	-0.0233	0.0695	0.0448
1	0	8	14	114.0	7.7	6.6	0.1992	0.0940	0.0801	0.0477	0.1106	0.0569
1	0	8	15	50.7	5.2	3.3	n.m.	n.m.	n.m.	n.m.	n.m.	n.m.
1	0	9	0	15964.1	93.4	862.7	0.0036	0.0077	0.0143	-0.0319	0.0078	0.0106
1	0	9	1	13956.3	106.4	766.5	n.m.	n.m.	n.m.	n.m.	n.m.	n.m.
1	0	9	2	12118.0	101.4	675.6	n.m.	n.m.	n.m.	n.m.	n.m.	n.m.
1	0	9	3	10158.3	130.6	606.4	n.m.	n.m.	n.m.	n.m.	n.m.	n.m.
1	0	9	4	8187.0	88.7	471.0	-0.0541	0.0190	0.0313	-0.0334	0.0144	0.0153
1	0	9	5	6382.6	57.2	340.8	-0.0707	0.0134	0.0204	-0.0462	0.0119	0.0092
1	0	9	6	5110.3	52.1	266.3	-0.0395	0.0149	0.0207	-0.0308	0.0137	0.0069
1	0	9	7	3794.0	45.8	200.0	-0.0431	0.0175	0.0178	-0.0273	0.0162	0.0097
1	0	9	8	2914.5	42.9	151.6	-0.0653	0.0213	0.0152	-0.0188	0.0198	0.0141
1	0	9	9	2110.8	38.6	112.6	-0.0517	0.0264	0.0157	-0.0264	0.0255	0.0157
1	0	9	10	1557.6	36.5	88.6	-0.0595	0.0335	0.0212	-0.0198	0.0325	0.0192
1	0	9	11	966.5	29.0	50.5	0.0409	0.0438	0.0264	0.0470	0.0400	0.0190
1	0	9	12	489.7	18.9	25.4	0.0014	0.0561	0.0386	0.0373	0.0500	0.0268
1	0	9	13	259.5	13.6	39.1	-0.0443	0.0761	0.2632	-0.0265	0.0723	0.2190
1	0	9	14	120.7	8.2	7.3	0.1367	0.0989	0.0565	0.0667	0.0939	0.0630
1	0	9	15	64.9	6.8	6.3	n.m.	n.m.	n.m.	n.m.	n.m.	n.m.
1	0	10	0	12636.1	79.9	652.6	0.0005	0.0082	0.0141	-0.0431	0.0084	0.0118
1	0	10	1	10833.2	139.5	684.9	n.m.	n.m.	n.m.	n.m.	n.m.	n.m.
1	0	10	2	9420.7	111.0	617.9	n.m.	n.m.	n.m.	n.m.	n.m.	n.m.
1	0	10	3	8032.6	109.4	472.6	n.m.	n.m.	n.m.	n.m.	n.m.	n.m.
1	0	10	4	6518.4	108.9	358.0	n.m.	n.m.	n.m.	n.m.	n.m.	n.m.
1	0	10	5	5017.9	92.4	279.7	n.m.	n.m.	n.m.	n.m.	n.m.	n.m.
1	0	10	6	4038.3	48.2	209.0	-0.0670	0.0182	0.0185	-0.0329	0.0158	0.0120
1	0	10	7	3237.7	44.5	172.5	-0.0800	0.0206	0.0165	-0.0199	0.0184	0.0123
1	0	10	8	2493.7	41.0	125.5	-0.1276	0.0245	0.0200	-0.0007	0.0226	0.0146
1	0	10	9	1753.4	35.1	89.3	-0.0509	0.0298	0.0230	0.0377	0.0275	0.0122
1	0	10	10	1360.4	34.2	64.7	-0.0398	0.0381	0.0311	0.0924	0.0334	0.0140
1	0	10	11	768.8	24.2	43.2	-0.0685	0.0468	0.0286	0.0665	0.0426	0.0256
1	0	10	12	445.5	18.1	26.7	0.0405	0.0583	0.0393	0.0013	0.0550	0.0326
1	0	10	13	218.6	11.9	13.5	-0.0570	0.0829	0.0553	0.1552	0.0739	0.0508

Continued on next page

Table B.1 – *Continued from previous page*

x	Q^2	z	$P_{h\perp}^2$	A_0	ΔA_0	δA_0	$A_{UU}^{\cos\phi_h}$	$\Delta A_{UU}^{\cos\phi_h}$	$\delta A_{UU}^{\cos\phi_h}$	$A_{UU}^{\cos 2\phi_h}$	$\Delta A_{UU}^{\cos 2\phi_h}$	$\delta A_{UU}^{\cos 2\phi_h}$
1	0	10	14	115.5	8.5	7.8	0.0675	0.1075	0.0692	0.0352	0.0993	0.0628
1	0	10	15	65.8	9.2	6.9	n.m.	n.m.	n.m.	n.m.	n.m.	n.m.
1	0	11	0	10518.0	71.4	600.7	0.0023	0.0088	0.0136	-0.0517	0.0090	0.0075
1	0	11	1	8216.9	148.0	525.0	n.m.	n.m.	n.m.	n.m.	n.m.	n.m.
1	0	11	2	7561.5	103.0	460.1	n.m.	n.m.	n.m.	n.m.	n.m.	n.m.
1	0	11	3	6057.7	92.6	389.4	n.m.	n.m.	n.m.	n.m.	n.m.	n.m.
1	0	11	4	5160.0	92.6	314.1	n.m.	n.m.	n.m.	n.m.	n.m.	n.m.
1	0	11	5	4241.7	96.7	256.0	n.m.	n.m.	n.m.	n.m.	n.m.	n.m.
1	0	11	6	3265.9	96.0	185.6	n.m.	n.m.	n.m.	n.m.	n.m.	n.m.
1	0	11	7	2758.1	83.0	150.8	n.m.	n.m.	n.m.	n.m.	n.m.	n.m.
1	0	11	8	2059.2	40.4	99.8	-0.0816	0.0302	0.0168	0.0122	0.0260	0.0099
1	0	11	9	1539.7	36.9	82.1	-0.0481	0.0369	0.0258	0.0600	0.0319	0.0173
1	0	11	10	1086.4	32.4	56.9	-0.0245	0.0456	0.0399	0.0684	0.0393	0.0201
1	0	11	11	624.1	23.3	34.0	-0.1507	0.0573	0.0423	0.0452	0.0540	0.0293
1	0	11	12	372.9	18.4	20.3	-0.0035	0.0757	0.0577	0.2098	0.0629	0.0326
1	0	11	13	192.2	13.4	15.3	n.m.	n.m.	n.m.	n.m.	n.m.	n.m.
1	0	11	14	101.9	14.4	12.1	n.m.	n.m.	n.m.	n.m.	n.m.	n.m.
1	0	12	0	8945.0	65.0	454.8	-0.0190	0.0093	0.0105	-0.0733	0.0098	0.0082
1	0	12	1	6727.0	180.0	393.8	n.m.	n.m.	n.m.	n.m.	n.m.	n.m.
1	0	12	2	5973.2	94.7	322.3	n.m.	n.m.	n.m.	n.m.	n.m.	n.m.
1	0	12	3	4960.1	84.0	241.1	n.m.	n.m.	n.m.	n.m.	n.m.	n.m.
1	0	12	4	4103.6	82.6	216.3	n.m.	n.m.	n.m.	n.m.	n.m.	n.m.
1	0	12	5	3362.1	84.3	185.5	n.m.	n.m.	n.m.	n.m.	n.m.	n.m.
1	0	12	6	2788.0	88.5	129.7	n.m.	n.m.	n.m.	n.m.	n.m.	n.m.
1	0	12	7	2090.2	78.7	127.9	n.m.	n.m.	n.m.	n.m.	n.m.	n.m.
1	0	12	8	1671.3	43.4	86.7	-0.1285	0.0420	0.0307	0.0082	0.0338	0.0176
1	0	12	9	1276.3	41.4	64.7	0.0201	0.0505	0.0740	0.0468	0.0408	0.0277
1	0	12	10	793.3	30.3	43.8	-0.0893	0.0607	0.0403	0.1200	0.0481	0.0254
1	0	12	11	421.2	21.1	22.9	-0.0755	0.0761	0.0658	0.0205	0.0648	0.0377
1	0	12	12	261.3	20.4	16.1	n.m.	n.m.	n.m.	n.m.	n.m.	n.m.
1	0	12	13	137.0	20.6	8.6	n.m.	n.m.	n.m.	n.m.	n.m.	n.m.
1	0	13	0	7570.2	58.9	389.6	-0.0057	0.0102	0.0111	-0.0379	0.0106	0.0126
1	0	13	1	6247.4	319.8	424.5	n.m.	n.m.	n.m.	n.m.	n.m.	n.m.
1	0	13	2	5027.1	166.9	292.7	n.m.	n.m.	n.m.	n.m.	n.m.	n.m.
1	0	13	3	4379.5	138.2	272.1	n.m.	n.m.	n.m.	n.m.	n.m.	n.m.
1	0	13	4	3604.6	132.5	305.6	n.m.	n.m.	n.m.	n.m.	n.m.	n.m.
1	0	13	5	2991.7	137.0	278.3	n.m.	n.m.	n.m.	n.m.	n.m.	n.m.
1	0	13	6	2271.1	129.2	157.7	n.m.	n.m.	n.m.	n.m.	n.m.	n.m.
1	0	13	7	1934.7	133.1	170.6	n.m.	n.m.	n.m.	n.m.	n.m.	n.m.

Continued on next page

Table B.1 – *Continued from previous page*

x	Q^2	z	$P_{h\perp}^2$	A_0	ΔA_0	δA_0	$A_{UU}^{\cos\phi_h}$	$\Delta A_{UU}^{\cos\phi_h}$	$\delta A_{UU}^{\cos\phi_h}$	$A_{UU}^{\cos 2\phi_h}$	$\Delta A_{UU}^{\cos 2\phi_h}$	$\delta A_{UU}^{\cos 2\phi_h}$
1	0	13	8	1367.4	99.6	90.0	n.m.	n.m.	n.m.	n.m.	n.m.	n.m.
1	0	13	9	761.7	39.2	72.6	n.m.	n.m.	n.m.	n.m.	n.m.	n.m.
1	0	13	10	499.0	39.0	32.5	n.m.	n.m.	n.m.	n.m.	n.m.	n.m.
1	0	13	11	298.7	37.4	17.6	n.m.	n.m.	n.m.	n.m.	n.m.	n.m.
1	0	14	0	6624.5	58.3	330.4	-0.0052	0.0117	0.0137	-0.0371	0.0120	0.0104
1	0	14	1	5283.8	408.6	578.6	n.m.	n.m.	n.m.	n.m.	n.m.	n.m.
1	0	14	2	4727.2	213.9	400.5	n.m.	n.m.	n.m.	n.m.	n.m.	n.m.
1	0	14	3	3780.2	572.5	915.1	n.m.	n.m.	n.m.	n.m.	n.m.	n.m.
1	0	14	4	3325.3	542.5	455.3	n.m.	n.m.	n.m.	n.m.	n.m.	n.m.
1	0	14	5	3308.9	98.6	312.9	n.m.	n.m.	n.m.	n.m.	n.m.	n.m.
1	0	14	6	2369.4	88.0	192.3	n.m.	n.m.	n.m.	n.m.	n.m.	n.m.
1	0	14	7	1830.1	93.1	294.5	n.m.	n.m.	n.m.	n.m.	n.m.	n.m.
1	0	14	8	732.5	369.1	215.5	n.m.	n.m.	n.m.	n.m.	n.m.	n.m.
1	0	15	0	6335.5	78.4	313.8	-0.0300	0.0163	0.0121	-0.0593	0.0167	0.0143
1	0	15	1	4386.1	103.0	707.6	n.m.	n.m.	n.m.	n.m.	n.m.	n.m.
1	0	15	2	3975.2	1128.3	524.9	n.m.	n.m.	n.m.	n.m.	n.m.	n.m.
1	0	15	3	4363.3	797.8	964.0	n.m.	n.m.	n.m.	n.m.	n.m.	n.m.
1	0	15	4	2446.5	861.3	692.7	n.m.	n.m.	n.m.	n.m.	n.m.	n.m.
1	0	15	5	1520.7	1.4	127.4	n.m.	n.m.	n.m.	n.m.	n.m.	n.m.
1	0	16	0	5387.9	175.8	262.9	0.0037	0.0438	0.0305	-0.0558	0.0426	0.0214
1	0	16	1	4476.5	736.7	453.3	n.m.	n.m.	n.m.	n.m.	n.m.	n.m.
1	1	1	0	192736.0	245.6	10660.2	-0.1537	0.0018	0.0306	-0.0274	0.0018	0.0031
1	1	2	0	89338.4	151.6	4615.3	-0.0664	0.0025	0.0108	-0.0029	0.0023	0.0027
1	1	2	1	60237.8	103.5	3044.2	-0.1548	0.0024	0.0219	-0.0105	0.0024	0.0038
1	1	2	2	30622.5	69.1	1601.0	-0.2259	0.0032	0.0323	0.0247	0.0032	0.0054
1	1	2	3	13576.7	44.4	726.3	-0.2960	0.0045	0.0473	0.0513	0.0046	0.0068
1	1	3	0	56073.3	148.5	2778.2	0.0179	0.0043	0.0175	-0.0036	0.0036	0.0089
1	1	3	1	40292.4	89.0	1978.7	-0.0286	0.0032	0.0194	-0.0009	0.0031	0.0039
1	1	3	2	25368.5	66.2	1252.2	-0.0906	0.0037	0.0246	-0.0048	0.0037	0.0042
1	1	3	3	15340.7	49.1	766.7	-0.1438	0.0046	0.0291	-0.0038	0.0046	0.0058
1	1	3	4	9069.8	36.3	455.2	-0.1949	0.0056	0.0340	0.0057	0.0057	0.0076
1	1	3	5	5109.2	26.4	262.6	-0.2518	0.0073	0.0400	0.0596	0.0073	0.0093
1	1	3	6	2766.5	19.1	149.6	-0.2606	0.0097	0.0446	0.0423	0.0097	0.0136
1	1	3	7	1453.2	14.5	84.6	-0.3288	0.0141	0.0641	0.1107	0.0138	0.0164
1	1	4	0	32296.6	128.5	1619.5	-0.0186	0.0069	0.0288	-0.0569	0.0057	0.0169
1	1	4	1	26399.3	91.6	1268.6	0.0445	0.0056	0.0211	0.0062	0.0047	0.0072
1	1	4	2	19087.5	59.2	924.4	-0.0237	0.0045	0.0258	0.0108	0.0043	0.0030
1	1	4	3	12982.6	47.9	630.9	-0.0658	0.0053	0.0290	0.0014	0.0052	0.0035
1	1	4	4	8685.4	38.8	427.8	-0.1044	0.0064	0.0321	0.0051	0.0063	0.0054

Continued on next page

Table B.1 – *Continued from previous page*

x	Q^2	z	$P_{h\perp}^2$	A_0	ΔA_0	δA_0	$A_{UU}^{\cos\phi_h}$	$\Delta A_{UU}^{\cos\phi_h}$	$\delta A_{UU}^{\cos\phi_h}$	$A_{UU}^{\cos 2\phi_h}$	$\Delta A_{UU}^{\cos 2\phi_h}$	$\delta A_{UU}^{\cos 2\phi_h}$
1	1	4	5	5788.5	31.5	281.9	-0.1275	0.0078	0.0341	0.0015	0.0078	0.0072
1	1	4	6	3695.3	24.5	186.3	-0.1467	0.0096	0.0357	0.0187	0.0095	0.0099
1	1	4	7	2342.0	19.4	119.3	-0.1828	0.0119	0.0370	0.0456	0.0118	0.0119
1	1	4	8	1397.1	14.7	74.5	-0.2144	0.0151	0.0385	0.0353	0.0150	0.0121
1	1	4	9	821.0	11.4	47.1	-0.1789	0.0196	0.0475	0.0178	0.0195	0.0215
1	1	4	10	486.0	9.3	28.3	-0.2125	0.0266	0.0605	0.0007	0.0269	0.0162
1	1	4	11	286.4	8.1	17.0	-0.2834	0.0414	0.0346	0.1860	0.0392	0.0765
1	1	5	0	19175.8	78.3	930.1	n.m.	n.m.	n.m.	n.m.	n.m.	n.m.
1	1	5	1	16996.5	79.4	803.5	0.0310	0.0078	0.0252	-0.0071	0.0062	0.0087
1	1	5	2	13568.2	50.3	647.5	0.0135	0.0054	0.0279	0.0022	0.0050	0.0046
1	1	5	3	10140.0	42.6	492.9	-0.0285	0.0060	0.0312	0.0035	0.0058	0.0036
1	1	5	4	7386.8	36.8	357.9	-0.0755	0.0071	0.0348	0.0193	0.0070	0.0044
1	1	5	5	5208.1	31.3	255.2	-0.0921	0.0086	0.0368	0.0224	0.0084	0.0058
1	1	5	6	3620.8	26.4	180.6	-0.1318	0.0104	0.0381	0.0211	0.0103	0.0078
1	1	5	7	2508.5	22.2	126.9	-0.1360	0.0128	0.0395	0.0429	0.0127	0.0084
1	1	5	8	1754.4	18.9	86.9	-0.1445	0.0158	0.0409	0.0735	0.0154	0.0107
1	1	5	9	1159.2	15.3	59.7	-0.1135	0.0195	0.0389	0.0850	0.0190	0.0128
1	1	5	10	737.4	12.2	38.1	-0.1294	0.0240	0.0383	0.0535	0.0236	0.0185
1	1	5	11	448.3	9.6	23.8	-0.0675	0.0318	0.0406	0.0959	0.0306	0.0204
1	1	5	12	268.8	7.5	15.8	-0.1420	0.0406	0.0467	0.0501	0.0391	0.0245
1	1	5	13	152.8	6.0	8.8	-0.0026	0.0601	0.0649	0.2171	0.0528	0.0341
1	1	6	0	11597.5	56.3	562.5	n.m.	n.m.	n.m.	n.m.	n.m.	n.m.
1	1	6	1	10813.2	87.1	504.8	n.m.	n.m.	n.m.	n.m.	n.m.	n.m.
1	1	6	2	9337.4	52.7	444.0	0.0191	0.0093	0.0320	0.0263	0.0074	0.0071
1	1	6	3	7360.3	35.9	351.2	-0.0205	0.0072	0.0355	0.0238	0.0066	0.0036
1	1	6	4	5634.6	31.4	268.7	-0.0482	0.0080	0.0384	0.0132	0.0076	0.0045
1	1	6	5	4213.0	27.8	201.1	-0.0694	0.0095	0.0410	0.0244	0.0091	0.0048
1	1	6	6	3048.6	24.3	151.0	-0.0902	0.0115	0.0433	0.0434	0.0112	0.0061
1	1	6	7	2254.4	21.6	107.9	-0.0990	0.0138	0.0448	0.0483	0.0136	0.0084
1	1	6	8	1564.7	18.2	75.4	-0.1545	0.0168	0.0457	0.0755	0.0162	0.0100
1	1	6	9	1138.4	15.9	60.3	-0.1411	0.0203	0.0468	0.0750	0.0193	0.0114
1	1	6	10	824.7	14.2	41.0	-0.1342	0.0252	0.0437	0.0961	0.0243	0.0139
1	1	6	11	552.3	11.7	28.1	-0.1036	0.0315	0.0427	0.1202	0.0302	0.0167
1	1	6	12	357.6	9.4	18.4	-0.0916	0.0395	0.0408	0.1722	0.0376	0.0180
1	1	6	13	234.2	7.7	12.1	-0.0069	0.0474	0.0451	0.0521	0.0461	0.0255
1	1	6	14	143.2	6.4	9.1	0.0100	0.0668	0.0531	0.1798	0.0605	0.0446
1	1	6	15	86.5	5.5	5.1	0.1802	0.0937	0.0734	0.2475	0.0833	0.0465
1	1	6	16	48.1	4.9	3.3	n.m.	n.m.	n.m.	n.m.	n.m.	n.m.
1	1	7	0	7420.4	42.4	350.7	n.m.	n.m.	n.m.	n.m.	n.m.	n.m.

Continued on next page

Table B.1 – *Continued from previous page*

x	Q^2	z	$P_{h\perp}^2$	A_0	ΔA_0	δA_0	$A_{UU}^{\cos\phi_h}$	$\Delta A_{UU}^{\cos\phi_h}$	$\delta A_{UU}^{\cos\phi_h}$	$A_{UU}^{\cos 2\phi_h}$	$\Delta A_{UU}^{\cos 2\phi_h}$	$\delta A_{UU}^{\cos 2\phi_h}$
1	1	7	1	7319.7	62.7	368.2	n.m.	n.m.	n.m.	n.m.	n.m.	n.m.
1	1	7	2	6163.1	44.4	397.0	-0.0612	0.0126	0.0958	-0.0218	0.0097	0.0610
1	1	7	3	5183.7	36.5	250.6	-0.0281	0.0117	0.0407	0.0123	0.0095	0.0093
1	1	7	4	4179.8	26.4	198.7	-0.0561	0.0093	0.0431	0.0191	0.0085	0.0071
1	1	7	5	3190.1	23.3	146.7	-0.0726	0.0106	0.0453	0.0287	0.0100	0.0065
1	1	7	6	2411.3	20.8	115.3	-0.1101	0.0126	0.0463	0.0519	0.0119	0.0087
1	1	7	7	1858.0	19.0	95.2	-0.1305	0.0146	0.0475	0.0203	0.0142	0.0083
1	1	7	8	1371.9	16.9	64.9	-0.1211	0.0179	0.0488	0.0614	0.0172	0.0098
1	1	7	9	1001.4	15.0	52.4	-0.1275	0.0215	0.0501	0.0513	0.0214	0.0115
1	1	7	10	721.7	13.0	34.8	-0.1885	0.0263	0.0501	0.1083	0.0253	0.0134
1	1	7	11	526.7	11.5	26.5	-0.1527	0.0320	0.0483	0.1202	0.0310	0.0137
1	1	7	12	378.8	10.2	18.6	-0.0681	0.0397	0.0449	0.0922	0.0372	0.0169
1	1	7	13	262.1	8.6	14.8	-0.1026	0.0482	0.0446	0.1079	0.0448	0.0274
1	1	7	14	161.9	6.7	9.1	0.0123	0.0606	0.0482	0.0687	0.0626	0.0293
1	1	7	15	101.9	5.4	6.0	-0.1059	0.0775	0.0552	0.0975	0.0756	0.0423
1	1	7	16	65.9	4.6	4.5	-0.1295	0.1024	0.0905	0.1124	0.0972	0.0598
1	1	7	17	44.1	4.8	3.5	n.m.	n.m.	n.m.	n.m.	n.m.	n.m.
1	1	8	0	5173.6	34.0	238.0	n.m.	n.m.	n.m.	n.m.	n.m.	n.m.
1	1	8	1	4856.9	209.7	487.1	n.m.	n.m.	n.m.	n.m.	n.m.	n.m.
1	1	8	2	4382.1	67.7	214.2	n.m.	n.m.	n.m.	n.m.	n.m.	n.m.
1	1	8	3	3557.1	49.7	165.5	n.m.	n.m.	n.m.	n.m.	n.m.	n.m.
1	1	8	4	2910.8	21.6	138.0	-0.1058	0.0112	0.0447	-0.0163	0.0099	0.0100
1	1	8	5	2399.1	19.6	115.7	-0.0772	0.0121	0.0483	0.0144	0.0110	0.0073
1	1	8	6	1871.1	17.6	90.8	-0.1103	0.0139	0.0509	0.0439	0.0129	0.0076
1	1	8	7	1457.0	16.0	72.7	-0.1159	0.0160	0.0515	0.0352	0.0153	0.0100
1	1	8	8	1138.1	14.8	50.9	-0.1381	0.0192	0.0526	0.0717	0.0183	0.0106
1	1	8	9	857.3	13.4	42.0	-0.1373	0.0230	0.0525	0.0960	0.0218	0.0120
1	1	8	10	633.2	11.9	29.6	-0.1843	0.0273	0.0495	0.0618	0.0263	0.0125
1	1	8	11	473.1	10.9	22.9	-0.1530	0.0344	0.0497	0.1570	0.0329	0.0180
1	1	8	12	365.4	10.1	18.3	-0.1261	0.0395	0.0433	0.0533	0.0395	0.0155
1	1	8	13	257.1	8.6	13.4	-0.1025	0.0484	0.0471	0.1037	0.0465	0.0169
1	1	8	14	182.7	7.5	9.3	-0.0570	0.0585	0.0436	0.0674	0.0579	0.0232
1	1	8	15	111.6	5.7	6.4	-0.1384	0.0768	0.0590	0.1657	0.0772	0.0398
1	1	8	16	72.7	4.8	4.1	-0.0552	0.0939	0.0915	0.0223	0.0996	0.0604
1	1	8	17	39.6	3.7	4.6	n.m.	n.m.	n.m.	n.m.	n.m.	n.m.
1	1	9	0	3948.8	29.0	184.0	n.m.	n.m.	n.m.	n.m.	n.m.	n.m.
1	1	9	1	3841.7	187.5	321.7	n.m.	n.m.	n.m.	n.m.	n.m.	n.m.
1	1	9	2	3319.2	155.9	166.9	n.m.	n.m.	n.m.	n.m.	n.m.	n.m.
1	1	9	3	2478.0	21.2	150.7	n.m.	n.m.	n.m.	n.m.	n.m.	n.m.

Continued on next page

Table B.1 – *Continued from previous page*

x	Q^2	z	$P_{h\perp}^2$	A_0	ΔA_0	δA_0	$A_{UU}^{\cos\phi_h}$	$\Delta A_{UU}^{\cos\phi_h}$	$\delta A_{UU}^{\cos\phi_h}$	$A_{UU}^{\cos 2\phi_h}$	$\Delta A_{UU}^{\cos 2\phi_h}$	$\delta A_{UU}^{\cos 2\phi_h}$
1	1	9	4	2196.3	127.9	137.9	n.m.	n.m.	n.m.	n.m.	n.m.	n.m.
1	1	9	5	1852.7	21.2	85.1	-0.1144	0.0193	0.0508	0.0053	0.0155	0.0100
1	1	9	6	1445.9	15.2	69.4	-0.1542	0.0157	0.0515	0.0185	0.0143	0.0106
1	1	9	7	1212.2	14.4	55.6	-0.0899	0.0176	0.0508	0.0027	0.0164	0.0098
1	1	9	8	932.6	12.9	44.4	-0.0956	0.0202	0.0523	0.0120	0.0194	0.0079
1	1	9	9	765.2	12.5	35.8	-0.0861	0.0244	0.0506	0.0835	0.0229	0.0143
1	1	9	10	584.1	11.3	26.6	-0.1268	0.0286	0.0486	0.0665	0.0268	0.0107
1	1	9	11	441.6	10.3	22.1	-0.1412	0.0341	0.0484	0.0754	0.0330	0.0122
1	1	9	12	340.4	9.5	17.0	-0.0834	0.0412	0.0447	0.0659	0.0383	0.0201
1	1	9	13	244.0	8.4	12.1	-0.2083	0.0498	0.0381	0.0913	0.0502	0.0215
1	1	9	14	164.1	6.9	8.5	-0.0100	0.0632	0.0536	0.1375	0.0596	0.0288
1	1	9	15	110.3	5.7	5.5	-0.2020	0.0764	0.0530	0.1919	0.0703	0.0332
1	1	9	16	82.2	5.3	5.2	-0.0822	0.0948	0.0812	0.1562	0.0885	0.0472
1	1	9	17	56.4	5.2	6.8	-0.0255	0.1098	0.1271	-0.1945	0.1145	0.1237
1	1	10	0	3172.5	25.4	144.1	n.m.	n.m.	n.m.	n.m.	n.m.	n.m.
1	1	10	1	2745.1	180.9	214.0	n.m.	n.m.	n.m.	n.m.	n.m.	n.m.
1	1	10	2	2439.9	142.8	160.4	n.m.	n.m.	n.m.	n.m.	n.m.	n.m.
1	1	10	3	2160.4	128.1	166.2	n.m.	n.m.	n.m.	n.m.	n.m.	n.m.
1	1	10	4	1617.0	17.3	92.9	n.m.	n.m.	n.m.	n.m.	n.m.	n.m.
1	1	10	5	1550.5	45.0	82.8	n.m.	n.m.	n.m.	n.m.	n.m.	n.m.
1	1	10	6	1215.5	41.9	64.7	n.m.	n.m.	n.m.	n.m.	n.m.	n.m.
1	1	10	7	968.8	12.9	45.5	-0.1535	0.0198	0.0474	-0.0231	0.0180	0.0086
1	1	10	8	814.2	12.2	37.1	-0.1357	0.0223	0.0446	0.0148	0.0206	0.0088
1	1	10	9	648.3	11.4	31.4	-0.1415	0.0260	0.0425	0.0243	0.0240	0.0123
1	1	10	10	514.3	10.7	27.1	-0.0900	0.0302	0.0406	0.0060	0.0283	0.0146
1	1	10	11	402.9	10.1	21.9	-0.1464	0.0381	0.0405	0.1596	0.0343	0.0142
1	1	10	12	300.2	8.8	15.0	-0.1420	0.0433	0.0367	0.0947	0.0420	0.0194
1	1	10	13	215.2	7.7	11.4	-0.2097	0.0528	0.0418	0.1165	0.0493	0.0156
1	1	10	14	161.6	7.0	8.1	-0.0707	0.0626	0.0436	-0.0465	0.0623	0.0293
1	1	10	15	118.9	6.4	6.4	-0.2669	0.0798	0.0383	0.2287	0.0716	0.0360
1	1	10	16	66.1	5.0	6.8	n.m.	n.m.	n.m.	n.m.	n.m.	n.m.
1	1	10	17	53.0	7.0	4.1	n.m.	n.m.	n.m.	n.m.	n.m.	n.m.
1	1	11	0	2636.2	22.7	129.9	n.m.	n.m.	n.m.	n.m.	n.m.	n.m.
1	1	11	1	2381.3	176.0	214.4	n.m.	n.m.	n.m.	n.m.	n.m.	n.m.
1	1	11	2	2045.5	140.0	149.2	n.m.	n.m.	n.m.	n.m.	n.m.	n.m.
1	1	11	3	1639.5	17.8	101.4	n.m.	n.m.	n.m.	n.m.	n.m.	n.m.
1	1	11	4	1404.7	108.4	117.7	n.m.	n.m.	n.m.	n.m.	n.m.	n.m.
1	1	11	5	1315.0	98.5	134.9	n.m.	n.m.	n.m.	n.m.	n.m.	n.m.
1	1	11	6	934.7	14.1	68.4	n.m.	n.m.	n.m.	n.m.	n.m.	n.m.

Continued on next page

Table B.1 – *Continued from previous page*

x	Q^2	z	$P_{h\perp}^2$	A_0	ΔA_0	δA_0	$A_{UU}^{\cos\phi_h}$	$\Delta A_{UU}^{\cos\phi_h}$	$\delta A_{UU}^{\cos\phi_h}$	$A_{UU}^{\cos 2\phi_h}$	$\Delta A_{UU}^{\cos 2\phi_h}$	$\delta A_{UU}^{\cos 2\phi_h}$
1	1	11	7	776.6	13.5	113.7	n.m.	n.m.	n.m.	n.m.	n.m.	n.m.
1	1	11	8	673.8	11.4	32.8	-0.2408	0.0248	0.0416	-0.0660	0.0224	0.0206
1	1	11	9	557.0	10.8	27.1	-0.1499	0.0284	0.0343	-0.0536	0.0260	0.0117
1	1	11	10	445.9	10.0	21.8	-0.1592	0.0336	0.0391	0.0261	0.0313	0.0148
1	1	11	11	363.3	9.6	16.7	-0.0969	0.0395	0.0365	0.0553	0.0365	0.0195
1	1	11	12	267.4	8.5	12.8	-0.1413	0.0467	0.0313	0.0015	0.0452	0.0195
1	1	11	13	185.8	7.2	9.7	-0.1251	0.0591	0.0328	0.1624	0.0535	0.0234
1	1	11	14	132.6	6.5	6.6	-0.1153	0.0739	0.0371	0.1157	0.0705	0.0556
1	1	11	15	87.7	5.8	7.8	-0.0346	0.0975	0.1162	-0.0847	0.0964	0.1244
1	1	11	16	69.9	6.4	5.3	n.m.	n.m.	n.m.	n.m.	n.m.	n.m.
1	1	12	0	2321.2	21.5	111.4	n.m.	n.m.	n.m.	n.m.	n.m.	n.m.
1	1	12	1	1973.1	187.5	110.3	n.m.	n.m.	n.m.	n.m.	n.m.	n.m.
1	1	12	2	1675.7	19.8	121.6	n.m.	n.m.	n.m.	n.m.	n.m.	n.m.
1	1	12	3	1435.2	17.7	163.3	n.m.	n.m.	n.m.	n.m.	n.m.	n.m.
1	1	12	4	1265.3	111.0	92.6	n.m.	n.m.	n.m.	n.m.	n.m.	n.m.
1	1	12	5	1030.0	15.1	49.6	n.m.	n.m.	n.m.	n.m.	n.m.	n.m.
1	1	12	6	805.5	15.9	53.5	n.m.	n.m.	n.m.	n.m.	n.m.	n.m.
1	1	12	7	669.9	12.6	38.0	n.m.	n.m.	n.m.	n.m.	n.m.	n.m.
1	1	12	8	553.4	11.5	26.9	n.m.	n.m.	n.m.	n.m.	n.m.	n.m.
1	1	12	9	469.3	10.7	22.7	-0.1795	0.0343	0.0354	-0.0949	0.0304	0.0234
1	1	12	10	370.7	9.7	17.9	-0.1884	0.0397	0.0351	-0.0528	0.0362	0.0201
1	1	12	11	299.4	9.4	15.5	-0.1245	0.0477	0.0274	0.0087	0.0435	0.0188
1	1	12	12	220.0	8.4	9.3	-0.1543	0.0583	0.0345	0.0874	0.0527	0.0199
1	1	12	13	162.9	7.6	9.6	-0.2406	0.0706	0.0302	0.1245	0.0634	0.0203
1	1	12	14	121.6	8.5	6.4	n.m.	n.m.	n.m.	n.m.	n.m.	n.m.
1	1	12	15	103.9	12.7	18.0	n.m.	n.m.	n.m.	n.m.	n.m.	n.m.
1	1	13	0	2035.9	20.1	100.0	n.m.	n.m.	n.m.	n.m.	n.m.	n.m.
1	1	13	1	2035.5	193.6	313.8	n.m.	n.m.	n.m.	n.m.	n.m.	n.m.
1	1	13	2	1593.1	148.9	164.9	n.m.	n.m.	n.m.	n.m.	n.m.	n.m.
1	1	13	3	1564.8	127.8	199.3	n.m.	n.m.	n.m.	n.m.	n.m.	n.m.
1	1	13	4	1027.7	15.7	56.5	n.m.	n.m.	n.m.	n.m.	n.m.	n.m.
1	1	13	5	869.4	14.5	45.1	n.m.	n.m.	n.m.	n.m.	n.m.	n.m.
1	1	13	6	772.5	91.3	82.2	n.m.	n.m.	n.m.	n.m.	n.m.	n.m.
1	1	13	7	701.9	85.0	126.8	n.m.	n.m.	n.m.	n.m.	n.m.	n.m.
1	1	13	8	483.5	11.9	23.4	n.m.	n.m.	n.m.	n.m.	n.m.	n.m.
1	1	13	9	401.9	14.2	27.5	-0.0839	0.0603	0.0917	-0.1027	0.0481	0.0611
1	1	13	10	323.7	12.0	17.1	-0.1196	0.0607	0.0313	0.0286	0.0497	0.0209
1	1	13	11	246.3	11.0	11.1	-0.0264	0.0693	0.0326	0.0022	0.0603	0.0180
1	1	13	12	181.9	11.3	12.2	0.0201	0.0970	0.1176	0.1088	0.0791	0.0459

Continued on next page

Table B.1 – *Continued from previous page*

x	Q^2	z	$P_{h\perp}^2$	A_0	ΔA_0	δA_0	$A_{UU}^{\cos\phi_h}$	$\Delta A_{UU}^{\cos\phi_h}$	$\delta A_{UU}^{\cos\phi_h}$	$A_{UU}^{\cos 2\phi_h}$	$\Delta A_{UU}^{\cos 2\phi_h}$	$\delta A_{UU}^{\cos 2\phi_h}$
1	1	13	13	174.0	17.8	15.8	n.m.	n.m.	n.m.	n.m.	n.m.	n.m.
1	1	14	0	1806.8	19.2	90.5	n.m.	n.m.	n.m.	n.m.	n.m.	n.m.
1	1	14	1	1448.4	21.8	334.7	n.m.	n.m.	n.m.	n.m.	n.m.	n.m.
1	1	14	2	1453.2	153.4	139.1	n.m.	n.m.	n.m.	n.m.	n.m.	n.m.
1	1	14	3	1308.6	128.1	184.5	n.m.	n.m.	n.m.	n.m.	n.m.	n.m.
1	1	14	4	979.9	115.7	135.2	n.m.	n.m.	n.m.	n.m.	n.m.	n.m.
1	1	14	5	1027.4	105.8	107.5	n.m.	n.m.	n.m.	n.m.	n.m.	n.m.
1	1	14	6	650.4	99.4	88.4	n.m.	n.m.	n.m.	n.m.	n.m.	n.m.
1	1	14	7	503.8	100.0	79.4	n.m.	n.m.	n.m.	n.m.	n.m.	n.m.
1	1	14	8	450.5	44.0	28.5	n.m.	n.m.	n.m.	n.m.	n.m.	n.m.
1	1	14	9	378.6	46.7	30.2	n.m.	n.m.	n.m.	n.m.	n.m.	n.m.
1	1	14	10	265.0	28.1	18.6	n.m.	n.m.	n.m.	n.m.	n.m.	n.m.
1	1	15	0	1542.8	19.7	76.3	n.m.	n.m.	n.m.	n.m.	n.m.	n.m.
1	1	15	1	1204.6	23.0	61.9	n.m.	n.m.	n.m.	n.m.	n.m.	n.m.
1	1	15	2	1039.4	25.1	314.3	n.m.	n.m.	n.m.	n.m.	n.m.	n.m.
1	1	15	3	1126.5	169.4	165.4	n.m.	n.m.	n.m.	n.m.	n.m.	n.m.
1	1	15	4	696.4	21.0	60.2	n.m.	n.m.	n.m.	n.m.	n.m.	n.m.
1	1	15	5	840.1	123.7	69.6	n.m.	n.m.	n.m.	n.m.	n.m.	n.m.
1	1	15	6	589.8	31.0	101.7	n.m.	n.m.	n.m.	n.m.	n.m.	n.m.
1	1	15	7	338.6	32.4	36.8	n.m.	n.m.	n.m.	n.m.	n.m.	n.m.
1	1	16	0	1190.9	31.8	52.8	n.m.	n.m.	n.m.	n.m.	n.m.	n.m.
1	1	16	1	959.3	46.8	77.7	n.m.	n.m.	n.m.	n.m.	n.m.	n.m.
1	1	16	2	1254.5	107.0	88.2	n.m.	n.m.	n.m.	n.m.	n.m.	n.m.
2	0	1	0	104588.0	286.6	4978.8	-0.0933	0.0039	0.0191	-0.0186	0.0038	0.0018
2	0	2	0	58642.3	134.9	2800.3	-0.0425	0.0034	0.0050	-0.0007	0.0032	0.0016
2	0	2	1	41642.4	111.6	1978.9	-0.1683	0.0038	0.0131	-0.0118	0.0037	0.0021
2	0	3	0	38700.6	121.7	1814.9	0.0508	0.0049	0.0079	0.0329	0.0043	0.0050
2	0	3	1	29321.5	89.7	1366.5	-0.0938	0.0044	0.0123	0.0013	0.0042	0.0020
2	0	3	2	16752.2	65.7	811.8	-0.1812	0.0055	0.0132	-0.0108	0.0055	0.0037
2	0	3	3	10117.6	55.1	499.0	-0.1910	0.0077	0.0072	-0.0012	0.0076	0.0038
2	0	3	4	5737.9	52.4	280.4	-0.2578	0.0128	0.0344	0.0317	0.0127	0.0059
2	0	4	0	26583.4	102.2	1234.4	0.0898	0.0059	0.0132	0.0179	0.0054	0.0088
2	0	4	1	20745.9	80.0	974.6	0.0237	0.0058	0.0114	0.0302	0.0052	0.0036
2	0	4	2	13964.9	62.2	670.0	-0.0744	0.0065	0.0144	0.0240	0.0061	0.0027
2	0	4	3	8692.0	48.2	415.1	-0.1481	0.0080	0.0151	-0.0021	0.0078	0.0038
2	0	4	4	5631.8	39.6	267.4	-0.1615	0.0099	0.0112	-0.0155	0.0099	0.0053
2	0	4	5	4423.5	44.2	222.2	-0.1349	0.0138	0.0222	-0.0514	0.0139	0.0104
2	0	4	6	2526.4	42.0	117.7	-0.2148	0.0230	0.0340	-0.0221	0.0231	0.0144
2	0	5	0	17472.5	75.6	820.6	0.0798	0.0063	0.0126	0.0012	0.0062	0.0078

Continued on next page

Table B.1 – *Continued from previous page*

x	Q^2	z	$P_{h\perp}^2$	A_0	ΔA_0	δA_0	$A_{UU}^{\cos\phi_h}$	$\Delta A_{UU}^{\cos\phi_h}$	$\delta A_{UU}^{\cos\phi_h}$	$A_{UU}^{\cos 2\phi_h}$	$\Delta A_{UU}^{\cos 2\phi_h}$	$\delta A_{UU}^{\cos 2\phi_h}$
2	0	5	1	14184.3	71.2	663.1	0.0265	0.0081	0.0150	-0.0091	0.0070	0.0054
2	0	5	2	10713.4	55.4	503.2	-0.0240	0.0076	0.0146	0.0046	0.0070	0.0031
2	0	5	3	7396.3	45.8	348.5	-0.0719	0.0090	0.0159	0.0082	0.0085	0.0039
2	0	5	4	5015.5	38.3	251.1	-0.0986	0.0110	0.0163	-0.0012	0.0106	0.0057
2	0	5	5	3447.9	32.9	169.3	-0.1359	0.0137	0.0162	0.0029	0.0136	0.0065
2	0	5	6	2956.5	38.8	132.7	-0.0806	0.0186	0.0235	-0.0257	0.0182	0.0110
2	0	5	7	2354.8	47.9	115.6	-0.0773	0.0292	0.0327	-0.0064	0.0278	0.0237
2	0	6	0	11764.9	59.2	548.8	0.0724	0.0070	0.0121	-0.0069	0.0071	0.0092
2	0	6	1	10205.3	94.0	527.5	n.m.	n.m.	n.m.	n.m.	n.m.	n.m.
2	0	6	2	8106.7	67.5	387.3	0.0160	0.0144	0.0275	-0.0134	0.0115	0.0155
2	0	6	3	5936.5	41.5	285.7	-0.0041	0.0102	0.0178	0.0019	0.0094	0.0064
2	0	6	4	4308.1	36.1	207.3	-0.0349	0.0122	0.0176	0.0184	0.0114	0.0057
2	0	6	5	2989.8	30.7	143.1	-0.0540	0.0148	0.0191	-0.0162	0.0140	0.0090
2	0	6	6	2182.8	28.8	105.7	-0.0134	0.0188	0.0169	-0.0216	0.0180	0.0091
2	0	6	7	1951.6	37.2	88.8	-0.0319	0.0283	0.0239	0.0559	0.0259	0.0137
2	0	6	8	1610.7	48.0	82.5	0.0931	0.0424	0.0519	-0.0139	0.0399	0.0264
2	0	6	9	727.2	35.1	38.8	0.1625	0.0687	0.0756	0.0597	0.0715	0.0351
2	0	7	0	8396.2	48.1	395.8	0.0409	0.0077	0.0123	-0.0322	0.0078	0.0126
2	0	7	1	7557.9	78.2	358.2	n.m.	n.m.	n.m.	n.m.	n.m.	n.m.
2	0	7	2	6089.3	55.3	288.8	0.0269	0.0160	0.0210	-0.0248	0.0133	0.0057
2	0	7	3	4651.7	38.2	217.6	0.0034	0.0125	0.0212	-0.0267	0.0111	0.0089
2	0	7	4	3572.2	33.0	166.5	0.0075	0.0133	0.0202	-0.0406	0.0125	0.0058
2	0	7	5	2582.0	28.4	124.3	-0.0311	0.0156	0.0236	-0.0392	0.0148	0.0064
2	0	7	6	1864.8	25.7	84.5	0.0078	0.0201	0.0199	0.0250	0.0188	0.0118
2	0	7	7	1450.1	27.9	64.8	0.0160	0.0284	0.0206	0.0729	0.0262	0.0123
2	0	7	8	1211.1	34.7	61.1	0.0571	0.0418	0.0320	0.0545	0.0374	0.0143
2	0	7	9	878.9	41.5	46.9	0.1270	0.0698	0.0567	0.0659	0.0604	0.0442
2	0	7	10	305.4	22.8	20.1	-0.0335	0.1093	0.0975	0.0342	0.1055	0.0564
2	0	8	0	6257.8	39.3	293.9	0.0269	0.0083	0.0113	-0.0250	0.0086	0.0092
2	0	8	1	5591.1	70.2	280.5	n.m.	n.m.	n.m.	n.m.	n.m.	n.m.
2	0	8	2	4642.4	41.1	222.4	0.0137	0.0155	0.0245	-0.0418	0.0140	0.0117
2	0	8	3	3622.0	44.5	180.6	-0.0386	0.0224	0.0266	-0.0905	0.0187	0.0146
2	0	8	4	2819.1	30.0	132.7	-0.0518	0.0159	0.0271	-0.0957	0.0144	0.0145
2	0	8	5	2203.7	26.7	104.1	0.0063	0.0177	0.0223	-0.0286	0.0163	0.0068
2	0	8	6	1590.5	23.3	79.4	-0.0043	0.0213	0.0221	0.0042	0.0195	0.0091
2	0	8	7	1195.4	24.2	56.4	0.0070	0.0292	0.0230	0.0116	0.0279	0.0114
2	0	8	8	854.5	24.6	45.1	0.0587	0.0423	0.0227	0.0787	0.0388	0.0192
2	0	8	9	678.8	30.9	39.9	0.1557	0.0627	0.0584	0.0044	0.0644	0.0348
2	0	8	10	327.1	24.6	18.9	0.1724	0.1085	0.0765	-0.0435	0.1124	0.0543

Continued on next page

Table B.1 – *Continued from previous page*

x	Q^2	z	$P_{h\perp}^2$	A_0	ΔA_0	δA_0	$A_{UU}^{\cos\phi_h}$	$\Delta A_{UU}^{\cos\phi_h}$	$\delta A_{UU}^{\cos\phi_h}$	$A_{UU}^{\cos 2\phi_h}$	$\Delta A_{UU}^{\cos 2\phi_h}$	$\delta A_{UU}^{\cos 2\phi_h}$
2	0	9	0	4661.6	32.3	224.3	0.0203	0.0090	0.0104	-0.0373	0.0095	0.0084
2	0	9	1	4178.4	66.3	222.9	n.m.	n.m.	n.m.	n.m.	n.m.	n.m.
2	0	9	2	3652.0	40.1	171.8	n.m.	n.m.	n.m.	n.m.	n.m.	n.m.
2	0	9	3	2932.8	35.1	151.6	-0.0370	0.0216	0.0247	-0.0832	0.0191	0.0089
2	0	9	4	2244.1	36.2	106.2	-0.0786	0.0298	0.0251	-0.0976	0.0245	0.0119
2	0	9	5	1736.4	32.6	93.2	-0.0103	0.0330	0.0460	-0.0573	0.0268	0.0288
2	0	9	6	1325.4	22.1	64.3	0.0046	0.0245	0.0262	-0.0144	0.0225	0.0116
2	0	9	7	983.5	22.2	48.1	0.0706	0.0327	0.0261	-0.0234	0.0300	0.0201
2	0	9	8	818.6	26.5	40.9	0.0756	0.0450	0.0314	-0.0559	0.0428	0.0177
2	0	9	9	529.0	26.4	24.4	0.1979	0.0694	0.0566	-0.0322	0.0624	0.0362
2	0	9	10	266.3	21.7	44.9	0.1801	0.1140	0.1931	-0.0097	0.1071	0.0895
2	0	10	0	3584.0	27.0	166.0	0.0226	0.0100	0.0108	-0.0154	0.0103	0.0071
2	0	10	1	3291.0	69.3	180.3	n.m.	n.m.	n.m.	n.m.	n.m.	n.m.
2	0	10	2	2783.7	47.6	135.9	n.m.	n.m.	n.m.	n.m.	n.m.	n.m.
2	0	10	3	2187.9	41.4	117.0	n.m.	n.m.	n.m.	n.m.	n.m.	n.m.
2	0	10	4	1737.3	38.2	77.5	n.m.	n.m.	n.m.	n.m.	n.m.	n.m.
2	0	10	5	1338.9	38.1	68.9	n.m.	n.m.	n.m.	n.m.	n.m.	n.m.
2	0	10	6	1028.2	22.5	48.4	-0.0889	0.0351	0.0225	-0.0401	0.0295	0.0178
2	0	10	7	811.7	23.2	40.4	0.0154	0.0426	0.0263	-0.0234	0.0371	0.0193
2	0	10	8	671.7	27.9	37.8	0.0535	0.0637	0.0474	0.0516	0.0564	0.0253
2	0	10	9	468.6	31.3	29.7	0.1757	0.1017	0.0746	0.2360	0.0757	0.0282
2	0	10	10	281.0	32.8	39.9	n.m.	n.m.	n.m.	n.m.	n.m.	n.m.
2	0	11	0	2846.8	23.2	132.7	0.0222	0.0109	0.0110	-0.0147	0.0114	0.0076
2	0	11	1	2573.4	153.7	234.1	n.m.	n.m.	n.m.	n.m.	n.m.	n.m.
2	0	11	2	2018.9	43.8	103.8	n.m.	n.m.	n.m.	n.m.	n.m.	n.m.
2	0	11	3	1615.4	34.9	84.4	n.m.	n.m.	n.m.	n.m.	n.m.	n.m.
2	0	11	4	1264.7	33.2	95.2	n.m.	n.m.	n.m.	n.m.	n.m.	n.m.
2	0	11	5	1021.6	35.3	59.3	n.m.	n.m.	n.m.	n.m.	n.m.	n.m.
2	0	11	6	855.8	41.7	62.0	n.m.	n.m.	n.m.	n.m.	n.m.	n.m.
2	0	11	7	651.4	29.9	32.4	-0.0904	0.0771	0.0438	-0.0375	0.0626	0.0412
2	0	11	8	479.3	35.6	76.1	n.m.	n.m.	n.m.	n.m.	n.m.	n.m.
2	0	11	9	433.0	54.1	48.1	n.m.	n.m.	n.m.	n.m.	n.m.	n.m.
2	0	12	0	2236.3	20.0	104.2	0.0170	0.0121	0.0111	-0.0053	0.0123	0.0066
2	0	12	1	1850.8	71.6	128.4	n.m.	n.m.	n.m.	n.m.	n.m.	n.m.
2	0	12	2	1582.2	44.1	87.5	n.m.	n.m.	n.m.	n.m.	n.m.	n.m.
2	0	12	3	1246.5	35.6	72.3	n.m.	n.m.	n.m.	n.m.	n.m.	n.m.
2	0	12	4	980.4	35.1	58.3	n.m.	n.m.	n.m.	n.m.	n.m.	n.m.
2	0	12	5	830.2	40.3	59.7	n.m.	n.m.	n.m.	n.m.	n.m.	n.m.
2	0	12	6	616.6	46.7	48.8	n.m.	n.m.	n.m.	n.m.	n.m.	n.m.

Continued on next page

Table B.1 – *Continued from previous page*

x	Q^2	z	$P_{h\perp}^2$	A_0	ΔA_0	δA_0	$A_{UU}^{\cos\phi_h}$	$\Delta A_{UU}^{\cos\phi_h}$	$\delta A_{UU}^{\cos\phi_h}$	$A_{UU}^{\cos 2\phi_h}$	$\Delta A_{UU}^{\cos 2\phi_h}$	$\delta A_{UU}^{\cos 2\phi_h}$
2	0	12	7	547.8	70.7	38.9	n.m.	n.m.	n.m.	n.m.	n.m.	n.m.
2	0	13	0	1736.5	17.5	82.4	0.0303	0.0135	0.0115	-0.0352	0.0141	0.0050
2	0	13	1	1396.8	69.3	99.2	n.m.	n.m.	n.m.	n.m.	n.m.	n.m.
2	0	13	2	1147.5	54.3	80.8	n.m.	n.m.	n.m.	n.m.	n.m.	n.m.
2	0	13	3	941.3	46.2	64.1	n.m.	n.m.	n.m.	n.m.	n.m.	n.m.
2	0	13	4	717.7	46.4	47.6	n.m.	n.m.	n.m.	n.m.	n.m.	n.m.
2	0	13	5	703.8	71.7	91.5	n.m.	n.m.	n.m.	n.m.	n.m.	n.m.
2	0	14	0	1351.6	20.5	67.3	0.0584	0.0205	0.0101	-0.0121	0.0211	0.0109
2	0	14	1	1026.2	34.7	50.0	-0.1180	0.0428	0.0334	-0.1193	0.0400	0.0289
2	0	14	2	951.7	175.6	179.2	n.m.	n.m.	n.m.	n.m.	n.m.	n.m.
2	0	14	3	867.5	327.6	146.8	n.m.	n.m.	n.m.	n.m.	n.m.	n.m.
2	0	15	0	1188.7	48.5	51.7	0.0274	0.0557	0.0284	0.0070	0.0584	0.0327
2	1	1	0	105037.0	176.2	5539.7	-0.1385	0.0024	0.0308	-0.0371	0.0023	0.0041
2	1	2	0	51889.1	111.5	2538.4	-0.0267	0.0032	0.0083	-0.0190	0.0030	0.0059
2	1	2	1	34405.2	76.0	1698.1	-0.1453	0.0031	0.0209	-0.0122	0.0031	0.0030
2	1	2	2	15949.7	48.8	818.0	-0.2337	0.0043	0.0308	0.0266	0.0043	0.0048
2	1	2	3	6489.2	31.1	349.5	-0.2826	0.0067	0.0500	0.0447	0.0067	0.0079
2	1	3	0	34015.1	104.0	1592.1	0.0679	0.0047	0.0163	0.0100	0.0042	0.0092
2	1	3	1	24751.3	68.7	1164.2	-0.0313	0.0040	0.0183	0.0088	0.0038	0.0023
2	1	3	2	15005.8	50.1	717.4	-0.0946	0.0048	0.0247	0.0160	0.0047	0.0032
2	1	3	3	8720.9	36.6	421.8	-0.1526	0.0060	0.0284	0.0142	0.0060	0.0046
2	1	3	4	4989.8	27.3	248.8	-0.1958	0.0078	0.0302	0.0184	0.0078	0.0057
2	1	3	5	2652.0	20.1	140.3	-0.2068	0.0108	0.0345	0.0267	0.0106	0.0128
2	1	3	6	1332.7	15.2	70.8	-0.3395	0.0160	0.0594	0.0972	0.0157	0.0116
2	1	4	0	20502.6	79.8	970.1	0.0251	0.0062	0.0237	-0.0320	0.0055	0.0135
2	1	4	1	16528.6	59.0	765.9	0.0333	0.0054	0.0210	0.0232	0.0048	0.0062
2	1	4	2	11705.9	45.8	551.6	-0.0206	0.0057	0.0248	0.0270	0.0054	0.0028
2	1	4	3	7872.7	36.9	377.7	-0.0714	0.0067	0.0284	0.0145	0.0065	0.0038
2	1	4	4	5123.0	29.6	244.5	-0.1239	0.0083	0.0311	0.0124	0.0081	0.0055
2	1	4	5	3374.6	24.4	161.0	-0.1274	0.0104	0.0314	0.0175	0.0103	0.0067
2	1	4	6	2214.4	20.5	108.1	-0.1486	0.0135	0.0312	0.0469	0.0132	0.0117
2	1	4	7	1325.7	16.4	65.7	-0.1588	0.0179	0.0279	0.0379	0.0179	0.0118
2	1	4	8	685.3	12.1	36.7	-0.1429	0.0255	0.0527	0.0168	0.0252	0.0222
2	1	4	9	317.4	8.3	19.0	-0.2593	0.0382	0.0752	0.1341	0.0358	0.0724
2	1	5	0	12474.5	55.8	571.3	0.0025	0.0069	0.0227	-0.0406	0.0063	0.0128
2	1	5	1	10813.5	61.7	500.8	0.0090	0.0098	0.0255	0.0028	0.0079	0.0060
2	1	5	2	8654.6	40.2	395.6	0.0112	0.0069	0.0279	0.0196	0.0062	0.0053
2	1	5	3	6354.4	33.7	299.8	-0.0319	0.0076	0.0315	0.0144	0.0072	0.0041
2	1	5	4	4531.9	28.8	214.2	-0.0803	0.0091	0.0337	0.0116	0.0089	0.0043

Continued on next page

Table B.1 – *Continued from previous page*

x	Q^2	z	$P_{h\perp}^2$	A_0	ΔA_0	δA_0	$A_{UU}^{\cos\phi_h}$	$\Delta A_{UU}^{\cos\phi_h}$	$\delta A_{UU}^{\cos\phi_h}$	$A_{UU}^{\cos 2\phi_h}$	$\Delta A_{UU}^{\cos 2\phi_h}$	$\delta A_{UU}^{\cos 2\phi_h}$
2	1	5	5	3125.1	24.3	150.3	-0.1114	0.0110	0.0363	0.0020	0.0109	0.0062
2	1	5	6	2159.6	21.0	103.5	-0.0997	0.0139	0.0354	0.0129	0.0137	0.0100
2	1	5	7	1554.4	19.0	76.6	-0.0996	0.0175	0.0318	0.0066	0.0175	0.0116
2	1	5	8	1106.7	17.6	56.5	-0.0995	0.0237	0.0273	0.0909	0.0228	0.0141
2	1	5	9	639.6	13.5	32.9	-0.0413	0.0308	0.0359	0.0609	0.0302	0.0210
2	1	5	10	342.5	10.0	17.3	-0.0878	0.0426	0.0445	0.0222	0.0422	0.0256
2	1	5	11	138.6	6.1	8.7	-0.1557	0.0616	0.0835	-0.0506	0.0657	0.0560
2	1	6	0	7960.8	41.3	374.4	-0.0343	0.0076	0.0227	-0.0563	0.0073	0.0111
2	1	6	1	7356.6	65.0	350.8	n.m.	n.m.	n.m.	n.m.	n.m.	n.m.
2	1	6	2	6215.7	45.1	288.7	0.0095	0.0122	0.0351	0.0076	0.0098	0.0121
2	1	6	3	4809.7	29.2	222.6	-0.0296	0.0090	0.0349	0.0021	0.0082	0.0047
2	1	6	4	3639.2	25.5	169.5	-0.0750	0.0101	0.0387	-0.0030	0.0095	0.0049
2	1	6	5	2653.2	22.4	127.9	-0.0598	0.0121	0.0401	0.0043	0.0116	0.0062
2	1	6	6	1917.1	19.9	88.0	-0.0858	0.0149	0.0411	0.0341	0.0143	0.0066
2	1	6	7	1357.8	17.6	63.5	-0.1140	0.0186	0.0392	0.0373	0.0184	0.0084
2	1	6	8	1000.3	16.5	47.4	-0.1281	0.0237	0.0383	0.0539	0.0235	0.0119
2	1	6	9	706.2	15.0	34.5	-0.1238	0.0313	0.0330	0.1181	0.0297	0.0172
2	1	6	10	471.1	13.1	23.1	-0.0094	0.0397	0.0382	0.0317	0.0396	0.0228
2	1	6	11	259.3	9.7	14.0	0.0165	0.0528	0.0470	-0.0034	0.0516	0.0326
2	1	6	12	124.8	6.3	7.4	-0.0613	0.0695	0.0817	-0.0347	0.0706	0.0341
2	1	6	13	26.1	2.3	1.9	0.3980	0.1210	0.1653	0.2455	0.0979	0.0830
2	1	7	0	5445.2	32.3	254.1	-0.0588	0.0085	0.0222	-0.0461	0.0082	0.0101
2	1	7	1	5187.8	51.4	238.7	n.m.	n.m.	n.m.	n.m.	n.m.	n.m.
2	1	7	2	4347.4	50.5	210.1	n.m.	n.m.	n.m.	n.m.	n.m.	n.m.
2	1	7	3	3535.6	51.6	171.5	n.m.	n.m.	n.m.	n.m.	n.m.	n.m.
2	1	7	4	2769.0	22.0	128.7	-0.0493	0.0118	0.0420	0.0032	0.0107	0.0065
2	1	7	5	2094.4	19.3	96.3	-0.0768	0.0135	0.0426	0.0177	0.0125	0.0046
2	1	7	6	1572.6	17.5	73.9	-0.0976	0.0162	0.0461	0.0325	0.0152	0.0071
2	1	7	7	1175.8	16.2	57.1	-0.1012	0.0203	0.0460	0.0722	0.0188	0.0081
2	1	7	8	851.0	14.8	42.5	-0.1060	0.0248	0.0451	0.0253	0.0237	0.0141
2	1	7	9	660.1	14.7	34.7	-0.1071	0.0317	0.0368	0.0374	0.0321	0.0146
2	1	7	10	444.1	12.8	21.7	-0.0341	0.0413	0.0342	0.0253	0.0409	0.0222
2	1	7	11	301.7	11.4	13.6	-0.1000	0.0541	0.0486	0.0206	0.0538	0.0330
2	1	7	12	164.2	8.1	9.0	0.0095	0.0705	0.0589	0.0753	0.0729	0.0387
2	1	7	13	98.0	7.2	7.6	-0.0534	0.0971	0.0864	-0.0777	0.1034	0.0499
2	1	7	14	44.8	6.5	5.5	n.m.	n.m.	n.m.	n.m.	n.m.	n.m.
2	1	8	0	4053.9	26.6	188.6	-0.0452	0.0091	0.0225	-0.0351	0.0088	0.0119
2	1	8	1	3664.4	43.1	180.7	n.m.	n.m.	n.m.	n.m.	n.m.	n.m.
2	1	8	2	3197.4	39.3	147.6	n.m.	n.m.	n.m.	n.m.	n.m.	n.m.

Continued on next page

Table B.1 – *Continued from previous page*

x	Q^2	z	$P_{h\perp}^2$	A_0	ΔA_0	δA_0	$A_{UU}^{\cos\phi_h}$	$\Delta A_{UU}^{\cos\phi_h}$	$\delta A_{UU}^{\cos\phi_h}$	$A_{UU}^{\cos 2\phi_h}$	$\Delta A_{UU}^{\cos 2\phi_h}$	$\delta A_{UU}^{\cos 2\phi_h}$
2	1	8	3	2659.7	40.2	127.1	n.m.	n.m.	n.m.	n.m.	n.m.	n.m.
2	1	8	4	2093.1	24.0	95.0	-0.1093	0.0197	0.0461	-0.0059	0.0160	0.0075
2	1	8	5	1673.3	17.4	78.1	-0.1051	0.0156	0.0454	0.0008	0.0140	0.0110
2	1	8	6	1281.2	15.6	56.1	-0.0765	0.0179	0.0470	0.0174	0.0167	0.0087
2	1	8	7	1005.2	14.7	47.2	-0.0372	0.0214	0.0433	0.0376	0.0202	0.0067
2	1	8	8	725.1	13.0	35.5	-0.0958	0.0258	0.0411	0.0149	0.0246	0.0090
2	1	8	9	536.5	12.3	25.2	-0.0782	0.0334	0.0478	0.0603	0.0315	0.0124
2	1	8	10	396.5	11.9	18.8	-0.0851	0.0431	0.0392	0.0378	0.0400	0.0189
2	1	8	11	272.5	10.9	14.1	-0.1776	0.0572	0.0400	0.0183	0.0566	0.0332
2	1	8	12	178.2	9.4	7.1	0.0165	0.0735	0.0657	0.0113	0.0743	0.0487
2	1	8	13	93.6	6.4	6.3	-0.0647	0.1057	0.0784	0.2459	0.0915	0.0634
2	1	8	14	52.7	5.7	4.3	0.0098	0.1316	0.1102	-0.1711	0.1380	0.0552
2	1	9	0	3130.4	22.5	138.6	-0.0545	0.0099	0.0218	-0.0404	0.0097	0.0109
2	1	9	1	2769.2	59.9	153.2	n.m.	n.m.	n.m.	n.m.	n.m.	n.m.
2	1	9	2	2399.5	32.8	110.5	n.m.	n.m.	n.m.	n.m.	n.m.	n.m.
2	1	9	3	2055.5	33.6	100.5	n.m.	n.m.	n.m.	n.m.	n.m.	n.m.
2	1	9	4	1694.9	45.4	98.9	n.m.	n.m.	n.m.	n.m.	n.m.	n.m.
2	1	9	5	1330.3	31.6	67.5	n.m.	n.m.	n.m.	n.m.	n.m.	n.m.
2	1	9	6	1034.8	14.1	51.5	-0.1840	0.0205	0.0440	-0.0323	0.0184	0.0112
2	1	9	7	835.5	13.4	38.5	-0.1206	0.0240	0.0421	0.0048	0.0219	0.0095
2	1	9	8	658.1	12.7	33.2	-0.1348	0.0281	0.0373	0.0007	0.0266	0.0132
2	1	9	9	498.3	12.0	23.7	-0.0546	0.0361	0.0378	0.0611	0.0320	0.0141
2	1	9	10	340.5	10.4	17.4	-0.1162	0.0445	0.0328	0.0317	0.0417	0.0242
2	1	9	11	235.4	9.6	11.8	0.0269	0.0617	0.0393	0.1738	0.0545	0.0256
2	1	9	12	159.5	8.4	9.7	0.0690	0.0780	0.0523	0.1015	0.0740	0.0309
2	1	9	13	94.5	7.0	4.9	-0.0786	0.1132	0.0535	0.2075	0.1009	0.0402
2	1	9	14	56.5	8.7	6.6	n.m.	n.m.	n.m.	n.m.	n.m.	n.m.
2	1	10	0	2568.8	20.0	118.6	-0.0478	0.0105	0.0195	-0.0490	0.0105	0.0054
2	1	10	1	2164.6	57.9	135.1	n.m.	n.m.	n.m.	n.m.	n.m.	n.m.
2	1	10	2	1950.6	46.6	99.8	n.m.	n.m.	n.m.	n.m.	n.m.	n.m.
2	1	10	3	1699.8	41.9	79.0	n.m.	n.m.	n.m.	n.m.	n.m.	n.m.
2	1	10	4	1312.4	38.3	64.6	n.m.	n.m.	n.m.	n.m.	n.m.	n.m.
2	1	10	5	1111.6	29.0	51.3	n.m.	n.m.	n.m.	n.m.	n.m.	n.m.
2	1	10	6	887.8	27.5	47.3	n.m.	n.m.	n.m.	n.m.	n.m.	n.m.
2	1	10	7	649.9	25.1	38.4	n.m.	n.m.	n.m.	n.m.	n.m.	n.m.
2	1	10	8	541.8	11.7	24.8	-0.1110	0.0329	0.0369	0.0169	0.0286	0.0144
2	1	10	9	401.2	10.4	18.8	-0.1764	0.0381	0.0347	-0.0034	0.0348	0.0113
2	1	10	10	299.0	9.8	17.9	-0.0753	0.0487	0.0293	0.0449	0.0457	0.0155
2	1	10	11	210.9	9.1	11.1	-0.0818	0.0654	0.0403	0.0934	0.0601	0.0248

Continued on next page

Table B.1 – *Continued from previous page*

x	Q^2	z	$P_{h\perp}^2$	A_0	ΔA_0	δA_0	$A_{UU}^{\cos\phi_h}$	$\Delta A_{UU}^{\cos\phi_h}$	$\delta A_{UU}^{\cos\phi_h}$	$A_{UU}^{\cos 2\phi_h}$	$\Delta A_{UU}^{\cos 2\phi_h}$	$\delta A_{UU}^{\cos 2\phi_h}$
2	1	10	12	152.8	8.9	9.6	-0.0816	0.0891	0.0624	0.1510	0.0745	0.0359
2	1	10	13	85.1	7.3	5.8	0.1525	0.1240	0.0627	0.1793	0.1089	0.0581
2	1	10	14	46.0	7.7	7.4	n.m.	n.m.	n.m.	n.m.	n.m.	n.m.
2	1	11	0	2112.7	17.8	98.7	-0.0629	0.0114	0.0196	-0.0438	0.0115	0.0050
2	1	11	1	1596.6	21.6	211.2	n.m.	n.m.	n.m.	n.m.	n.m.	n.m.
2	1	11	2	1765.0	418.4	319.8	n.m.	n.m.	n.m.	n.m.	n.m.	n.m.
2	1	11	3	1158.0	19.3	83.0	n.m.	n.m.	n.m.	n.m.	n.m.	n.m.
2	1	11	4	1055.3	97.5	101.3	n.m.	n.m.	n.m.	n.m.	n.m.	n.m.
2	1	11	5	786.6	13.5	69.3	n.m.	n.m.	n.m.	n.m.	n.m.	n.m.
2	1	11	6	697.1	31.4	33.1	n.m.	n.m.	n.m.	n.m.	n.m.	n.m.
2	1	11	7	538.0	22.5	29.3	n.m.	n.m.	n.m.	n.m.	n.m.	n.m.
2	1	11	8	434.4	13.8	26.4	-0.1201	0.0550	0.0608	-0.0021	0.0427	0.0308
2	1	11	9	342.5	10.7	17.6	-0.1509	0.0482	0.0403	0.0288	0.0427	0.0230
2	1	11	10	240.2	9.5	11.3	-0.1594	0.0611	0.0402	0.0407	0.0559	0.0215
2	1	11	11	177.0	9.2	9.2	-0.0716	0.0802	0.0584	0.1397	0.0699	0.0272
2	1	11	12	115.0	8.9	8.5	-0.1204	0.1260	0.1479	0.1470	0.0982	0.0599
2	1	12	0	1732.4	15.9	83.1	-0.0533	0.0126	0.0179	-0.0277	0.0126	0.0060
2	1	12	1	1288.7	19.4	62.0	n.m.	n.m.	n.m.	n.m.	n.m.	n.m.
2	1	12	2	1108.0	18.9	183.2	n.m.	n.m.	n.m.	n.m.	n.m.	n.m.
2	1	12	3	1353.7	324.0	236.8	n.m.	n.m.	n.m.	n.m.	n.m.	n.m.
2	1	12	4	817.2	90.5	70.9	n.m.	n.m.	n.m.	n.m.	n.m.	n.m.
2	1	12	5	674.8	86.3	58.2	n.m.	n.m.	n.m.	n.m.	n.m.	n.m.
2	1	12	6	580.1	80.9	49.3	n.m.	n.m.	n.m.	n.m.	n.m.	n.m.
2	1	12	7	415.4	11.7	20.3	n.m.	n.m.	n.m.	n.m.	n.m.	n.m.
2	1	12	8	356.2	21.9	25.7	n.m.	n.m.	n.m.	n.m.	n.m.	n.m.
2	1	12	9	282.3	15.4	16.4	-0.0025	0.0921	0.0986	0.0646	0.0708	0.0642
2	1	12	10	191.9	11.6	9.2	-0.0720	0.0992	0.0652	-0.0919	0.0895	0.0406
2	1	12	11	154.8	16.1	10.5	n.m.	n.m.	n.m.	n.m.	n.m.	n.m.
2	1	13	0	1362.0	13.8	64.0	-0.0931	0.0137	0.0162	-0.0494	0.0140	0.0103
2	1	13	1	1056.4	18.1	404.1	n.m.	n.m.	n.m.	n.m.	n.m.	n.m.
2	1	13	2	869.6	17.5	226.3	n.m.	n.m.	n.m.	n.m.	n.m.	n.m.
2	1	13	3	927.6	340.8	230.9	n.m.	n.m.	n.m.	n.m.	n.m.	n.m.
2	1	13	4	624.5	17.0	35.0	n.m.	n.m.	n.m.	n.m.	n.m.	n.m.
2	1	13	5	522.4	16.3	118.3	n.m.	n.m.	n.m.	n.m.	n.m.	n.m.
2	1	13	6	439.3	17.1	181.7	n.m.	n.m.	n.m.	n.m.	n.m.	n.m.
2	1	13	7	488.5	23.1	48.7	n.m.	n.m.	n.m.	n.m.	n.m.	n.m.
2	1	13	8	285.2	36.0	25.3	n.m.	n.m.	n.m.	n.m.	n.m.	n.m.
2	1	13	9	215.1	73.8	40.1	n.m.	n.m.	n.m.	n.m.	n.m.	n.m.
2	1	14	0	1106.7	13.2	54.0	-0.0513	0.0162	0.0132	-0.0413	0.0164	0.0084

Continued on next page

Table B.1 – *Continued from previous page*

x	Q^2	z	$P_{h\perp}^2$	A_0	ΔA_0	δA_0	$A_{UU}^{\cos\phi_h}$	$\Delta A_{UU}^{\cos\phi_h}$	$\delta A_{UU}^{\cos\phi_h}$	$A_{UU}^{\cos 2\phi_h}$	$\Delta A_{UU}^{\cos 2\phi_h}$	$\delta A_{UU}^{\cos 2\phi_h}$
2	1	14	1	809.8	16.8	37.9	n.m.	n.m.	n.m.	n.m.	n.m.	n.m.
2	1	14	2	712.5	18.4	117.9	n.m.	n.m.	n.m.	n.m.	n.m.	n.m.
2	1	14	3	947.5	30.7	49.0	n.m.	n.m.	n.m.	n.m.	n.m.	n.m.
2	1	14	4	779.0	32.2	149.6	n.m.	n.m.	n.m.	n.m.	n.m.	n.m.
2	1	14	5	416.3	22.0	56.4	n.m.	n.m.	n.m.	n.m.	n.m.	n.m.
2	1	14	6	361.5	26.3	133.9	n.m.	n.m.	n.m.	n.m.	n.m.	n.m.
2	1	15	0	939.3	17.2	43.4	-0.1001	0.0253	0.0153	-0.0721	0.0250	0.0162
2	1	15	1	795.1	528.1	272.9	n.m.	n.m.	n.m.	n.m.	n.m.	n.m.
2	1	15	2	589.2	29.9	179.0	n.m.	n.m.	n.m.	n.m.	n.m.	n.m.
2	1	15	3	787.6	61.4	146.9	n.m.	n.m.	n.m.	n.m.	n.m.	n.m.
2	1	16	0	1108.2	104.5	94.4	n.m.	n.m.	n.m.	n.m.	n.m.	n.m.
3	0	1	0	17519.4	89.2	806.3	-0.0871	0.0073	0.0287	-0.0236	0.0071	0.0021
3	0	2	0	9286.2	46.5	412.7	-0.0386	0.0075	0.0092	-0.0024	0.0070	0.0031
3	0	2	1	6304.4	35.9	284.9	-0.1742	0.0080	0.0225	-0.0164	0.0080	0.0032
3	0	3	0	6658.7	45.2	304.6	0.0844	0.0105	0.0117	0.0531	0.0094	0.0057
3	0	3	1	4982.7	32.8	230.5	-0.0764	0.0096	0.0183	0.0164	0.0091	0.0030
3	0	3	2	2762.0	23.8	124.0	-0.1618	0.0123	0.0225	-0.0027	0.0122	0.0045
3	0	3	3	1551.0	18.2	72.1	-0.1976	0.0166	0.0317	-0.0050	0.0166	0.0080
3	0	4	0	4598.6	36.6	205.7	0.0814	0.0121	0.0179	0.0334	0.0113	0.0104
3	0	4	1	3553.0	30.0	165.8	0.0088	0.0128	0.0171	0.0033	0.0115	0.0051
3	0	4	2	2407.6	23.1	112.9	-0.0997	0.0141	0.0201	0.0366	0.0132	0.0045
3	0	4	3	1475.6	18.1	66.4	-0.1391	0.0181	0.0219	0.0501	0.0170	0.0072
3	0	4	4	853.2	13.4	37.5	-0.1465	0.0224	0.0301	-0.0233	0.0223	0.0079
3	0	4	5	667.4	15.2	35.6	-0.1965	0.0328	0.0337	0.0049	0.0324	0.0158
3	0	5	0	3118.0	28.0	141.5	0.0683	0.0129	0.0165	-0.0025	0.0126	0.0114
3	0	5	1	2530.1	30.4	116.7	0.0116	0.0209	0.0207	-0.0170	0.0181	0.0068
3	0	5	2	1940.4	21.8	91.2	-0.0404	0.0168	0.0236	0.0044	0.0154	0.0080
3	0	5	3	1299.8	17.5	57.5	-0.0642	0.0196	0.0266	0.0269	0.0181	0.0087
3	0	5	4	868.2	14.4	35.4	-0.1231	0.0235	0.0265	-0.0072	0.0230	0.0071
3	0	5	5	535.8	11.4	25.4	-0.1109	0.0304	0.0345	-0.0188	0.0286	0.0106
3	0	5	6	433.7	13.8	21.7	-0.1843	0.0472	0.0397	0.0413	0.0462	0.0179
3	0	6	0	2129.4	22.1	97.4	0.0529	0.0143	0.0145	-0.0171	0.0141	0.0093
3	0	6	1	1900.7	24.1	91.9	0.0553	0.0214	0.0408	0.0037	0.0195	0.0281
3	0	6	2	1435.9	24.6	69.0	-0.0515	0.0305	0.0320	-0.0484	0.0260	0.0192
3	0	6	3	1031.3	15.9	46.4	-0.0217	0.0226	0.0286	-0.0183	0.0208	0.0129
3	0	6	4	716.3	13.1	32.9	-0.0788	0.0262	0.0361	-0.0113	0.0242	0.0134
3	0	6	5	491.6	11.0	24.1	-0.0642	0.0308	0.0370	-0.0496	0.0310	0.0120
3	0	6	6	335.6	9.9	14.2	-0.0626	0.0414	0.0442	-0.0217	0.0388	0.0259
3	0	6	7	251.7	11.9	17.0	-0.1208	0.0693	0.0652	0.0336	0.0649	0.0349

Continued on next page

Table B.1 – *Continued from previous page*

x	Q^2	z	$P_{h\perp}^2$	A_0	ΔA_0	δA_0	$A_{UU}^{\cos\phi_h}$	$\Delta A_{UU}^{\cos\phi_h}$	$\delta A_{UU}^{\cos\phi_h}$	$A_{UU}^{\cos 2\phi_h}$	$\Delta A_{UU}^{\cos 2\phi_h}$	$\delta A_{UU}^{\cos 2\phi_h}$
3	0	7	0	1609.2	18.6	71.5	0.0219	0.0156	0.0133	-0.0278	0.0159	0.0076
3	0	7	1	1461.9	21.7	71.1	0.0833	0.0246	0.0443	-0.0167	0.0233	0.0339
3	0	7	2	1078.6	19.0	48.7	-0.0245	0.0308	0.0273	-0.0824	0.0272	0.0160
3	0	7	3	869.2	16.9	40.4	0.0561	0.0307	0.0259	-0.0233	0.0272	0.0079
3	0	7	4	625.1	13.1	28.5	0.0329	0.0311	0.0329	-0.0093	0.0281	0.0125
3	0	7	5	440.4	10.8	22.6	-0.0195	0.0354	0.0355	-0.0232	0.0347	0.0137
3	0	7	6	293.5	8.9	12.9	-0.0450	0.0408	0.0482	-0.0826	0.0402	0.0223
3	0	7	7	191.2	9.1	10.8	-0.0945	0.0664	0.0604	-0.0552	0.0627	0.0384
3	0	7	8	119.5	12.3	11.2	n.m.	n.m.	n.m.	n.m.	n.m.	n.m.
3	0	8	0	1240.9	15.8	56.0	0.0215	0.0169	0.0127	-0.0291	0.0173	0.0099
3	0	8	1	1054.5	31.5	50.3	n.m.	n.m.	n.m.	n.m.	n.m.	n.m.
3	0	8	2	840.4	24.5	46.7	n.m.	n.m.	n.m.	n.m.	n.m.	n.m.
3	0	8	3	694.2	22.7	45.9	n.m.	n.m.	n.m.	n.m.	n.m.	n.m.
3	0	8	4	522.8	23.3	34.6	n.m.	n.m.	n.m.	n.m.	n.m.	n.m.
3	0	8	5	340.5	9.4	16.4	-0.0495	0.0419	0.0378	-0.0450	0.0377	0.0248
3	0	8	6	256.6	8.5	11.8	-0.0304	0.0468	0.0381	-0.0737	0.0443	0.0220
3	0	8	7	186.3	9.8	11.3	-0.0264	0.0794	0.0379	0.1594	0.0669	0.0219
3	0	8	8	111.8	14.9	10.7	n.m.	n.m.	n.m.	n.m.	n.m.	n.m.
3	0	9	0	876.7	12.6	39.4	0.0653	0.0191	0.0142	0.0041	0.0197	0.0105
3	0	9	1	754.6	29.0	40.9	n.m.	n.m.	n.m.	n.m.	n.m.	n.m.
3	0	9	2	704.2	23.2	37.6	n.m.	n.m.	n.m.	n.m.	n.m.	n.m.
3	0	9	3	501.9	18.9	39.0	n.m.	n.m.	n.m.	n.m.	n.m.	n.m.
3	0	9	4	382.6	16.8	18.2	n.m.	n.m.	n.m.	n.m.	n.m.	n.m.
3	0	9	5	266.9	10.9	15.4	-0.2034	0.0787	0.0762	-0.1065	0.0658	0.0538
3	0	9	6	198.2	8.7	12.1	0.0232	0.0681	0.0493	0.0266	0.0572	0.0255
3	0	9	7	147.1	11.8	12.0	n.m.	n.m.	n.m.	n.m.	n.m.	n.m.
3	0	10	0	668.4	10.4	29.7	-0.0053	0.0208	0.0121	-0.0324	0.0214	0.0061
3	0	10	1	558.2	27.4	38.2	n.m.	n.m.	n.m.	n.m.	n.m.	n.m.
3	0	10	2	507.5	20.6	29.1	n.m.	n.m.	n.m.	n.m.	n.m.	n.m.
3	0	10	3	399.4	17.0	22.4	n.m.	n.m.	n.m.	n.m.	n.m.	n.m.
3	0	10	4	289.8	14.0	15.3	n.m.	n.m.	n.m.	n.m.	n.m.	n.m.
3	0	10	5	212.1	13.4	11.8	n.m.	n.m.	n.m.	n.m.	n.m.	n.m.
3	0	10	6	136.7	17.8	12.3	n.m.	n.m.	n.m.	n.m.	n.m.	n.m.
3	0	11	0	506.5	8.7	23.1	0.0425	0.0232	0.0143	-0.0008	0.0234	0.0090
3	0	11	1	402.0	10.6	19.5	-0.1070	0.0352	0.0256	-0.0791	0.0347	0.0202
3	0	11	2	329.2	10.9	19.2	-0.0135	0.0553	0.0522	-0.0759	0.0502	0.0303
3	0	11	3	277.2	8.6	13.2	-0.0358	0.0523	0.0434	-0.0693	0.0508	0.0309
3	0	11	4	214.8	9.0	11.0	-0.0303	0.0751	0.0497	-0.0306	0.0693	0.0402
3	0	11	5	182.0	18.2	15.7	n.m.	n.m.	n.m.	n.m.	n.m.	n.m.

Continued on next page

Table B.1 – *Continued from previous page*

x	Q^2	z	$P_{h\perp}^2$	A_0	ΔA_0	δA_0	$A_{UU}^{\cos\phi_h}$	$\Delta A_{UU}^{\cos\phi_h}$	$\delta A_{UU}^{\cos\phi_h}$	$A_{UU}^{\cos 2\phi_h}$	$\Delta A_{UU}^{\cos 2\phi_h}$	$\delta A_{UU}^{\cos 2\phi_h}$
3	0	12	0	367.8	6.9	16.9	0.0075	0.0260	0.0156	0.0311	0.0264	0.0143
3	0	12	1	310.2	9.1	13.3	-0.0380	0.0367	0.0281	-0.1214	0.0367	0.0221
3	0	12	2	244.9	18.4	18.4	n.m.	n.m.	n.m.	n.m.	n.m.	n.m.
3	0	12	3	212.1	18.9	20.9	n.m.	n.m.	n.m.	n.m.	n.m.	n.m.
3	0	12	4	178.0	22.0	17.5	n.m.	n.m.	n.m.	n.m.	n.m.	n.m.
3	0	13	0	257.4	6.0	12.4	-0.0268	0.0325	0.0202	0.0220	0.0326	0.0186
3	0	13	1	219.7	10.0	11.6	0.0042	0.0529	0.0326	-0.1591	0.0560	0.0271
3	0	13	2	272.8	33.3	22.9	n.m.	n.m.	n.m.	n.m.	n.m.	n.m.
3	0	14	0	219.8	12.9	6.6	0.0008	0.0818	0.0693	0.0251	0.0814	0.0559
3	1	1	0	34460.8	102.0	1805.1	-0.1087	0.0042	0.0277	-0.0415	0.0042	0.0049
3	1	2	0	18553.4	69.7	905.0	-0.0054	0.0056	0.0071	-0.0108	0.0052	0.0059
3	1	2	1	11787.4	46.6	590.0	-0.1401	0.0056	0.0190	-0.0182	0.0056	0.0023
3	1	2	2	5295.3	30.3	269.6	-0.1962	0.0082	0.0223	0.0534	0.0081	0.0063
3	1	2	3	2381.4	23.3	128.1	-0.2528	0.0139	0.0337	0.0601	0.0137	0.0065
3	1	3	0	12650.7	66.0	602.0	0.0593	0.0081	0.0162	0.0130	0.0072	0.0101
3	1	3	1	9261.2	44.9	441.9	-0.0249	0.0071	0.0163	0.0281	0.0067	0.0032
3	1	3	2	5449.2	32.5	260.0	-0.1141	0.0086	0.0210	0.0140	0.0084	0.0037
3	1	3	3	2995.3	23.2	142.9	-0.1295	0.0112	0.0239	0.0169	0.0110	0.0058
3	1	3	4	1768.9	18.7	94.7	-0.1754	0.0154	0.0194	0.0384	0.0153	0.0081
3	1	3	5	1038.5	17.2	61.3	-0.2563	0.0237	0.0194	0.0555	0.0236	0.0102
3	1	4	0	8094.1	50.8	374.2	0.0246	0.0099	0.0205	-0.0230	0.0089	0.0140
3	1	4	1	6459.7	50.0	310.1	0.0273	0.0128	0.0180	0.0383	0.0105	0.0043
3	1	4	2	4516.3	31.1	217.8	-0.0253	0.0100	0.0213	0.0236	0.0095	0.0050
3	1	4	3	2960.8	24.8	139.9	-0.0775	0.0120	0.0238	0.0053	0.0117	0.0052
3	1	4	4	1825.8	19.3	89.9	-0.1224	0.0153	0.0252	0.0223	0.0148	0.0059
3	1	4	5	1187.7	16.2	58.2	-0.1407	0.0194	0.0239	-0.0061	0.0196	0.0095
3	1	4	6	813.3	15.6	44.5	-0.1215	0.0277	0.0239	-0.0091	0.0280	0.0200
3	1	4	7	506.6	15.2	32.5	-0.1124	0.0438	0.0406	0.0149	0.0427	0.0260
3	1	5	0	5217.6	37.6	237.5	0.0122	0.0109	0.0185	-0.0352	0.0102	0.0106
3	1	5	1	4369.9	40.7	203.8	0.0079	0.0159	0.0252	-0.0101	0.0134	0.0112
3	1	5	2	3426.6	35.0	173.8	0.0065	0.0169	0.0317	0.0380	0.0138	0.0140
3	1	5	3	2499.1	23.5	118.4	-0.0408	0.0138	0.0257	0.0366	0.0129	0.0056
3	1	5	4	1716.5	19.7	82.2	-0.0600	0.0164	0.0279	0.0091	0.0161	0.0069
3	1	5	5	1120.0	16.0	53.7	-0.1256	0.0201	0.0285	-0.0103	0.0198	0.0074
3	1	5	6	802.4	14.7	39.8	-0.1387	0.0262	0.0260	0.0129	0.0255	0.0136
3	1	5	7	587.7	14.7	31.6	-0.0758	0.0366	0.0238	0.0589	0.0346	0.0141
3	1	5	8	386.7	14.2	20.4	-0.0264	0.0516	0.0432	-0.0066	0.0534	0.0226
3	1	5	9	181.5	11.6	11.4	-0.0168	0.0942	0.0984	0.0734	0.0905	0.0514
3	1	6	0	3498.1	29.1	167.0	0.0001	0.0121	0.0202	-0.0286	0.0113	0.0106

Continued on next page

Table B.1 – *Continued from previous page*

x	Q^2	z	$P_{h\perp}^2$	A_0	ΔA_0	δA_0	$A_{UU}^{\cos\phi_h}$	$\Delta A_{UU}^{\cos\phi_h}$	$\delta A_{UU}^{\cos\phi_h}$	$A_{UU}^{\cos 2\phi_h}$	$\Delta A_{UU}^{\cos 2\phi_h}$	$\delta A_{UU}^{\cos 2\phi_h}$
3	1	6	1	3152.9	45.3	144.0	n.m.	n.m.	n.m.	n.m.	n.m.	n.m.
3	1	6	2	2557.5	46.5	122.0	n.m.	n.m.	n.m.	n.m.	n.m.	n.m.
3	1	6	3	1920.3	20.9	88.9	-0.0202	0.0165	0.0297	0.0181	0.0147	0.0090
3	1	6	4	1426.1	18.2	67.8	-0.0472	0.0188	0.0296	0.0302	0.0177	0.0092
3	1	6	5	1062.8	16.4	51.3	-0.0938	0.0226	0.0320	0.0453	0.0215	0.0098
3	1	6	6	725.8	14.1	37.7	-0.0787	0.0276	0.0324	0.0042	0.0263	0.0130
3	1	6	7	493.9	12.5	26.4	-0.1524	0.0364	0.0331	0.0577	0.0336	0.0144
3	1	6	8	388.3	13.7	18.8	-0.0537	0.0494	0.0302	-0.0336	0.0481	0.0248
3	1	6	9	278.6	14.1	14.6	-0.0860	0.0736	0.0566	0.0254	0.0708	0.0407
3	1	6	10	127.5	12.1	23.7	-0.1473	0.1522	0.2665	0.1956	0.1349	0.0651
3	1	7	0	2546.9	23.6	121.5	-0.0088	0.0131	0.0207	-0.0388	0.0126	0.0145
3	1	7	1	2298.1	38.6	114.5	n.m.	n.m.	n.m.	n.m.	n.m.	n.m.
3	1	7	2	1868.1	36.0	95.6	n.m.	n.m.	n.m.	n.m.	n.m.	n.m.
3	1	7	3	1528.9	37.2	82.6	n.m.	n.m.	n.m.	n.m.	n.m.	n.m.
3	1	7	4	1176.1	17.1	55.2	-0.0698	0.0219	0.0320	-0.0322	0.0199	0.0104
3	1	7	5	873.6	14.8	42.3	-0.0443	0.0249	0.0297	-0.0013	0.0229	0.0099
3	1	7	6	639.6	13.2	32.2	-0.0955	0.0295	0.0302	-0.0090	0.0281	0.0110
3	1	7	7	448.3	12.0	21.0	-0.0629	0.0400	0.0335	0.1165	0.0378	0.0189
3	1	7	8	331.2	12.0	17.6	-0.0591	0.0539	0.0309	0.0973	0.0527	0.0173
3	1	7	9	251.9	13.3	14.9	-0.1380	0.0735	0.0421	-0.0132	0.0718	0.0556
3	1	7	10	183.8	16.0	13.9	-0.0311	0.1249	0.1053	0.0133	0.1246	0.0576
3	1	7	11	89.4	25.0	9.0	n.m.	n.m.	n.m.	n.m.	n.m.	n.m.
3	1	8	0	1900.1	19.3	88.3	-0.0099	0.0139	0.0213	-0.0391	0.0137	0.0129
3	1	8	1	1679.7	34.7	83.0	n.m.	n.m.	n.m.	n.m.	n.m.	n.m.
3	1	8	2	1448.7	30.2	69.0	n.m.	n.m.	n.m.	n.m.	n.m.	n.m.
3	1	8	3	1178.8	30.0	57.8	n.m.	n.m.	n.m.	n.m.	n.m.	n.m.
3	1	8	4	926.3	29.7	51.1	n.m.	n.m.	n.m.	n.m.	n.m.	n.m.
3	1	8	5	693.2	26.8	34.9	n.m.	n.m.	n.m.	n.m.	n.m.	n.m.
3	1	8	6	523.1	12.0	24.4	-0.0275	0.0343	0.0335	0.0255	0.0315	0.0098
3	1	8	7	404.9	11.8	19.3	-0.0251	0.0416	0.0352	-0.0203	0.0401	0.0212
3	1	8	8	284.8	10.7	12.9	-0.1400	0.0536	0.0338	-0.0207	0.0528	0.0401
3	1	8	9	186.1	10.0	9.8	-0.0655	0.0710	0.0443	-0.1218	0.0727	0.0279
3	1	8	10	137.8	11.4	7.3	-0.0651	0.1143	0.0725	-0.0654	0.1072	0.0470
3	1	9	0	1514.8	16.9	69.3	-0.0200	0.0151	0.0198	-0.0317	0.0151	0.0121
3	1	9	1	1374.1	36.2	80.6	n.m.	n.m.	n.m.	n.m.	n.m.	n.m.
3	1	9	2	1171.1	27.8	57.5	n.m.	n.m.	n.m.	n.m.	n.m.	n.m.
3	1	9	3	936.6	25.4	47.7	n.m.	n.m.	n.m.	n.m.	n.m.	n.m.
3	1	9	4	783.3	24.6	61.4	n.m.	n.m.	n.m.	n.m.	n.m.	n.m.
3	1	9	5	595.7	23.8	33.9	n.m.	n.m.	n.m.	n.m.	n.m.	n.m.

Continued on next page

Table B.1 – *Continued from previous page*

x	Q^2	z	$P_{h\perp}^2$	A_0	ΔA_0	δA_0	$A_{UU}^{\cos\phi_h}$	$\Delta A_{UU}^{\cos\phi_h}$	$\delta A_{UU}^{\cos\phi_h}$	$A_{UU}^{\cos 2\phi_h}$	$\Delta A_{UU}^{\cos 2\phi_h}$	$\delta A_{UU}^{\cos 2\phi_h}$
3	1	9	6	418.8	11.3	21.1	-0.1530	0.0423	0.0368	-0.0576	0.0372	0.0154
3	1	9	7	323.8	10.9	17.3	0.0691	0.0506	0.0411	0.0197	0.0450	0.0236
3	1	9	8	257.9	11.4	14.1	-0.0400	0.0645	0.0310	-0.0845	0.0632	0.0381
3	1	9	9	158.7	9.5	12.3	-0.0913	0.0880	0.1155	-0.0531	0.0838	0.0800
3	1	9	10	106.9	10.9	8.4	n.m.	n.m.	n.m.	n.m.	n.m.	n.m.
3	1	10	0	1183.0	13.8	56.4	-0.0613	0.0162	0.0159	-0.0171	0.0165	0.0102
3	1	10	1	998.0	19.3	50.4	n.m.	n.m.	n.m.	n.m.	n.m.	n.m.
3	1	10	2	904.2	25.7	44.7	n.m.	n.m.	n.m.	n.m.	n.m.	n.m.
3	1	10	3	730.9	21.7	37.3	n.m.	n.m.	n.m.	n.m.	n.m.	n.m.
3	1	10	4	607.9	21.1	32.6	n.m.	n.m.	n.m.	n.m.	n.m.	n.m.
3	1	10	5	457.6	19.8	37.2	n.m.	n.m.	n.m.	n.m.	n.m.	n.m.
3	1	10	6	374.4	21.2	23.3	n.m.	n.m.	n.m.	n.m.	n.m.	n.m.
3	1	10	7	275.8	11.8	15.8	-0.0758	0.0706	0.0461	0.0070	0.0602	0.0309
3	1	10	8	202.6	11.9	12.0	-0.0713	0.0930	0.0492	0.1369	0.0719	0.0263
3	1	10	9	159.7	15.1	16.4	n.m.	n.m.	n.m.	n.m.	n.m.	n.m.
3	1	11	0	938.8	12.4	41.5	-0.0260	0.0179	0.0190	-0.0293	0.0186	0.0065
3	1	11	1	728.5	16.3	36.9	n.m.	n.m.	n.m.	n.m.	n.m.	n.m.
3	1	11	2	649.2	22.5	32.8	n.m.	n.m.	n.m.	n.m.	n.m.	n.m.
3	1	11	3	540.9	19.3	27.1	n.m.	n.m.	n.m.	n.m.	n.m.	n.m.
3	1	11	4	404.0	16.0	27.6	n.m.	n.m.	n.m.	n.m.	n.m.	n.m.
3	1	11	5	348.4	18.1	24.5	n.m.	n.m.	n.m.	n.m.	n.m.	n.m.
3	1	11	6	261.4	16.9	13.5	n.m.	n.m.	n.m.	n.m.	n.m.	n.m.
3	1	11	7	217.5	21.4	18.0	n.m.	n.m.	n.m.	n.m.	n.m.	n.m.
3	1	11	8	195.2	39.7	47.0	n.m.	n.m.	n.m.	n.m.	n.m.	n.m.
3	1	12	0	711.4	10.4	33.0	-0.0735	0.0197	0.0155	-0.0694	0.0203	0.0082
3	1	12	1	547.4	13.3	26.5	n.m.	n.m.	n.m.	n.m.	n.m.	n.m.
3	1	12	2	487.2	22.2	37.5	n.m.	n.m.	n.m.	n.m.	n.m.	n.m.
3	1	12	3	392.5	18.1	25.1	n.m.	n.m.	n.m.	n.m.	n.m.	n.m.
3	1	12	4	330.6	17.7	26.1	n.m.	n.m.	n.m.	n.m.	n.m.	n.m.
3	1	12	5	272.3	18.2	22.3	n.m.	n.m.	n.m.	n.m.	n.m.	n.m.
3	1	12	6	209.5	12.3	13.0	n.m.	n.m.	n.m.	n.m.	n.m.	n.m.
3	1	13	0	519.0	8.8	23.8	-0.0501	0.0230	0.0167	-0.0346	0.0232	0.0134
3	1	13	1	414.4	13.2	19.0	n.m.	n.m.	n.m.	n.m.	n.m.	n.m.
3	1	13	2	347.1	32.1	32.5	n.m.	n.m.	n.m.	n.m.	n.m.	n.m.
3	1	13	3	363.6	35.4	52.0	n.m.	n.m.	n.m.	n.m.	n.m.	n.m.
3	1	13	4	272.6	35.1	40.0	n.m.	n.m.	n.m.	n.m.	n.m.	n.m.
3	1	13	5	239.4	29.8	17.1	n.m.	n.m.	n.m.	n.m.	n.m.	n.m.
3	1	14	0	410.9	10.2	23.4	-0.0114	0.0335	0.0184	-0.0423	0.0349	0.0190
3	1	14	1	307.6	15.6	17.4	n.m.	n.m.	n.m.	n.m.	n.m.	n.m.

Continued on next page

Table B.1 – *Continued from previous page*

x	Q^2	z	$P_{h\perp}^2$	A_0	ΔA_0	δA_0	$A_{UU}^{\cos\phi_h}$	$\Delta A_{UU}^{\cos\phi_h}$	$\delta A_{UU}^{\cos\phi_h}$	$A_{UU}^{\cos 2\phi_h}$	$\Delta A_{UU}^{\cos 2\phi_h}$	$\delta A_{UU}^{\cos 2\phi_h}$
3	1	14	2	476.0	48.5	118.4	n.m.	n.m.	n.m.	n.m.	n.m.	n.m.
4	0	1	0	8154.8	58.0	473.4	-0.0808	0.0103	0.0284	-0.0136	0.0101	0.0034
4	0	2	0	4729.1	41.9	262.9	0.0145	0.0133	0.0091	-0.0114	0.0124	0.0066
4	0	2	1	3038.7	29.4	168.2	-0.1362	0.0138	0.0208	-0.0088	0.0138	0.0066
4	0	2	2	1296.7	19.3	73.4	-0.1421	0.0218	0.0202	0.0641	0.0215	0.0087
4	0	2	3	608.4	18.8	38.5	-0.2160	0.0435	0.0419	-0.0286	0.0430	0.0217
4	0	3	0	3262.7	39.8	172.5	0.0446	0.0192	0.0156	0.0231	0.0168	0.0121
4	0	3	1	2534.0	29.0	138.7	-0.0270	0.0170	0.0188	0.0419	0.0157	0.0046
4	0	3	2	1421.1	21.0	77.2	-0.0941	0.0217	0.0224	0.0382	0.0207	0.0102
4	0	3	3	711.6	14.1	40.4	-0.1574	0.0286	0.0229	0.0189	0.0285	0.0121
4	0	3	4	442.1	13.4	28.1	-0.1156	0.0444	0.0239	0.0339	0.0424	0.0235
4	0	3	5	350.7	51.9	28.6	n.m.	n.m.	n.m.	n.m.	n.m.	n.m.
4	0	4	0	2255.2	32.2	121.9	0.0334	0.0224	0.0224	0.0175	0.0201	0.0100
4	0	4	1	1740.4	26.2	93.0	0.0151	0.0235	0.0262	0.0359	0.0206	0.0148
4	0	4	2	1232.9	20.3	67.7	-0.0368	0.0242	0.0219	0.0272	0.0226	0.0109
4	0	4	3	738.0	15.5	42.0	-0.0749	0.0294	0.0233	-0.0373	0.0292	0.0110
4	0	4	4	434.4	11.7	25.4	-0.1199	0.0393	0.0274	-0.0006	0.0379	0.0119
4	0	4	5	262.2	10.1	15.8	-0.1068	0.0558	0.0329	0.0230	0.0518	0.0194
4	0	4	6	254.5	25.9	16.7	n.m.	n.m.	n.m.	n.m.	n.m.	n.m.
4	0	5	0	1555.7	25.4	81.2	0.0351	0.0238	0.0293	-0.0601	0.0224	0.0208
4	0	5	1	1308.8	27.8	70.9	0.0233	0.0359	0.0409	-0.0294	0.0313	0.0284
4	0	5	2	965.9	19.0	51.4	-0.1018	0.0295	0.0207	-0.0158	0.0266	0.0086
4	0	5	3	649.7	15.1	36.7	-0.0653	0.0339	0.0233	0.0088	0.0316	0.0156
4	0	5	4	440.6	12.6	25.8	-0.0892	0.0407	0.0231	-0.0043	0.0392	0.0151
4	0	5	5	265.7	9.5	16.2	-0.1304	0.0510	0.0318	0.0099	0.0499	0.0248
4	0	5	6	164.7	8.9	11.8	-0.0580	0.0809	0.0447	0.0718	0.0857	0.0461
4	0	5	7	259.2	50.4	213.8	n.m.	n.m.	n.m.	n.m.	n.m.	n.m.
4	0	6	0	1113.0	20.5	55.5	-0.0326	0.0263	0.0196	-0.0301	0.0253	0.0173
4	0	6	1	981.3	22.4	53.0	0.0060	0.0381	0.0495	-0.0577	0.0352	0.0332
4	0	6	2	715.1	21.7	39.8	-0.0602	0.0538	0.0500	-0.0774	0.0455	0.0346
4	0	6	3	544.2	19.9	33.0	0.0396	0.0612	0.0676	0.0615	0.0493	0.0456
4	0	6	4	387.8	12.5	20.5	0.0128	0.0469	0.0307	0.0028	0.0443	0.0114
4	0	6	5	252.9	9.9	13.2	-0.0581	0.0561	0.0378	-0.0165	0.0558	0.0134
4	0	6	6	177.1	9.2	12.5	-0.0366	0.0735	0.0534	-0.0140	0.0703	0.0268
4	0	6	7	141.8	14.7	8.5	n.m.	n.m.	n.m.	n.m.	n.m.	n.m.
4	0	7	0	851.6	17.7	45.7	-0.0347	0.0284	0.0201	-0.0437	0.0280	0.0170
4	0	7	1	719.9	19.2	44.7	0.0004	0.0448	0.0783	-0.0657	0.0407	0.0539
4	0	7	2	534.1	17.3	29.3	0.0037	0.0561	0.0423	-0.0308	0.0475	0.0306
4	0	7	3	450.4	19.3	28.2	0.0951	0.0706	0.0738	0.0568	0.0547	0.0474

Continued on next page

Table B.1 – *Continued from previous page*

x	Q^2	z	$P_{h\perp}^2$	A_0	ΔA_0	δA_0	$A_{UU}^{\cos\phi_h}$	$\Delta A_{UU}^{\cos\phi_h}$	$\delta A_{UU}^{\cos\phi_h}$	$A_{UU}^{\cos 2\phi_h}$	$\Delta A_{UU}^{\cos 2\phi_h}$	$\delta A_{UU}^{\cos 2\phi_h}$
4	0	7	4	300.0	11.6	17.0	-0.1016	0.0605	0.0504	-0.0004	0.0557	0.0206
4	0	7	5	227.7	10.4	15.7	0.1447	0.0687	0.0510	0.1017	0.0599	0.0316
4	0	7	6	162.9	9.1	11.5	-0.0735	0.0839	0.0488	0.0694	0.0769	0.0354
4	0	7	7	123.1	14.9	11.9	n.m.	n.m.	n.m.	n.m.	n.m.	n.m.
4	0	8	0	648.0	15.2	34.2	-0.0355	0.0325	0.0221	-0.0191	0.0319	0.0153
4	0	8	1	547.8	28.4	40.4	n.m.	n.m.	n.m.	n.m.	n.m.	n.m.
4	0	8	2	476.3	24.3	27.0	n.m.	n.m.	n.m.	n.m.	n.m.	n.m.
4	0	8	3	338.5	19.9	17.9	n.m.	n.m.	n.m.	n.m.	n.m.	n.m.
4	0	8	4	210.8	18.4	15.7	n.m.	n.m.	n.m.	n.m.	n.m.	n.m.
4	0	8	5	192.9	19.0	16.2	n.m.	n.m.	n.m.	n.m.	n.m.	n.m.
4	0	8	6	123.2	9.1	7.9	-0.1039	0.1202	0.0674	0.2169	0.1006	0.0261
4	0	8	7	153.6	24.9	56.0	n.m.	n.m.	n.m.	n.m.	n.m.	n.m.
4	0	9	0	461.4	12.1	25.8	-0.0221	0.0351	0.0211	-0.0546	0.0366	0.0168
4	0	9	1	453.1	29.7	45.0	n.m.	n.m.	n.m.	n.m.	n.m.	n.m.
4	0	9	2	390.9	23.4	26.5	n.m.	n.m.	n.m.	n.m.	n.m.	n.m.
4	0	9	3	303.2	20.0	23.9	n.m.	n.m.	n.m.	n.m.	n.m.	n.m.
4	0	9	4	230.7	18.6	36.2	n.m.	n.m.	n.m.	n.m.	n.m.	n.m.
4	0	9	5	152.2	15.1	13.9	n.m.	n.m.	n.m.	n.m.	n.m.	n.m.
4	0	9	6	91.4	8.9	9.0	n.m.	n.m.	n.m.	n.m.	n.m.	n.m.
4	0	10	0	372.4	10.3	19.9	-0.0596	0.0377	0.0198	-0.0148	0.0383	0.0230
4	0	10	1	326.9	26.3	22.2	n.m.	n.m.	n.m.	n.m.	n.m.	n.m.
4	0	10	2	234.4	17.1	23.7	n.m.	n.m.	n.m.	n.m.	n.m.	n.m.
4	0	10	3	197.5	15.3	20.3	n.m.	n.m.	n.m.	n.m.	n.m.	n.m.
4	0	10	4	153.6	9.4	9.6	0.0105	0.1038	0.0592	-0.0243	0.0913	0.0310
4	0	10	5	104.4	1.3	8.9	n.m.	n.m.	n.m.	n.m.	n.m.	n.m.
4	0	11	0	263.7	7.9	12.8	-0.0823	0.0407	0.0202	-0.0015	0.0432	0.0135
4	0	11	1	217.4	20.9	16.9	n.m.	n.m.	n.m.	n.m.	n.m.	n.m.
4	0	11	2	169.9	17.3	21.1	n.m.	n.m.	n.m.	n.m.	n.m.	n.m.
4	0	11	3	137.4	12.3	9.5	n.m.	n.m.	n.m.	n.m.	n.m.	n.m.
4	0	11	4	146.9	17.4	14.2	n.m.	n.m.	n.m.	n.m.	n.m.	n.m.
4	0	12	0	178.4	6.3	7.8	-0.0072	0.0474	0.0299	-0.0507	0.0483	0.0219
4	0	12	1	194.1	12.3	22.7	n.m.	n.m.	n.m.	n.m.	n.m.	n.m.
4	0	12	2	191.4	20.6	41.7	n.m.	n.m.	n.m.	n.m.	n.m.	n.m.
4	0	13	0	139.2	7.5	12.7	-0.1233	0.0749	0.0623	0.0135	0.0741	0.0300

Table B.2: Table of results for π^-. The Δ quantities are statistical uncertainty and the δ quantities are systematic uncertainty. The x, Q^2, z, and $P_{h\perp}^2$ values refer to the bin number (starting with 0), not the value. Bins where nothing is measure are omitted; in bins where only the multiplicity is measured, the moments have a value of "n.m." for no measurement.

x	Q^2	z	$P_{h\perp}^2$	A_0	ΔA_0	δA_0	$A_{UU}^{\cos\phi_h}$	$\Delta A_{UU}^{\cos\phi_h}$	$\delta A_{UU}^{\cos\phi_h}$	$A_{UU}^{\cos 2\phi_h}$	$\Delta A_{UU}^{\cos 2\phi_h}$	$\delta A_{UU}^{\cos 2\phi_h}$
0	0	1	0	303685.0	1230.8	15867.9	n.m.	n.m.	n.m.	n.m.	n.m.	n.m.
0	0	2	0	171326.0	31534.4	42469.6	n.m.	n.m.	n.m.	n.m.	n.m.	n.m.
0	0	2	1	104688.0	350.7	5501.8	n.m.	n.m.	n.m.	n.m.	n.m.	n.m.
0	0	2	2	53921.4	158.6	2902.9	-0.0563	0.0043	0.0041	0.0123	0.0042	0.0031
0	0	2	3	21566.3	83.5	1133.9	-0.0820	0.0055	0.0044	0.0247	0.0055	0.0054
0	0	3	0	83156.2	3257.1	7478.6	n.m.	n.m.	n.m.	n.m.	n.m.	n.m.
0	0	3	1	58130.8	317.1	5298.1	n.m.	n.m.	n.m.	n.m.	n.m.	n.m.
0	0	3	2	45027.9	224.1	2245.8	-0.0339	0.0081	0.0054	-0.0000	0.0066	0.0036
0	0	3	3	29538.1	131.5	1509.4	-0.0045	0.0066	0.0042	0.0314	0.0064	0.0047
0	0	3	4	18023.6	92.2	921.4	-0.0488	0.0074	0.0047	0.0409	0.0073	0.0046
0	0	3	5	10194.3	63.1	559.2	-0.0788	0.0090	0.0095	0.0616	0.0088	0.0054
0	0	3	6	5171.0	41.0	273.8	-0.0698	0.0115	0.0113	0.0642	0.0112	0.0065
0	0	3	7	2492.6	26.5	129.7	-0.0983	0.0155	0.0043	0.0885	0.0150	0.0112
0	0	3	8	1162.9	18.0	61.2	-0.1433	0.0225	0.0116	0.1115	0.0215	0.0163
0	0	4	0	80671.7	26673.9	51964.7	n.m.	n.m.	n.m.	n.m.	n.m.	n.m.
0	0	4	1	37097.3	391.2	2036.2	n.m.	n.m.	n.m.	n.m.	n.m.	n.m.
0	0	4	2	34597.4	928.4	1685.6	n.m.	n.m.	n.m.	n.m.	n.m.	n.m.
0	0	4	3	23594.8	179.9	1092.6	0.0096	0.0121	0.0150	0.0097	0.0096	0.0091
0	0	4	4	16220.6	106.7	796.9	-0.0016	0.0100	0.0069	0.0307	0.0092	0.0066
0	0	4	5	11357.4	82.2	555.3	-0.0018	0.0107	0.0081	0.0351	0.0103	0.0063
0	0	4	6	7700.9	64.5	392.5	-0.0097	0.0122	0.0096	0.0327	0.0119	0.0123
0	0	4	7	5077.2	49.8	272.7	-0.0404	0.0142	0.0091	0.0571	0.0139	0.0086
0	0	4	8	3069.6	36.5	166.5	-0.0136	0.0174	0.0119	0.0887	0.0166	0.0082
0	0	4	9	1731.7	25.8	95.0	-0.0176	0.0218	0.0087	0.0958	0.0209	0.0094

Continued on next page

Table B.2 – *Continued from previous page*

x	Q^2	z	$P_{h\perp}^2$	A_0	ΔA_0	δA_0	$A_{UU}^{\cos\phi_h}$	$\Delta A_{UU}^{\cos\phi_h}$	$\delta A_{UU}^{\cos\phi_h}$	$A_{UU}^{\cos 2\phi_h}$	$\Delta A_{UU}^{\cos 2\phi_h}$	$\delta A_{UU}^{\cos 2\phi_h}$
0	0	4	10	938.1	18.1	51.7	-0.0501	0.0283	0.0108	0.0972	0.0273	0.0073
0	0	4	11	469.5	12.5	23.0	0.0167	0.0396	0.0181	0.1351	0.0377	0.0222
0	0	4	12	255.3	9.5	16.7	-0.1241	0.0555	0.0242	0.1717	0.0510	0.0291
0	0	5	0	66196.8	34570.6	30378.3	n.m.	n.m.	n.m.	n.m.	n.m.	n.m.
0	0	5	1	27638.8	666.3	2302.3	n.m.	n.m.	n.m.	n.m.	n.m.	n.m.
0	0	5	2	19181.9	187.8	1595.7	n.m.	n.m.	n.m.	n.m.	n.m.	n.m.
0	0	5	3	18047.4	965.8	1217.3	n.m.	n.m.	n.m.	n.m.	n.m.	n.m.
0	0	5	4	13349.8	159.3	655.2	0.0633	0.0187	0.0186	0.0540	0.0139	0.0108
0	0	5	5	9542.4	91.5	478.8	0.0273	0.0147	0.0100	0.0142	0.0133	0.0155
0	0	5	6	6935.6	71.2	343.1	0.0050	0.0154	0.0086	0.0183	0.0146	0.0117
0	0	5	7	4936.5	57.4	256.1	-0.0180	0.0173	0.0116	0.0533	0.0165	0.0091
0	0	5	8	3477.6	46.7	186.7	-0.0387	0.0200	0.0118	0.0809	0.0189	0.0105
0	0	5	9	2426.8	37.6	125.7	0.0087	0.0229	0.0144	0.0853	0.0217	0.0125
0	0	5	10	1525.0	28.1	86.2	-0.0117	0.0268	0.0166	0.0660	0.0268	0.0129
0	0	5	11	979.9	21.9	51.1	0.0229	0.0324	0.0309	0.0799	0.0316	0.0178
0	0	5	12	607.9	16.7	31.9	0.0714	0.0408	0.0211	0.1620	0.0367	0.0225
0	0	5	13	325.0	11.6	18.7	0.0460	0.0510	0.0288	0.0293	0.0499	0.0381
0	0	5	14	202.5	9.5	12.1	0.0278	0.0716	0.0849	0.2836	0.0627	0.0222
0	0	5	15	114.1	7.8	8.2	n.m.	n.m.	n.m.	n.m.	n.m.	n.m.
0	0	6	0	55583.8	23468.8	32239.7	n.m.	n.m.	n.m.	n.m.	n.m.	n.m.
0	0	6	1	18775.9	1006.4	8877.0	n.m.	n.m.	n.m.	n.m.	n.m.	n.m.
0	0	6	2	13629.9	215.1	2163.6	n.m.	n.m.	n.m.	n.m.	n.m.	n.m.
0	0	6	3	10381.3	123.3	552.2	n.m.	n.m.	n.m.	n.m.	n.m.	n.m.
0	0	6	4	10956.1	649.7	601.5	n.m.	n.m.	n.m.	n.m.	n.m.	n.m.
0	0	6	5	7518.2	200.1	710.3	n.m.	n.m.	n.m.	n.m.	n.m.	n.m.
0	0	6	6	5416.6	77.1	257.6	0.0787	0.0215	0.0118	0.0783	0.0179	0.0130
0	0	6	7	3844.4	54.5	191.3	0.0037	0.0213	0.0201	0.0193	0.0195	0.0156
0	0	6	8	2918.7	46.6	146.4	-0.0287	0.0241	0.0119	0.0597	0.0221	0.0109
0	0	6	9	2198.0	40.1	111.7	0.0085	0.0273	0.0296	0.0184	0.0263	0.0133
0	0	6	10	1593.3	33.4	84.4	0.0061	0.0314	0.0297	0.0866	0.0296	0.0115
0	0	6	11	1091.5	26.6	56.2	-0.0788	0.0362	0.0253	0.0928	0.0341	0.0160
0	0	6	12	836.1	24.1	40.7	0.0963	0.0422	0.0303	0.0738	0.0398	0.0189
0	0	6	13	504.0	17.3	27.2	-0.0206	0.0516	0.0231	0.1609	0.0469	0.0330
0	0	6	14	324.6	13.6	24.1	0.0533	0.0624	0.0465	0.2001	0.0569	0.0510
0	0	6	15	205.8	11.1	10.9	0.0668	0.0808	0.0389	0.1510	0.0762	0.0545
0	0	6	16	119.8	8.5	8.5	0.0072	0.1083	0.0670	0.1455	0.1066	0.0335
0	0	6	17	96.9	11.4	5.6	n.m.	n.m.	n.m.	n.m.	n.m.	n.m.
0	0	7	0	11368.9	1140.7	21652.3	n.m.	n.m.	n.m.	n.m.	n.m.	n.m.
0	0	7	1	20168.0	5027.7	9956.0	n.m.	n.m.	n.m.	n.m.	n.m.	n.m.

Continued on next page

Table B.2 – *Continued from previous page*

x	Q^2	z	$P_{h\perp}^2$	A_0	ΔA_0	δA_0	$A_{UU}^{\cos\phi_h}$	$\Delta A_{UU}^{\cos\phi_h}$	$\delta A_{UU}^{\cos\phi_h}$	$A_{UU}^{\cos 2\phi_h}$	$\Delta A_{UU}^{\cos 2\phi_h}$	$\delta A_{UU}^{\cos 2\phi_h}$
0	0	7	2	10079.8	277.2	624.5	n.m.	n.m.	n.m.	n.m.	n.m.	n.m.
0	0	7	3	7385.8	120.2	432.3	n.m.	n.m.	n.m.	n.m.	n.m.	n.m.
0	0	7	4	6589.6	1805.3	1138.6	n.m.	n.m.	n.m.	n.m.	n.m.	n.m.
0	0	7	5	5566.0	504.1	501.5	n.m.	n.m.	n.m.	n.m.	n.m.	n.m.
0	0	7	6	4004.5	157.3	373.9	n.m.	n.m.	n.m.	n.m.	n.m.	n.m.
0	0	7	7	3009.9	64.2	168.9	0.0950	0.0327	0.0115	0.0428	0.0262	0.0183
0	0	7	8	2165.4	43.1	108.1	0.0046	0.0301	0.0236	0.0353	0.0265	0.0344
0	0	7	9	1702.6	36.9	94.8	0.0405	0.0325	0.0215	0.0796	0.0294	0.0196
0	0	7	10	1254.7	31.6	72.6	0.0827	0.0379	0.0203	0.0369	0.0357	0.0290
0	0	7	11	988.6	28.2	58.1	0.0201	0.0435	0.0366	0.1228	0.0398	0.0135
0	0	7	12	673.5	22.1	37.9	0.0205	0.0496	0.0324	0.1077	0.0456	0.0501
0	0	7	13	480.4	17.7	26.4	0.0007	0.0552	0.0331	0.0942	0.0517	0.0241
0	0	7	14	337.9	15.0	21.7	-0.0690	0.0678	0.0351	0.2323	0.0632	0.0394
0	0	7	15	233.6	13.1	12.9	0.0791	0.0875	0.0555	0.1402	0.0829	0.0422
0	0	7	16	166.6	11.5	8.7	-0.0466	0.1046	0.0526	0.1248	0.1012	0.0360
0	0	7	17	98.0	9.0	9.1	n.m.	n.m.	n.m.	n.m.	n.m.	n.m.
0	0	7	18	87.0	12.3	10.3	n.m.	n.m.	n.m.	n.m.	n.m.	n.m.
0	0	8	1	11424.1	9339.7	12645.9	n.m.	n.m.	n.m.	n.m.	n.m.	n.m.
0	0	8	2	7614.8	399.8	3816.4	n.m.	n.m.	n.m.	n.m.	n.m.	n.m.
0	0	8	3	5573.3	128.8	532.5	n.m.	n.m.	n.m.	n.m.	n.m.	n.m.
0	0	8	4	4261.5	83.6	478.0	n.m.	n.m.	n.m.	n.m.	n.m.	n.m.
0	0	8	5	3274.6	65.4	320.6	n.m.	n.m.	n.m.	n.m.	n.m.	n.m.
0	0	8	6	2437.8	53.3	149.0	n.m.	n.m.	n.m.	n.m.	n.m.	n.m.
0	0	8	7	2192.2	122.3	330.3	n.m.	n.m.	n.m.	n.m.	n.m.	n.m.
0	0	8	8	1791.7	92.2	122.4	n.m.	n.m.	n.m.	n.m.	n.m.	n.m.
0	0	8	9	1311.2	36.8	68.0	0.0790	0.0424	0.0392	0.0751	0.0354	0.0278
0	0	8	10	977.8	27.2	52.4	-0.0469	0.0411	0.0399	-0.0288	0.0381	0.0298
0	0	8	11	758.1	24.4	41.4	0.0719	0.0475	0.0304	0.0818	0.0443	0.0228
0	0	8	12	545.8	19.8	30.6	0.0799	0.0529	0.0319	0.0366	0.0506	0.0449
0	0	8	13	437.8	18.0	20.6	0.0555	0.0616	0.0441	0.0710	0.0594	0.0477
0	0	8	14	313.2	15.0	13.3	-0.0390	0.0704	0.0610	-0.1018	0.0717	0.0649
0	0	8	15	208.3	12.2	15.1	n.m.	n.m.	n.m.	n.m.	n.m.	n.m.
0	0	8	16	179.4	13.1	14.6	n.m.	n.m.	n.m.	n.m.	n.m.	n.m.
0	0	8	17	113.5	11.2	26.1	n.m.	n.m.	n.m.	n.m.	n.m.	n.m.
0	0	8	18	95.8	11.7	13.5	n.m.	n.m.	n.m.	n.m.	n.m.	n.m.
0	0	9	1	16105.6	3188.5	5447.5	n.m.	n.m.	n.m.	n.m.	n.m.	n.m.
0	0	9	2	10191.5	1287.3	4456.6	n.m.	n.m.	n.m.	n.m.	n.m.	n.m.
0	0	9	3	8226.2	904.9	2549.6	n.m.	n.m.	n.m.	n.m.	n.m.	n.m.
0	0	9	4	3806.2	270.3	2618.6	n.m.	n.m.	n.m.	n.m.	n.m.	n.m.

Continued on next page

Table B.2 – *Continued from previous page*

x	Q^2	z	$P_{h\perp}^2$	A_0	ΔA_0	δA_0	$A_{UU}^{\cos\phi_h}$	$\Delta A_{UU}^{\cos\phi_h}$	$\delta A_{UU}^{\cos\phi_h}$	$A_{UU}^{\cos 2\phi_h}$	$\Delta A_{UU}^{\cos 2\phi_h}$	$\delta A_{UU}^{\cos 2\phi_h}$
0	0	9	5	2499.2	60.9	443.1	n.m.	n.m.	n.m.	n.m.	n.m.	n.m.
0	0	9	6	2696.6	69.8	676.3	n.m.	n.m.	n.m.	n.m.	n.m.	n.m.
0	0	9	7	1534.0	246.0	306.6	n.m.	n.m.	n.m.	n.m.	n.m.	n.m.
0	0	9	8	1136.5	216.4	128.7	n.m.	n.m.	n.m.	n.m.	n.m.	n.m.
0	0	9	9	1027.0	73.5	110.0	n.m.	n.m.	n.m.	n.m.	n.m.	n.m.
0	0	9	10	802.1	59.1	69.4	n.m.	n.m.	n.m.	n.m.	n.m.	n.m.
0	0	9	11	601.8	23.6	29.4	0.0057	0.0600	0.0434	0.0811	0.0506	0.0379
0	0	9	12	469.5	19.4	32.4	-0.0696	0.0611	0.0562	0.0051	0.0546	0.0580
0	0	9	13	345.2	16.5	21.8	0.0038	0.0715	0.0498	0.0663	0.0681	0.0456
0	0	9	14	248.5	13.6	16.2	-0.1517	0.0843	0.0498	0.0278	0.0853	0.0549
0	0	9	15	185.7	12.5	13.7	n.m.	n.m.	n.m.	n.m.	n.m.	n.m.
0	0	9	16	153.3	12.8	8.1	n.m.	n.m.	n.m.	n.m.	n.m.	n.m.
0	0	9	17	92.7	9.0	18.5	n.m.	n.m.	n.m.	n.m.	n.m.	n.m.
0	0	9	18	124.1	24.2	46.6	n.m.	n.m.	n.m.	n.m.	n.m.	n.m.
0	0	10	1	16678.5	728.1	4761.4	n.m.	n.m.	n.m.	n.m.	n.m.	n.m.
0	0	10	2	7243.9	2029.7	2062.5	n.m.	n.m.	n.m.	n.m.	n.m.	n.m.
0	0	10	3	5223.8	20.5	3370.1	n.m.	n.m.	n.m.	n.m.	n.m.	n.m.
0	0	10	4	4066.0	966.7	1362.7	n.m.	n.m.	n.m.	n.m.	n.m.	n.m.
0	0	10	5	2046.0	14276.1	891.0	n.m.	n.m.	n.m.	n.m.	n.m.	n.m.
0	0	10	6	1569.9	49.4	154.6	n.m.	n.m.	n.m.	n.m.	n.m.	n.m.
0	0	10	7	1078.1	35.5	107.8	n.m.	n.m.	n.m.	n.m.	n.m.	n.m.
0	0	10	8	1248.8	44.7	428.4	n.m.	n.m.	n.m.	n.m.	n.m.	n.m.
0	0	10	9	908.0	36.2	74.6	n.m.	n.m.	n.m.	n.m.	n.m.	n.m.
0	0	10	10	468.3	19.1	41.0	n.m.	n.m.	n.m.	n.m.	n.m.	n.m.
0	0	10	11	377.3	16.7	44.7	n.m.	n.m.	n.m.	n.m.	n.m.	n.m.
0	0	10	12	359.5	19.9	17.8	n.m.	n.m.	n.m.	n.m.	n.m.	n.m.
0	0	10	13	311.9	18.6	18.4	n.m.	n.m.	n.m.	n.m.	n.m.	n.m.
0	0	10	14	201.5	12.7	15.5	n.m.	n.m.	n.m.	n.m.	n.m.	n.m.
0	0	10	15	178.9	12.6	16.3	n.m.	n.m.	n.m.	n.m.	n.m.	n.m.
0	0	10	16	129.8	11.2	12.7	n.m.	n.m.	n.m.	n.m.	n.m.	n.m.
0	0	10	17	102.5	12.7	20.4	n.m.	n.m.	n.m.	n.m.	n.m.	n.m.
0	0	11	1	4918.2	2071.8	5097.0	n.m.	n.m.	n.m.	n.m.	n.m.	n.m.
0	0	11	2	4515.6	762.4	698.4	n.m.	n.m.	n.m.	n.m.	n.m.	n.m.
0	0	11	3	7209.9	2546.9	1497.4	n.m.	n.m.	n.m.	n.m.	n.m.	n.m.
0	0	11	4	4571.6	611.8	1901.8	n.m.	n.m.	n.m.	n.m.	n.m.	n.m.
0	0	11	5	1487.1	59.8	95.1	n.m.	n.m.	n.m.	n.m.	n.m.	n.m.
0	0	11	6	1186.9	45.0	97.5	n.m.	n.m.	n.m.	n.m.	n.m.	n.m.
0	0	11	7	1289.0	50.8	464.0	n.m.	n.m.	n.m.	n.m.	n.m.	n.m.
0	0	11	8	1038.8	43.6	339.9	n.m.	n.m.	n.m.	n.m.	n.m.	n.m.

Continued on next page

Table B.2 – *Continued from previous page*

x	Q^2	z	$P_{h\perp}^2$	A_0	ΔA_0	δA_0	$A_{UU}^{\cos\phi_h}$	$\Delta A_{UU}^{\cos\phi_h}$	$\delta A_{UU}^{\cos\phi_h}$	$A_{UU}^{\cos 2\phi_h}$	$\Delta A_{UU}^{\cos 2\phi_h}$	$\delta A_{UU}^{\cos 2\phi_h}$
0	0	11	9	510.5	23.3	291.6	n.m.	n.m.	n.m.	n.m.	n.m.	n.m.
0	0	11	10	493.4	441.4	228.2	n.m.	n.m.	n.m.	n.m.	n.m.	n.m.
0	0	11	11	466.6	26.8	64.7	n.m.	n.m.	n.m.	n.m.	n.m.	n.m.
0	0	11	12	349.1	19.9	50.6	n.m.	n.m.	n.m.	n.m.	n.m.	n.m.
0	0	11	13	211.4	32.0	36.4	n.m.	n.m.	n.m.	n.m.	n.m.	n.m.
0	0	11	14	215.0	16.2	38.5	n.m.	n.m.	n.m.	n.m.	n.m.	n.m.
0	0	11	15	150.1	28.9	24.0	n.m.	n.m.	n.m.	n.m.	n.m.	n.m.
0	0	12	1	7989.9	4397.4	2801.9	n.m.	n.m.	n.m.	n.m.	n.m.	n.m.
0	0	12	2	4764.0	953.1	2205.4	n.m.	n.m.	n.m.	n.m.	n.m.	n.m.
0	0	12	3	4554.3	758.4	1077.1	n.m.	n.m.	n.m.	n.m.	n.m.	n.m.
0	0	12	4	3023.6	673.6	1302.6	n.m.	n.m.	n.m.	n.m.	n.m.	n.m.
0	0	12	5	1241.7	73.3	479.6	n.m.	n.m.	n.m.	n.m.	n.m.	n.m.
0	0	12	6	1243.0	59.8	438.4	n.m.	n.m.	n.m.	n.m.	n.m.	n.m.
0	0	12	7	840.6	752.7	341.3	n.m.	n.m.	n.m.	n.m.	n.m.	n.m.
0	0	12	8	771.7	39.3	258.8	n.m.	n.m.	n.m.	n.m.	n.m.	n.m.
0	0	12	9	560.4	30.7	145.2	n.m.	n.m.	n.m.	n.m.	n.m.	n.m.
0	0	12	10	478.8	28.2	112.9	n.m.	n.m.	n.m.	n.m.	n.m.	n.m.
0	0	12	11	268.3	17.9	41.0	n.m.	n.m.	n.m.	n.m.	n.m.	n.m.
0	0	12	12	326.7	21.2	25.5	n.m.	n.m.	n.m.	n.m.	n.m.	n.m.
0	0	12	13	242.8	18.9	33.0	n.m.	n.m.	n.m.	n.m.	n.m.	n.m.
0	0	12	14	189.8	18.0	13.7	n.m.	n.m.	n.m.	n.m.	n.m.	n.m.
0	0	13	1	4444.2	2083.3	2419.9	n.m.	n.m.	n.m.	n.m.	n.m.	n.m.
0	0	13	2	5302.1	994.7	2061.5	n.m.	n.m.	n.m.	n.m.	n.m.	n.m.
0	0	13	3	3105.8	1109.5	1611.8	n.m.	n.m.	n.m.	n.m.	n.m.	n.m.
0	0	13	4	1781.0	1078.4	1474.6	n.m.	n.m.	n.m.	n.m.	n.m.	n.m.
0	0	13	5	1084.6	97.5	575.4	n.m.	n.m.	n.m.	n.m.	n.m.	n.m.
0	0	13	6	711.6	48.9	491.3	n.m.	n.m.	n.m.	n.m.	n.m.	n.m.
0	0	13	7	598.6	38.1	199.9	n.m.	n.m.	n.m.	n.m.	n.m.	n.m.
0	0	13	8	508.8	664.7	255.0	n.m.	n.m.	n.m.	n.m.	n.m.	n.m.
0	0	13	9	321.1	23.5	61.2	n.m.	n.m.	n.m.	n.m.	n.m.	n.m.
0	0	13	10	292.5	22.8	43.8	n.m.	n.m.	n.m.	n.m.	n.m.	n.m.
0	0	13	11	205.7	18.0	70.8	n.m.	n.m.	n.m.	n.m.	n.m.	n.m.
0	0	14	1	1635.6	1604.3	3497.8	n.m.	n.m.	n.m.	n.m.	n.m.	n.m.
0	0	14	2	2622.1	773.8	847.2	n.m.	n.m.	n.m.	n.m.	n.m.	n.m.
0	0	14	3	2350.7	1063.5	854.2	n.m.	n.m.	n.m.	n.m.	n.m.	n.m.
0	0	14	4	2688.0	971.1	1121.1	n.m.	n.m.	n.m.	n.m.	n.m.	n.m.
0	0	14	5	1206.6	253.7	648.5	n.m.	n.m.	n.m.	n.m.	n.m.	n.m.
0	0	14	6	668.9	71.8	550.4	n.m.	n.m.	n.m.	n.m.	n.m.	n.m.
0	0	14	7	735.2	105.8	449.4	n.m.	n.m.	n.m.	n.m.	n.m.	n.m.

Continued on next page

Table B.2 – *Continued from previous page*

x	Q^2	z	$P_{h\perp}^2$	A_0	ΔA_0	δA_0	$A_{UU}^{\cos\phi_h}$	$\Delta A_{UU}^{\cos\phi_h}$	$\delta A_{UU}^{\cos\phi_h}$	$A_{UU}^{\cos 2\phi_h}$	$\Delta A_{UU}^{\cos 2\phi_h}$	$\delta A_{UU}^{\cos 2\phi_h}$
0	0	14	8	407.8	45.8	285.0	n.m.	n.m.	n.m.	n.m.	n.m.	n.m.
0	0	15	1	6019.3	11534.5	4525.0	n.m.	n.m.	n.m.	n.m.	n.m.	n.m.
0	0	15	2	2525.6	19541.1	4212.2	n.m.	n.m.	n.m.	n.m.	n.m.	n.m.
0	0	15	3	2367.3	15172.1	1757.6	n.m.	n.m.	n.m.	n.m.	n.m.	n.m.
0	0	15	4	1913.9	10430.5	1899.0	n.m.	n.m.	n.m.	n.m.	n.m.	n.m.
0	1	1	0	80056.3	364.2	4196.5	-0.2135	0.0068	0.0043	-0.0002	0.0062	0.0027
0	1	1	1	25914.6	69.3	1307.0	-0.1504	0.0038	0.0017	-0.0051	0.0038	0.0034
0	1	2	0	35632.3	441.5	1886.0	n.m.	n.m.	n.m.	n.m.	n.m.	n.m.
0	1	2	1	27219.2	108.5	1326.1	-0.1451	0.0064	0.0030	-0.0300	0.0053	0.0019
0	1	2	2	15704.7	53.2	773.7	-0.0821	0.0049	0.0021	-0.0017	0.0048	0.0038
0	1	2	3	8047.0	34.8	405.2	-0.0839	0.0062	0.0022	0.0268	0.0061	0.0047
0	1	2	4	3305.0	21.2	166.9	-0.1231	0.0092	0.0023	0.0496	0.0090	0.0062
0	1	2	5	1172.4	12.3	60.2	-0.1478	0.0152	0.0053	0.0843	0.0147	0.0096
0	1	2	6	330.0	6.6	17.8	-0.2117	0.0285	0.0112	0.0701	0.0279	0.0142
0	1	3	0	29071.1	5002.8	2021.6	n.m.	n.m.	n.m.	n.m.	n.m.	n.m.
0	1	3	1	15747.5	98.4	892.7	n.m.	n.m.	n.m.	n.m.	n.m.	n.m.
0	1	3	2	12260.9	72.4	589.6	-0.0749	0.0096	0.0029	-0.0055	0.0077	0.0033
0	1	3	3	8124.8	41.7	395.9	-0.0375	0.0077	0.0021	0.0104	0.0074	0.0053
0	1	3	4	5206.8	30.7	260.2	-0.0595	0.0086	0.0056	0.0240	0.0085	0.0045
0	1	3	5	3327.1	23.6	166.3	-0.0916	0.0103	0.0052	0.0634	0.0101	0.0056
0	1	3	6	1981.6	17.5	100.5	-0.0820	0.0129	0.0030	0.0832	0.0124	0.0068
0	1	3	7	1052.3	12.4	51.1	-0.0812	0.0173	0.0050	0.0963	0.0165	0.0084
0	1	3	8	487.8	8.3	26.3	-0.0764	0.0249	0.0092	0.1015	0.0238	0.0089
0	1	3	9	192.8	5.2	11.7	-0.0480	0.0399	0.0159	0.0974	0.0377	0.0177
0	1	3	10	83.8	3.8	5.1	0.0347	0.0661	0.0251	0.0823	0.0638	0.0247
0	1	4	0	13102.0	25496.8	12025.7	n.m.	n.m.	n.m.	n.m.	n.m.	n.m.
0	1	4	1	9828.8	125.6	470.3	n.m.	n.m.	n.m.	n.m.	n.m.	n.m.
0	1	4	2	8702.3	307.5	643.9	n.m.	n.m.	n.m.	n.m.	n.m.	n.m.
0	1	4	3	6491.1	60.9	308.0	-0.0248	0.0152	0.0067	0.0056	0.0116	0.0058
0	1	4	4	4604.7	34.8	229.3	-0.0210	0.0115	0.0040	0.0235	0.0106	0.0066
0	1	4	5	3232.5	26.8	154.9	-0.0377	0.0123	0.0039	0.0299	0.0119	0.0068
0	1	4	6	2251.1	21.7	108.1	-0.0715	0.0142	0.0046	0.0433	0.0138	0.0090
0	1	4	7	1557.6	17.6	77.2	-0.0625	0.0165	0.0071	0.0466	0.0162	0.0055
0	1	4	8	1019.1	13.8	53.3	-0.0524	0.0199	0.0067	0.0633	0.0190	0.0098
0	1	4	9	635.9	10.7	32.7	-0.0261	0.0243	0.0145	0.0583	0.0238	0.0093
0	1	4	10	371.9	8.1	17.8	-0.0288	0.0324	0.0125	0.1624	0.0301	0.0114
0	1	4	11	199.8	5.8	10.8	-0.0188	0.0425	0.0113	0.0772	0.0412	0.0132
0	1	4	12	111.3	4.7	7.4	-0.0445	0.0604	0.0315	0.0738	0.0612	0.1708
0	1	4	13	58.9	3.9	2.1	0.1710	0.0952	0.0418	0.1540	0.0850	0.0470

Continued on next page

Table B.2 – *Continued from previous page*

x	Q^2	z	$P_{h\perp}^2$	A_0	ΔA_0	δA_0	$A_{UU}^{\cos\phi_h}$	$\Delta A_{UU}^{\cos\phi_h}$	$\delta A_{UU}^{\cos\phi_h}$	$A_{UU}^{\cos 2\phi_h}$	$\Delta A_{UU}^{\cos 2\phi_h}$	$\delta A_{UU}^{\cos 2\phi_h}$
0	1	5	1	6231.9	192.6	306.5	n.m.	n.m.	n.m.	n.m.	n.m.	n.m.
0	1	5	2	5196.3	58.5	235.7	n.m.	n.m.	n.m.	n.m.	n.m.	n.m.
0	1	5	3	4945.8	318.9	752.0	n.m.	n.m.	n.m.	n.m.	n.m.	n.m.
0	1	5	4	3673.7	56.1	166.7	0.0547	0.0242	0.0102	0.0234	0.0172	0.0068
0	1	5	5	2675.5	30.0	125.3	0.0084	0.0172	0.0048	0.0017	0.0152	0.0076
0	1	5	6	1978.4	23.0	98.2	-0.0259	0.0174	0.0064	0.0530	0.0163	0.0116
0	1	5	7	1477.0	19.4	75.1	-0.0370	0.0194	0.0069	0.0308	0.0186	0.0094
0	1	5	8	1058.8	16.2	51.6	-0.0853	0.0225	0.0068	0.0371	0.0219	0.0086
0	1	5	9	732.2	13.2	36.6	-0.0853	0.0264	0.0082	0.0322	0.0268	0.0114
0	1	5	10	512.3	10.8	23.9	-0.0910	0.0303	0.0120	-0.0039	0.0301	0.0105
0	1	5	11	338.2	8.6	17.8	-0.1112	0.0379	0.0155	0.1037	0.0362	0.0155
0	1	5	12	232.9	7.3	11.2	-0.0305	0.0470	0.0168	0.1637	0.0453	0.0169
0	1	5	13	135.5	5.5	7.2	-0.0324	0.0622	0.0212	0.2472	0.0558	0.0167
0	1	5	14	87.6	4.7	5.2	0.1136	0.0781	0.0356	0.1636	0.0776	0.0677
0	1	5	15	50.2	4.1	5.3	n.m.	n.m.	n.m.	n.m.	n.m.	n.m.
0	1	6	1	4718.7	451.4	360.2	n.m.	n.m.	n.m.	n.m.	n.m.	n.m.
0	1	6	2	3411.4	62.8	178.2	n.m.	n.m.	n.m.	n.m.	n.m.	n.m.
0	1	6	3	2759.0	38.1	131.5	n.m.	n.m.	n.m.	n.m.	n.m.	n.m.
0	1	6	4	2924.9	186.4	200.9	n.m.	n.m.	n.m.	n.m.	n.m.	n.m.
0	1	6	5	1970.0	64.8	155.3	n.m.	n.m.	n.m.	n.m.	n.m.	n.m.
0	1	6	6	1480.3	24.8	68.1	-0.0384	0.0266	0.0140	0.0125	0.0217	0.0133
0	1	6	7	1176.6	19.7	58.2	0.0455	0.0250	0.0101	0.0107	0.0233	0.0112
0	1	6	8	894.4	16.2	41.4	0.0252	0.0270	0.0103	0.0433	0.0259	0.0138
0	1	6	9	665.0	13.8	31.9	-0.0545	0.0309	0.0199	0.0470	0.0300	0.0151
0	1	6	10	472.0	11.3	20.5	-0.0750	0.0354	0.0203	0.0519	0.0342	0.0164
0	1	6	11	341.4	9.6	18.3	-0.0044	0.0424	0.0149	0.1196	0.0390	0.0142
0	1	6	12	227.9	7.6	12.2	-0.0549	0.0500	0.0207	0.1522	0.0468	0.0164
0	1	6	13	165.9	6.5	8.8	-0.0975	0.0581	0.0243	0.1487	0.0583	0.0227
0	1	6	14	115.0	5.7	5.8	0.1286	0.0734	0.0209	0.1781	0.0661	0.0312
0	1	6	15	73.6	4.5	4.3	0.2031	0.0883	0.0265	0.1234	0.0857	0.0354
0	1	6	16	48.4	4.0	2.4	n.m.	n.m.	n.m.	n.m.	n.m.	n.m.
0	1	6	17	40.8	6.5	3.9	n.m.	n.m.	n.m.	n.m.	n.m.	n.m.
0	1	7	1	2964.0	665.3	1615.1	n.m.	n.m.	n.m.	n.m.	n.m.	n.m.
0	1	7	2	2930.9	1825.8	881.6	n.m.	n.m.	n.m.	n.m.	n.m.	n.m.
0	1	7	3	1989.1	37.8	103.2	n.m.	n.m.	n.m.	n.m.	n.m.	n.m.
0	1	7	4	1755.8	562.9	266.6	n.m.	n.m.	n.m.	n.m.	n.m.	n.m.
0	1	7	5	1588.1	155.9	131.3	n.m.	n.m.	n.m.	n.m.	n.m.	n.m.
0	1	7	6	1197.2	61.8	78.3	n.m.	n.m.	n.m.	n.m.	n.m.	n.m.
0	1	7	7	864.3	22.8	45.4	0.0463	0.0418	0.0202	0.0241	0.0321	0.0148

Continued on next page

Table B.2 – *Continued from previous page*

x	Q^2	z	$P_{h\perp}^2$	A_0	ΔA_0	δA_0	$A_{UU}^{\cos\phi_h}$	$\Delta A_{UU}^{\cos\phi_h}$	$\delta A_{UU}^{\cos\phi_h}$	$A_{UU}^{\cos 2\phi_h}$	$\Delta A_{UU}^{\cos 2\phi_h}$	$\delta A_{UU}^{\cos 2\phi_h}$
0	1	7	8	670.5	16.1	30.4	0.0075	0.0367	0.0389	0.0462	0.0307	0.0277
0	1	7	9	510.4	12.7	24.4	0.0194	0.0375	0.0137	0.0864	0.0337	0.0176
0	1	7	10	392.9	10.9	19.0	-0.0444	0.0407	0.0112	0.0046	0.0383	0.0145
0	1	7	11	287.1	9.0	12.7	-0.0690	0.0456	0.0250	0.0159	0.0442	0.0190
0	1	7	12	209.5	7.5	11.8	-0.0285	0.0536	0.0213	0.0503	0.0487	0.0295
0	1	7	13	169.4	7.2	8.5	-0.0218	0.0649	0.0301	0.1686	0.0590	0.0358
0	1	7	14	103.1	5.2	6.3	-0.2165	0.0753	0.0391	0.0959	0.0810	0.0257
0	1	7	15	80.9	4.9	4.9	-0.1356	0.0916	0.0328	0.0563	0.0888	0.0452
0	1	7	16	63.7	5.0	4.3	0.1235	0.1161	0.0536	0.2486	0.1007	0.0551
0	1	7	17	48.0	6.1	2.7	n.m.	n.m.	n.m.	n.m.	n.m.	n.m.
0	1	8	1	1674.3	1041.0	1456.5	n.m.	n.m.	n.m.	n.m.	n.m.	n.m.
0	1	8	2	1800.7	111.9	894.7	n.m.	n.m.	n.m.	n.m.	n.m.	n.m.
0	1	8	3	1472.0	39.4	124.9	n.m.	n.m.	n.m.	n.m.	n.m.	n.m.
0	1	8	4	1163.6	26.2	54.3	n.m.	n.m.	n.m.	n.m.	n.m.	n.m.
0	1	8	5	1301.8	30.5	327.5	n.m.	n.m.	n.m.	n.m.	n.m.	n.m.
0	1	8	6	678.0	17.1	276.5	n.m.	n.m.	n.m.	n.m.	n.m.	n.m.
0	1	8	7	641.3	47.7	72.9	n.m.	n.m.	n.m.	n.m.	n.m.	n.m.
0	1	8	8	485.0	29.2	47.9	n.m.	n.m.	n.m.	n.m.	n.m.	n.m.
0	1	8	9	369.4	13.5	17.3	-0.0600	0.0598	0.0201	0.0044	0.0481	0.0266
0	1	8	10	293.1	10.3	15.0	-0.0069	0.0545	0.0168	0.0686	0.0449	0.0221
0	1	8	11	238.1	8.7	10.1	-0.0433	0.0542	0.0312	0.0033	0.0503	0.0265
0	1	8	12	178.4	7.1	8.4	-0.0297	0.0604	0.0230	0.0672	0.0557	0.0381
0	1	8	13	130.1	6.0	5.2	-0.0993	0.0687	0.0210	-0.0181	0.0685	0.0254
0	1	8	14	92.8	5.2	5.4	0.0219	0.0827	0.0680	0.0625	0.0818	0.0239
0	1	8	15	75.3	5.0	3.4	-0.0973	0.1007	0.0997	0.0014	0.0902	0.0751
0	1	8	16	58.4	5.0	3.4	n.m.	n.m.	n.m.	n.m.	n.m.	n.m.
0	1	8	17	43.9	5.5	3.7	n.m.	n.m.	n.m.	n.m.	n.m.	n.m.
0	1	9	1	1300.0	62.2	733.3	n.m.	n.m.	n.m.	n.m.	n.m.	n.m.
0	1	9	2	1554.9	219.3	133.3	n.m.	n.m.	n.m.	n.m.	n.m.	n.m.
0	1	9	3	1369.7	3537.1	801.3	n.m.	n.m.	n.m.	n.m.	n.m.	n.m.
0	1	9	4	1016.6	86.4	522.4	n.m.	n.m.	n.m.	n.m.	n.m.	n.m.
0	1	9	5	717.2	20.3	291.4	n.m.	n.m.	n.m.	n.m.	n.m.	n.m.
0	1	9	6	804.2	328.9	212.3	n.m.	n.m.	n.m.	n.m.	n.m.	n.m.
0	1	9	7	424.5	82.2	36.1	n.m.	n.m.	n.m.	n.m.	n.m.	n.m.
0	1	9	8	372.2	73.8	40.7	n.m.	n.m.	n.m.	n.m.	n.m.	n.m.
0	1	9	9	275.0	26.4	29.1	n.m.	n.m.	n.m.	n.m.	n.m.	n.m.
0	1	9	10	254.3	21.0	16.3	n.m.	n.m.	n.m.	n.m.	n.m.	n.m.
0	1	9	11	188.0	10.0	9.4	n.m.	n.m.	n.m.	n.m.	n.m.	n.m.
0	1	9	12	124.3	6.5	6.0	n.m.	n.m.	n.m.	n.m.	n.m.	n.m.

Continued on next page

Table B.2 – *Continued from previous page*

x	Q^2	z	$P_{h\perp}^2$	A_0	ΔA_0	δA_0	$A_{UU}^{\cos\phi_h}$	$\Delta A_{UU}^{\cos\phi_h}$	$\delta A_{UU}^{\cos\phi_h}$	$A_{UU}^{\cos 2\phi_h}$	$\Delta A_{UU}^{\cos 2\phi_h}$	$\delta A_{UU}^{\cos 2\phi_h}$
0	1	9	13	115.5	6.6	5.9	0.1226	0.0853	0.0341	0.1565	0.0740	0.0340
0	1	9	14	82.2	5.0	5.1	n.m.	n.m.	n.m.	n.m.	n.m.	n.m.
0	1	9	15	66.8	5.2	3.8	n.m.	n.m.	n.m.	n.m.	n.m.	n.m.
0	1	9	16	59.0	6.0	4.4	n.m.	n.m.	n.m.	n.m.	n.m.	n.m.
0	1	9	17	47.3	5.4	3.7	n.m.	n.m.	n.m.	n.m.	n.m.	n.m.
0	1	10	1	1674.7	1255.5	1054.1	n.m.	n.m.	n.m.	n.m.	n.m.	n.m.
0	1	10	2	2181.9	328.5	291.0	n.m.	n.m.	n.m.	n.m.	n.m.	n.m.
0	1	10	3	1615.5	229.2	477.0	n.m.	n.m.	n.m.	n.m.	n.m.	n.m.
0	1	10	4	1199.9	212.2	836.7	n.m.	n.m.	n.m.	n.m.	n.m.	n.m.
0	1	10	5	580.8	20.4	109.6	n.m.	n.m.	n.m.	n.m.	n.m.	n.m.
0	1	10	6	622.8	22.2	54.3	n.m.	n.m.	n.m.	n.m.	n.m.	n.m.
0	1	10	7	369.5	254.1	118.9	n.m.	n.m.	n.m.	n.m.	n.m.	n.m.
0	1	10	8	368.2	15.4	17.7	n.m.	n.m.	n.m.	n.m.	n.m.	n.m.
0	1	10	9	188.0	8.5	69.0	n.m.	n.m.	n.m.	n.m.	n.m.	n.m.
0	1	10	10	160.6	44.3	24.7	n.m.	n.m.	n.m.	n.m.	n.m.	n.m.
0	1	10	11	137.3	17.3	30.1	n.m.	n.m.	n.m.	n.m.	n.m.	n.m.
0	1	10	12	107.1	8.1	5.1	n.m.	n.m.	n.m.	n.m.	n.m.	n.m.
0	1	10	13	101.4	8.3	5.2	n.m.	n.m.	n.m.	n.m.	n.m.	n.m.
0	1	10	14	66.4	5.0	4.3	n.m.	n.m.	n.m.	n.m.	n.m.	n.m.
0	1	10	15	45.3	4.2	4.3	n.m.	n.m.	n.m.	n.m.	n.m.	n.m.
0	1	10	16	50.2	6.3	4.1	n.m.	n.m.	n.m.	n.m.	n.m.	n.m.
0	1	11	1	1244.5	564.7	1675.0	n.m.	n.m.	n.m.	n.m.	n.m.	n.m.
0	1	11	2	1361.8	316.4	551.2	n.m.	n.m.	n.m.	n.m.	n.m.	n.m.
0	1	11	3	664.8	3681.1	518.2	n.m.	n.m.	n.m.	n.m.	n.m.	n.m.
0	1	11	4	749.0	151.0	225.8	n.m.	n.m.	n.m.	n.m.	n.m.	n.m.
0	1	11	5	470.5	436.4	185.2	n.m.	n.m.	n.m.	n.m.	n.m.	n.m.
0	1	11	6	460.3	20.3	121.8	n.m.	n.m.	n.m.	n.m.	n.m.	n.m.
0	1	11	7	366.0	214.2	106.3	n.m.	n.m.	n.m.	n.m.	n.m.	n.m.
0	1	11	8	285.8	13.9	74.8	n.m.	n.m.	n.m.	n.m.	n.m.	n.m.
0	1	11	9	219.4	11.6	50.1	n.m.	n.m.	n.m.	n.m.	n.m.	n.m.
0	1	11	10	100.3	6.1	40.4	n.m.	n.m.	n.m.	n.m.	n.m.	n.m.
0	1	11	11	84.5	5.6	39.8	n.m.	n.m.	n.m.	n.m.	n.m.	n.m.
0	1	11	12	75.7	30.1	37.0	n.m.	n.m.	n.m.	n.m.	n.m.	n.m.
0	1	11	13	66.0	5.1	14.5	n.m.	n.m.	n.m.	n.m.	n.m.	n.m.
0	1	11	14	75.8	20.4	14.5	n.m.	n.m.	n.m.	n.m.	n.m.	n.m.
0	1	11	15	42.7	4.5	14.0	n.m.	n.m.	n.m.	n.m.	n.m.	n.m.
0	1	12	1	2060.3	2803.1	757.7	n.m.	n.m.	n.m.	n.m.	n.m.	n.m.
0	1	12	2	518.6	26.5	56.3	n.m.	n.m.	n.m.	n.m.	n.m.	n.m.
0	1	12	3	732.0	7.2	349.9	n.m.	n.m.	n.m.	n.m.	n.m.	n.m.

Continued on next page

Table B.2 – *Continued from previous page*

x	Q^2	z	$P_{h\perp}^2$	A_0	ΔA_0	δA_0	$A_{UU}^{\cos\phi_h}$	$\Delta A_{UU}^{\cos\phi_h}$	$\delta A_{UU}^{\cos\phi_h}$	$A_{UU}^{\cos 2\phi_h}$	$\Delta A_{UU}^{\cos 2\phi_h}$	$\delta A_{UU}^{\cos 2\phi_h}$
0	1	12	4	820.1	150.3	55.0	n.m.	n.m.	n.m.	n.m.	n.m.	n.m.
0	1	12	5	318.8	19.6	161.2	n.m.	n.m.	n.m.	n.m.	n.m.	n.m.
0	1	12	6	403.0	24.8	104.8	n.m.	n.m.	n.m.	n.m.	n.m.	n.m.
0	1	12	7	180.0	10.4	49.1	n.m.	n.m.	n.m.	n.m.	n.m.	n.m.
0	1	12	8	171.6	172.2	65.7	n.m.	n.m.	n.m.	n.m.	n.m.	n.m.
0	1	12	9	158.4	10.5	12.1	n.m.	n.m.	n.m.	n.m.	n.m.	n.m.
0	1	12	10	91.2	6.1	32.7	n.m.	n.m.	n.m.	n.m.	n.m.	n.m.
0	1	12	11	78.0	6.2	37.0	n.m.	n.m.	n.m.	n.m.	n.m.	n.m.
0	1	12	12	88.0	36.1	26.2	n.m.	n.m.	n.m.	n.m.	n.m.	n.m.
0	1	12	13	90.5	8.3	20.4	n.m.	n.m.	n.m.	n.m.	n.m.	n.m.
0	1	12	14	74.8	7.6	12.3	n.m.	n.m.	n.m.	n.m.	n.m.	n.m.
0	1	13	1	585.0	569.6	608.8	n.m.	n.m.	n.m.	n.m.	n.m.	n.m.
0	1	13	2	812.2	410.2	148.6	n.m.	n.m.	n.m.	n.m.	n.m.	n.m.
0	1	13	3	307.3	17.3	51.3	n.m.	n.m.	n.m.	n.m.	n.m.	n.m.
0	1	13	4	488.1	114.8	239.6	n.m.	n.m.	n.m.	n.m.	n.m.	n.m.
0	1	13	5	228.3	24.0	67.7	n.m.	n.m.	n.m.	n.m.	n.m.	n.m.
0	1	13	6	188.8	14.7	23.6	n.m.	n.m.	n.m.	n.m.	n.m.	n.m.
0	1	13	7	143.3	1.6	41.8	n.m.	n.m.	n.m.	n.m.	n.m.	n.m.
0	1	13	8	131.9	9.5	14.1	n.m.	n.m.	n.m.	n.m.	n.m.	n.m.
0	1	13	9	95.7	7.5	7.5	n.m.	n.m.	n.m.	n.m.	n.m.	n.m.
0	1	13	10	65.4	5.6	27.2	n.m.	n.m.	n.m.	n.m.	n.m.	n.m.
0	1	13	12	88.0	8.6	20.8	n.m.	n.m.	n.m.	n.m.	n.m.	n.m.
0	1	14	2	324.4	24.2	362.9	n.m.	n.m.	n.m.	n.m.	n.m.	n.m.
0	1	14	3	375.3	126.7	60.4	n.m.	n.m.	n.m.	n.m.	n.m.	n.m.
0	1	14	4	346.2	105.3	36.5	n.m.	n.m.	n.m.	n.m.	n.m.	n.m.
0	1	14	5	265.6	89.0	47.0	n.m.	n.m.	n.m.	n.m.	n.m.	n.m.
0	1	14	6	300.2	203.4	196.4	n.m.	n.m.	n.m.	n.m.	n.m.	n.m.
0	1	14	7	150.3	22.3	62.9	n.m.	n.m.	n.m.	n.m.	n.m.	n.m.
1	0	1	0	335227.0	1377.6	17640.9	-0.2048	0.0062	0.0051	-0.0124	0.0055	0.0032
1	0	2	0	245826.0	5705.1	29477.1	n.m.	n.m.	n.m.	n.m.	n.m.	n.m.
1	0	2	1	124848.0	319.2	6430.5	-0.1303	0.0039	0.0057	-0.0303	0.0035	0.0021
1	0	2	2	38523.3	119.4	1922.2	-0.0939	0.0045	0.0059	0.0417	0.0044	0.0049
1	0	3	0	125627.0	1038.0	6782.2	n.m.	n.m.	n.m.	n.m.	n.m.	n.m.
1	0	3	1	89742.6	5894.3	19504.3	n.m.	n.m.	n.m.	n.m.	n.m.	n.m.
1	0	3	2	57101.7	218.7	2901.3	-0.0063	0.0059	0.0020	0.0094	0.0052	0.0058
1	0	3	3	33922.5	139.5	1724.7	-0.0358	0.0061	0.0074	0.0719	0.0058	0.0038
1	0	3	4	15465.4	83.2	793.0	-0.0859	0.0079	0.0092	0.0838	0.0075	0.0073
1	0	3	5	5554.9	43.4	273.6	-0.1496	0.0114	0.0078	0.1037	0.0110	0.0067
1	0	4	0	91452.4	12101.1	40644.8	n.m.	n.m.	n.m.	n.m.	n.m.	n.m.

Continued on next page

Table B.2 – *Continued from previous page*

x	Q^2	z	$P_{h\perp}^2$	A_0	ΔA_0	δA_0	$A_{UU}^{\cos\phi_h}$	$\Delta A_{UU}^{\cos\phi_h}$	$\delta A_{UU}^{\cos\phi_h}$	$A_{UU}^{\cos 2\phi_h}$	$\Delta A_{UU}^{\cos 2\phi_h}$	$\delta A_{UU}^{\cos 2\phi_h}$
1	0	4	1	54090.2	5803.4	9194.3	n.m.	n.m.	n.m.	n.m.	n.m.	n.m.
1	0	4	2	44551.2	601.0	2464.1	n.m.	n.m.	n.m.	n.m.	n.m.	n.m.
1	0	4	3	27619.5	159.9	1379.5	0.0236	0.0091	0.0040	0.0367	0.0077	0.0078
1	0	4	4	20693.5	119.5	1024.6	0.0187	0.0087	0.0096	0.0872	0.0080	0.0075
1	0	4	5	14548.5	99.8	743.4	-0.0347	0.0102	0.0114	0.1066	0.0097	0.0088
1	0	4	6	7812.6	68.4	396.9	-0.0396	0.0129	0.0056	0.1124	0.0123	0.0115
1	0	4	7	3299.9	39.1	162.4	-0.0684	0.0176	0.0104	0.1453	0.0166	0.0169
1	0	4	8	1302.1	22.2	67.1	-0.1167	0.0257	0.0111	0.2180	0.0237	0.0247
1	0	5	0	80084.8	5377.7	24427.1	n.m.	n.m.	n.m.	n.m.	n.m.	n.m.
1	0	5	1	40821.5	5804.2	9184.3	n.m.	n.m.	n.m.	n.m.	n.m.	n.m.
1	0	5	2	25338.3	175.0	2049.8	n.m.	n.m.	n.m.	n.m.	n.m.	n.m.
1	0	5	3	22178.2	841.2	1884.4	n.m.	n.m.	n.m.	n.m.	n.m.	n.m.
1	0	5	4	16091.7	145.2	808.1	0.0660	0.0143	0.0094	0.0786	0.0111	0.0068
1	0	5	5	11803.8	98.0	594.1	0.0370	0.0127	0.0134	0.0853	0.0115	0.0061
1	0	5	6	10097.1	94.4	502.3	0.0395	0.0140	0.0087	0.1160	0.0129	0.0131
1	0	5	7	6948.9	78.5	346.5	-0.0361	0.0169	0.0087	0.1300	0.0160	0.0161
1	0	5	8	3676.4	52.4	181.9	-0.0459	0.0211	0.0100	0.1220	0.0201	0.0171
1	0	5	9	1636.9	31.2	81.4	-0.0560	0.0285	0.0092	0.1565	0.0271	0.0174
1	0	5	10	720.4	18.6	37.3	-0.0480	0.0387	0.0106	0.1730	0.0367	0.0153
1	0	6	0	49900.8	4625.3	11139.5	n.m.	n.m.	n.m.	n.m.	n.m.	n.m.
1	0	6	1	28716.0	5854.9	8144.4	n.m.	n.m.	n.m.	n.m.	n.m.	n.m.
1	0	6	2	18258.4	163.8	1135.0	n.m.	n.m.	n.m.	n.m.	n.m.	n.m.
1	0	6	3	13867.6	4906.7	1245.6	n.m.	n.m.	n.m.	n.m.	n.m.	n.m.
1	0	6	4	13980.0	444.6	901.1	n.m.	n.m.	n.m.	n.m.	n.m.	n.m.
1	0	6	5	10075.1	225.2	547.4	n.m.	n.m.	n.m.	n.m.	n.m.	n.m.
1	0	6	6	7229.5	88.4	357.2	0.0769	0.0189	0.0120	0.0912	0.0162	0.0092
1	0	6	7	6219.6	82.3	311.4	0.0353	0.0202	0.0128	0.1351	0.0180	0.0100
1	0	6	8	4825.8	75.5	240.0	0.0701	0.0236	0.0152	0.1767	0.0212	0.0188
1	0	6	9	2791.5	53.3	137.3	-0.0210	0.0289	0.0147	0.1505	0.0272	0.0173
1	0	6	10	1489.0	35.7	77.2	-0.0079	0.0359	0.0214	0.1523	0.0336	0.0216
1	0	6	11	686.6	21.4	39.3	0.0153	0.0464	0.0143	0.1091	0.0449	0.0183
1	0	6	12	335.0	14.4	21.7	-0.0242	0.0647	0.0284	0.1763	0.0617	0.0313
1	0	7	0	22598.0	4835.0	12746.9	n.m.	n.m.	n.m.	n.m.	n.m.	n.m.
1	0	7	1	17036.0	1262.8	8782.5	n.m.	n.m.	n.m.	n.m.	n.m.	n.m.
1	0	7	2	13072.6	159.1	854.0	n.m.	n.m.	n.m.	n.m.	n.m.	n.m.
1	0	7	3	10053.7	115.3	536.7	n.m.	n.m.	n.m.	n.m.	n.m.	n.m.
1	0	7	4	8655.2	1927.4	1283.0	n.m.	n.m.	n.m.	n.m.	n.m.	n.m.
1	0	7	5	8107.1	494.6	607.9	n.m.	n.m.	n.m.	n.m.	n.m.	n.m.
1	0	7	6	5893.7	198.2	334.3	n.m.	n.m.	n.m.	n.m.	n.m.	n.m.

Continued on next page

Table B.2 – *Continued from previous page*

x	Q^2	z	$P_{h\perp}^2$	A_0	ΔA_0	δA_0	$A_{UU}^{\cos\phi_h}$	$\Delta A_{UU}^{\cos\phi_h}$	$\delta A_{UU}^{\cos\phi_h}$	$A_{UU}^{\cos 2\phi_h}$	$\Delta A_{UU}^{\cos 2\phi_h}$	$\delta A_{UU}^{\cos 2\phi_h}$
1	0	7	7	4509.6	81.9	262.7	0.1048	0.0282	0.0118	0.0492	0.0228	0.0111
1	0	7	8	3727.5	71.5	187.6	0.0847	0.0294	0.0111	0.1151	0.0252	0.0103
1	0	7	9	2568.5	56.2	130.2	0.0270	0.0336	0.0165	0.1490	0.0295	0.0205
1	0	7	10	1656.3	43.7	80.8	0.0056	0.0402	0.0118	0.1159	0.0354	0.0184
1	0	7	11	892.6	29.6	47.4	0.0028	0.0509	0.0361	0.1526	0.0470	0.0223
1	0	7	12	456.1	19.5	28.3	0.0472	0.0643	0.0244	0.1634	0.0587	0.0321
1	0	7	13	232.2	13.1	12.8	0.0168	0.0865	0.0233	0.1932	0.0745	0.0521
1	0	7	14	154.1	13.0	8.2	n.m.	n.m.	n.m.	n.m.	n.m.	n.m.
1	0	8	0	15980.5	2905.4	5688.6	n.m.	n.m.	n.m.	n.m.	n.m.	n.m.
1	0	8	1	17745.5	1612.8	6231.0	n.m.	n.m.	n.m.	n.m.	n.m.	n.m.
1	0	8	2	9804.6	169.0	2290.5	n.m.	n.m.	n.m.	n.m.	n.m.	n.m.
1	0	8	3	7475.1	108.3	382.4	n.m.	n.m.	n.m.	n.m.	n.m.	n.m.
1	0	8	4	5648.1	85.5	2184.1	n.m.	n.m.	n.m.	n.m.	n.m.	n.m.
1	0	8	5	4257.6	70.7	562.2	n.m.	n.m.	n.m.	n.m.	n.m.	n.m.
1	0	8	6	4025.6	1220.2	897.4	n.m.	n.m.	n.m.	n.m.	n.m.	n.m.
1	0	8	7	3441.9	183.4	295.2	n.m.	n.m.	n.m.	n.m.	n.m.	n.m.
1	0	8	8	2692.5	131.9	227.2	n.m.	n.m.	n.m.	n.m.	n.m.	n.m.
1	0	8	9	2089.2	63.2	109.0	0.2259	0.0445	0.0148	0.1208	0.0350	0.0160
1	0	8	10	1364.5	44.9	76.5	0.2196	0.0477	0.0262	0.1256	0.0401	0.0251
1	0	8	11	806.0	31.0	47.4	0.1224	0.0565	0.0321	0.0889	0.0473	0.0260
1	0	8	12	473.5	22.9	34.4	0.2157	0.0696	0.0460	0.2075	0.0586	0.0348
1	0	8	13	244.7	14.8	13.7	0.1224	0.0897	0.0320	0.0584	0.0812	0.0251
1	0	8	14	137.0	10.8	5.4	0.2734	0.1136	0.0548	0.1318	0.1028	0.0382
1	0	9	0	8554.7	3410.7	5561.1	n.m.	n.m.	n.m.	n.m.	n.m.	n.m.
1	0	9	1	12782.4	7.8	6019.9	n.m.	n.m.	n.m.	n.m.	n.m.	n.m.
1	0	9	2	7078.2	263.4	2884.2	n.m.	n.m.	n.m.	n.m.	n.m.	n.m.
1	0	9	3	8849.8	358.4	3431.4	n.m.	n.m.	n.m.	n.m.	n.m.	n.m.
1	0	9	4	6183.2	251.0	401.5	n.m.	n.m.	n.m.	n.m.	n.m.	n.m.
1	0	9	5	3216.0	63.0	178.9	n.m.	n.m.	n.m.	n.m.	n.m.	n.m.
1	0	9	6	2479.6	54.9	351.9	n.m.	n.m.	n.m.	n.m.	n.m.	n.m.
1	0	9	7	2556.7	55.7	136.1	n.m.	n.m.	n.m.	n.m.	n.m.	n.m.
1	0	9	8	1622.1	249.3	242.8	n.m.	n.m.	n.m.	n.m.	n.m.	n.m.
1	0	9	9	1320.1	96.6	120.1	n.m.	n.m.	n.m.	n.m.	n.m.	n.m.
1	0	9	10	964.6	72.2	82.6	n.m.	n.m.	n.m.	n.m.	n.m.	n.m.
1	0	9	11	617.2	32.0	43.6	n.m.	n.m.	n.m.	n.m.	n.m.	n.m.
1	0	9	12	393.6	23.5	25.4	0.1186	0.0878	0.0756	0.0885	0.0797	0.0392
1	0	9	13	216.9	14.4	15.5	n.m.	n.m.	n.m.	n.m.	n.m.	n.m.
1	0	9	14	122.6	14.5	8.2	n.m.	n.m.	n.m.	n.m.	n.m.	n.m.
1	0	10	0	12373.9	54178.3	5808.5	n.m.	n.m.	n.m.	n.m.	n.m.	n.m.

Continued on next page

Table B.2 – *Continued from previous page*

x	Q^2	z	$P_{h\perp}^2$	A_0	ΔA_0	δA_0	$A_{UU}^{\cos\phi_h}$	$\Delta A_{UU}^{\cos\phi_h}$	$\delta A_{UU}^{\cos\phi_h}$	$A_{UU}^{\cos 2\phi_h}$	$\Delta A_{UU}^{\cos 2\phi_h}$	$\delta A_{UU}^{\cos 2\phi_h}$
1	0	10	1	10112.1	3.7	4645.3	n.m.	n.m.	n.m.	n.m.	n.m.	n.m.
1	0	10	2	8436.3	346.6	3950.8	n.m.	n.m.	n.m.	n.m.	n.m.	n.m.
1	0	10	3	4099.1	195.1	321.5	n.m.	n.m.	n.m.	n.m.	n.m.	n.m.
1	0	10	4	3046.6	151.6	1368.1	n.m.	n.m.	n.m.	n.m.	n.m.	n.m.
1	0	10	5	2386.2	1473.7	579.0	n.m.	n.m.	n.m.	n.m.	n.m.	n.m.
1	0	10	6	2335.9	895.0	696.9	n.m.	n.m.	n.m.	n.m.	n.m.	n.m.
1	0	10	7	1314.5	38.1	540.5	n.m.	n.m.	n.m.	n.m.	n.m.	n.m.
1	0	10	8	1503.9	52.5	178.9	n.m.	n.m.	n.m.	n.m.	n.m.	n.m.
1	0	10	9	786.0	33.0	68.1	n.m.	n.m.	n.m.	n.m.	n.m.	n.m.
1	0	10	10	827.2	36.4	39.7	n.m.	n.m.	n.m.	n.m.	n.m.	n.m.
1	0	10	11	580.9	31.7	48.8	n.m.	n.m.	n.m.	n.m.	n.m.	n.m.
1	0	10	12	307.7	27.3	21.7	n.m.	n.m.	n.m.	n.m.	n.m.	n.m.
1	0	10	13	172.8	23.2	20.8	n.m.	n.m.	n.m.	n.m.	n.m.	n.m.
1	0	10	14	134.8	76.7	31.8	n.m.	n.m.	n.m.	n.m.	n.m.	n.m.
1	0	11	0	20872.7	630.5	12859.3	n.m.	n.m.	n.m.	n.m.	n.m.	n.m.
1	0	11	1	8772.6	2.2	2750.1	n.m.	n.m.	n.m.	n.m.	n.m.	n.m.
1	0	11	2	7029.3	305.5	449.1	n.m.	n.m.	n.m.	n.m.	n.m.	n.m.
1	0	11	3	5276.9	275.8	393.0	n.m.	n.m.	n.m.	n.m.	n.m.	n.m.
1	0	11	4	2801.0	6442.2	1935.2	n.m.	n.m.	n.m.	n.m.	n.m.	n.m.
1	0	11	5	2190.7	1093.9	664.1	n.m.	n.m.	n.m.	n.m.	n.m.	n.m.
1	0	11	6	2111.9	66.1	643.0	n.m.	n.m.	n.m.	n.m.	n.m.	n.m.
1	0	11	7	1575.3	56.1	289.3	n.m.	n.m.	n.m.	n.m.	n.m.	n.m.
1	0	11	8	866.7	35.7	57.5	n.m.	n.m.	n.m.	n.m.	n.m.	n.m.
1	0	11	9	822.2	41.1	49.3	n.m.	n.m.	n.m.	n.m.	n.m.	n.m.
1	0	11	10	403.3	24.3	37.8	n.m.	n.m.	n.m.	n.m.	n.m.	n.m.
1	0	11	11	238.4	20.5	111.8	n.m.	n.m.	n.m.	n.m.	n.m.	n.m.
1	0	11	12	263.0	22.9	15.0	n.m.	n.m.	n.m.	n.m.	n.m.	n.m.
1	0	12	0	17378.8	562.2	8612.3	n.m.	n.m.	n.m.	n.m.	n.m.	n.m.
1	0	12	1	5092.8	725.3	6657.8	n.m.	n.m.	n.m.	n.m.	n.m.	n.m.
1	0	12	2	3926.8	168.7	341.2	n.m.	n.m.	n.m.	n.m.	n.m.	n.m.
1	0	12	3	4487.6	252.9	2513.3	n.m.	n.m.	n.m.	n.m.	n.m.	n.m.
1	0	12	4	2090.6	143.6	888.7	n.m.	n.m.	n.m.	n.m.	n.m.	n.m.
1	0	12	5	1738.9	63.9	143.1	n.m.	n.m.	n.m.	n.m.	n.m.	n.m.
1	0	12	6	1325.1	55.5	560.2	n.m.	n.m.	n.m.	n.m.	n.m.	n.m.
1	0	12	7	1439.5	64.9	77.3	n.m.	n.m.	n.m.	n.m.	n.m.	n.m.
1	0	12	8	751.7	40.6	49.0	n.m.	n.m.	n.m.	n.m.	n.m.	n.m.
1	0	12	9	523.0	33.5	246.3	n.m.	n.m.	n.m.	n.m.	n.m.	n.m.
1	0	12	10	519.8	46.6	158.2	n.m.	n.m.	n.m.	n.m.	n.m.	n.m.
1	0	13	0	15713.9	539.6	8265.2	n.m.	n.m.	n.m.	n.m.	n.m.	n.m.

Continued on next page

Table B.2 – *Continued from previous page*

x	Q^2	z	$P_{h\perp}^2$	A_0	ΔA_0	δA_0	$A_{UU}^{\cos\phi_h}$	$\Delta A_{UU}^{\cos\phi_h}$	$\delta A_{UU}^{\cos\phi_h}$	$A_{UU}^{\cos 2\phi_h}$	$\Delta A_{UU}^{\cos 2\phi_h}$	$\delta A_{UU}^{\cos 2\phi_h}$
1	0	13	1	5359.1	7.8	1922.0	n.m.	n.m.	n.m.	n.m.	n.m.	n.m.
1	0	13	2	3819.9	180.1	322.6	n.m.	n.m.	n.m.	n.m.	n.m.	n.m.
1	0	13	3	2502.7	163.8	3132.9	n.m.	n.m.	n.m.	n.m.	n.m.	n.m.
1	0	13	4	3129.1	286.0	243.1	n.m.	n.m.	n.m.	n.m.	n.m.	n.m.
1	0	13	5	2100.6	1315.6	569.2	n.m.	n.m.	n.m.	n.m.	n.m.	n.m.
1	0	13	6	1753.9	105.8	612.5	n.m.	n.m.	n.m.	n.m.	n.m.	n.m.
1	0	13	7	790.1	59.7	391.0	n.m.	n.m.	n.m.	n.m.	n.m.	n.m.
1	0	13	8	1083.9	101.8	300.1	n.m.	n.m.	n.m.	n.m.	n.m.	n.m.
1	0	14	0	6984.9	35068.3	2133.9	n.m.	n.m.	n.m.	n.m.	n.m.	n.m.
1	0	14	1	4492.2	8810.6	2963.8	n.m.	n.m.	n.m.	n.m.	n.m.	n.m.
1	0	14	2	3472.6	233.1	1683.1	n.m.	n.m.	n.m.	n.m.	n.m.	n.m.
1	0	14	3	3552.8	391.8	2365.6	n.m.	n.m.	n.m.	n.m.	n.m.	n.m.
1	0	14	4	2037.7	245.5	316.9	n.m.	n.m.	n.m.	n.m.	n.m.	n.m.
1	0	14	5	2075.8	2905.7	885.1	n.m.	n.m.	n.m.	n.m.	n.m.	n.m.
1	0	14	6	1851.6	259.5	556.9	n.m.	n.m.	n.m.	n.m.	n.m.	n.m.
1	0	15	0	14483.6	915.8	8315.5	n.m.	n.m.	n.m.	n.m.	n.m.	n.m.
1	0	15	1	10397.9	1030.1	6102.1	n.m.	n.m.	n.m.	n.m.	n.m.	n.m.
1	0	15	2	7631.8	568.7	3105.7	n.m.	n.m.	n.m.	n.m.	n.m.	n.m.
1	1	1	0	113239.0	424.8	5747.3	-0.2448	0.0057	0.0029	-0.0124	0.0050	0.0010
1	1	2	0	61414.5	4780.0	3701.1	n.m.	n.m.	n.m.	n.m.	n.m.	n.m.
1	1	2	1	38114.7	116.9	1818.2	-0.1569	0.0050	0.0016	-0.0522	0.0040	0.0011
1	1	2	2	20506.8	57.2	981.2	-0.0685	0.0041	0.0029	-0.0007	0.0040	0.0021
1	1	2	3	9262.4	35.7	455.9	-0.1074	0.0056	0.0025	0.0311	0.0055	0.0046
1	1	3	0	35166.6	584.9	1651.1	n.m.	n.m.	n.m.	n.m.	n.m.	n.m.
1	1	3	1	24698.3	2118.8	4708.1	n.m.	n.m.	n.m.	n.m.	n.m.	n.m.
1	1	3	2	17622.5	82.7	838.0	-0.0590	0.0076	0.0034	-0.0303	0.0061	0.0022
1	1	3	3	11329.0	46.4	541.4	-0.0195	0.0061	0.0025	0.0163	0.0058	0.0029
1	1	3	4	7031.6	34.2	334.3	-0.0353	0.0072	0.0031	0.0590	0.0070	0.0045
1	1	3	5	4070.3	25.0	198.8	-0.0667	0.0090	0.0036	0.0564	0.0088	0.0038
1	1	3	6	2144.1	17.7	104.0	-0.0794	0.0121	0.0038	0.0794	0.0116	0.0060
1	1	3	7	1086.9	12.8	53.0	-0.1250	0.0172	0.0063	0.0865	0.0165	0.0108
1	1	4	0	20469.0	3010.0	10777.2	n.m.	n.m.	n.m.	n.m.	n.m.	n.m.
1	1	4	1	15374.8	111.3	725.2	n.m.	n.m.	n.m.	n.m.	n.m.	n.m.
1	1	4	2	14272.0	309.2	703.2	n.m.	n.m.	n.m.	n.m.	n.m.	n.m.
1	1	4	3	9441.4	72.0	437.5	-0.0237	0.0124	0.0090	-0.0011	0.0093	0.0048
1	1	4	4	6676.4	40.5	313.6	0.0077	0.0092	0.0048	0.0396	0.0084	0.0039
1	1	4	5	4585.4	30.6	217.5	-0.0020	0.0099	0.0033	0.0628	0.0094	0.0039
1	1	4	6	3021.2	23.8	147.8	-0.0400	0.0117	0.0053	0.0734	0.0111	0.0039
1	1	4	7	2006.0	19.3	96.1	-0.0564	0.0143	0.0062	0.0997	0.0136	0.0053

Continued on next page

Table B.2 – *Continued from previous page*

x	Q^2	z	$P_{h\perp}^2$	A_0	ΔA_0	δA_0	$A_{UU}^{\cos\phi_h}$	$\Delta A_{UU}^{\cos\phi_h}$	$\delta A_{UU}^{\cos\phi_h}$	$A_{UU}^{\cos 2\phi_h}$	$\Delta A_{UU}^{\cos 2\phi_h}$	$\delta A_{UU}^{\cos 2\phi_h}$
1	1	4	8	1170.2	14.4	57.7	-0.0566	0.0182	0.0064	0.0939	0.0173	0.0066
1	1	4	9	677.3	10.9	30.9	-0.0334	0.0237	0.0062	0.0855	0.0228	0.0080
1	1	4	10	363.0	8.1	19.5	-0.0463	0.0333	0.0134	0.1267	0.0320	0.0111
1	1	4	11	235.4	7.7	10.4	-0.0783	0.0501	0.0169	0.3161	0.0431	0.0486
1	1	5	0	13329.6	8.5	4666.4	n.m.	n.m.	n.m.	n.m.	n.m.	n.m.
1	1	5	1	13734.8	2506.4	2368.0	n.m.	n.m.	n.m.	n.m.	n.m.	n.m.
1	1	5	2	9351.4	1252.5	1358.3	n.m.	n.m.	n.m.	n.m.	n.m.	n.m.
1	1	5	3	7421.7	325.2	617.9	n.m.	n.m.	n.m.	n.m.	n.m.	n.m.
1	1	5	4	5617.1	70.5	252.5	0.0465	0.0201	0.0069	0.0190	0.0139	0.0044
1	1	5	5	4056.3	37.9	182.4	0.0289	0.0146	0.0057	0.0374	0.0125	0.0047
1	1	5	6	2937.5	27.6	140.2	0.0248	0.0141	0.0052	0.0531	0.0129	0.0054
1	1	5	7	2029.0	21.6	96.9	-0.0061	0.0157	0.0066	0.0646	0.0149	0.0048
1	1	5	8	1475.2	18.4	69.8	-0.0415	0.0185	0.0055	0.0931	0.0180	0.0083
1	1	5	9	975.6	14.8	46.3	-0.0485	0.0225	0.0077	0.0861	0.0215	0.0095
1	1	5	10	631.9	11.9	31.0	-0.0150	0.0283	0.0101	0.1335	0.0267	0.0133
1	1	5	11	386.8	9.3	17.1	-0.0157	0.0357	0.0078	0.1245	0.0335	0.0108
1	1	5	12	232.7	7.4	12.4	0.0306	0.0473	0.0208	0.0984	0.0454	0.0114
1	1	5	13	128.4	5.6	6.9	0.1454	0.0643	0.0233	0.2259	0.0622	0.0253
1	1	6	0	6639.3	1269.6	7977.4	n.m.	n.m.	n.m.	n.m.	n.m.	n.m.
1	1	6	1	8687.0	2669.1	1932.6	n.m.	n.m.	n.m.	n.m.	n.m.	n.m.
1	1	6	2	5544.9	62.8	346.3	n.m.	n.m.	n.m.	n.m.	n.m.	n.m.
1	1	6	3	4718.8	854.8	599.8	n.m.	n.m.	n.m.	n.m.	n.m.	n.m.
1	1	6	4	4395.1	175.9	259.2	n.m.	n.m.	n.m.	n.m.	n.m.	n.m.
1	1	6	5	3435.1	92.4	182.8	n.m.	n.m.	n.m.	n.m.	n.m.	n.m.
1	1	6	6	2451.2	35.5	117.0	0.0609	0.0229	0.0058	0.0605	0.0180	0.0069
1	1	6	7	1765.3	23.8	82.1	-0.0172	0.0208	0.0050	0.0388	0.0185	0.0076
1	1	6	8	1306.8	19.0	60.4	-0.0319	0.0219	0.0066	0.0665	0.0201	0.0121
1	1	6	9	929.2	15.7	46.5	-0.0017	0.0251	0.0135	0.0824	0.0236	0.0080
1	1	6	10	678.4	13.6	31.2	-0.0747	0.0302	0.0109	0.1300	0.0282	0.0126
1	1	6	11	466.4	11.3	24.6	0.0210	0.0371	0.0133	0.1930	0.0321	0.0117
1	1	6	12	299.7	8.8	15.0	-0.0758	0.0435	0.0204	0.0890	0.0425	0.0170
1	1	6	13	192.7	7.2	10.1	0.0341	0.0564	0.0225	0.1752	0.0528	0.0190
1	1	6	14	123.5	6.2	6.3	0.1004	0.0765	0.0316	0.2175	0.0711	0.0343
1	1	6	15	77.2	5.0	3.2	-0.0322	0.0948	0.0472	0.0817	0.0979	0.0536
1	1	6	16	74.7	9.8	8.7	n.m.	n.m.	n.m.	n.m.	n.m.	n.m.
1	1	7	0	7044.5	6.3	3202.3	n.m.	n.m.	n.m.	n.m.	n.m.	n.m.
1	1	7	1	6826.1	715.4	3282.2	n.m.	n.m.	n.m.	n.m.	n.m.	n.m.
1	1	7	2	3846.6	62.6	181.8	n.m.	n.m.	n.m.	n.m.	n.m.	n.m.
1	1	7	3	3527.8	815.1	421.6	n.m.	n.m.	n.m.	n.m.	n.m.	n.m.

Continued on next page

Table B.2 – *Continued from previous page*

x	Q^2	z	$P_{h\perp}^2$	A_0	ΔA_0	δA_0	$A_{UU}^{\cos\phi_h}$	$\Delta A_{UU}^{\cos\phi_h}$	$\delta A_{UU}^{\cos\phi_h}$	$A_{UU}^{\cos 2\phi_h}$	$\Delta A_{UU}^{\cos 2\phi_h}$	$\delta A_{UU}^{\cos 2\phi_h}$
1	1	7	4	2800.5	639.2	448.4	n.m.	n.m.	n.m.	n.m.	n.m.	n.m.
1	1	7	5	2618.8	177.1	216.1	n.m.	n.m.	n.m.	n.m.	n.m.	n.m.
1	1	7	6	1872.1	74.8	109.5	n.m.	n.m.	n.m.	n.m.	n.m.	n.m.
1	1	7	7	1419.0	31.5	62.6	0.0859	0.0344	0.0100	0.0548	0.0255	0.0083
1	1	7	8	1071.7	22.2	50.5	0.0717	0.0322	0.0131	0.0755	0.0261	0.0088
1	1	7	9	783.4	16.5	36.4	0.0402	0.0322	0.0144	0.1016	0.0281	0.0093
1	1	7	10	567.6	13.2	27.2	0.0115	0.0350	0.0101	0.0636	0.0320	0.0127
1	1	7	11	413.0	10.9	21.1	-0.0337	0.0396	0.0182	0.0830	0.0369	0.0137
1	1	7	12	290.1	9.1	15.0	0.0470	0.0469	0.0117	0.1115	0.0418	0.0127
1	1	7	13	208.6	7.7	10.2	-0.0956	0.0548	0.0251	0.0813	0.0534	0.0177
1	1	7	14	133.4	6.3	6.6	-0.2236	0.0676	0.0229	0.0687	0.0684	0.0236
1	1	7	15	88.3	5.3	4.2	0.0387	0.0923	0.0213	0.3201	0.0751	0.0347
1	1	7	16	48.6	4.3	3.0	n.m.	n.m.	n.m.	n.m.	n.m.	n.m.
1	1	8	0	5504.6	1945.9	2129.3	n.m.	n.m.	n.m.	n.m.	n.m.	n.m.
1	1	8	1	3390.0	630.1	1016.6	n.m.	n.m.	n.m.	n.m.	n.m.	n.m.
1	1	8	2	2734.6	64.7	1141.9	n.m.	n.m.	n.m.	n.m.	n.m.	n.m.
1	1	8	3	2489.5	744.5	587.1	n.m.	n.m.	n.m.	n.m.	n.m.	n.m.
1	1	8	4	2031.1	578.6	266.7	n.m.	n.m.	n.m.	n.m.	n.m.	n.m.
1	1	8	5	1403.7	514.6	300.5	n.m.	n.m.	n.m.	n.m.	n.m.	n.m.
1	1	8	6	1465.8	28.9	145.1	n.m.	n.m.	n.m.	n.m.	n.m.	n.m.
1	1	8	7	1139.7	66.0	73.8	n.m.	n.m.	n.m.	n.m.	n.m.	n.m.
1	1	8	8	793.3	39.5	94.7	n.m.	n.m.	n.m.	n.m.	n.m.	n.m.
1	1	8	9	641.9	20.4	33.0	0.1545	0.0474	0.0120	0.1107	0.0358	0.0078
1	1	8	10	467.1	14.8	18.2	0.1354	0.0471	0.0316	0.0571	0.0382	0.0193
1	1	8	11	345.2	11.2	18.7	0.1138	0.0488	0.0149	0.0723	0.0450	0.0178
1	1	8	12	258.4	9.5	15.1	0.0675	0.0557	0.0189	0.1484	0.0495	0.0196
1	1	8	13	174.6	7.2	9.4	0.0164	0.0635	0.0268	0.1858	0.0537	0.0260
1	1	8	14	124.8	6.1	7.9	-0.0352	0.0720	0.0553	0.0558	0.0700	0.0303
1	1	8	15	85.5	5.3	6.1	-0.0449	0.0935	0.0550	0.1109	0.0802	0.0304
1	1	8	16	54.2	4.5	3.4	n.m.	n.m.	n.m.	n.m.	n.m.	n.m.
1	1	8	17	55.0	8.8	3.8	n.m.	n.m.	n.m.	n.m.	n.m.	n.m.
1	1	9	0	5608.9	13886.4	3384.7	n.m.	n.m.	n.m.	n.m.	n.m.	n.m.
1	1	9	1	2611.8	539.1	1278.2	n.m.	n.m.	n.m.	n.m.	n.m.	n.m.
1	1	9	2	2092.9	100.4	133.4	n.m.	n.m.	n.m.	n.m.	n.m.	n.m.
1	1	9	3	2704.4	118.4	721.6	n.m.	n.m.	n.m.	n.m.	n.m.	n.m.
1	1	9	4	1996.5	80.6	692.6	n.m.	n.m.	n.m.	n.m.	n.m.	n.m.
1	1	9	5	1049.5	451.4	139.7	n.m.	n.m.	n.m.	n.m.	n.m.	n.m.
1	1	9	6	757.2	17.8	73.8	n.m.	n.m.	n.m.	n.m.	n.m.	n.m.
1	1	9	7	861.5	19.3	59.0	n.m.	n.m.	n.m.	n.m.	n.m.	n.m.

Continued on next page

Table B.2 – *Continued from previous page*

x	Q^2	z	$P_{h\perp}^2$	A_0	ΔA_0	δA_0	$A_{UU}^{\cos\phi_h}$	$\Delta A_{UU}^{\cos\phi_h}$	$\delta A_{UU}^{\cos\phi_h}$	$A_{UU}^{\cos 2\phi_h}$	$\Delta A_{UU}^{\cos 2\phi_h}$	$\delta A_{UU}^{\cos 2\phi_h}$
1	1	9	8	593.7	81.0	46.5	n.m.	n.m.	n.m.	n.m.	n.m.	n.m.
1	1	9	9	474.2	32.4	42.3	n.m.	n.m.	n.m.	n.m.	n.m.	n.m.
1	1	9	10	319.1	23.8	25.5	n.m.	n.m.	n.m.	n.m.	n.m.	n.m.
1	1	9	11	262.2	11.8	13.7	0.0892	0.0694	0.0260	0.1006	0.0539	0.0171
1	1	9	12	203.3	10.4	10.9	0.0545	0.0789	0.0226	0.1267	0.0648	0.0182
1	1	9	13	140.2	7.4	8.2	0.0440	0.0802	0.0271	0.1151	0.0695	0.0327
1	1	9	14	103.8	5.8	5.4	-0.0390	0.0852	0.0542	-0.0335	0.0807	0.0198
1	1	9	15	70.5	5.2	3.5	n.m.	n.m.	n.m.	n.m.	n.m.	n.m.
1	1	9	16	58.1	5.7	4.1	n.m.	n.m.	n.m.	n.m.	n.m.	n.m.
1	1	10	0	1571.0	149.8	1190.6	n.m.	n.m.	n.m.	n.m.	n.m.	n.m.
1	1	10	1	2872.0	5.9	766.6	n.m.	n.m.	n.m.	n.m.	n.m.	n.m.
1	1	10	2	2617.6	137.1	123.8	n.m.	n.m.	n.m.	n.m.	n.m.	n.m.
1	1	10	3	1291.6	67.3	96.2	n.m.	n.m.	n.m.	n.m.	n.m.	n.m.
1	1	10	4	1111.5	57.9	675.3	n.m.	n.m.	n.m.	n.m.	n.m.	n.m.
1	1	10	5	746.5	19.9	37.1	n.m.	n.m.	n.m.	n.m.	n.m.	n.m.
1	1	10	6	641.1	329.2	135.8	n.m.	n.m.	n.m.	n.m.	n.m.	n.m.
1	1	10	7	473.1	36.6	166.6	n.m.	n.m.	n.m.	n.m.	n.m.	n.m.
1	1	10	8	348.6	11.6	38.2	n.m.	n.m.	n.m.	n.m.	n.m.	n.m.
1	1	10	9	267.1	9.9	13.6	n.m.	n.m.	n.m.	n.m.	n.m.	n.m.
1	1	10	10	308.0	11.7	15.2	n.m.	n.m.	n.m.	n.m.	n.m.	n.m.
1	1	10	11	165.4	22.6	20.5	n.m.	n.m.	n.m.	n.m.	n.m.	n.m.
1	1	10	12	150.8	10.2	11.2	n.m.	n.m.	n.m.	n.m.	n.m.	n.m.
1	1	10	13	122.0	8.8	9.3	n.m.	n.m.	n.m.	n.m.	n.m.	n.m.
1	1	10	14	100.6	8.8	11.3	n.m.	n.m.	n.m.	n.m.	n.m.	n.m.
1	1	10	15	71.6	7.7	5.7	n.m.	n.m.	n.m.	n.m.	n.m.	n.m.
1	1	11	0	1481.8	90.6	877.8	n.m.	n.m.	n.m.	n.m.	n.m.	n.m.
1	1	11	1	2102.1	4.4	869.5	n.m.	n.m.	n.m.	n.m.	n.m.	n.m.
1	1	11	2	1981.3	121.7	117.5	n.m.	n.m.	n.m.	n.m.	n.m.	n.m.
1	1	11	3	1501.0	98.9	892.2	n.m.	n.m.	n.m.	n.m.	n.m.	n.m.
1	1	11	4	1304.1	83.9	509.6	n.m.	n.m.	n.m.	n.m.	n.m.	n.m.
1	1	11	5	594.9	386.6	144.4	n.m.	n.m.	n.m.	n.m.	n.m.	n.m.
1	1	11	6	453.2	293.7	194.1	n.m.	n.m.	n.m.	n.m.	n.m.	n.m.
1	1	11	7	508.3	18.3	49.4	n.m.	n.m.	n.m.	n.m.	n.m.	n.m.
1	1	11	8	354.5	183.5	89.8	n.m.	n.m.	n.m.	n.m.	n.m.	n.m.
1	1	11	9	194.4	8.6	19.2	n.m.	n.m.	n.m.	n.m.	n.m.	n.m.
1	1	11	10	167.1	8.1	9.3	n.m.	n.m.	n.m.	n.m.	n.m.	n.m.
1	1	11	11	178.6	135.2	46.2	n.m.	n.m.	n.m.	n.m.	n.m.	n.m.
1	1	11	12	159.7	38.2	13.4	n.m.	n.m.	n.m.	n.m.	n.m.	n.m.
1	1	11	13	89.0	6.0	23.5	n.m.	n.m.	n.m.	n.m.	n.m.	n.m.

Continued on next page

Table B.2 – *Continued from previous page*

x	Q^2	z	$P_{h\perp}^2$	A_0	ΔA_0	δA_0	$A_{UU}^{\cos\phi_h}$	$\Delta A_{UU}^{\cos\phi_h}$	$\delta A_{UU}^{\cos\phi_h}$	$A_{UU}^{\cos 2\phi_h}$	$\Delta A_{UU}^{\cos 2\phi_h}$	$\delta A_{UU}^{\cos 2\phi_h}$
1	1	11	14	59.2	5.5	5.3	n.m.	n.m.	n.m.	n.m.	n.m.	n.m.
1	1	12	0	1137.6	382.9	1195.6	n.m.	n.m.	n.m.	n.m.	n.m.	n.m.
1	1	12	1	2506.5	444.7	906.0	n.m.	n.m.	n.m.	n.m.	n.m.	n.m.
1	1	12	2	1750.8	115.5	104.8	n.m.	n.m.	n.m.	n.m.	n.m.	n.m.
1	1	12	3	1133.2	80.7	311.2	n.m.	n.m.	n.m.	n.m.	n.m.	n.m.
1	1	12	4	531.1	40.3	238.0	n.m.	n.m.	n.m.	n.m.	n.m.	n.m.
1	1	12	5	631.4	26.7	133.2	n.m.	n.m.	n.m.	n.m.	n.m.	n.m.
1	1	12	6	330.4	13.3	21.2	n.m.	n.m.	n.m.	n.m.	n.m.	n.m.
1	1	12	7	284.4	12.1	115.7	n.m.	n.m.	n.m.	n.m.	n.m.	n.m.
1	1	12	8	322.4	14.6	15.7	n.m.	n.m.	n.m.	n.m.	n.m.	n.m.
1	1	12	9	241.6	12.6	26.7	n.m.	n.m.	n.m.	n.m.	n.m.	n.m.
1	1	12	10	147.3	8.4	9.9	n.m.	n.m.	n.m.	n.m.	n.m.	n.m.
1	1	12	11	111.9	7.9	55.5	n.m.	n.m.	n.m.	n.m.	n.m.	n.m.
1	1	12	12	103.4	7.6	19.1	n.m.	n.m.	n.m.	n.m.	n.m.	n.m.
1	1	12	13	101.1	52.0	31.2	n.m.	n.m.	n.m.	n.m.	n.m.	n.m.
1	1	13	0	905.0	291.7	830.6	n.m.	n.m.	n.m.	n.m.	n.m.	n.m.
1	1	13	1	993.2	594.8	432.8	n.m.	n.m.	n.m.	n.m.	n.m.	n.m.
1	1	13	2	1242.9	88.6	228.7	n.m.	n.m.	n.m.	n.m.	n.m.	n.m.
1	1	13	3	680.6	49.1	47.1	n.m.	n.m.	n.m.	n.m.	n.m.	n.m.
1	1	13	4	579.7	1639.4	440.0	n.m.	n.m.	n.m.	n.m.	n.m.	n.m.
1	1	13	5	360.1	19.6	177.5	n.m.	n.m.	n.m.	n.m.	n.m.	n.m.
1	1	13	6	394.7	276.0	120.7	n.m.	n.m.	n.m.	n.m.	n.m.	n.m.
1	1	13	7	253.2	294.2	121.1	n.m.	n.m.	n.m.	n.m.	n.m.	n.m.
1	1	13	8	274.5	16.9	29.8	n.m.	n.m.	n.m.	n.m.	n.m.	n.m.
1	1	13	9	149.4	10.9	95.2	n.m.	n.m.	n.m.	n.m.	n.m.	n.m.
1	1	13	10	137.6	11.9	51.4	n.m.	n.m.	n.m.	n.m.	n.m.	n.m.
1	1	14	0	810.0	102.8	637.3	n.m.	n.m.	n.m.	n.m.	n.m.	n.m.
1	1	14	1	778.2	382.8	965.8	n.m.	n.m.	n.m.	n.m.	n.m.	n.m.
1	1	14	2	1112.0	93.4	312.6	n.m.	n.m.	n.m.	n.m.	n.m.	n.m.
1	1	14	3	749.7	76.9	78.5	n.m.	n.m.	n.m.	n.m.	n.m.	n.m.
1	1	14	4	597.3	78.4	88.2	n.m.	n.m.	n.m.	n.m.	n.m.	n.m.
1	1	14	5	380.0	770.3	325.1	n.m.	n.m.	n.m.	n.m.	n.m.	n.m.
1	1	14	6	260.3	24.1	279.3	n.m.	n.m.	n.m.	n.m.	n.m.	n.m.
1	1	14	7	178.9	25.8	173.4	n.m.	n.m.	n.m.	n.m.	n.m.	n.m.
1	1	15	1	945.7	5273.8	1000.3	n.m.	n.m.	n.m.	n.m.	n.m.	n.m.
1	1	15	2	481.7	157.2	642.8	n.m.	n.m.	n.m.	n.m.	n.m.	n.m.
1	1	15	3	1431.9	2746.1	1260.2	n.m.	n.m.	n.m.	n.m.	n.m.	n.m.
2	0	1	0	77232.2	530.7	4019.4	n.m.	n.m.	n.m.	n.m.	n.m.	n.m.
2	0	2	0	60953.1	5769.2	10623.8	n.m.	n.m.	n.m.	n.m.	n.m.	n.m.

Continued on next page

Table B.2 – *Continued from previous page*

x	Q^2	z	$P_{h\perp}^2$	A_0	ΔA_0	δA_0	$A_{UU}^{\cos\phi_h}$	$\Delta A_{UU}^{\cos\phi_h}$	$\delta A_{UU}^{\cos\phi_h}$	$A_{UU}^{\cos 2\phi_h}$	$\Delta A_{UU}^{\cos 2\phi_h}$	$\delta A_{UU}^{\cos 2\phi_h}$
2	0	2	1	25689.5	101.0	1278.2	n.m.	n.m.	n.m.	n.m.	n.m.	n.m.
2	0	3	0	27908.8	402.1	3795.8	n.m.	n.m.	n.m.	n.m.	n.m.	n.m.
2	0	3	1	19120.4	284.5	969.5	n.m.	n.m.	n.m.	n.m.	n.m.	n.m.
2	0	3	2	10580.6	61.8	514.4	-0.0292	0.0090	0.0040	0.0388	0.0081	0.0027
2	0	3	3	7188.8	49.0	353.9	-0.0889	0.0101	0.0050	0.0686	0.0096	0.0041
2	0	3	4	4825.0	52.4	239.4	-0.1313	0.0160	0.0111	0.0992	0.0153	0.0089
2	0	4	0	18518.9	15604.6	5534.4	n.m.	n.m.	n.m.	n.m.	n.m.	n.m.
2	0	4	1	14542.5	560.4	833.8	n.m.	n.m.	n.m.	n.m.	n.m.	n.m.
2	0	4	2	9432.1	173.0	490.9	n.m.	n.m.	n.m.	n.m.	n.m.	n.m.
2	0	4	3	5620.8	52.5	260.3	0.0452	0.0147	0.0089	0.0809	0.0124	0.0059
2	0	4	4	3909.3	36.5	200.7	-0.0434	0.0142	0.0073	0.1007	0.0131	0.0051
2	0	4	5	3602.2	44.8	179.9	-0.0838	0.0187	0.0102	0.1429	0.0172	0.0078
2	0	4	6	2357.0	46.8	113.8	-0.1049	0.0299	0.0094	0.1760	0.0275	0.0133
2	0	5	0	16676.6	394.2	1072.5	n.m.	n.m.	n.m.	n.m.	n.m.	n.m.
2	0	5	1	9971.8	1556.8	2043.3	n.m.	n.m.	n.m.	n.m.	n.m.	n.m.
2	0	5	2	6701.1	332.8	499.2	n.m.	n.m.	n.m.	n.m.	n.m.	n.m.
2	0	5	3	5166.4	155.1	288.9	n.m.	n.m.	n.m.	n.m.	n.m.	n.m.
2	0	5	4	3402.1	46.8	168.8	0.0505	0.0218	0.0215	0.0891	0.0173	0.0112
2	0	5	5	2382.2	31.6	115.1	-0.0240	0.0204	0.0107	0.1269	0.0183	0.0064
2	0	5	6	2230.4	37.5	105.8	-0.0235	0.0255	0.0101	0.1202	0.0238	0.0087
2	0	5	7	1973.8	48.8	96.5	-0.0349	0.0379	0.0156	0.2028	0.0328	0.0119
2	0	6	0	10566.5	275.4	2744.1	n.m.	n.m.	n.m.	n.m.	n.m.	n.m.
2	0	6	1	8118.7	813.3	613.4	n.m.	n.m.	n.m.	n.m.	n.m.	n.m.
2	0	6	2	5109.7	313.4	435.9	n.m.	n.m.	n.m.	n.m.	n.m.	n.m.
2	0	6	3	4156.9	252.5	392.1	n.m.	n.m.	n.m.	n.m.	n.m.	n.m.
2	0	6	4	3157.4	128.7	171.0	n.m.	n.m.	n.m.	n.m.	n.m.	n.m.
2	0	6	5	2268.6	75.5	124.5	n.m.	n.m.	n.m.	n.m.	n.m.	n.m.
2	0	6	6	1643.7	33.9	85.5	-0.0243	0.0332	0.0231	0.1485	0.0268	0.0111
2	0	6	7	1577.1	39.7	86.2	-0.0279	0.0391	0.0181	0.1619	0.0338	0.0108
2	0	6	8	1365.7	48.9	74.0	-0.0303	0.0557	0.0182	0.2431	0.0463	0.0141
2	0	6	9	770.8	43.3	55.8	-0.1483	0.0894	0.0419	0.2318	0.0817	0.0296
2	0	7	0	6864.8	194.4	2108.0	n.m.	n.m.	n.m.	n.m.	n.m.	n.m.
2	0	7	1	5633.4	110.8	421.4	n.m.	n.m.	n.m.	n.m.	n.m.	n.m.
2	0	7	2	3749.6	502.1	376.9	n.m.	n.m.	n.m.	n.m.	n.m.	n.m.
2	0	7	3	3274.4	224.9	436.8	n.m.	n.m.	n.m.	n.m.	n.m.	n.m.
2	0	7	4	2081.4	203.6	190.3	n.m.	n.m.	n.m.	n.m.	n.m.	n.m.
2	0	7	5	1777.7	188.5	255.3	n.m.	n.m.	n.m.	n.m.	n.m.	n.m.
2	0	7	6	1418.9	88.2	76.9	n.m.	n.m.	n.m.	n.m.	n.m.	n.m.
2	0	7	7	1147.6	66.3	69.5	n.m.	n.m.	n.m.	n.m.	n.m.	n.m.

Continued on next page

Table B.2 – *Continued from previous page*

x	Q^2	z	$P_{h\perp}^2$	A_0	ΔA_0	δA_0	$A_{UU}^{\cos\phi_h}$	$\Delta A_{UU}^{\cos\phi_h}$	$\delta A_{UU}^{\cos\phi_h}$	$A_{UU}^{\cos 2\phi_h}$	$\Delta A_{UU}^{\cos 2\phi_h}$	$\delta A_{UU}^{\cos 2\phi_h}$
2	0	7	8	1047.7	43.7	43.5	0.0836	0.0657	0.0264	0.1285	0.0545	0.0223
2	0	7	9	771.5	45.8	35.9	0.1355	0.0895	0.0262	0.2418	0.0689	0.0358
2	0	7	10	469.9	39.9	34.1	n.m.	n.m.	n.m.	n.m.	n.m.	n.m.
2	0	8	0	4823.2	142.9	1387.1	n.m.	n.m.	n.m.	n.m.	n.m.	n.m.
2	0	8	1	3925.8	99.2	199.2	n.m.	n.m.	n.m.	n.m.	n.m.	n.m.
2	0	8	2	3196.7	56.0	153.0	n.m.	n.m.	n.m.	n.m.	n.m.	n.m.
2	0	8	3	2471.3	40.3	360.4	n.m.	n.m.	n.m.	n.m.	n.m.	n.m.
2	0	8	4	1774.2	180.0	146.2	n.m.	n.m.	n.m.	n.m.	n.m.	n.m.
2	0	8	5	1627.5	34.4	90.1	n.m.	n.m.	n.m.	n.m.	n.m.	n.m.
2	0	8	6	1162.0	75.5	61.6	n.m.	n.m.	n.m.	n.m.	n.m.	n.m.
2	0	8	7	749.8	57.3	116.9	n.m.	n.m.	n.m.	n.m.	n.m.	n.m.
2	0	8	8	721.3	69.8	55.0	n.m.	n.m.	n.m.	n.m.	n.m.	n.m.
2	0	8	9	535.9	87.1	61.4	n.m.	n.m.	n.m.	n.m.	n.m.	n.m.
2	0	8	10	356.9	70.1	43.4	n.m.	n.m.	n.m.	n.m.	n.m.	n.m.
2	0	9	0	3241.7	2199.0	1513.1	n.m.	n.m.	n.m.	n.m.	n.m.	n.m.
2	0	9	1	2824.3	80.2	1347.8	n.m.	n.m.	n.m.	n.m.	n.m.	n.m.
2	0	9	2	1630.7	433.4	162.4	n.m.	n.m.	n.m.	n.m.	n.m.	n.m.
2	0	9	3	1289.8	25.1	68.6	n.m.	n.m.	n.m.	n.m.	n.m.	n.m.
2	0	9	4	1389.5	150.2	176.9	n.m.	n.m.	n.m.	n.m.	n.m.	n.m.
2	0	9	5	846.1	153.9	100.9	n.m.	n.m.	n.m.	n.m.	n.m.	n.m.
2	0	9	6	959.3	28.1	70.6	n.m.	n.m.	n.m.	n.m.	n.m.	n.m.
2	0	9	7	653.8	140.9	132.9	n.m.	n.m.	n.m.	n.m.	n.m.	n.m.
2	0	9	8	586.1	32.5	137.4	n.m.	n.m.	n.m.	n.m.	n.m.	n.m.
2	0	9	9	282.7	22.2	34.2	n.m.	n.m.	n.m.	n.m.	n.m.	n.m.
2	0	10	0	2619.6	86.2	335.9	n.m.	n.m.	n.m.	n.m.	n.m.	n.m.
2	0	10	1	2222.3	67.1	98.8	n.m.	n.m.	n.m.	n.m.	n.m.	n.m.
2	0	10	2	1170.4	32.8	113.2	n.m.	n.m.	n.m.	n.m.	n.m.	n.m.
2	0	10	3	1202.0	169.8	122.9	n.m.	n.m.	n.m.	n.m.	n.m.	n.m.
2	0	10	4	1027.0	136.3	71.9	n.m.	n.m.	n.m.	n.m.	n.m.	n.m.
2	0	10	5	600.7	17.1	65.0	n.m.	n.m.	n.m.	n.m.	n.m.	n.m.
2	0	10	6	647.1	113.9	91.1	n.m.	n.m.	n.m.	n.m.	n.m.	n.m.
2	0	10	7	347.2	17.4	137.2	n.m.	n.m.	n.m.	n.m.	n.m.	n.m.
2	0	10	8	414.8	30.5	23.0	n.m.	n.m.	n.m.	n.m.	n.m.	n.m.
2	0	11	0	1459.8	47.9	175.8	n.m.	n.m.	n.m.	n.m.	n.m.	n.m.
2	0	11	1	1206.4	1196.2	327.3	n.m.	n.m.	n.m.	n.m.	n.m.	n.m.
2	0	11	2	1193.4	417.1	385.4	n.m.	n.m.	n.m.	n.m.	n.m.	n.m.
2	0	11	3	882.9	154.6	161.3	n.m.	n.m.	n.m.	n.m.	n.m.	n.m.
2	0	11	4	792.4	24.5	121.7	n.m.	n.m.	n.m.	n.m.	n.m.	n.m.
2	0	11	5	466.4	117.9	77.4	n.m.	n.m.	n.m.	n.m.	n.m.	n.m.

Continued on next page

Table B.2 – *Continued from previous page*

x	Q^2	z	$P_{h\perp}^2$	A_0	ΔA_0	δA_0	$A_{UU}^{\cos\phi_h}$	$\Delta A_{UU}^{\cos\phi_h}$	$\delta A_{UU}^{\cos\phi_h}$	$A_{UU}^{\cos 2\phi_h}$	$\Delta A_{UU}^{\cos 2\phi_h}$	$\delta A_{UU}^{\cos 2\phi_h}$
2	0	11	6	465.6	24.2	85.0	n.m.	n.m.	n.m.	n.m.	n.m.	n.m.
2	0	11	7	265.7	18.5	70.9	n.m.	n.m.	n.m.	n.m.	n.m.	n.m.
2	0	12	0	1571.5	768.1	495.7	n.m.	n.m.	n.m.	n.m.	n.m.	n.m.
2	0	12	1	1010.1	39.5	362.1	n.m.	n.m.	n.m.	n.m.	n.m.	n.m.
2	0	12	2	1186.7	51.0	53.2	n.m.	n.m.	n.m.	n.m.	n.m.	n.m.
2	0	12	3	600.2	31.1	37.4	n.m.	n.m.	n.m.	n.m.	n.m.	n.m.
2	0	12	4	468.5	28.9	305.1	n.m.	n.m.	n.m.	n.m.	n.m.	n.m.
2	0	12	5	475.0	182.6	119.8	n.m.	n.m.	n.m.	n.m.	n.m.	n.m.
2	0	12	6	507.0	49.0	117.7	n.m.	n.m.	n.m.	n.m.	n.m.	n.m.
2	0	13	0	1346.7	31.9	293.2	n.m.	n.m.	n.m.	n.m.	n.m.	n.m.
2	0	13	1	982.9	45.1	414.1	n.m.	n.m.	n.m.	n.m.	n.m.	n.m.
2	0	13	2	717.4	51.3	59.6	n.m.	n.m.	n.m.	n.m.	n.m.	n.m.
2	0	13	3	845.2	88.5	330.2	n.m.	n.m.	n.m.	n.m.	n.m.	n.m.
2	0	13	4	770.2	161.2	260.4	n.m.	n.m.	n.m.	n.m.	n.m.	n.m.
2	0	14	0	1139.0	48.7	474.6	n.m.	n.m.	n.m.	n.m.	n.m.	n.m.
2	0	14	1	1268.4	113.0	125.4	n.m.	n.m.	n.m.	n.m.	n.m.	n.m.
2	1	1	0	66726.2	349.4	3302.3	n.m.	n.m.	n.m.	n.m.	n.m.	n.m.
2	1	2	0	40972.2	5219.1	3914.6	n.m.	n.m.	n.m.	n.m.	n.m.	n.m.
2	1	2	1	21827.2	90.8	1027.0	n.m.	n.m.	n.m.	n.m.	n.m.	n.m.
2	1	2	2	11044.2	42.3	523.7	-0.0646	0.0056	0.0016	0.0133	0.0054	0.0016
2	1	2	3	4562.2	26.4	222.2	-0.0925	0.0084	0.0034	0.0445	0.0082	0.0036
2	1	3	0	24089.3	483.8	9714.8	n.m.	n.m.	n.m.	n.m.	n.m.	n.m.
2	1	3	1	17459.2	404.0	819.3	n.m.	n.m.	n.m.	n.m.	n.m.	n.m.
2	1	3	2	10224.2	66.2	480.0	-0.0498	0.0106	0.0057	-0.0148	0.0082	0.0030
2	1	3	3	6214.6	34.2	291.4	-0.0276	0.0082	0.0035	0.0338	0.0078	0.0028
2	1	3	4	3838.3	25.9	180.4	-0.0474	0.0099	0.0050	0.0467	0.0096	0.0026
2	1	3	5	2163.7	19.9	99.4	-0.0575	0.0137	0.0028	0.0926	0.0131	0.0046
2	1	3	6	1038.0	14.2	51.4	-0.0762	0.0202	0.0055	0.0898	0.0192	0.0103
2	1	4	0	22261.7	710.2	5968.9	n.m.	n.m.	n.m.	n.m.	n.m.	n.m.
2	1	4	1	11446.4	647.1	937.4	n.m.	n.m.	n.m.	n.m.	n.m.	n.m.
2	1	4	2	8526.6	212.5	436.0	n.m.	n.m.	n.m.	n.m.	n.m.	n.m.
2	1	4	3	5600.6	60.9	259.1	-0.0008	0.0178	0.0052	0.0039	0.0129	0.0031
2	1	4	4	3710.6	30.5	170.7	-0.0094	0.0126	0.0042	0.0327	0.0113	0.0043
2	1	4	5	2580.8	23.2	120.2	-0.0068	0.0133	0.0053	0.0540	0.0127	0.0045
2	1	4	6	1783.0	19.7	84.6	-0.0152	0.0165	0.0045	0.1017	0.0156	0.0040
2	1	4	7	1110.8	16.0	48.6	-0.0317	0.0213	0.0071	0.0978	0.0207	0.0057
2	1	4	8	568.9	11.6	27.4	-0.0008	0.0305	0.0115	0.1481	0.0286	0.0087
2	1	4	9	333.5	10.1	18.6	-0.1295	0.0459	0.0148	0.2324	0.0426	0.0502
2	1	5	0	9563.2	33105.0	5703.5	n.m.	n.m.	n.m.	n.m.	n.m.	n.m.

Continued on next page

Table B.2 – *Continued from previous page*

x	Q^2	z	$P_{h\perp}^2$	A_0	ΔA_0	δA_0	$A_{UU}^{\cos\phi_h}$	$\Delta A_{UU}^{\cos\phi_h}$	$\delta A_{UU}^{\cos\phi_h}$	$A_{UU}^{\cos 2\phi_h}$	$\Delta A_{UU}^{\cos 2\phi_h}$	$\delta A_{UU}^{\cos 2\phi_h}$
2	1	5	1	9487.0	1533.8	1829.6	n.m.	n.m.	n.m.	n.m.	n.m.	n.m.
2	1	5	2	5895.6	327.8	453.6	n.m.	n.m.	n.m.	n.m.	n.m.	n.m.
2	1	5	3	4878.6	162.2	264.5	n.m.	n.m.	n.m.	n.m.	n.m.	n.m.
2	1	5	4	3471.9	62.0	153.8	0.1216	0.0276	0.0103	0.0545	0.0182	0.0081
2	1	5	5	2435.2	30.9	112.9	-0.0044	0.0201	0.0081	0.0518	0.0168	0.0044
2	1	5	6	1672.1	21.5	78.0	0.0181	0.0194	0.0055	0.0683	0.0176	0.0063
2	1	5	7	1245.4	18.2	58.1	-0.0042	0.0218	0.0090	0.0841	0.0207	0.0112
2	1	5	8	855.0	15.5	44.5	-0.0097	0.0270	0.0074	0.1171	0.0248	0.0073
2	1	5	9	528.0	12.4	27.2	-0.0057	0.0345	0.0099	0.0968	0.0333	0.0175
2	1	5	10	300.2	9.4	14.1	-0.0722	0.0462	0.0167	0.1121	0.0439	0.0144
2	1	5	11	168.5	7.6	10.0	0.0671	0.0677	0.0198	0.1781	0.0616	0.0432
2	1	6	0	8227.9	391.2	492.6	n.m.	n.m.	n.m.	n.m.	n.m.	n.m.
2	1	6	1	4533.5	84.7	234.8	n.m.	n.m.	n.m.	n.m.	n.m.	n.m.
2	1	6	2	4564.7	325.0	334.9	n.m.	n.m.	n.m.	n.m.	n.m.	n.m.
2	1	6	3	3351.5	217.6	337.5	n.m.	n.m.	n.m.	n.m.	n.m.	n.m.
2	1	6	4	2626.9	113.0	126.5	n.m.	n.m.	n.m.	n.m.	n.m.	n.m.
2	1	6	5	2059.1	70.2	145.8	n.m.	n.m.	n.m.	n.m.	n.m.	n.m.
2	1	6	6	1541.5	32.2	74.1	0.0494	0.0335	0.0121	0.0834	0.0252	0.0081
2	1	6	7	1086.1	20.9	47.5	0.0036	0.0304	0.0152	0.0590	0.0261	0.0123
2	1	6	8	763.6	15.8	36.1	-0.0497	0.0317	0.0118	0.0999	0.0282	0.0094
2	1	6	9	563.2	13.7	26.5	-0.0839	0.0366	0.0113	0.1173	0.0343	0.0096
2	1	6	10	401.0	12.3	19.1	0.0188	0.0461	0.0223	0.1601	0.0420	0.0173
2	1	6	11	241.0	9.8	12.7	0.0919	0.0611	0.0214	0.1687	0.0542	0.0254
2	1	6	12	159.1	8.7	8.9	-0.0065	0.0796	0.0353	0.0713	0.0797	0.0387
2	1	6	13	123.1	12.0	9.8	n.m.	n.m.	n.m.	n.m.	n.m.	n.m.
2	1	7	0	5509.4	280.5	310.0	n.m.	n.m.	n.m.	n.m.	n.m.	n.m.
2	1	7	1	4682.0	126.3	1017.9	n.m.	n.m.	n.m.	n.m.	n.m.	n.m.
2	1	7	2	2430.1	37.0	297.5	n.m.	n.m.	n.m.	n.m.	n.m.	n.m.
2	1	7	3	2222.7	193.4	199.5	n.m.	n.m.	n.m.	n.m.	n.m.	n.m.
2	1	7	4	1939.4	158.9	160.2	n.m.	n.m.	n.m.	n.m.	n.m.	n.m.
2	1	7	5	1401.9	136.9	126.3	n.m.	n.m.	n.m.	n.m.	n.m.	n.m.
2	1	7	6	1294.0	77.9	79.3	n.m.	n.m.	n.m.	n.m.	n.m.	n.m.
2	1	7	7	951.5	48.7	54.7	n.m.	n.m.	n.m.	n.m.	n.m.	n.m.
2	1	7	8	676.4	21.1	30.3	0.1012	0.0486	0.0117	0.0827	0.0377	0.0092
2	1	7	9	481.9	15.4	20.0	-0.0017	0.0495	0.0296	0.0605	0.0420	0.0168
2	1	7	10	375.3	13.9	14.1	0.0516	0.0571	0.0242	0.1894	0.0450	0.0200
2	1	7	11	249.6	11.2	14.8	-0.0153	0.0688	0.0250	0.1198	0.0658	0.0148
2	1	7	12	152.2	8.7	8.3	0.0719	0.0874	0.0736	0.2066	0.0720	0.0200
2	1	7	13	104.1	8.0	6.2	0.0831	0.1163	0.0944	0.0556	0.1126	0.0774

Continued on next page

Table B.2 – *Continued from previous page*

x	Q^2	z	$P_{h\perp}^2$	A_0	ΔA_0	δA_0	$A_{UU}^{\cos\phi_h}$	$\Delta A_{UU}^{\cos\phi_h}$	$\delta A_{UU}^{\cos\phi_h}$	$A_{UU}^{\cos 2\phi_h}$	$\Delta A_{UU}^{\cos 2\phi_h}$	$\delta A_{UU}^{\cos 2\phi_h}$
2	1	7	14	94.5	18.3	10.6	n.m.	n.m.	n.m.	n.m.	n.m.	n.m.
2	1	8	0	3577.9	198.7	178.7	n.m.	n.m.	n.m.	n.m.	n.m.	n.m.
2	1	8	1	3067.8	1754.2	1279.1	n.m.	n.m.	n.m.	n.m.	n.m.	n.m.
2	1	8	2	1712.3	35.1	391.5	n.m.	n.m.	n.m.	n.m.	n.m.	n.m.
2	1	8	3	1692.4	191.0	275.0	n.m.	n.m.	n.m.	n.m.	n.m.	n.m.
2	1	8	4	1440.6	143.9	229.3	n.m.	n.m.	n.m.	n.m.	n.m.	n.m.
2	1	8	5	1086.7	118.9	100.7	n.m.	n.m.	n.m.	n.m.	n.m.	n.m.
2	1	8	6	842.0	64.6	47.5	n.m.	n.m.	n.m.	n.m.	n.m.	n.m.
2	1	8	7	737.4	52.7	44.5	n.m.	n.m.	n.m.	n.m.	n.m.	n.m.
2	1	8	8	576.1	40.1	46.0	n.m.	n.m.	n.m.	n.m.	n.m.	n.m.
2	1	8	9	369.8	26.1	29.5	n.m.	n.m.	n.m.	n.m.	n.m.	n.m.
2	1	8	10	279.1	23.6	28.9	n.m.	n.m.	n.m.	n.m.	n.m.	n.m.
2	1	8	11	214.5	12.4	9.8	-0.0395	0.0934	0.0184	0.1429	0.0761	0.0212
2	1	8	12	137.7	9.5	7.5	n.m.	n.m.	n.m.	n.m.	n.m.	n.m.
2	1	8	13	96.9	8.2	5.2	n.m.	n.m.	n.m.	n.m.	n.m.	n.m.
2	1	9	0	2646.6	152.7	152.8	n.m.	n.m.	n.m.	n.m.	n.m.	n.m.
2	1	9	1	1521.4	60.1	634.4	n.m.	n.m.	n.m.	n.m.	n.m.	n.m.
2	1	9	2	1904.3	53.0	467.5	n.m.	n.m.	n.m.	n.m.	n.m.	n.m.
2	1	9	3	1341.9	178.4	119.0	n.m.	n.m.	n.m.	n.m.	n.m.	n.m.
2	1	9	4	944.3	118.9	156.9	n.m.	n.m.	n.m.	n.m.	n.m.	n.m.
2	1	9	5	743.8	98.9	111.6	n.m.	n.m.	n.m.	n.m.	n.m.	n.m.
2	1	9	6	709.8	17.7	116.7	n.m.	n.m.	n.m.	n.m.	n.m.	n.m.
2	1	9	7	404.2	79.2	68.2	n.m.	n.m.	n.m.	n.m.	n.m.	n.m.
2	1	9	8	394.6	66.5	26.7	n.m.	n.m.	n.m.	n.m.	n.m.	n.m.
2	1	9	9	327.8	13.7	59.5	n.m.	n.m.	n.m.	n.m.	n.m.	n.m.
2	1	9	10	250.5	14.2	20.0	n.m.	n.m.	n.m.	n.m.	n.m.	n.m.
2	1	9	11	158.2	14.9	6.8	n.m.	n.m.	n.m.	n.m.	n.m.	n.m.
2	1	9	12	129.7	17.0	8.2	n.m.	n.m.	n.m.	n.m.	n.m.	n.m.
2	1	9	13	73.3	12.1	5.0	n.m.	n.m.	n.m.	n.m.	n.m.	n.m.
2	1	10	0	2018.8	114.3	160.7	n.m.	n.m.	n.m.	n.m.	n.m.	n.m.
2	1	10	1	1148.1	1427.2	608.8	n.m.	n.m.	n.m.	n.m.	n.m.	n.m.
2	1	10	2	1394.2	52.4	144.2	n.m.	n.m.	n.m.	n.m.	n.m.	n.m.
2	1	10	3	857.3	162.1	137.5	n.m.	n.m.	n.m.	n.m.	n.m.	n.m.
2	1	10	4	726.5	115.9	141.8	n.m.	n.m.	n.m.	n.m.	n.m.	n.m.
2	1	10	5	582.3	90.2	41.0	n.m.	n.m.	n.m.	n.m.	n.m.	n.m.
2	1	10	6	456.0	72.9	54.8	n.m.	n.m.	n.m.	n.m.	n.m.	n.m.
2	1	10	7	321.7	58.1	58.5	n.m.	n.m.	n.m.	n.m.	n.m.	n.m.
2	1	10	8	232.0	67.0	22.3	n.m.	n.m.	n.m.	n.m.	n.m.	n.m.
2	1	10	9	229.0	49.2	18.3	n.m.	n.m.	n.m.	n.m.	n.m.	n.m.

Continued on next page

Table B.2 – *Continued from previous page*

x	Q^2	z	$P_{h\perp}^2$	A_0	ΔA_0	δA_0	$A_{UU}^{\cos\phi_h}$	$\Delta A_{UU}^{\cos\phi_h}$	$\delta A_{UU}^{\cos\phi_h}$	$A_{UU}^{\cos 2\phi_h}$	$\Delta A_{UU}^{\cos 2\phi_h}$	$\delta A_{UU}^{\cos 2\phi_h}$
2	1	10	10	184.8	10.4	9.3	n.m.	n.m.	n.m.	n.m.	n.m.	n.m.
2	1	10	11	127.4	34.5	20.5	n.m.	n.m.	n.m.	n.m.	n.m.	n.m.
2	1	10	12	86.2	9.2	7.0	n.m.	n.m.	n.m.	n.m.	n.m.	n.m.
2	1	11	0	1275.1	69.6	625.9	n.m.	n.m.	n.m.	n.m.	n.m.	n.m.
2	1	11	1	1065.1	2243.9	562.4	n.m.	n.m.	n.m.	n.m.	n.m.	n.m.
2	1	11	2	1000.0	47.2	52.9	n.m.	n.m.	n.m.	n.m.	n.m.	n.m.
2	1	11	3	543.3	18.0	28.7	n.m.	n.m.	n.m.	n.m.	n.m.	n.m.
2	1	11	4	427.2	13.2	50.9	n.m.	n.m.	n.m.	n.m.	n.m.	n.m.
2	1	11	5	507.6	16.1	25.8	n.m.	n.m.	n.m.	n.m.	n.m.	n.m.
2	1	11	6	293.7	68.7	31.9	n.m.	n.m.	n.m.	n.m.	n.m.	n.m.
2	1	11	7	307.3	12.5	28.0	n.m.	n.m.	n.m.	n.m.	n.m.	n.m.
2	1	11	8	213.8	10.6	36.1	n.m.	n.m.	n.m.	n.m.	n.m.	n.m.
2	1	11	9	144.7	35.0	11.4	n.m.	n.m.	n.m.	n.m.	n.m.	n.m.
2	1	11	10	106.6	7.2	7.5	n.m.	n.m.	n.m.	n.m.	n.m.	n.m.
2	1	11	11	73.8	6.9	4.5	n.m.	n.m.	n.m.	n.m.	n.m.	n.m.
2	1	12	0	1562.0	68.6	79.8	n.m.	n.m.	n.m.	n.m.	n.m.	n.m.
2	1	12	1	1062.9	57.5	270.4	n.m.	n.m.	n.m.	n.m.	n.m.	n.m.
2	1	12	2	856.0	45.5	49.4	n.m.	n.m.	n.m.	n.m.	n.m.	n.m.
2	1	12	3	665.8	35.6	125.2	n.m.	n.m.	n.m.	n.m.	n.m.	n.m.
2	1	12	4	519.1	26.5	45.7	n.m.	n.m.	n.m.	n.m.	n.m.	n.m.
2	1	12	5	367.5	15.0	51.3	n.m.	n.m.	n.m.	n.m.	n.m.	n.m.
2	1	12	6	213.6	62.5	52.3	n.m.	n.m.	n.m.	n.m.	n.m.	n.m.
2	1	12	7	189.0	41.2	12.0	n.m.	n.m.	n.m.	n.m.	n.m.	n.m.
2	1	12	8	164.3	9.8	9.9	n.m.	n.m.	n.m.	n.m.	n.m.	n.m.
2	1	12	9	118.7	53.5	20.5	n.m.	n.m.	n.m.	n.m.	n.m.	n.m.
2	1	13	0	1103.0	484.7	320.8	n.m.	n.m.	n.m.	n.m.	n.m.	n.m.
2	1	13	1	662.7	1645.1	330.4	n.m.	n.m.	n.m.	n.m.	n.m.	n.m.
2	1	13	2	683.9	47.2	254.7	n.m.	n.m.	n.m.	n.m.	n.m.	n.m.
2	1	13	3	682.7	52.6	43.2	n.m.	n.m.	n.m.	n.m.	n.m.	n.m.
2	1	13	4	294.4	28.5	53.0	n.m.	n.m.	n.m.	n.m.	n.m.	n.m.
2	1	13	5	375.4	22.7	51.6	n.m.	n.m.	n.m.	n.m.	n.m.	n.m.
2	1	13	6	318.4	22.7	20.5	n.m.	n.m.	n.m.	n.m.	n.m.	n.m.
2	1	13	7	281.5	22.6	39.9	n.m.	n.m.	n.m.	n.m.	n.m.	n.m.
2	1	14	0	1005.3	56.8	201.7	n.m.	n.m.	n.m.	n.m.	n.m.	n.m.
2	1	14	1	805.8	62.1	226.1	n.m.	n.m.	n.m.	n.m.	n.m.	n.m.
2	1	14	2	315.2	20.3	64.9	n.m.	n.m.	n.m.	n.m.	n.m.	n.m.
2	1	14	3	368.2	53.8	29.9	n.m.	n.m.	n.m.	n.m.	n.m.	n.m.
2	1	14	4	337.8	31.7	48.3	n.m.	n.m.	n.m.	n.m.	n.m.	n.m.
3	0	1	0	12797.8	156.4	621.7	n.m.	n.m.	n.m.	n.m.	n.m.	n.m.

Continued on next page

Table B.2 – *Continued from previous page*

x	Q^2	z	$P_{h\perp}^2$	A_0	ΔA_0	δA_0	$A_{UU}^{\cos\phi_h}$	$\Delta A_{UU}^{\cos\phi_h}$	$\delta A_{UU}^{\cos\phi_h}$	$A_{UU}^{\cos 2\phi_h}$	$\Delta A_{UU}^{\cos 2\phi_h}$	$\delta A_{UU}^{\cos 2\phi_h}$
3	0	2	0	7811.0	101.9	375.5	n.m.	n.m.	n.m.	n.m.	n.m.	n.m.
3	0	2	1	3774.2	37.0	184.9	n.m.	n.m.	n.m.	n.m.	n.m.	n.m.
3	0	3	0	7063.7	1361.5	1919.8	n.m.	n.m.	n.m.	n.m.	n.m.	n.m.
3	0	3	1	3422.9	217.6	365.3	n.m.	n.m.	n.m.	n.m.	n.m.	n.m.
3	0	3	2	1676.3	27.2	82.8	-0.0484	0.0270	0.0256	0.0042	0.0223	0.0173
3	0	3	3	1056.4	19.2	52.1	0.0047	0.0289	0.0294	0.1051	0.0264	0.0228
3	0	4	0	4470.6	172.4	204.4	n.m.	n.m.	n.m.	n.m.	n.m.	n.m.
3	0	4	1	1928.0	761.7	268.2	n.m.	n.m.	n.m.	n.m.	n.m.	n.m.
3	0	4	2	1384.3	129.5	142.1	n.m.	n.m.	n.m.	n.m.	n.m.	n.m.
3	0	4	3	933.8	23.0	49.8	0.0453	0.0397	0.0213	0.0871	0.0297	0.0129
3	0	4	4	577.6	13.3	29.2	-0.0934	0.0372	0.0112	0.1301	0.0331	0.0135
3	0	4	5	596.7	17.7	30.0	-0.0063	0.0458	0.0134	0.2187	0.0396	0.0151
3	0	5	0	1658.1	139.8	783.1	n.m.	n.m.	n.m.	n.m.	n.m.	n.m.
3	0	5	1	2005.4	44.5	330.4	n.m.	n.m.	n.m.	n.m.	n.m.	n.m.
3	0	5	2	1267.8	123.6	159.5	n.m.	n.m.	n.m.	n.m.	n.m.	n.m.
3	0	5	3	846.2	54.0	48.9	n.m.	n.m.	n.m.	n.m.	n.m.	n.m.
3	0	5	4	582.9	31.7	38.6	n.m.	n.m.	n.m.	n.m.	n.m.	n.m.
3	0	5	5	418.9	14.6	23.3	0.0769	0.0545	0.0335	0.1453	0.0444	0.0221
3	0	5	6	380.6	15.7	17.6	-0.0665	0.0647	0.0255	0.2446	0.0566	0.0191
3	0	6	0	1092.1	102.5	186.0	n.m.	n.m.	n.m.	n.m.	n.m.	n.m.
3	0	6	1	910.9	27.4	160.6	n.m.	n.m.	n.m.	n.m.	n.m.	n.m.
3	0	6	2	813.0	115.2	126.5	n.m.	n.m.	n.m.	n.m.	n.m.	n.m.
3	0	6	3	697.8	91.8	48.5	n.m.	n.m.	n.m.	n.m.	n.m.	n.m.
3	0	6	4	509.2	43.6	31.2	n.m.	n.m.	n.m.	n.m.	n.m.	n.m.
3	0	6	5	390.7	40.5	42.7	n.m.	n.m.	n.m.	n.m.	n.m.	n.m.
3	0	6	6	259.6	15.7	15.5	n.m.	n.m.	n.m.	n.m.	n.m.	n.m.
3	0	6	7	265.0	26.5	24.3	n.m.	n.m.	n.m.	n.m.	n.m.	n.m.
3	0	7	0	1174.1	136.6	132.8	n.m.	n.m.	n.m.	n.m.	n.m.	n.m.
3	0	7	1	875.8	34.0	44.1	n.m.	n.m.	n.m.	n.m.	n.m.	n.m.
3	0	7	2	607.6	105.4	102.6	n.m.	n.m.	n.m.	n.m.	n.m.	n.m.
3	0	7	3	502.9	88.6	55.7	n.m.	n.m.	n.m.	n.m.	n.m.	n.m.
3	0	7	4	342.2	38.6	19.3	n.m.	n.m.	n.m.	n.m.	n.m.	n.m.
3	0	7	5	354.4	14.5	22.4	n.m.	n.m.	n.m.	n.m.	n.m.	n.m.
3	0	7	6	230.9	30.8	17.5	n.m.	n.m.	n.m.	n.m.	n.m.	n.m.
3	0	7	7	185.0	25.0	37.3	n.m.	n.m.	n.m.	n.m.	n.m.	n.m.
3	0	8	0	949.6	110.3	429.5	n.m.	n.m.	n.m.	n.m.	n.m.	n.m.
3	0	8	1	439.1	20.5	193.7	n.m.	n.m.	n.m.	n.m.	n.m.	n.m.
3	0	8	2	335.8	11.8	17.2	n.m.	n.m.	n.m.	n.m.	n.m.	n.m.
3	0	8	3	422.1	15.4	26.5	n.m.	n.m.	n.m.	n.m.	n.m.	n.m.

Continued on next page

Table B.2 – *Continued from previous page*

x	Q^2	z	$P_{h\perp}^2$	A_0	ΔA_0	δA_0	$A_{UU}^{\cos\phi_h}$	$\Delta A_{UU}^{\cos\phi_h}$	$\delta A_{UU}^{\cos\phi_h}$	$A_{UU}^{\cos 2\phi_h}$	$\Delta A_{UU}^{\cos 2\phi_h}$	$\delta A_{UU}^{\cos 2\phi_h}$
3	0	8	4	265.7	9.9	21.8	n.m.	n.m.	n.m.	n.m.	n.m.	n.m.
3	0	8	5	234.4	25.3	33.4	n.m.	n.m.	n.m.	n.m.	n.m.	n.m.
3	0	8	6	169.3	25.5	5.8	n.m.	n.m.	n.m.	n.m.	n.m.	n.m.
3	0	8	7	143.5	12.2	6.4	n.m.	n.m.	n.m.	n.m.	n.m.	n.m.
3	0	9	0	491.9	81.8	168.3	n.m.	n.m.	n.m.	n.m.	n.m.	n.m.
3	0	9	1	275.7	14.5	14.3	n.m.	n.m.	n.m.	n.m.	n.m.	n.m.
3	0	9	2	369.2	16.1	18.3	n.m.	n.m.	n.m.	n.m.	n.m.	n.m.
3	0	9	3	292.0	64.7	35.2	n.m.	n.m.	n.m.	n.m.	n.m.	n.m.
3	0	9	4	234.0	29.2	17.3	n.m.	n.m.	n.m.	n.m.	n.m.	n.m.
3	0	9	5	192.0	21.9	18.8	n.m.	n.m.	n.m.	n.m.	n.m.	n.m.
3	0	9	6	135.4	24.8	8.4	n.m.	n.m.	n.m.	n.m.	n.m.	n.m.
3	0	9	7	102.7	14.9	40.1	n.m.	n.m.	n.m.	n.m.	n.m.	n.m.
3	0	10	0	449.1	71.1	158.7	n.m.	n.m.	n.m.	n.m.	n.m.	n.m.
3	0	10	1	345.3	19.8	15.0	n.m.	n.m.	n.m.	n.m.	n.m.	n.m.
3	0	10	2	281.2	16.3	25.3	n.m.	n.m.	n.m.	n.m.	n.m.	n.m.
3	0	10	3	228.6	57.8	42.4	n.m.	n.m.	n.m.	n.m.	n.m.	n.m.
3	0	10	4	191.8	9.9	8.8	n.m.	n.m.	n.m.	n.m.	n.m.	n.m.
3	0	10	5	139.5	24.0	12.4	n.m.	n.m.	n.m.	n.m.	n.m.	n.m.
3	0	10	6	110.5	52.1	12.8	n.m.	n.m.	n.m.	n.m.	n.m.	n.m.
3	0	11	0	399.6	68.7	164.5	n.m.	n.m.	n.m.	n.m.	n.m.	n.m.
3	0	11	1	251.5	15.3	40.2	n.m.	n.m.	n.m.	n.m.	n.m.	n.m.
3	0	11	2	145.9	10.8	87.6	n.m.	n.m.	n.m.	n.m.	n.m.	n.m.
3	0	11	3	153.3	59.5	22.2	n.m.	n.m.	n.m.	n.m.	n.m.	n.m.
3	0	11	4	105.1	15.9	8.8	n.m.	n.m.	n.m.	n.m.	n.m.	n.m.
3	0	12	0	295.2	15.3	15.9	n.m.	n.m.	n.m.	n.m.	n.m.	n.m.
3	0	12	1	164.3	14.0	43.6	n.m.	n.m.	n.m.	n.m.	n.m.	n.m.
3	0	12	2	93.4	12.3	77.7	n.m.	n.m.	n.m.	n.m.	n.m.	n.m.
3	0	13	0	200.8	11.9	93.3	n.m.	n.m.	n.m.	n.m.	n.m.	n.m.
3	0	13	1	141.4	18.0	55.4	n.m.	n.m.	n.m.	n.m.	n.m.	n.m.
3	1	1	0	24677.9	255.8	1268.1	n.m.	n.m.	n.m.	n.m.	n.m.	n.m.
3	1	2	0	16022.9	3486.7	3513.6	n.m.	n.m.	n.m.	n.m.	n.m.	n.m.
3	1	2	1	7303.5	59.1	337.5	n.m.	n.m.	n.m.	n.m.	n.m.	n.m.
3	1	2	2	3749.7	27.7	184.9	-0.0490	0.0109	0.0036	0.0210	0.0105	0.0026
3	1	2	3	1800.0	21.8	96.3	-0.0581	0.0180	0.0059	0.0661	0.0172	0.0066
3	1	3	0	8716.7	195.0	396.0	n.m.	n.m.	n.m.	n.m.	n.m.	n.m.
3	1	3	1	6907.8	369.7	623.1	n.m.	n.m.	n.m.	n.m.	n.m.	n.m.
3	1	3	2	3605.2	52.8	162.2	-0.0231	0.0243	0.0094	0.0018	0.0176	0.0054
3	1	3	3	2092.1	25.9	101.5	-0.0240	0.0201	0.0084	0.0443	0.0178	0.0073
3	1	3	4	1339.3	17.7	65.5	-0.0099	0.0196	0.0072	0.0920	0.0187	0.0089

Continued on next page

Table B.2 – *Continued from previous page*

x	Q^2	z	$P_{h\perp}^2$	A_0	ΔA_0	δA_0	$A_{UU}^{\cos\phi_h}$	$\Delta A_{UU}^{\cos\phi_h}$	$\delta A_{UU}^{\cos\phi_h}$	$A_{UU}^{\cos 2\phi_h}$	$\Delta A_{UU}^{\cos 2\phi_h}$	$\delta A_{UU}^{\cos 2\phi_h}$
3	1	3	5	894.1	17.9	49.5	-0.0459	0.0300	0.0112	0.1423	0.0279	0.0111
3	1	4	0	9310.5	454.4	491.8	n.m.	n.m.	n.m.	n.m.	n.m.	n.m.
3	1	4	1	3930.9	1014.7	370.1	n.m.	n.m.	n.m.	n.m.	n.m.	n.m.
3	1	4	2	2856.0	211.5	194.4	n.m.	n.m.	n.m.	n.m.	n.m.	n.m.
3	1	4	3	1954.2	44.6	82.3	0.0020	0.0377	0.0121	0.0243	0.0256	0.0057
3	1	4	4	1288.7	22.1	60.5	-0.0267	0.0276	0.0228	0.0505	0.0236	0.0161
3	1	4	5	917.7	15.8	41.4	0.0001	0.0257	0.0121	0.0908	0.0242	0.0092
3	1	4	6	687.1	15.5	36.7	-0.0626	0.0329	0.0117	0.0607	0.0321	0.0093
3	1	4	7	496.8	16.8	22.4	0.0081	0.0504	0.0128	0.1356	0.0455	0.0166
3	1	5	0	3338.9	961.8	3086.4	n.m.	n.m.	n.m.	n.m.	n.m.	n.m.
3	1	5	1	2472.3	48.7	984.7	n.m.	n.m.	n.m.	n.m.	n.m.	n.m.
3	1	5	2	2442.1	204.4	253.6	n.m.	n.m.	n.m.	n.m.	n.m.	n.m.
3	1	5	3	1771.9	101.3	92.6	n.m.	n.m.	n.m.	n.m.	n.m.	n.m.
3	1	5	4	1199.3	54.4	96.9	n.m.	n.m.	n.m.	n.m.	n.m.	n.m.
3	1	5	5	867.6	24.1	38.3	0.0533	0.0448	0.0179	0.0664	0.0336	0.0105
3	1	5	6	634.4	16.6	30.4	-0.0033	0.0411	0.0148	0.1066	0.0363	0.0118
3	1	5	7	470.3	14.3	25.1	-0.0829	0.0458	0.0188	0.1068	0.0412	0.0116
3	1	5	8	302.5	12.7	14.8	-0.1525	0.0614	0.0303	0.0785	0.0627	0.0189
3	1	5	9	237.0	15.8	12.6	0.0060	0.0937	0.0425	-0.0124	0.0929	0.0225
3	1	6	0	2544.0	4354.1	1276.5	n.m.	n.m.	n.m.	n.m.	n.m.	n.m.
3	1	6	1	2733.9	81.1	537.2	n.m.	n.m.	n.m.	n.m.	n.m.	n.m.
3	1	6	2	1472.7	193.9	136.2	n.m.	n.m.	n.m.	n.m.	n.m.	n.m.
3	1	6	3	1491.2	28.1	147.0	n.m.	n.m.	n.m.	n.m.	n.m.	n.m.
3	1	6	4	1067.8	76.0	49.7	n.m.	n.m.	n.m.	n.m.	n.m.	n.m.
3	1	6	5	725.1	60.8	68.4	n.m.	n.m.	n.m.	n.m.	n.m.	n.m.
3	1	6	6	516.3	23.0	27.3	n.m.	n.m.	n.m.	n.m.	n.m.	n.m.
3	1	6	7	416.8	20.8	37.7	n.m.	n.m.	n.m.	n.m.	n.m.	n.m.
3	1	6	8	299.9	16.8	18.2	n.m.	n.m.	n.m.	n.m.	n.m.	n.m.
3	1	6	9	266.7	16.8	12.9	0.0023	0.0964	0.0532	0.1137	0.0893	0.0284
3	1	6	10	159.6	22.9	12.2	n.m.	n.m.	n.m.	n.m.	n.m.	n.m.
3	1	7	0	1192.2	166.7	123.1	n.m.	n.m.	n.m.	n.m.	n.m.	n.m.
3	1	7	1	1142.9	3723.3	675.2	n.m.	n.m.	n.m.	n.m.	n.m.	n.m.
3	1	7	2	973.6	23.4	39.0	n.m.	n.m.	n.m.	n.m.	n.m.	n.m.
3	1	7	3	893.2	134.4	102.6	n.m.	n.m.	n.m.	n.m.	n.m.	n.m.
3	1	7	4	825.0	68.2	49.5	n.m.	n.m.	n.m.	n.m.	n.m.	n.m.
3	1	7	5	536.3	52.3	39.3	n.m.	n.m.	n.m.	n.m.	n.m.	n.m.
3	1	7	6	498.3	48.6	35.2	n.m.	n.m.	n.m.	n.m.	n.m.	n.m.
3	1	7	7	349.2	27.0	55.1	n.m.	n.m.	n.m.	n.m.	n.m.	n.m.
3	1	7	8	272.0	30.2	22.1	n.m.	n.m.	n.m.	n.m.	n.m.	n.m.

Continued on next page

Table B.2 – *Continued from previous page*

x	Q^2	z	$P_{h\perp}^2$	A_0	ΔA_0	δA_0	$A_{UU}^{\cos\phi_h}$	$\Delta A_{UU}^{\cos\phi_h}$	$\delta A_{UU}^{\cos\phi_h}$	$A_{UU}^{\cos 2\phi_h}$	$\Delta A_{UU}^{\cos 2\phi_h}$	$\delta A_{UU}^{\cos 2\phi_h}$
3	1	7	9	187.2	15.0	10.8	-0.0368	0.1289	0.0347	-0.0644	0.1168	0.0439
3	1	7	10	146.3	16.3	10.6	n.m.	n.m.	n.m.	n.m.	n.m.	n.m.
3	1	8	0	908.5	6.2	580.1	n.m.	n.m.	n.m.	n.m.	n.m.	n.m.
3	1	8	1	1121.8	53.6	65.9	n.m.	n.m.	n.m.	n.m.	n.m.	n.m.
3	1	8	2	850.9	199.7	161.6	n.m.	n.m.	n.m.	n.m.	n.m.	n.m.
3	1	8	3	772.3	112.5	47.1	n.m.	n.m.	n.m.	n.m.	n.m.	n.m.
3	1	8	4	658.3	18.9	34.5	n.m.	n.m.	n.m.	n.m.	n.m.	n.m.
3	1	8	5	432.5	45.7	28.8	n.m.	n.m.	n.m.	n.m.	n.m.	n.m.
3	1	8	6	333.2	43.0	15.6	n.m.	n.m.	n.m.	n.m.	n.m.	n.m.
3	1	8	7	209.8	9.8	10.4	n.m.	n.m.	n.m.	n.m.	n.m.	n.m.
3	1	8	8	243.2	46.3	23.6	n.m.	n.m.	n.m.	n.m.	n.m.	n.m.
3	1	8	9	148.7	39.0	9.2	n.m.	n.m.	n.m.	n.m.	n.m.	n.m.
3	1	8	10	122.5	17.2	17.1	n.m.	n.m.	n.m.	n.m.	n.m.	n.m.
3	1	9	0	926.2	166.7	339.9	n.m.	n.m.	n.m.	n.m.	n.m.	n.m.
3	1	9	1	813.6	46.9	44.6	n.m.	n.m.	n.m.	n.m.	n.m.	n.m.
3	1	9	2	646.6	174.2	93.4	n.m.	n.m.	n.m.	n.m.	n.m.	n.m.
3	1	9	3	395.6	96.4	87.1	n.m.	n.m.	n.m.	n.m.	n.m.	n.m.
3	1	9	4	459.5	15.8	22.2	n.m.	n.m.	n.m.	n.m.	n.m.	n.m.
3	1	9	5	352.2	13.1	19.4	n.m.	n.m.	n.m.	n.m.	n.m.	n.m.
3	1	9	6	281.9	12.4	20.3	n.m.	n.m.	n.m.	n.m.	n.m.	n.m.
3	1	9	7	234.8	32.1	15.2	n.m.	n.m.	n.m.	n.m.	n.m.	n.m.
3	1	9	8	153.3	44.2	16.1	n.m.	n.m.	n.m.	n.m.	n.m.	n.m.
3	1	9	9	104.7	10.1	9.2	n.m.	n.m.	n.m.	n.m.	n.m.	n.m.
3	1	10	0	815.7	147.7	416.8	n.m.	n.m.	n.m.	n.m.	n.m.	n.m.
3	1	10	1	565.6	36.5	31.2	n.m.	n.m.	n.m.	n.m.	n.m.	n.m.
3	1	10	2	487.0	26.4	29.2	n.m.	n.m.	n.m.	n.m.	n.m.	n.m.
3	1	10	3	379.1	16.3	35.5	n.m.	n.m.	n.m.	n.m.	n.m.	n.m.
3	1	10	4	327.4	53.8	24.3	n.m.	n.m.	n.m.	n.m.	n.m.	n.m.
3	1	10	5	220.4	39.8	21.3	n.m.	n.m.	n.m.	n.m.	n.m.	n.m.
3	1	10	6	202.8	11.1	10.3	n.m.	n.m.	n.m.	n.m.	n.m.	n.m.
3	1	10	7	153.9	34.2	15.7	n.m.	n.m.	n.m.	n.m.	n.m.	n.m.
3	1	10	8	95.9	8.3	9.8	n.m.	n.m.	n.m.	n.m.	n.m.	n.m.
3	1	11	0	502.8	8.6	280.2	n.m.	n.m.	n.m.	n.m.	n.m.	n.m.
3	1	11	1	459.4	28.5	24.6	n.m.	n.m.	n.m.	n.m.	n.m.	n.m.
3	1	11	2	382.4	25.7	22.3	n.m.	n.m.	n.m.	n.m.	n.m.	n.m.
3	1	11	3	305.3	18.9	14.3	n.m.	n.m.	n.m.	n.m.	n.m.	n.m.
3	1	11	4	244.9	13.1	15.7	n.m.	n.m.	n.m.	n.m.	n.m.	n.m.
3	1	11	5	194.3	48.9	14.4	n.m.	n.m.	n.m.	n.m.	n.m.	n.m.
3	1	11	6	168.9	12.6	17.6	n.m.	n.m.	n.m.	n.m.	n.m.	n.m.

Continued on next page

Table B.2 – *Continued from previous page*

x	Q^2	z	$P_{h\perp}^2$	A_0	ΔA_0	δA_0	$A_{UU}^{\cos\phi_h}$	$\Delta A_{UU}^{\cos\phi_h}$	$\delta A_{UU}^{\cos\phi_h}$	$A_{UU}^{\cos 2\phi_h}$	$\Delta A_{UU}^{\cos 2\phi_h}$	$\delta A_{UU}^{\cos 2\phi_h}$
3	1	12	0	518.5	32.5	25.6	n.m.	n.m.	n.m.	n.m.	n.m.	n.m.
3	1	12	1	224.5	18.6	115.7	n.m.	n.m.	n.m.	n.m.	n.m.	n.m.
3	1	12	2	305.4	25.8	18.9	n.m.	n.m.	n.m.	n.m.	n.m.	n.m.
3	1	12	3	323.5	34.6	88.9	n.m.	n.m.	n.m.	n.m.	n.m.	n.m.
3	1	12	4	207.9	90.0	28.5	n.m.	n.m.	n.m.	n.m.	n.m.	n.m.
3	1	13	0	427.0	32.2	18.9	n.m.	n.m.	n.m.	n.m.	n.m.	n.m.
3	1	13	1	312.3	33.3	20.9	n.m.	n.m.	n.m.	n.m.	n.m.	n.m.
3	1	13	2	257.4	39.6	22.1	n.m.	n.m.	n.m.	n.m.	n.m.	n.m.
4	0	1	0	6026.4	194.4	374.8	-0.2577	0.0560	0.0173	0.0546	0.0370	0.0110
4	0	2	0	3878.4	162.2	222.2	n.m.	n.m.	n.m.	n.m.	n.m.	n.m.
4	0	2	1	1757.1	52.8	103.2	n.m.	n.m.	n.m.	n.m.	n.m.	n.m.
4	0	2	2	872.8	17.4	48.4	-0.0334	0.0301	0.0092	0.0736	0.0282	0.0103
4	0	2	3	540.3	21.1	30.1	-0.0157	0.0567	0.0355	0.0342	0.0559	0.0150
4	0	3	0	3265.7	238.1	845.5	n.m.	n.m.	n.m.	n.m.	n.m.	n.m.
4	0	3	1	1627.4	215.0	280.1	n.m.	n.m.	n.m.	n.m.	n.m.	n.m.
4	0	3	2	815.4	42.9	90.8	n.m.	n.m.	n.m.	n.m.	n.m.	n.m.
4	0	3	3	453.2	12.5	25.3	-0.0605	0.0418	0.0128	0.0238	0.0382	0.0180
4	0	3	4	351.9	13.3	19.1	-0.0319	0.0545	0.0260	-0.0089	0.0545	0.0194
4	0	4	0	2297.8	258.1	132.2	n.m.	n.m.	n.m.	n.m.	n.m.	n.m.
4	0	4	1	885.4	28.0	489.1	n.m.	n.m.	n.m.	n.m.	n.m.	n.m.
4	0	4	2	750.2	115.7	95.5	n.m.	n.m.	n.m.	n.m.	n.m.	n.m.
4	0	4	3	481.9	39.6	38.6	n.m.	n.m.	n.m.	n.m.	n.m.	n.m.
4	0	4	4	299.4	13.8	18.0	-0.1421	0.0773	0.0337	0.0669	0.0640	0.0265
4	0	4	5	227.1	11.5	15.5	0.0128	0.0778	0.0321	0.0931	0.0696	0.0181
4	0	5	0	635.3	41.8	306.3	n.m.	n.m.	n.m.	n.m.	n.m.	n.m.
4	0	5	1	612.3	27.6	163.9	n.m.	n.m.	n.m.	n.m.	n.m.	n.m.
4	0	5	2	497.7	311.6	199.7	n.m.	n.m.	n.m.	n.m.	n.m.	n.m.
4	0	5	3	489.8	19.5	36.5	n.m.	n.m.	n.m.	n.m.	n.m.	n.m.
4	0	5	4	286.5	44.5	24.1	n.m.	n.m.	n.m.	n.m.	n.m.	n.m.
4	0	5	5	188.2	20.9	12.4	n.m.	n.m.	n.m.	n.m.	n.m.	n.m.
4	0	5	6	154.8	13.6	19.3	n.m.	n.m.	n.m.	n.m.	n.m.	n.m.
4	0	6	0	441.1	37.4	144.5	n.m.	n.m.	n.m.	n.m.	n.m.	n.m.
4	0	6	1	546.0	487.3	190.4	n.m.	n.m.	n.m.	n.m.	n.m.	n.m.
4	0	6	2	469.5	325.2	138.3	n.m.	n.m.	n.m.	n.m.	n.m.	n.m.
4	0	6	3	339.6	79.0	53.5	n.m.	n.m.	n.m.	n.m.	n.m.	n.m.
4	0	6	4	295.0	15.2	18.1	n.m.	n.m.	n.m.	n.m.	n.m.	n.m.
4	0	6	5	197.9	40.8	16.9	n.m.	n.m.	n.m.	n.m.	n.m.	n.m.
4	0	6	6	155.3	32.0	17.4	n.m.	n.m.	n.m.	n.m.	n.m.	n.m.
4	0	6	7	177.6	31.3	10.4	n.m.	n.m.	n.m.	n.m.	n.m.	n.m.

Continued on next page

Table B.2 – *Continued from previous page*

x	Q^2	z	$P_{h\perp}^2$	A_0	ΔA_0	δA_0	$A_{UU}^{\cos\phi_h}$	$\Delta A_{UU}^{\cos\phi_h}$	$\delta A_{UU}^{\cos\phi_h}$	$A_{UU}^{\cos 2\phi_h}$	$\Delta A_{UU}^{\cos 2\phi_h}$	$\delta A_{UU}^{\cos 2\phi_h}$
4	0	7	0	817.4	352.6	486.8	n.m.	n.m.	n.m.	n.m.	n.m.	n.m.
4	0	7	1	411.1	44.1	35.4	n.m.	n.m.	n.m.	n.m.	n.m.	n.m.
4	0	7	2	224.0	15.5	28.1	n.m.	n.m.	n.m.	n.m.	n.m.	n.m.
4	0	7	3	211.5	72.4	36.4	n.m.	n.m.	n.m.	n.m.	n.m.	n.m.
4	0	7	4	171.9	10.8	17.1	n.m.	n.m.	n.m.	n.m.	n.m.	n.m.
4	0	7	5	169.2	44.9	15.4	n.m.	n.m.	n.m.	n.m.	n.m.	n.m.
4	0	7	6	104.5	41.6	16.5	n.m.	n.m.	n.m.	n.m.	n.m.	n.m.
4	0	8	1	362.5	50.9	102.3	n.m.	n.m.	n.m.	n.m.	n.m.	n.m.
4	0	8	2	270.9	28.2	23.1	n.m.	n.m.	n.m.	n.m.	n.m.	n.m.
4	0	8	3	204.1	57.3	27.1	n.m.	n.m.	n.m.	n.m.	n.m.	n.m.
4	0	8	4	155.1	10.8	8.8	n.m.	n.m.	n.m.	n.m.	n.m.	n.m.
4	0	8	5	120.9	34.9	12.8	n.m.	n.m.	n.m.	n.m.	n.m.	n.m.
4	0	8	6	122.9	13.9	8.7	n.m.	n.m.	n.m.	n.m.	n.m.	n.m.
4	0	9	1	228.0	36.9	14.4	n.m.	n.m.	n.m.	n.m.	n.m.	n.m.
4	0	9	2	189.4	27.2	62.3	n.m.	n.m.	n.m.	n.m.	n.m.	n.m.
4	0	9	3	136.7	66.6	57.2	n.m.	n.m.	n.m.	n.m.	n.m.	n.m.
4	0	9	4	136.7	11.6	11.1	n.m.	n.m.	n.m.	n.m.	n.m.	n.m.
4	0	9	5	88.3	9.0	9.8	n.m.	n.m.	n.m.	n.m.	n.m.	n.m.